Structural and Functional Analysis of the Protein Network Controlling Centriole Biogenesis

Thesis

How to cite:

Schneider, Manuela Sandra (2017). Structural and Functional Analysis of the Protein Network Controlling Centriole Biogenesis. PhD thesis The Open University.

Structural and functional analysis of the protein network controlling centriole biogenesis

M. Sandra Schneider BSc MSc

This thesis is submitted for the degree of Doctor of Philosophy in
Faculty of Science
Department of Life, Health & Chemical Sciences at
the Open University

June 2016

Acknowledgements

My sincere thanks goes to Professor David M. Glover, who gave me the opportunity to join his research group as research assistant and undertake my PhD research in his laboratory (Cell Cycle Genetics group, Department of Genetics, University of Cambridge, UK). This thesis would not have been possible without his support and kindness, for which I am utmost grateful.

I also greatly thank Dr. Robert Saunders for his everlasting optimism and support over the past years as my supervisor at The Open University. I also thank Dr. Nacho Romero for being my internal supervisor.

A great thank you goes to everyone in David’s lab, past and present, for their support, food for thoughts on my research and for an ambitious lab environment. In particular, I would like to thank Dr. Dzhindzhev, Dr. Lipinszki, Dr. Tzolovsky and Miss Chu for their collaborations and discussions.

A special thanks goes to my family, friends and especially Dan for his continuous support and believe in me. Cambridge, you have been great.

Abstract

Centrosomes function as microtubules organising centres in mitosis or as basal bodies in cilia and flagella formation. The duplication of centrioles, which are at the core of each centrosome, is tightly regulated and occurs only once per cell cycle, which allows for correct segregation of chromosomes. In *C. elegans*, only five proteins are essential for centriole duplication. How their *Drosophila* counterparts interact with each other on a molecular level still remains largely unknown.

To further our understanding of the protein interactions governing centriole duplication, I applied *in vivo* and *in vitro* methods to design a protein interaction network at the centriole. I analysed mass spectrometry data from purifications of ProteinA-tagged centriole duplication proteins to identify *in vivo* protein complexes; and performed direct *in vitro* and *in vivo* protein-protein interaction assays.

Additionally, I studied the *Drosophila* proteins Ana2 and Sas6; showing that Plk4 phosphorylates S318, S365, S370, and S373 of the Ana2-STAN motif; which identifies a direct substrate of Plk4. By *in vitro* interaction studies I show that Sas6 aa276-432 and Ana2-STAN interact directly, if the latter is phosphorylated by Plk4. The depletion of Ana2 or expression of Ana2-4A causes loss of centrosomes in *Drosophila* cell culture, which was not observed when expressing Ana2-4D. This supports the importance of Plk4-mediated phosphorylation of Ana2-STAN in centriole duplication.

Mass spectrometry analysis of Sas6 purifications from cultured *Drosophila* cells identified the uncharacterised protein CG33052 (Dragon) and reciprocal purifications of tagged Dragon from *Drosophila* cell culture and syncytial embryos identified Sas6. By *in vitro* interaction studies I confirm that Dragon aa191-318/GoRab and Sas6 aa351-462/HsSas6 interact directly. The deletion mutant Dragon∆aa260-286 does not interact with Sas6 *in vitro* or *in vivo*, and fails to rescue centriole duplication after Dragon depletion. Dragon localises to the *trans*-Golgi and co-localises with Sas6 at the centriole throughout the cell cycle.

Table of Contents

4 Interaction of Ana2 and Sas6 – Mediated by Plk4 phosphorylation of Ana2 and enabling procentriole formation 89

5 The novel direct interaction and centrosome localisation of Dragon (CG33052) with the cartwheel protein Sas6.........................137

List of Figures

List of Tables

List of Abbreviations

AD	Activation Domain
AKAP450	A-kinase anchor proteins, *Drosophila* homologue Plp
AL	Activation Loop
Ana1, 2, 3	anastral spindle 1, 2, 3
Asl	Asterless
BD	Binding Domain
Cdk1	cyclin-dependent kinase 1
CLASPs	cytoplasmic linker-associated proteins
Cnn	centrosomin
CtBP	C-terminal binding protein
D-Plp	Drosophila pericentrin-like protein
DRE	downstream regulatory element
ER	endoplasmic reticulum
GMAP210	Golgi microtubules associated protein of 210kDa
IFT	intraflagellar transport
IM	interaction motif
IVTT	*in vitro* transcription translation
KDEL	Lysine-Aspartic acid-Glutamic acid-Leucine
KLP10A	kinesin-like protein 10A
LC8	dynein light chain
MDM2	mouse double minute gene number 2
MTOC	microtubules organising centre
Nap1	Nucleosome assembly protein 1
PB	polo box
PCM	pericentriolar material
PISA	present in Sas6
Plk	Polo like kinase
Poly-Ub/ pUb	poly-Ubiquitin
PP2A	protein phosphatase 2A

PPH4	protein phosphatase 4
Rcd4	Reduction in Cnn dots 4
RNAi	ribonucleic acid interferance
Sas4, 6	spindle assembly abnormal 4, 6
Spd2	spindle defective 2
STAN	STIL Ana2
TGN	*trans*-Golgi-network
TIM	truncated in microcephaly
Zyg-1	zygote defective-1

Chapter 1

Introduction

1 Introduction

1.1 The cell cycle

The cell cycle is a series of events that are categorised into interphase and mitosis; with interphase being separated into G_1-, S-, G_2- and M-phases (Figure 1-1). During each cell cycle the cell's DNA is replicated in S-phase and the duplicated chromatids are segregated to the opposite poles of the mitotic spindle during M-phase followed by the division of the cell into two identical daughters at cytokinesis.

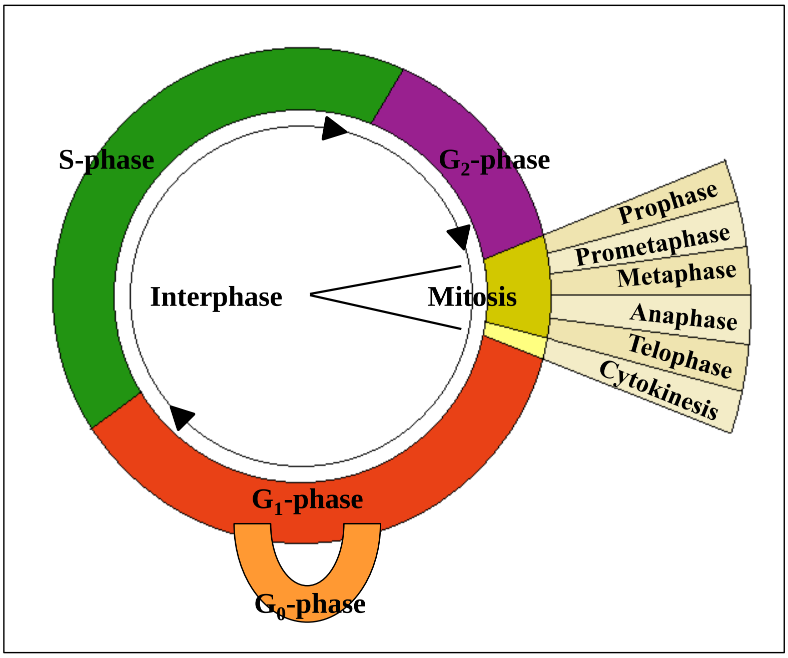

Figure 1-1 Cell cycle phases. The cell division cycle is divided into interphase and mitosis. Interphase composes of G_1-phase where cell growth occurs and centriole duplication begins, S-phase in which the DNA replicates and G_2-phase which is characterised by final cell growth and the completion of centriole duplication. During mitosis the duplicated DNA copies are separated into daughter cells. G_0-phase is a dormancy phase of the cell when conditions do not favour to progress through G_1-phase and into S-phase.

M phase initiates with prophase, when the chromatin fibres condense to chromosomes, followed by the beginning of nuclear envelope breakdown at the end of prophase; and the migration of the two centrosomes to opposite sides of the nucleus. Centrosomes are the major MTOCs (microtubules organising centres) and are also important for mitotic progression as they recruit the mitotic kinases Plk [1] and Aurora A [2]. The minus ends of the microtubules are nucleated from the spindle poles and the plus ends of the microtubules grow towards the chromosomes, which progress to the equator of the cell. The kinetochores at the centromere of each chromosome function as the attachment site for microtubules from each spindle pole, to form bipolar attachments (Figure 1-2). Kinetochores are conserved multiprotein complexes and they support the spindle microtubule anchoring by nucleating short microtubule stubs themselves [3,4]. Only end-on, balanced microtubule attachments stabilise each sister kinetochore to its respective pole. Incorrect attachments are labile and become disattached through the activity of Aurora B [5–9]. At metaphase, all chromosomes align at an equatorial plan and in some species oscillate due to fluctuations in the balance of microtubule tension (Figure 1-2). During anaphase, the sister chromatids are separated by separase protease that cleaves cohesin at the kinetochores (Figure 1-2) [10], and the separated sister chromatids segregate to opposite cell poles as a result of depolymerisation of the plus-ends of microtubules and the acting of minus-end directed motors. A surveillance mechanism, the ‘Spindle Assembly Checkpoint’ (SAC), functions at kinetochores to prevent the separation of any sister chromatids until all kinetochores are attached to microtubules and the chromosomes are perfectly aligned at the metaphase plate [11]. The cell poles move further apart in anaphase B as a result of the sliding of overlapping spindle pole microtubules of opposite polarity. The spindle reorganises in late anaphase and the resulting ‘central spindle’ participates in organising the cleavage furrow that enables cell membranes to form between the telophase nuclei. Cytokinesis divides the cell into two identical daughters.

The interphase that follows mitosis is separated into three events, G_1-phase, S-phase and G_2-phase. Cells can enter an additional state in G_1-phase, the dormancy or G_0-phase, when they do not progress to S-phase due to unfavourable conditions such as limiting growth factors or lack of nutrients. Otherwise, G_1-phase is the main phase of cell growth and the time at which centrosome duplication begins. Chromosomal DNA is regulated during S-phase, and the subsequent G_2-phase is characterised by final cell growth and the completion of centrosome duplication.

The centrosome comprises of a pair of centrioles (mother and daughter) surrounded by PCM (pericentriolar material). In addition to their mitotic function as MTOCs to organise the formation of the bipolar spindle, the mother centriole at their core can template formation of cilia and flagella.

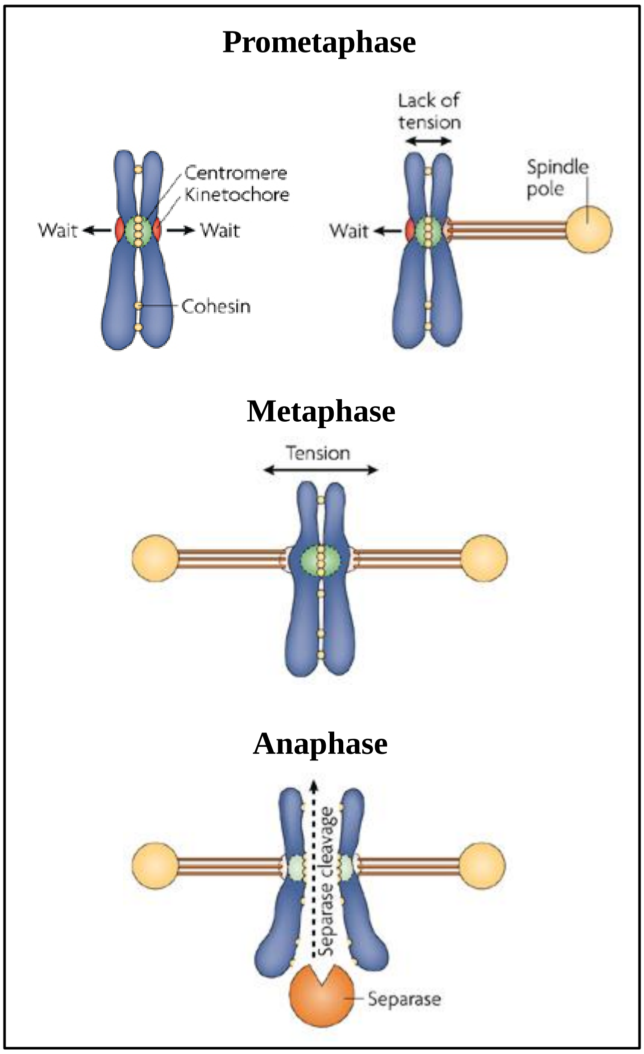

Figure 1-2 Attachment of microtubules to the kinetochores and subsequent sister chromatid separation. In prometaphase the spindle microtubules attach to the kinetochores of the centromeres, leading to bipolar attachment. The chromosomes oscillate, align at the central metaphase plate and the attached spindle microtubules cause tension at the centromere. Activated separase then cleaves the sister chromatids at anaphase and they are pulled to opposite poles. Figure reproduced with modifications and permission from [11].

1.2 The Centrosome and cell cycle

In the late 19th century, Van Beneden and Theodor Boveri described two dots within the spindle poles that Boveri named the centrosome. But only in the mid 20th century did electron microscopy reveal the organisation of centrioles at their core [12,13]. In a little more than a decade, we have begun to understand the assembly and function of centrioles and centrosomes at the molecular level.

Centrioles are present in eukaryotic species which form cilia and flagella but not in higher plants and higher fungi, which do not form these structures. Centrosomes participate in many cellular and developmental processes, including cell polarity, cell motility and cell division. To form a cilium or flagellum, the mother centriole of a centriole pair converts into the basal body at the cell membrane in the G_0 phase of the cell cycle. The basal body then assembles cilia and flagella which function in signal transduction and cell motility. Many diseases are linked to structural, functional and numerical abnormal centrioles, including ciliopathies and cancer.

The duplication cycle of centrioles is generalised in Figure 1-3. This process begins at the G_1- to S-phase transition when one new daughter centriole (procentriole) begins to form orthogonally at the proximal end of each of the two linked mother centrioles; progresses through S-phase and into G_2-phase where the daughter centrioles elongate to their full size. At this point the only physical difference between mother and daughter centrioles are distal and subdistal appendages at the mother centrioles. At entry into mitosis, the linker between the two mother centrioles dissociates, the mother centrioles recruit PCM, and the two centrosomes separate and migrate to opposite sides of the nucleus where they will function as MTOCs. Each centrosome consists of a mother-daughter pair of centrioles with PCM recruited to surround the mother and each centrosome forms one spindle pole of the mitotic spindle. As mitosis progresses, the daughter centriole becomes licensed to recruit PCM in the next cycle. After mitosis, each of the two resulting daughter cells receives one centriole pair that consist of a mother and daughter centriole that separate but remain connected by a protein linker.

The coupling of centrosome duplication and the cell cycle is a major regulating mechanism. But each can occur independently, for example Aphidicolin blocks α-DNA polymerase and therefore DNA replication but centrosome duplication remains unperturbed in many cell types.

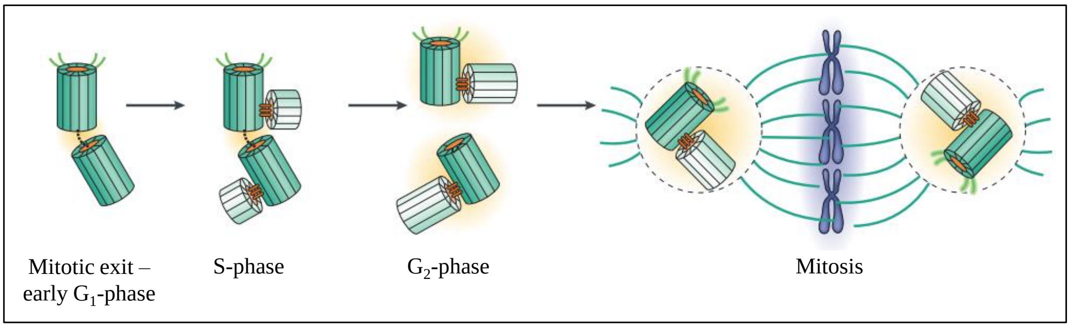

Figure 1-3 Centriole duplication. After mitotic exit two centrioles are loosely linked by a protein linker. At the G_1/S-phase transition, each of the centrioles functions as a mother centriole and procentriole formation is initiated at their proximal ends. The daughter centriole assembly continues throughout S-phase until it reaches its full length in G_2-phase. The mother centriole then recruits pericentriolar material and the two centrosomes separate by the removal of the protein linker. Each of the centrosomes then migrates to opposite sites of the nucleus where they function as MTOCs and generate the mitotic spindle. Figure reproduced with modifications and permission from [14].

1.3 Centriole structure and cartwheel

The process of centriole duplication is tightly regulated and linked to cell cycle progression to guarantee correct centriole numbers. The initial step in centriole duplication is the formation of the procentriole at one single site on the proximal end of the mother centriole. The hierarchy of protein recruitment to form the daughter centriole was first described in *C. elegans* and extensive RNA interference (RNAi) and genetic screens identified five proteins as essential for centriole duplication; Spd2 (spindle defective 2), the Serine/Threonine kinase Zyg-1 (zygotic defective: embryonic lethal 1), Sas6 (spindle assembly abnormal 6), Sas5 and Sas4 (spindle assembly abnormal 5 and 4 respectively) [15–23]. Table 1-1 shows the homologues of *C. elegans* in *Drosophila* and *Homo sapiens*. Their sequential recruitment was analysed by electron tomography of staged *C. elegans* one-cell embryos. This revealed firstly, the formation and elongation of a central tube and secondly, the assembly of nine singlet microtubules during daughter centriole formation. The pathway of centriole formation is believed to be conserved between species and in *C. elegans* it requires the coiled-coil protein Spd2 to recruit the protein kinase Zyg-1, followed by recruitment of the Sas6-Sas5-protein-complex as prerequisite for procentriole assembly, and Sas4 recruitment for microtubules assemble onto the central tube.

In this section I will discuss what we know of the structure of these proteins or their orthologues in *C. elegans* and other organisms. I will return to what we know of their role in centriole duplication in section 1.4.

Table 1-1 Homologues of centriole duplication proteins of *C. elegans*, *Drosophila* and *Homo sapiens*.

Homologues		
C. elegans	*Drosophila*	*Homo sapiens*
Spd2	-	Cep192
Zyg-1	Plk4	Plk4
-	Asterless	Cep152
Sas6	Sas6	Sas6
Sas5	Ana2	STIL
Sas4	Sas4	CPAP
-	Bld10	Cep135

The microscopy techniques, especially in the area of super-resolution, have advanced in the recent years, and in *Drosophila*, it is now possible to view the centriole as a cylinder which can be differentiated into five different regions and into which different centriole duplication proteins have been localised (Figure 1-4) [24–30].

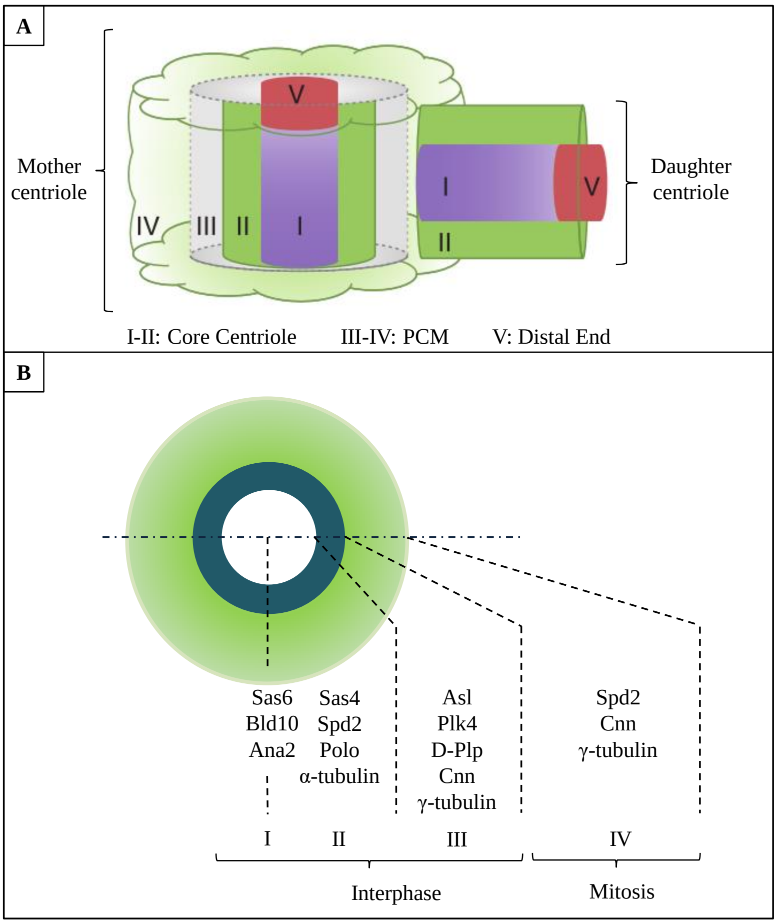

Figure 1-4 The division of *Drosophila* centrosome into five zones. (A) The schemata shows the mother and daughter centriole and PCM. Zones I-II represent the core centriole; zone III-IV represent the PCM and zone V represents the distal end. Figure reproduced with modifications and permission from [24]. (B) Schematic proximal view of a centriole; indicating the localisation of the named proteins at each zone during interphase and mitosis.

Centrioles are characterised by a precise 9-fold symmetry evident in the central cartwheel and in the organisation of its microtubules [31–33]. The cartwheel is believed to represent a conserved building mechanism. The cartwheel appears first during procentriole formation at the proximal end of the centriole. It consists of an inner hub from which nine spokes radiate outwards, which then each connect to an A-microtubule (Figure 1-5). These microtubules are stable due to tubulin modifications (e.g. tubulin glutamylation) [34] and comprise of triplets in most species but in *Drosophila* and *C. elegans*, duplets or singlets respectively predominate. Each A-microtubule is comprised of 13 α- and β-tubulin-containing protofilaments, followed by anti-clockwise assembly of the B- and C-microtubules of which each comprises 10 α- and β-tubulin-containing protofilaments [35–37]. Each of the partial microtubules forms a complete tubule by sharing 3 protofilaments with the preceding microtubule and each A-microtubule links with the neighbouring spoke's microtubule, to form the outer cylindrical ring of the centriole. The centriole microtubules show polarity, with the minus ends located at the proximal end of the centriole, which coincides with the site of cartwheel assembly. Sas4 protein is necessary for polymerisation of centriolar microtubules and it localises to the microtubules wall [24]. Overexpression of the human homologue of Sas4, CPAP, causes centriole elongation [38–40]; Sas4/CPAP also interacts with STIL and Cep135 [41–44] but the function of these interactions are still unknown. Additionally, γ-tubulin is necessary for the assembly of microtubules. It is part of the γ-tubulin ring complex and localises to the minus end microtubules of the A-microtubules [45–49].

Mother centrioles carry appendages at their distal end (Figure 1-5 B and C). The subdistal appendages function in anchoring of the minus ends of the cytoplasmic microtubules to organise radial arrays of microtubules. And the distal appendages function in anchoring the basal body to the cell membrane during ciliogenesis. Once the daughter centriole has passed through mitosis it will mature into a mother centriole and also carry these appendages [50].

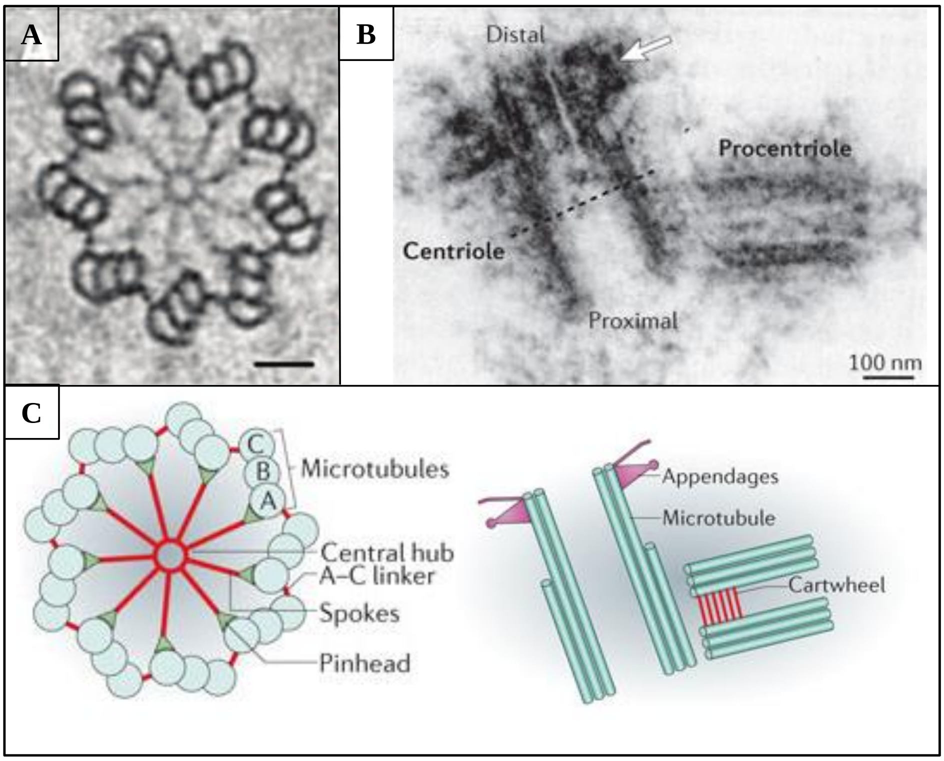

Figure 1-5 Centriole and cartwheel structure. (A) Ultrastructure of a cross-section of the proximal end of a *Trichonympha* reveals the cartwheel. At the central hub there are nine radiating spokes, which join the microtubules triplets. (B) Ultrastructure of a human centriole and procentriole; arrow indicates the distal and subdistal appendages next to the mother centriole. (C) Schemata of A and B. Additionally indicating the pinhead structures connecting the cartwheel spokes with the A-microtubules, which are in turn connected to the B-microtubules, and to the C-microtubules (left); the A-C-microtubules-linker (left); and the stack of cartwheels (right). Figures reproduced with modifications and permission; (A) from [51]; (B) and (C) from [52].

During procentriole formation, stacks of cartwheel form in the proximal part of the centriole, which vary in size between species, e.g. in *Drosophila* sperm, basal bodies are 2.5µm long whereas *C. elegans* centrioles are 150nm [53]. Mammalian centrioles lose their cartwheels during mitosis [37,54,55]. The *Trichonympha* centriole on the other hand is formed of many hundred cartwheels in approximately 90% of its centriole length [56]. This proves ideal for structural studies by cryo-electron tomography [36,51]. These reveal that neighbouring spokes of the cartwheel layers merge 20nm from the hub and end in a pinhead structure, which consist of the pinbody and two pinfeet that connect it to the A-microtubules (Figure 1-6) [36].

The vertical distance between the merged spokes is 17nm, that correlates with the size of two tubulin dimers.

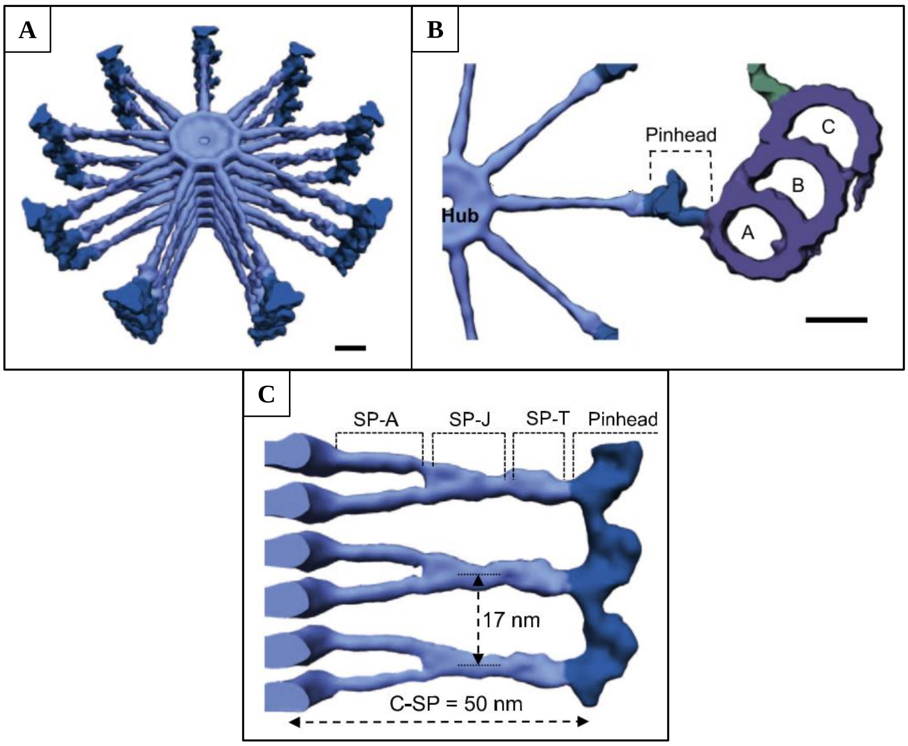

Figure 1-6 Characteristics of the proximal centriole region and cartwheel stack. (A) 3D representation of *Trichonympha* cartwheel stack showing the individual layers which show the central hub and nine radiating spokes each, which end in the pinhead structure. (B) 3D representation of the *Chlamydomonas* cartwheel-pinhead-microtubules triplet. (C) Longitudinal section of the cartwheel spokes (C-SP), which comprise of the spoke arm (SP-A), the spoke junction (SP-J), and the spoke tip (SP-T); connecting to the pinhead (partially indicated). Figure reproduced with modifications and permission from [36].

Despite the structural knowledge of the cartwheel and the microtubules the basis for the 9-fold symmetry is still unknown. In most organisms, the cartwheel appears before microtubule assembly [57–60] but *C. elegans* centrioles adopt 9-fold symmetry in the absence of any cartwheel structure [53]. Moreover, in *Paramecium*, the circular microtubules become arranged before cartwheel formation in basal bodies [61]. That the cartwheel contributes to the 9-fold structure has been demonstrated by multiple mutants that show structural defects. Also a

Chlamydomonas null-mutant in Bld10p, which encodes a Sas6-interacting protein, lacks centriolar microtubules [62] and a truncated Bld10p mutant leads to cartwheels with nine shorter spokes that recruit only eight microtubules due to reduced circumference based on shorter cartwheel spokes [62,63]. On the other hand, depletion of its respective homologue in *Drosophila* and human, Bld10 and Cep135 respectively, still permits centriole formation but they appear unstable [32,64–66]. This suggests that Bld10p/Bld10/Cep135 localis to the distal part of the cartwheel spokes and might function in extending the cartwheel to its full length and/or in stabilising the connection between cartwheel and microtubules [65,67]. This is supported by the observations that Bld10p/Cep135's N-terminus interacts with microtubules in human cells [43,68]; and that Bld10p/Cep135 C-terminus interacts with the cartwheel protein Sas6 [43,63].

Additionally the cartwheel protein Sas6 is required for the 9-fold symmetry of centrioles in zebrafish, human cells, *Drosophila*, *C. elegans* and *C. reinhardtii* [63,69–71]. A null-mutant of the homologue bld12 in *Chlamydomonas* causes loss of the central hub and cartwheel spokes [70]; and a mutant leads to 20% of cells with circular centrioles of which 30% have abnormal numbers of microtubules ranging between seven to 11 triplets [71]. Similar findings were made in *Drosophila*. Thus, bld10p/Bld10/Cep135 and bld12/Sas6 all contribute to the 9-fold symmetry of the centriole [54,72,73].

Structurally, Sas6 is characterised by a N-terminal head domain with a PISA motif (present in Sas6; region of homology), a coiled-coil domain and a small, poorly conserved and unstructured C-terminal domain [72]. The protein forms parallel homodimers via its coiled-coil domains, which exhibit a coiled-coil rod with two N-terminal globular domains, with the latter being positioned next to each other but in mirror image position (Figure 1-8). Each N-terminal head of the dimer weakly interacts via hydrophobic bonds with an N-terminal head of another Sas6 dimer, leading to the assembly of nine Sas6 dimers to the inner hub/ring like structure with the nine homodimerised coiled-coil domains of the protein radiating out (Figure 1-8). Its structure has been elucidated for *C. elegans*, *C. reinhardtii*, *Chlamydomonas* and zebrafish using X-ray crystallography, analytical gel-filtration, and *in silico* structural modelling [63,69,74,75]. In solution, Sas6 molecules are able to oligomerise and form ring like structures similar to the cartwheel hub [63,69]. This gives important insight into the nature of the 9-fold symmetry of centrioles. It predicts a 42° angle between the homodimers and a ring of 23nm diameter, which is close to the expected 40° angle from a 9-fold radially symmetry cartwheel and the observed 20-25nm diameter observed for the central hub by electron microscopy [60,69,76], with the model for Sas6 *C. reinhardtii* in Figure 1-7. On the other hand, *C. elegans* exhibits a tube like structure rather than a cartwheel [53] and X-ray crystallography shows that its Sas6 dimerise to a right-handed helical filament with 9-fold radial symmetry, leading to the tube rather than cartwheel formation (Figure 1-9) [77,78]. Just like the cartwheel, the tube can function as a scaffold for microtubule assembly. It was also suggested that two Sas6-spirals might be intertwined to form the central tube in *C. elegans* (Figure 1-9 C and D) [78]. The ability of Sas6 to self-assemble might explain why some centrioles can form *de novo*. But it also suggests there must be a tightly regulated process for Sas6 oligomerisation to prevent spontaneous cartwheel assembly. Therefore, Sas6 is the likely candidate to establish the universal 9-fold symmetry of centrioles.

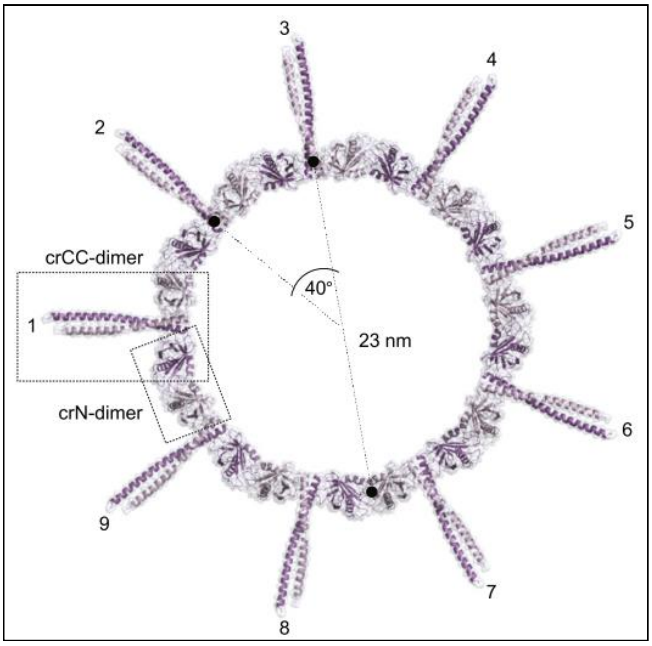

Figure 1-7 Bld12p (Sas6 homologue) oligomer model of *C. reinhardtii*. Organisation of nine coiled-coil homodimers according to their interacting N-terminal domains leads to a 9-fold symmetric cartwheel ring, exhibiting a diameter of 23nm, with nine radiating spokes. Figure reproduced with modifications from [69].

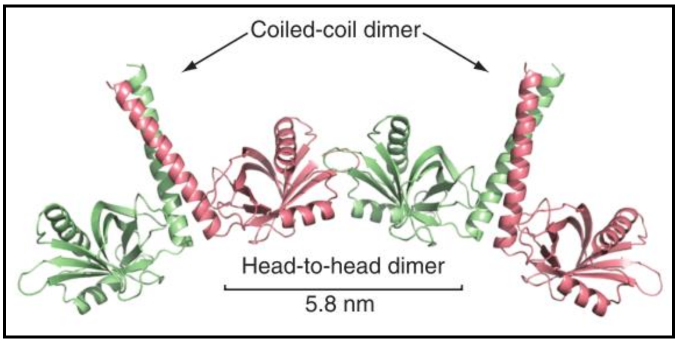

Figure 1-8 3D model of a Sas6 ring assembly. Sas6 dimers form by homodimerisation of their coiled-coil domains. Nine homodimers interact weakly via their N-terminal head domains and form the 9-fold symmetry of the centriolar cartwheel. Figure reproduced with modifications and permission from [63].

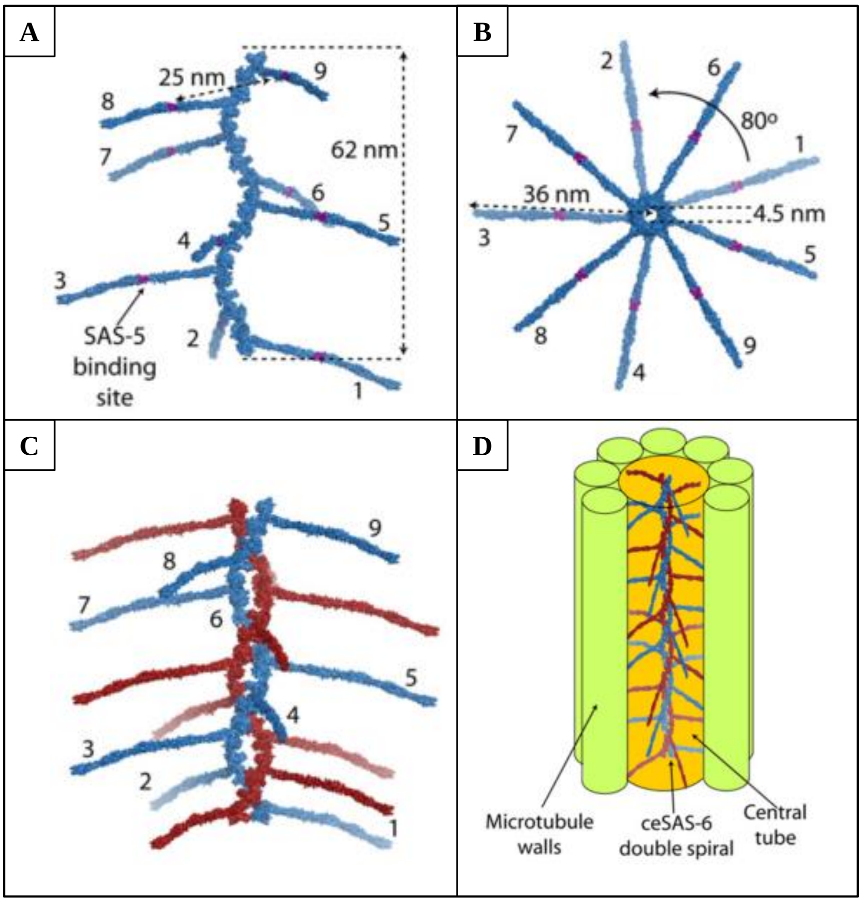

Figure 1-9 Sas6 forms a spiral in *C. elegans* which provides the basis for the 9-fold symmetry of the centriole. (A and B) Model of a single Sas6 spiral with nine homodimers (numbered, orthogonally viewed). (C) Model of two Sas6 spirals intertwined. (D) Centrosomal model of *C. elegans* containing the Sas6 double spiral, of which four turns account for the central tube. Original figure reproduced from [78].

Zone 5 of the centriole was described as a distal ‘cap’ to which the centriolar proteins CP110 and Cep97 localise and function in the regulation of centriole length [39,79,80]. The two proteins are co-ordinately recruited with Cep97 being required to stabilise CP110 at the centriole [81]. The loss or depletion of CP110 from human cell culture leads to elongated centriole microtubules [39]. In contrast, the depletion of CP110 in *Drosophila* cells leads to shortened centriolar microtubule apparently as a result of the ‘exposure’ of the centriole to Klp10A, a depolymerizing kinesin-like protein [82].

1.4 Centriole duplication and its proteins Plk4, Sas6 and Ana2

1.4.1 Plk4

Plk4 is the conserved master kinase of centriole duplication [73,83–85]. Its counterpart in *C. elegans* is Zyg-1 which, although more divergent, has the distinct domains of all other Plk4 kinases [86]. *Drosophila* Plk4 is structurally similar to other members of the polo-like kinase family but there are some significant differences; all Plks carry an N-terminal catalytic domain but Plk4’s C-terminal part contains three Polo box (PB) motifs compared to the two PBs in other family members (Figure 1-10) [87]. The polo-box motifs function to direct protein interactions, intracellular targeting, substrate binding, dimerization and auto-inhibition of kinase activity [1,86,88–90].

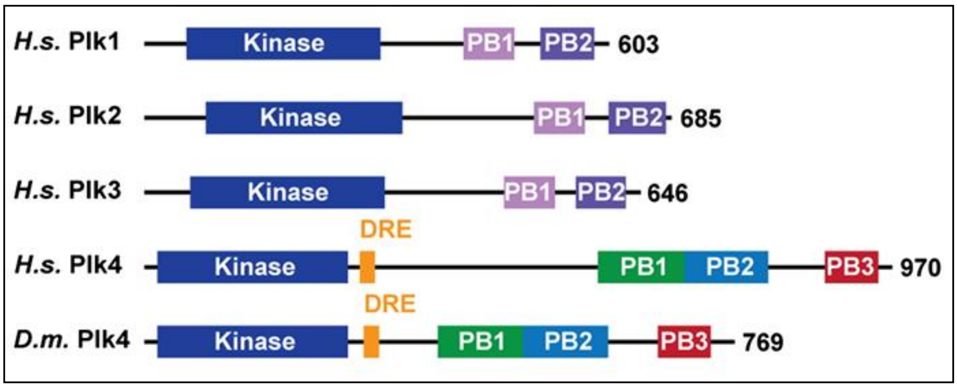

Figure 1-10 Polo-like kinase family and their domains of *Homo sapiens* and *Drosophila*. All kinases contain an N-terminal kinase domain. Plk1-3 contain two Polo box domains. But Plk4 is characterised by three polo boxes (PB) of which PB1 and PB2 function as a cryptic polo box. After homodimer-dependent autophosphorylation of Plk4, SCF$^{\mathrm{Slimb/\beta TrCP}}$ ubiquitin ligase recognises the phosphodegron 'downstream regulatory element' (DRE), leading to degradation (see Figure 1-11). Figure reproduced with modifications and permission from [87].

The localisation of Zyg-1/Plk4 to the site of centriole duplication requires Spd2 in *C. elegans* [53,91], Asterless in *Drosophila* [92] and the homologues of both proteins, Cep192 and Cep152 respectively, in mammalian cells [93,94]. Plk4 localises around the whole circumference of zone 3 of the centriole in G1 but becomes focused at a single site at the initiation of duplication [95]. This cannot be explained by its interaction with Cep192/Spd2 and Cep152/Asterless, as both localise around the entire centriole following the completion of centriole to centrosome conversion. How Plk4 becomes localised at a single site is not clear. The important role of Plk4 in centriole duplication is reflected by loss of centrioles after depletion of Plk4, and by the over-amplification of centrioles in many cell types and species when Plk4 is overexpressed [73,83–85,96,97]. Overexpression can also lead to *de novo* centriole formation in *Drosophila* eggs which lose their centrioles during oogenesis [20]. When Plk4 is overexpressed, multiple sites of centriole duplication are observed on the mother centriole to form a 'centriole rosette' [73,84]. Both, upregulation and downregulation of Plk4 have been associated with tumorigenesis [99–101].

The regulation of Plk4's activity for centriole duplication requires transcriptional control, localisation, regulated degradation and auto-inhibition of the kinase activity (Figure 1-11) [1,90,102–106]. A major mode of regulation of Plk4 appears to be through autoinhibition, achieved through homodimerisation of polo-box 1 and polo-box 2 (cryptic polo box; Figure 1-11 A and B) [87]. Homodimerisation itself or the recruitment of an unknown binding partner of PB3 to move the linker 1 (L1) away from the kinase's activation loop allows for auto-phosphorylation of a phosphodegron [104,107–109] (Figure 1-11C). This permitts for binding of the ubiquitin ligase complex SCF$^{Slimb/\beta TrCP}$ [103–105,107,110,111] (Figure 1-11D) and initiates Plk4 self-destruction by targeting it to the proteasome (Figure 1-11E) [103,105,108,109,112]. Although we have this outline of this aspect of Plk4 regulation, we still have much more to learn to fully understand how it controls centriole duplication.

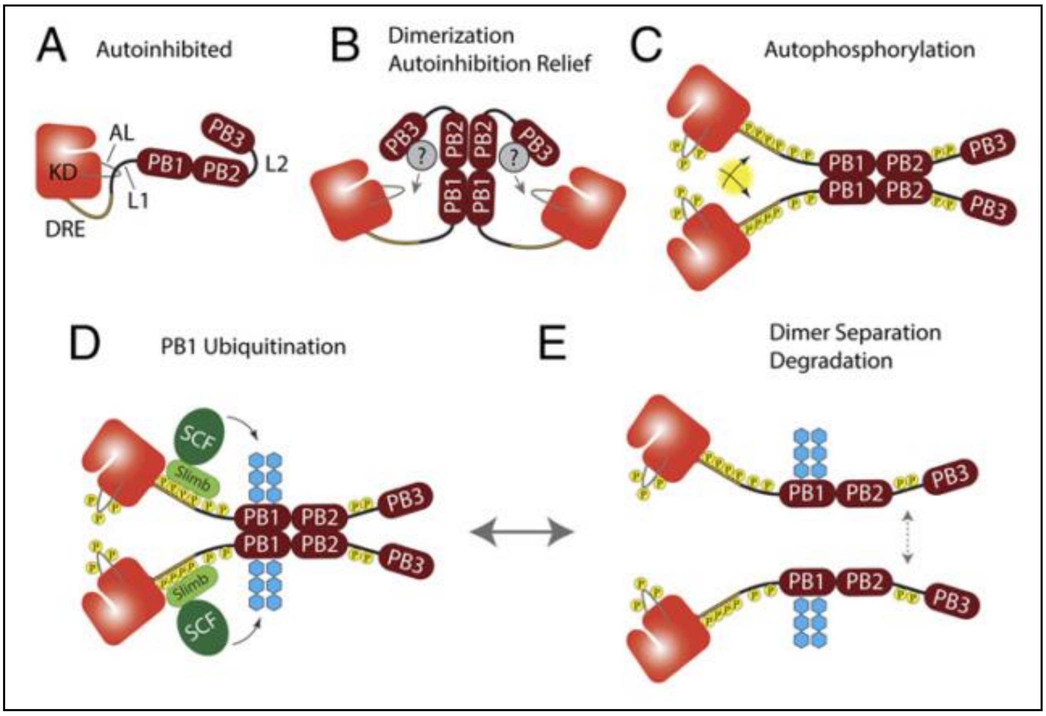

Figure 1-11 Speculative model for activation and regulation of Plk4. (A) Plk4 is autoinhibited by a link of Linker 1 (L1) and Activation loop (AL), which allows for homodimerisation by Polo Box 1 and 2 (PB1, PB2). (B) In the homodimerised stage, a binding partner of PB3 moves L1 away from AL which leads to autoinhibition relief. (C) This allows for autophosphorylation of Plk4. (D) Followed by SCF$^{Slimb/\beta TrCP}$ recruitment and ubiquitination of PB1. (E) And separation of the dimers. Original figure reproduced from [106].

1.4.2 Sas6

The recruitment of Sas6 to the procentriole in human cells is independent of Plk4. However its maintenance at the procentriole depends upon Plk4. This is similar to the relationship between Sas6 and Zyg-1 in *C. elegans,* where recruitment of Sas6 is directly regulated by Zyg-1 but is independent of Zyg-1 kinase activity [15,91], whereas the Zyg-1-phosphorylation of Sas6 at Ser123 is suggested for Sas6 maintenance [54,113]. However, this residue is not conserved in other species. Also, the recruitment hierarchy of human Sas6 and CPAP corresponds to that of Sas6 and Sas4 in *C. elegans*; HsSas6 depletion prevents the recruitment of CPAP whereas HsSas6 is still recruited after CPAP depletion, suggesting Sas6 is recruited upstream of CPAP/Sas4. Some species-specific differences are also seen from overexpression experiments. Overexpression of non-degradable HsSas6 causes amplification of centrioles whereas overexpression of DmSas6 in syncytial embryos leads to *de novo* formation of MTOCs that lack centrioles at their core [71]. However, when *Drosophila* Sas6 and Ana2 are co-expressed, they assemble into extended tubes that interact with proximal ends of centrioles and bear structural resemblance to the inner cartwheel of centrioles, when also co-overexpressed with Plk4 [114]. This suggests, that *Drosophila* Sas6 and Ana2 together drive cartwheel formation of centrioles, in a Plk4 dependent manner.

It is of great interest to know how the basic ring of Sas6 homodimers is stabilized to promote formation of a mature centriole. Two mechanisms have been proposed for regulating HsSas6 protein levels. First, that Sas6 is targeted for degradation by APC/C^{Cdh1} through its C-terminal KEN-box [54,115]. This keeps Sas6 levels low and could limit the number of procentrioles per mother centriole to one. Second, that SCF targets Sas6 for degradation by ubiquitination via Fbxw5 (Fbox protein) [115]. Fbxw5 on the other hand is regulated by degradation by the APC/C in mitosis before it accumulates at G_1/S-phase. Plk4 phosphorylates Fbxw5 which then suppresses the ubiquitination and consequently full degradation of Sas6 in S-phase [115]. This linkage would guarantee a timely increase and decrease of Sas6 protein levels to control centriole assembly. But there is still little structural information on how the mother centriole recruits Sas6 to a single site of procentriole formation and how the nascent cartwheel and centriole are linked to the mother centriole.

1.4.3 Ana2

It has been suggested that *Drosophila* Ana2 and human STIL are homologues of *C. elegans* Sas5, despite their limited sequence homology. Significantly, there is an approximately 20aa coiled-coil domain in the central part of each protein together with a conserved STAN motif in the C-terminus. The STAN motif is a region off approximately 90aa that exhibits 31% sequence identity between Ana2 and STIL and is even more distantly related to Sas5 [116]. Finally there is a conserved TIM (truncated in microcephaly) motif at the very C-termial end of Ana2, STIL and Sas5 that has been identified [117]. In human cells, STIL exhibits an asymmetric localisation to the daughter centriole and is essential for procentriole formation. In cultured human cells Sas6 is thought essential for STIL recruitment [41,117]. However there it is uncertain whether reciprocally STIL supports the recruitment of HsSas6 to centrioles [41,117,118]. This is in contrast to *C. elegans*, where Sas5 and Sas6 protein localisation is co-dependent [72]. Additionally, when Sas6 and/or Sas5/Ana2/STIL are overexpressed, it leads to over-amplification of centrioles, which is similar to Plk4 overexpression, which causes over-amplification and *de novo* formation (in unfertilized eggs) of centrioles [41,54,72,117–119]. In *Drosophila* spermatocytes, co-overexpression of Sas6 and Ana2 leads to the assembly of cartwheel-like structures [114]. Recently, it was suggested that the Ana2-Sas6 complex could function as the so far poorly understood linker between the procentriole and mother centriole, which retains the linkage between the two centrioles until their disengagement late in cell division [114]. STIL is recruited to the proximal end of the mother centriole after the G_1-S phase transition, where its signal increases gradually and reaches its maximum at the poles of pro- and prometaphase cells. This is followed by degrease in intensity from the metaphase-to-anaphase transition onwards until it appears absent in late anaphase and telophase cells [117]. A similar path of regulation to the one described above for Sas6 is claimed for STIL. The $APC/C^{Cdc20–Cdh1}$ brings about dependent proteasomal degradation of

STIL after the metaphase-anaphase transition, with Cdc20 being the major APC/C adaptor and the C-terminal Ana2 KEN box being recognised by APC/C at the end of mitosis [117]. Interestingly, the KEN box was observed to be lost in MCPH mutants of STIL, leading to accumulation of STIL protein in the cytoplasm and resulting in centriole amplification rather than interference with STIL function [120]. The degradation of STIL is initiated by its re-localisation from the centriole to the cytoplasm at nuclear envelope breakdown, dependent on Cdk1 (cyclin-dependent kinase 1) [117,120]. The mother and daughter centriole linkage also provides a physical input for regulating STIL levels, whereas their disengagement at the end of mitosis licenses them for reduplication in the next cell cycle [121,122]. It was shown that over-expressed STIL localises as a ring around the proximal end of the mother centriole and causes the near-simultaneous formation of multiple daughter centrioles, which co-localise with Sas6 [117]. This observation supports the theory that STIL and Sas6 function together in centriole duplication in human cells, just as do Sas5 and Sas6 in *C. elegans*. Therefore, it was the more surprising that it has not been possible to detect stable STIL-Sas6-complexes. On the other hand, depletion of STIL by siRNA has a negative effect and suppresses centriole duplication [41,117] but it did not affect the localisation of Plk4 nor Cep152 to the centrioles. By contrast, Plk4 depletion disrupts STIL localisation to the centriole [41]. This suggests that STIL is recruited to the daughter centriole downstream of Cep152 and Plk4. Indeed, STIL recruitment to the centriole was shown to depend on the interaction of its central coiled-coil domain with Plk4 [95,123]. Structurally, it has been shown that Ana2 and Sas6 both form homo-oligomers, and that the central coiled-coil domain of Ana2 is necessary to form a tetramer with an unusual parallel-coil topology, which occurs also but more weakly with STIL [124]. An Ana2 mutant that cannot tetramerise *in vitro* lacks ability for efficient centriole duplication *in vivo* but still allows for the formation of some centrosome like structures which can concentrate at spindle poles [124]. Controversially, an Ana2 tetramer was also observed but requiring dynein light chain (LC8) [125]. This led to the suggestion that the previously mentioned central coiled-coil domain of Ana2 might lead to the Ana2 tetramer formation and that the Ana2-LC8 interaction might rather be important for spindle orientation. Our knowledge of Ana2, its precise role in centriole duplication, and its interaction with other centriole duplication proteins is still very limited and requires further study.

1.5 Centriole maturation and PCM recruitment

The process of daughter centriole assembly to the mother centriole is followed by maturation of the centriole to centrosome conversion for which the mother centriole recruits PCM material. The PCM serves multiple functions: it is the site of microtubule nucleation from tubulin subunits [126], it organises the formation and anchors the mitotic spindle, and it is important for the accumulation of cell cycle regulators [14]. In the past it was believed that the PCM is an amorphous unstructured cloud of proteins surrounding the centriole but more advanced microscopy techniques in recent years, especially super-resolution microscopy, has started to elucidate that the PCM is a highly ordered layer system with hierarchical protein recruitment [24,26,28,127,128]. Many proteins of the PCM have been identified from purified centrosomes and RNAi and localisation screens in *C. elegans* [129], *Drosophila* [130,131] and human cells [132,133]. The molecular interactions of PCM components with each other begin to be uncovered but further study is necessary to understand their complex interacting network at the centriole, how the PCM is regulated and how it functions.

Asterless, which localises to zone III of the centriole, was suggested as a PCM recruiting protein[134], as it links the centriole with the PCM by direct interaction with Sas4 (zone II) [92] and as it is necessary for Cnn recruitment (zone IV) [135,136]. Sas4 also has PCM functions, as Sas4 null-mutant flies show reduced levels of PCM in testes [137,138]. But how the PCM expands to zone IV of the centrosome is still unknown. A possible regulator is Polo kinase whose inhibition prevents γ-tubulin assembly, phosphorylation of Cnn and Pericentrin (zone IV) and PCM expansion [131,139–141]. Additionally, Plk1 maintains the PCM at the centrosome throughout mitosis [142]. Aurora A, which assembles microtubule-nucleating complexes and proteins such as γ-tubulin [143,144], activates Plk1 in conjunction with Bora [145,146].

How the PCM and its proteins are dissociated from the centrosome after mitosis is not fully known. It is suggested that dephosphorylation plays an important part. Inhibition of Polo kinase activity leads to the removal of Pericentrin and γ-tubulin in human centrosomes [142]. Candidate phosphatases that might mediate this are protein phosphatase 4 (PPH4)[147–149] and/or protein phosphatase 2A (PP2A) [150,151]. Alternatively, PCM proteins could be removed from the centrioles by 'flaring', which is observed in telophase and interphase of *C. elegans* and *Drosophila* embryos [137,152–154].

1.6 Centriole disengagement

Once the cell has gone through mitosis and the mitotic spindle and the centrosomal PCM are disassembled, the two centrioles disengage by loosening their orthogonal connection but they remain connected by a linker. How this process is regulated still remains unknown but it licences the daughter centriole for duplication in the next cell cycle [122,155]. It is suggested that Plk1 and separase regulate the disengagement [156]. Plk1 is suggested to activate separase which in turn loosens cohesion at the centrioles and leads to disengagement [122,156–160]. Supporting this suggestion is the finding that overexpression of Plk1 leads to centriole disengagement in G_2-phase. Cohesion cleavage by Plk1 dependent separase activity also occurs earlier during the metaphase to anaphase transition at the sister chromatids. However a mechanism that would regulate dissociation of two different targets at two different time points has not been found [157,161–164]. Pericentrin has been suggested to be the separase substrate permitting disengagement as it gets cleaved at the meta-/anaphase transition but remains at the centrosome until anaphase [165].

After disengagement, the two centrioles remain linked and both function as mothers in the following cell cycle when new daughter centrioles are assembled. The details about the linker are still emerging but dependency studies suggest that C-Nap1 (Nucleosome assembly protein 1) localises and functions as a docking site for rootletin connecting the two centrioles at their proximal ends [166–169]. Bld10 is a candidate for the connection between the linker and the centriole [170]. The eventual separation of the two centrioles at the G_2/M-phase transition is proposed to be triggered by Nek2 phosphorylation of C-Nap1 and rootletin because overexpression of Nek2 leads spontaneous separation of the centrioles and decreased Nek2 levels inhibit separation [167,168,171–174]. Additionally, the motor protein Eg5 might support the linker separation by forcefully pulling the centrosomes apart before it separates them spatially [175].

1.7 The Golgi, GoRab and cilia signalling pathways

Both the centrosome and the Golgi apparatus have microtubule nucleation abilities [176,177]. At the centrosome, microtubule nucleation and anchoring occurs in the PCM and relies on γ-tubulin complexes [178]. Similar multiprotein complexes are also necessary for microtubule nucleation at the *cis*-Golgi. A well organised microtubule cytoskeleton is important for the organisation of the cell and the regulation of cellular processes. In general, the Golgi apparatus of the cell functions in organising secretory pathways, but interestingly, its structure varies depending on the organism (Figure 1-12). In yeast, the Golgi apparatus consists of dispersed cisterns [179]; in green algae, it consists of parallel aligned stacks of cisterns [180]; in fungi, plants and *Drosophila* multiple Golgi stacks are individually scattered in the cytoplasm but always linked to an individual ER exit site [181–183]; and in mammalian cells multiple Golgi stacks are laterally connected to form a ribbon-like structure [184,185], that localises near the centrosome and the nucleus in a manner dependent on centrosomal microtubules [186,187] and dynein [188]. In mammalian cells, the Golgi apparatus undergoes fragmentation in late G_2-phase, and this appears to be necessary for Golgi inheritance and mitotic entry [189,190]. The protein GMAP210 (Golgi microtubules associated protein of 210kDa) has been suggested to anchor the Golgi to the centrosome [191,192]. In *C. elegans*, GMAP210 functions in Golgi organisation and regulation of cilium length [193], reflecting its role as a receptor of the intraflagellar transport protein IFT20 (see also below). It is suggested that GMAP210 and IFT20 function together in the sorting or transport of cargo destined for cilia in mammalian cells [194]. Microtubules originate directly from the Golgi membrane [195] and their nucleation is dependent on PCM and the *cis*-Golgi protein AKAP450 (A-kinase anchor proteins, *Drosophila* homologue Plp), that in turn is recruited by the *cis*-Golgi protein GM130 [196], the *trans*-Golgi CLASPs (cytoplasmic linker-associated proteins) [177], and additional proteins in a multiprotein complex [197,198]. Whereas the precise role of AKAP450 in nucleating microtubules at the Golgi is not understood yet, such microtubules formation is independent of the centrosome [177] and might serve to link and fuse Golgi stacks [199,200]. Coordinated function of the centrosome, Golgi and Golgi microtubules are required in cell polarity and migration [186,196,201].

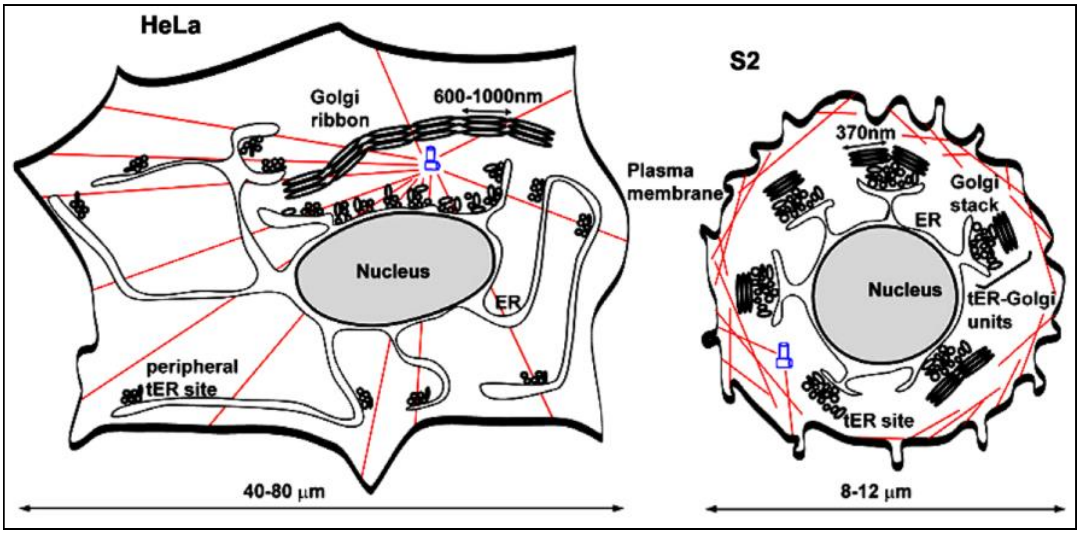

Figure 1-12 Golgi apparatus forms Golgi stacks in *Drosophila* S2 cells and Golgi ribbon in mammalian HeLa cells. The function of the Golgi apparatus for secretory pathways is conserved but it exhibits structural differences. In fungi, plant and *Drosophila*, Golgi stacks are dispersed in the cell but always linked to an ER exit site (example: *Drosophila* S2 cells). The mammalian Golgi apparatus consists of Golgi stacks that are laterally connected and form the Golgi ribbon. At late G_2-phase, the Golgi ribbon gets fractioned into Golgi stacks, which then disassemble for mitosis. Figure reproduced with modifications and permission from [183].

In this study I will focus on the uncharacterised Golgi protein CG33052, which is named Dragon from here onwards. GoRab, also known as SCYL1BP1 (Scyl1 binding partner), is the human counterpart of Dragon and it is highly expressed in skin and osteoblasts. The protein GoRab localises to the Golgi and appears to be an effector of the GTPase Rab6 since it binds the active GTP-bound form of Rab6 [202]. The Golgi apparatus consists of stacked cisternae, through which biosynthetic cargo proteins pass and are modified (Figure 1-13) [203]. It is also the site of synthesis of complex polysaccharides [204–206]. The function of

GoRab at the Golgi is unknown. However, a null mutant of GoRab has been identified in patients exhibiting gerodermia osteodysplastica [202]. A missense mutation resulting in similar phenotypes as the null mutant has also been described [207]. The phenotypes of this autosomal recessive disorder include osteoporosis, spontaneous bone fractures, above average joint dislocations, anomalies in the white matter of the brain but normal mental development. Patients have characteristic facial features with jaw hypoplasia, variable levels of growth retardation and wrinkly skin with severe elastin abnormalities [208–213]. GoRab was previously identified as an interactor with the pseudo protein kinase Scyl1, that is found in association with COPI vesicles and appears to be required for retrograde flow from the Golgi to the ER [214,215]. But the function of their interaction is unknown, particularly as Scyl1 localises to the *cis*-Golgi and GoRab polarises to the *trans*-Golgi-network (TGN) [202,216]. However, depletion of Scyl1 affects Golgi homeostasis which leads to an increased Golgi volume and surface area, decreased order in Golgi structure, and decrease in trafficking of the KDEL (Lysine/ Aspartic acid/ Glutamic acid/ Leucine) receptor by COPI [215]. But the Golgi polarity remains undisturbed. Similarly, the closely related Scyl3 associates with clathrin-coated vesicles [217], which are derivatives of Golgi transport vesicles. However, fibroblasts of patients carrying the GoRab null-mutant do not show any defects in Golgi or changes in the distribution of the Golgi proteins γadaption (a TGN marker), Rab6 (a *trans* Golgi marker) or GM130 (a *cis* Golgi marker) [202]. It is debatable whether GoRab should be classed as a Golgin since although it interacts with Rab6 and Golgi it has a single characteristic C-terminal coiled-coil domain, whereas Golgin proteins typically exhibit poorly structured coiled-coil domains throughout the whole protein. An understanding of the disease resulting from GoRab mutations is desirable, to understand how it leads to the typically ageing-related features on skin and bone, potentially by interfering with functional or secretory pathways [218]. A function of GoRab as a regulator of the MDM2-p53 feedback loop has also been suggested in which case it would function indirectly as a tumour suppressor [219]. GoRab triggers the self-ubiquitination and degradation of MDM2 (mouse double minute gene number 2) and thereby stabilising p53 levels [220–222]. This results in apoptosis, cell growth inhibition and tumour prevention [219].

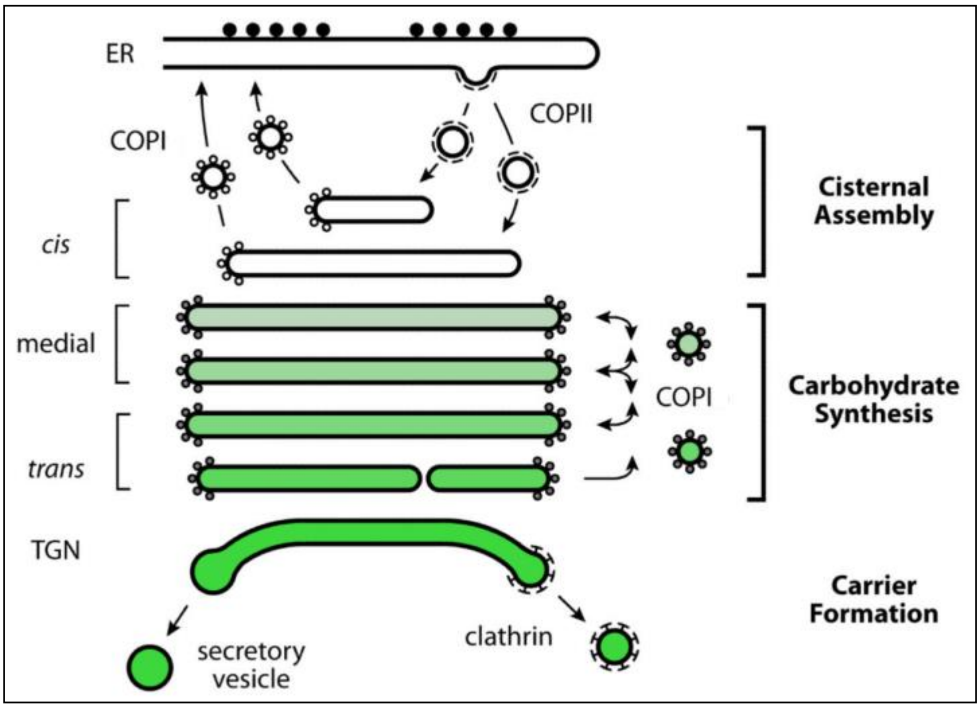

Figure 1-13 The currently proposed model of Golgi compartments and maturation. Structurally, COPI vesicles functions in the carbohydrate synthesis stage by transferring proteins between medial and *trans*-Golgi, as well as protein recycling from the *cis*-Golgi to the ER. COPII vesicles export proteins from the ER and bud into new *cis* Golgi cisterna, during the cisternal assembly stage. And carrier formation occurs at the TGN where cisterna disintegration leads to secretory and clathrin-coated vesicles. Figure reproduced with modifications and permission from [223].

Centrioles function not only at the core of centrosomal MTOCs but also as basal bodies to template cilia. There are two types of cilia, mobile and primary or non-mobile cilia. One obvious difference between the two forms is the composition of their axonemes. These originate from the basal body that is derived from the mother centriole of the cell's centrosome. Motile cilia have 9 peripherally arranged microtubule doublets plus one microtubule pair in their centre, which together with radial spokes and dynein arms enable its motility (9+2) [224]. Primary cilia assemble in G_0-phase and disassemble prior to mitotic entry. They consist only of 9 peripheral microtubule pairs and are missing the central microtubule pair (9+0) [224,225]. Primary cilia play an important part in cell signalling/signalling pathways [226,227] and regulate key processes during embryo development and tissue homeostasis, such as differentiation, re-entry into the cell cycle, cell division and apoptosis. Therefore, defects in the cilia structure or function lead to developmental abnormalities and diseases affecting many organs, known as ciliopathies. These include skeletal defects, blindness, obesity, polycystic kidney disease, retinal degeneration, infertility, Bardet-Biedl syndrome and many more [228–234]. To assemble the primary cilium, the centriole pair migrates to the plasma membrane, allowing the mother centriole to function as the basal body by anchoring itself to the plasma membrane by its distal appendages (Figure 1-14A). This is followed by elongation of the axoneme from the mother centriole on the surface of the plasma membrane. It is also proposed that the mother centriole may also attach with its distal appendages to a nearby Golgi vesicle (Figure 1-14A). The axoneme of the primary cilium grows from the mother centriole then indents the vesicle, which in turn extends with the growing axoneme by budding and fusion with other secondary vesicles, while remaining connected to the appendages/transition fibres. The structure then migrates to the cell surface where the Golgi vesicle fuses to the plasma membrane; and the primary cilium emerges on the cell surface, where it matures to its full length [235,236]. In this second intracellular path of cilia assembly, the primary cilia is partially intracellular and protrudes from the ciliary pocket, that is a membrane invagination. This ciliary pocket is important in membrane trafficking and signalling pathways, and consists of the ciliary membrane, transition fibres (the transformed distal appendages of the mother centriole) and the ciliary necklace (proposed to be the original site of docking to the Golgi vesicle) [237]. Despite being continuous, the ciliary membrane has a denser and distinct composition compared to the plasma membrane [238–241]. It is a complex barrier that restricts the diffusion of proteins between the plasma and the ciliary membrane, and functions in the selection of proteins that can transit into the ciliary membrane and intra-ciliary space from vesicle trafficking [242–244]. The primary cilia does not synthesise proteins itself. Instead, proteins are supplied by vesicles that travel to, dock and fuse with the ciliary membrane [245]. These vesicles are derived from the Golgi [246,247] and carry ciliary specific cargo that is pre-sorted mainly in the *trans*-Golgi network [248]. Their delivery requires specific ciliary targeting signals needed for the sorting and fusion into the primary cilia. The movement of selected cargo in the mammalian primary cilia is organised by intraflagellar transport complexes (IFT) (Figure

1-14B), which are essential for the growth and maintenance of the primary cilia [242]. Proteins are transported by the anterograde path from the primary cilia base, along the microtubules of the axoneme and to the primary cilia tip, and by the retrograde path from the primary cilia tip to the base [249–254]. Transport is mediated by IFT-particles/IFT-trains together with ciliary building complexes, as well as kinesin 2 motor proteins for the anterograde path and cytoplasmic dynein 2 for the retrograde path [255–258]. The primary cilia has highly significant but highly diverse functions in signalling pathways, with one primary cilia being able to have different receptors and channels at the same or at different times. Signalling via primary cilia is used in sensory (Rhodopsin) and in a variety of developmental pathways in vertebrates (Hedgehog and Wingless) in response to, for example, mechanical force, hormones and growth factors [233,259–268]. The abnormal activation or lack of cilia and therefore disrupted cilia signalling is linked to abnormal cell division and cancer [269–281]. In summary, vesicle trafficking and protein sorting dictate the assembly of the primary cilia and participate in their function in development and cell-cycle regulation. This accounts for the pleiotropic phenotypes associated with ciliopathies.

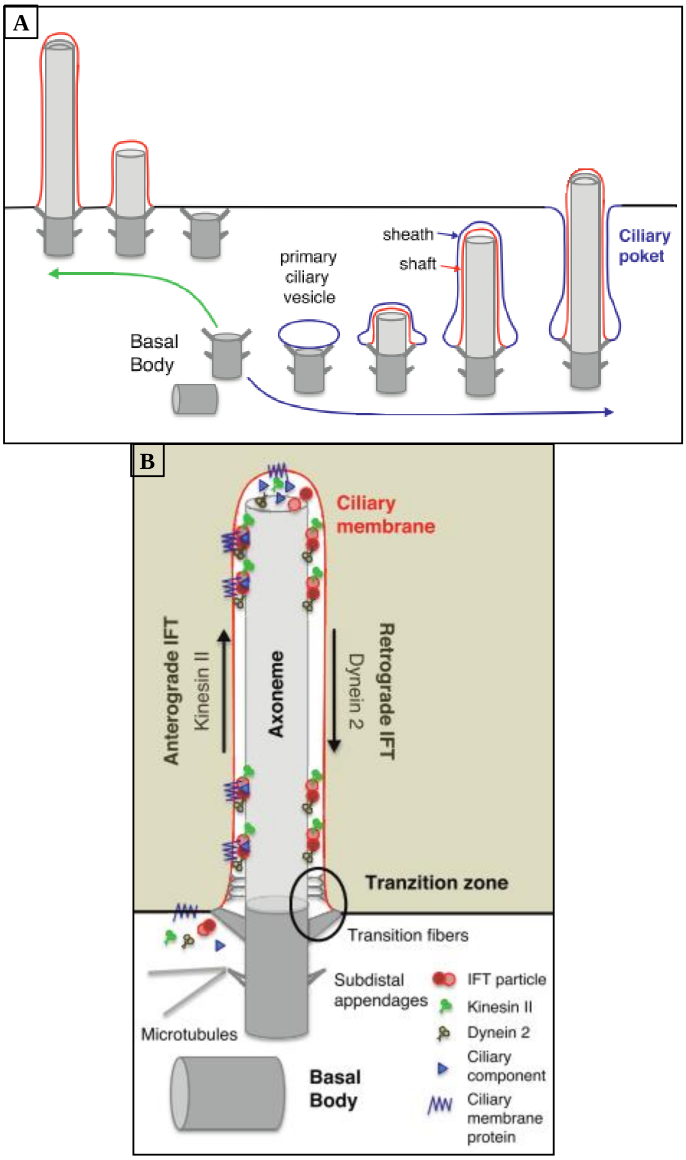

Figure 1-14 Cilia assembly and intraflagellar transport (IFT). (A) The mother centriole of a centriole pair functions as basal body in cilia assembly. Two different pathways are suggested. Firstly, the mother centriole anchors at the plasma membrane and the cilia is assembled from there on the cell surface. Alternatively, a Golgi vesicle is anchored by the distal appendages of the mother centriole in the cytoplasm, followed by the growth of the axoneme and the according growth of the vesicle by vesicle fusion. The growing cilia then migrates to the plasma membrane, where it is exposed to the cell surface by fusion of vesicle and plasma membrane. This creates the ciliary pocket at the cilia base. (B) Golgi vesicles are transported to the cilia, where they fuse with the ciliary membrane and release their cargo for anterograde and retrograde intraflagellar transport (IFT) by IFT particles and ciliary complexes, with the aid of Kinesin II and Dynein 2 respectively. The transition zone contains transition fibres and the ciliary necklace. It restricts protein diffusion from the cytoplasm, and functions as a protein selection barrier to the ciliary membrane and intraciliary space. Figure reproduced with modifications and permission from [245].

1.8 Aims of this thesis

The tight regulation of centriole duplication is important for the maintenance of genomic stability, but only little is known about the molecular regulation of centriole duplication. Therefore the overall goal of this thesis is to further elucidate the protein interactions at the centriole and the mechanisms that govern centriole duplication.

My aim was to identify the physical and functional interactions of the centriole duplication proteins. I approached this by re-analysing and performing *in vivo* protein purifications from cultured *Drosophila* cells and syncytial *Drosophila* embryos; performing a direct *in vitro* protein-protein interaction assay screen; and performing yeast-2-hybrid protein interaction assays to design a centriole protein network of protein-protein interactions in relation to their localisation at the centriole (Chapter 3).

I further aimed to specifically elucidate the interaction of Ana2 and Sas6, as it is known from *C. elegans* that their homologues Sas5 and Sas6 interact with each other and that a Sas5-Sas6-complex is recruited to the procentriole. My objective was to perform *in vitro* interaction studies of Ana2, Sas6 and Plk4, with the latter being the master kinase of centriole duplication. In collaboration with Dr. Dzhindzhev, I showed that Plk4 phosphorylates Ana2 at its STAN motif. Thus, I aimed to study non-phosphorylatable Ana2 versus phospho-mimicking Ana2 and to identify their effect on centriole duplication in *Drosophila* cell culture in collaboration with Dr. Dzhindzhev (Chapter 4). My next objective was to study the effect of Plk4-mediated Ana2-STAN phosphorylation on Ana2’s ability to interact with other centriole duplication proteins and specifically Sas6 by combined phosphorylation and direct binding assays *in vitro* (Chapter 4). This identified an interaction between Ana2 and Sas6 that is dependent on Plk4-phosphorylation of the Ana2-STAN motif. This led me to determine the minimal structural domains within Ana2 and Sas6 that are necessary for protein-protein interaction. To this end, I generated truncated protein constructs of both proteins and tested their direct binding abilities *in vitro* (Chapter 4).

The studies of *in vivo* Sas6 purifications from *Drosophila* cell culture repeatedly identified the uncharacterised protein CG33052, which we named Dragon. Its human homologue GoRab localises to the Golgi. My aim was to confirm or deny Dragon localisation at the Golgi and the centrosome. Additionally, I aimed to identify if Dragon is essential for centriole duplication by studying its effect on centrosome numbers after Dragon depletion; and to determine if Dragon interacts directly with the centriolar cartwheel protein Sas6 (Chapter 5). Centriolar localisation of Dragon by structured illumination microscopy was shown in collaboration with Dr. Tzolovsky. After showing that Dragon localises to the centriole and directly interacts with the centriolar cartwheel protein Sas6, I aimed to identify the smallest protein domains of Sas6 and Dragon necessary for their interaction (Chapter 5). My next objective was to generate a Dragon mutant that abolishes interaction with Sas6 and study its effect on centriole duplication by performing rescue experiments in *Drosophila* cell culture (Chapter 5). For my final objective I asked whether there is a similar requirement for the human homologue GoRab for centriole duplication (Chapter 5).

Chapter 2

Materials and Methods

2 Materials and Methods

2.1 Cloning

2.1.1 Gateway cloning to generate tagged protein constructs

Gateway® cloning is an Invitrogen^{TM} cloning system, applying recombination att sequence sites and BP and LR Clonase® enzyme mixes to transfer DNA fragments between plasmids and generate tagged proteins.

Full-length cDNAs (BDGP Gold Collection, *Drosophila* Genomics Resource Center) were amplified by PCR, using Pfu Ultra™ DNA Polymerase AD (Agilent, 600389-51), followed by agarose gel electrophoresis analysis and gel extraction (QIAquick® Gel Extraction Kit, QIAGEN, 28706). Utilised were the following cDNAs from the *Drosophila* Genomics Resource Centre (DGRC): Ana1 (LD07765 and IP16240 to generate a full-length Ana1 cDNA), Ana2 (LD22033), Asterless (GH02902), Bld10 (LD35990), Cep97 (RE26466), Rcd4 (SD16838), Sas6 (AT29216), Plk4 (RE70136), Dragon (RE68977). To generate the pENTR clones, the cDNA products were recombined with pDONR221 (Invitrogen^{TM}, Thermo Fisher Scientific, 12536-017) using BP Clonase® II Enzyme Mix (InvitrogenTM, Thermo Fisher Scientific, 11789-020). The fusion vectors were transformed into Library Efficiency® DH5α™ Competent Cells (InvitrogenTM, Thermo Fisher Scientific, 18263-012), amplified, purified (QIAprep® Spin Miniprep Kit, QIAGEN, 27106) and sequenced (Source BioScience LifeScience or GATC Biotech). To generate the pDEST clones, the pENTR clones were recombined with the Gateway® destination vectors, using LR Clonase® II Enzyme Mix (InvitrogenTM, Thermo Fisher Scientific, 11791-100). The *Drosophila* Gateway Vectors were used to generate expression vectors that drive expression of proteins with the N- or C-terminal tag eGFP (pAGW, pAWG, Thermo Fisher Scientific), 3xFLAG (pAFW, pAWF, Thermo Fisher Scientific), 6xmyc (pAWM, Thermo Fisher Scientific), 6xHis (pDEST42, Thermo Fisher Scientific), GST (pDEST24, Thermo Fisher Scientific) or MBP (pKM596, Addgene plasmid 8837). Additionally, pAct5c-PrA and pMT-cPrA (with the copper-inducible *Metallothionein* A (CG9470) promotor) were used, that were originally generated in the lab [282]. To generate plasmids that express untagged proteins, the pENTRs with the protein sequence and a C-terminal STOP codon were recombined into destination vectors for C-terminal tagging. The STOP-codon between the coding sequence and the tag leads to protein translation without the tag.

2.1.2 Regular cloning to generate constructs for Yeast-2-Hybrid method

PCR products that carry specific restriction enzyme sequences upstream and downstream of the protein sequences were amplified and cloned into the yeast-2-hybrid vectors pGBT9 and pGAD424. Pfu Ultra™ DNA Polymerase AD (Agilent, 600389-51) was utilised for the PCRs. Digests were performed consecutively or simultaneously, depending on the buffer conditions of the restriction enzymes used. The digested vectors were additionally treated with CIP (Alkaline Phosphatase, Calf Intestinal; New England BioLabs, M0290S) for 1 hour at 37°C, which catalyses the dephosphorylation of the 5' and 3' endings of the linearised vectors to prevent religation, followed by 15 minutes at 75°C to inactivate the CIP enzyme. The linearised vectors and digested PCR products were subjected to ligation at 16°C over night, using T4 ligase and reaction buffer (10x reaction buffer is 300mM Tris-HCl (pH 7.8 at 25°C), 100mM $MgCl_2$, 100mM DTT and 10mM ATP) (Promega, M1801). The ligation reaction was transformed into XL10-Gold ultracompetent cells (Stratagene, Agilent Technologies, 200314) according to the manufacturer protocol.

2.2 Site-directed mutagenesis

Table 2-1 Primers used for site-directed mutagenesis reactions. Listed are the forward (FW) and reverse (RV) primers applied in site-directed mutagenesis reactions of protein vectors to create the listed mutated protein (name). Blue represents final mutated sequence; red represents deletion between the two highlighted nucleotides.

Name	Primer	Primer sequence 5' to 3'
Dragon sequence correction	FW	CCAGAAGACGGCGGCGGAGTCGCGAAAGATCGAGGAGATCCGCCACGAGCTGT
	RV	ACAGCTCGTGGCGGATCTCCTCGATCTTTCGCGACTCCGCCGCCGTCTTCTGG
Dragon∆aa197-259	FW	CATCTCGCTGAAGGACTTCGAACAGTGCATACATTTTGCCAATGTAGAAA
	RV	TTTCTACATTGGCAAAATGTATGCACTGTTCGAAGTCCTTCAGCGAGATG
Dragon∆aa219-244	FW	AATGCTGTACCAGGCCATCGAGCAGCTGGCCGTGGACGTAGCTCTGCTGA
	RV	TCAGCAGAGCTACGTCCACGGCCAGCTGCTCGATGGCCTGGTACAGCATT
Dragon∆aa244-259	FW	CGAGCTGTCCAAGCTGGAAAGTGATTGCATACATTTTGCCAATGTAGAAA
	RV	TTTCTACATTGGCAAAATGTATGCAATCACTTTCCAGCTTGGACAGCTCG
Dragon∆aa286-320	FW	GCGGGCCAAGATAGAGCTGCACAATGGTCTGTCGCCAACCGATGATTGCC
	RV	GGCAATCATCGGTTGGCGACAGACCATTGTGCAGCTCTATCTTGGCCCGC
Dragon∆aa303-320	FW	AGAGCATCTATGCACAGTAATTGCCGGTCTGTCGCCAACCGATGATTGCC
	RV	GGCAATCATCGGTTGGCGACAGACCGGCAATTACTGTGCATAGATGCTCT
Dragon∆aa220-318	FW	AATGCTGTACCAGGCCATCGAGCAGAAAGTGGGTCTGTCGCCAACCGATG
	RV	CATCGGTTGGCGACAGACCCACTTTCTGCTCGATGGCCTGGTACAGCATT
Dragon∆aa220-286	FW	AATGCTGTACCAGGCCATCGAGCAGGCATCCGAAAAGAAGGAGCTGCTCA
	RV	TGAGCAGCTCCTTCTTTTCGGATGCCTGCTCGATGGCCTGGTACAGCATT
Dragon∆aa260-286	FW	GCTGAGGAAGCAGATCGACAATGCCGCATCCGAAAAGAAGGAGCTGCTCA
	RV	TGAGCAGCTCCTTCTTTTCGGATGCGGCATTGTCGATCTGCTTCCTCAGC
Dragon∆aa260-266	FW	GCTGAGGAAGCAGATCGACAATGCCGAAAAACAATACGTCAAAATCGAGG
	RV	CCTCGATTTTGACGTATTGTTTTTCGGCATTGTCGATCTGCTTCCTCAGC
Dragon∆aa267-281	FW	CTGCATACATTTTGCCAATGTAGAAATAGAGCTGCACAATGCATCCGAAA
	RV	TTTCGGATGCATTGTGCAGCTCTATTTCTACATTGGCAAAATGTATGCAG
Dragon∆aa282-286	FW	CGAGGCTCAGTTCTTGCGGGCCAAGGCATCCGAAAAGAAGGAGCTGCTCA
	RV	TGAGCAGCTCCTTCTTTTCGGATGCCTTGGCCCGCAAGAACTGAGCCTCG
Plk4-T172E	FW	AGCGACCTGATGAGCGCCATATGGAGATGTGTGGAACTCCGAACTATAT
	RV	ATATAGTTCGGAGTTCCACACATCTCCATATGGCGCTCATCAGGTCGCT
Plk4-K43M	FW	ACACTCACCAGGATGTGGCCATAATGATGATCGATAAAAAACTAATCCA
	RV	TGGATTAGTTTTTTATCGATCATCATTATGGCCACATCCTGGTGAGTGT
Ana2-S318A	FW	ACTGGCCAAGCCCAACACCGAGAAGGCAATGGTGATGAACGAGCTGGCGCTGA
	RV	TCAGCGCCAGCTCGTTCATCACCATTGCCTTCTCGGTGTTGGGCTTGGCCAGT
Ana2-S365A	FW	GATCGACAACATAGGCCACGCGCAGGCACCAAACGACATATCCAATGCTTCGT
	RV	ACGAAGCATTGGATATGTCGTTTGGTGCCTGCGCGTGGCCTATGTTGTCGATC
Ana2-S370A	FW	CCACGCGCAGAGTCCAAACGACATAGCAAATGCTTCGTACAAGTATCTCAAAA
	RV	TTTTGAGATACTTGTACGAAGCATTTGCTATGTCGTTTGGACTCTGCGCGTGG
Ana2-S373A	FW	GAGTCCAAACGACATATCCAATGCTGCATACAAGTATCTCAAAAAATACCGTC
	RV	GACGGTATTTTTTGAGATACTTGTATGCAGCATTGGATATGTCGTTTGGACTC
Ana2-3A	FW	CCACGCGCAGGCACCAAACGACATAGCAAATGCTGCATACAAGTATCTCAAAAAATACCGTC
	RV	GACGGTATTTTTTGAGATACTTGTATGCAGCATTTGCTATGTCGTTTGGTGCCTGCGCGTGG

To introduce point mutations or deletions within Dragon, the QuikChange II XL Site-Directed Mutagenesis Kit (Agilent Technologies, 200521) was used with Dragon cDNA or Dragon+STOP in pDEST42 (invitrogen^{TM}, Thermo Fisher Scientific, 12276010). The mutagenesis reaction mixes of 25µl final volume contained: 50ng DNA, 1x buffer, 600µM NTPs, 240nM forward primer, 240nM reverse primer, 1.5µl Quik Solution, 0.5µl *Pfu* Ultra high-fidelity DNA Polymerase; and the following temperature cycling program was used: 1. 95°C for 1 minute, 2. 18x cycles of 95°C for 50 seconds, 60°C for 50 seconds and 68°C for 3 minutes, 3. 68°C for 10 minutes, 4. Final storage at 4°C. The method uses the supercoiled double-stranded DNA vector and two primers that are complementary to opposite strands of the vector and contain the desired mutation. The primers are extended during the temperature cycles and contain staggered nicks. After the cycling program, the template DNA was digested by DpnI enzyme for 1 hour at 37°C, which targets for methylated and hemimethylated DNA (target sequence: 5´-Gm6ATC-3´). The remaining generated nicked vector products were transformed into DH5α cells.

2.3 Immuno-Histo-Staining and Microscopy

2.3.1 Immuno-Histo Stainings

For immune-staining of *Drosophila* cell culture 22 x 22 mm cover slides (VWR, 48376-049) were used. Therefore, the cell culture concentration was counted with a Hemocytometer and diluted to 500,000 to 800,000 cells per ml culture. Cover slides were pre-treated with concanavalinA (ConA, Sigma), which stretches the cells horizontally and allows an easier observation of the centrioles. The cells were incubated on the cover slide for 3 hours at 25°C before fixation with ice cold methanol. To fix the cells, the medium was taken off, 3ml ice cold methanol (left on dry-ice for 30 minutes beforehand) was flushed quickly onto the cover slides and remained on dry ice for 5 minutes. The methanol was taken off quickly and the cover slides were washed twice with 1x PBS. For long term storage, PBS-0.1%NaN_3 was added to prevent bacteria growth. To prepare the cells for staining, the cover slides were washed with PBS-0.1%TritonX-100 and transferred onto parafilm. The cells were blocked with PBS-10%FBS-0.1%TritonX-100 for 1 hour at room temperature, followed by incubation with primary antibodies (in PBS-10%FBS-0.1%TritonX-100) over night at 4°C, 3 washes with PBS-0.1%TritonX-100, and incubation with secondary antibodies (in PBS-10%FBS-0.1%TritonX-100) for 1 to 3 hours at room temperature (commonly Alexa Fluor® antibodies from Novex^{TM} (Thermo Fisher Scientific) were used). After incubation, the cover slides were washed 3 times with PBS-0.1%TritonX-100 and stored in 1x PBS until mounting the same day. The cover slides were briefly rinsed in ddH_2O before mounting to microscope slides with VECTORSHIELD mounting medium for fluorescence with DAPI (for DNA staining) (Vector Laboratories, H-1200) and nail varnish was used to seal off the edges.

Table 2-2 Summary of primary antibodies that were used in IF analyses.

Antibody	Dilution	Raised in	Location
Anti-Ana2	1:1000	Rabbit	Glover lab
Anti-Asterless	1:2000	Sheep	Glover lab
Anti-Dragon	1:1000	Guinea-pig	Glover lab
Anti-FLAG M2	1:1000	Mouse	Sigma, F3165
Anti-GM130	1:1000	Rabbit	Abcam, ab52649
Anti-Golgin245 G-7	1:1000	Mouse	Santa Cruz Biotechnology, sc-514775
Anti-D-Plp	1:1000	Chicken	Glover lab
Anti-Sas6	1:1000	Rat	Glover lab
Anti-GFP	1:600	Mouse	Thermo Fisher Scientific, A6455
Anti-myc 9E10	1:1000	Mouse	Thermo Fisher Scientific, 13-2500
Anti-α-tubulin DM1A	1:1000	Mouse	Sigma, T6199
Anti-γ-tubulin	1:250	Mouse	Sigma, T6557

Table 2-3 Summary of secondary antibodies that were used in IF analyses.

Antibody	Dilution	Species	Location
AlexaFluor® 488	1:333	Goat anti-chicken	Thermo Fisher Scientific, A11039
AlexaFluor® 568	1:333	Goat anti-chicken	Thermo Fisher Scientific, A11041
AlexaFluor® 594	1:333	Goat anti-chicken	Thermo Fisher Scientific, A11042
AlexaFluor® 647	1:333	Goat anti-chicken	Thermo Fisher Scientific, A21449
AlexaFluor® 488	1:333	Goat anti-guinea-pig	Thermo Fisher Scientific, A11073
AlexaFluor® 568	1:333	Goat anti-guinea-pig	Thermo Fisher Scientific, A11075
AlexaFluor® 594	1:333	Donkey anti-guinea-pig	Jackson ImmunoResearch, 70-586-148
AlexaFluor® 488	1:333	Donkey anti-mouse	Thermo Fisher Scientific, A21202
AlexaFluor® 594	1:333	Donkey anti-mouse	Thermo Fisher Scientific, A21203
AlexaFluor® 488	1:333	Donkey anti-rabbit	Thermo Fisher Scientific, A21206
AlexaFluor® 594	1:333	Goat anti-rabbit	Thermo Fisher Scientific, A11012
AlexaFluor® 405	1:333	Goat anti-rabbit	Thermo Fisher Scientific, A-31556
AlexaFluor® 488	1:333	Goat anti-rat	Thermo Fisher Scientific, A11006
AlexaFluor® 594	1:333	Goat anti-rat	Thermo Fisher Scientific, A21213
AlexaFluor® 488	1:333	Donkey anti-sheep	Jackson ImmunoResearch, 713-546-147

2.3.2 Microscopy

2.3.2.1 Structured illumination microscopy

The method was applied in collaboration with Dr. Tzolovsky and as describes in [24]. In short, the OMX-V3 system was used with a 63x/1.4NA oil Olympus lens to acquire super-resolution images (512x512ppi), followed by images being reconstructed and registered using the package SoftWorx Linux and processing of the images to obtain the maximum intensity projections. Final figures were cropped and assembled in Photoshop v6.

2.3.2.2 Fluorescent microscopy

Microscopic analyses of *Drosophila* cells and U2OS cells after histo-immuno-staining were performed on a Carl Zeiss Axiovert 200M microscope with 40x/1; 63x/1.25 and 100x/1.4 Plan Apochromat objectives. Acquiring of images was performed with a Photometrics Cool SNAP HQ2 camera, analyses of images were performed with the Metamorph software (v7.7).

2.4 Western Blot

For Western Blotting, proteins were run on a SDS-PAGE gel and transferred onto Hybond-ECL membran (GE Healthcare, RPN3032). Membranes were stained with Amido Black to visualise total protein. The membranes were then blocked for 1 hour in PBS-0.1%Tween-4% milk solution, followed by incubation over night with the primary antibody in PBS-0.1%Tween-4% milk solution at 4°C. The membranes were washed 3 times for 5 minutes in PBS-0.1%Tween and incubated for one hour with the secondary peroxidase conjugated antibody in PBS-0.1%Tween-4% milk solution at 4°C. After 3 washes in PBS-0.1%Tween for 5 minutes at room temperature the proteins were detected using Immobilon Western Chemiluminescent HRP Substrate reagent (WBKLS0500, Millipore). For this membrane was incubated with the mixed solutions (5ml ddH_2O, 2.5ml substrate solution, 2.5ml luminol solution) for 5 minutes, the majority of the solution was aspirated off and the membrane developed in the dark room.

Table 2-4 Summary of primary antibodies that were used in Western Blot analyses.

Antibody	Dilution used	Raised in	Location
Anti-DragonN (aa1-171)	1:1500	guinea-pig	Glover lab
Anti-FLAG M2	1:20,000	mouse	Sigma, F3165
Anti-GFP	1:2000 or 1:10,000	rabbit	Thermo Fisher Scientific, A6455
Anti-myc	1:5000	mouse	Abcam, ab18185
Anti-myc 9E10	1:6000	mouse	Thermo Fisher Scientific, 13-2500
Anti-Plk4	1:2000	sheep	Glover lab
Anti-α-tubulin DM1A	1:1000	mouse	Sigma, T6199

Table 2-5 Summary of secondary antibodies that were used in Western Blot analyses.

Antibody	Dilution	Location
Peroxidase AffiniPure Goat Anti-Guinea Pig IgG (H+L)	1:333	Jackson ImmunoResearch, 106-035-003
Peroxidase AffiniPure Goat Anti-mouse IgG (H+L)	1:333	Jackson ImmunoResearch, 115-035-003
Peroxidase AffiniPure Goat Anti-rabbit IgG (H+L)	1:333	Jackson ImmunoResearch, 111-035-144
Peroxidase AffiniPure Rabbit Anti-sheep IgG (H+L)	1:333	Jackson ImmunoResearch, 313-035-045

2.5 Expression and purification of tagged proteins from *E. coli* for *in vitro* assays and antibody generation

2.5.1 Expression and purification of tagged proteins from *E. coli*

Proteins were tagged with GST (Glutatione S-Transferase) or MBP (Maltose Binding Protein) using gateway cloning technology and transformed into Chemically Competent *E. coli* cells One Shot® BL21 Star™ (DE3) or BL21 Star (DE3) pLysS (Thermo Fisher Scientific). Colonies were tested for protein expression by inoculation of an overnight culture at 37°C, 220 rpm, followed by dilution to 1:50 and growth of the culture until it reached an OD of 0.4 to 0.6. At this time point a 1 ml sample of bacteria culture was taken for further analysis on SDS-PAGE and 1mM IPTG was added to the main culture to induce protein expression. The culture was left at 37°C and 1 ml culture samples were taken at different time points, up to 6 hours after induction, to analyse the level of protein expression on SDS-PAGE. After the timed protein expression, the cell cultures were centrifuged at 8600 rpm for 12 minutes, resuspended in 1x PBS and instantly stored at -20°C or -80°C. The samples for SDS-PAGE analysis were centrifuged at 13.000 rpm for 1 minute, the pellets were resuspended in PBS/1%Benzonase, left for 1 minute at RT, followed by adding 3x sample buffer containing 15%β-Mercaptoethanol to the sample and boiled at 96°C for 5 minutes.

Alterations of the expression conditions were undertaken where the above described protocol did not result in efficient protein expression. Expression levels were tested at 25°C or 16°C with increased expression times of up to 20 hours. The construct containing the HsSas6 protein sequence was kindly provided by Dr. Tzolovsky, followed by PCR to attach att overhangs for Gateway® cloning into pDONR221 and the expression construct pDEST15 (N-terminal GST tag).

For the protein purification, the bacteria suspension was defrosted and 1x Protease Inhibitor mix (cocktail tablets, complete EDTA-free, Roche, 11873580001), 10% PMSF (Sigma, 93482), 4% TritonX-100 (Sigma, T8787) and 10% Glycerol (Sigma, G5516) were added. In the case of Sas6 purification, PMSF was not added. Additionally, for the proteins stored on resin described in chapter 3, Sodium lauroyl sarcosinate (Sarkosyl, Sigma, 61747) was used instead of Glycerol, to increase solubility of GST fusion proteins [283]. The bacteria mix was then sonicated at 4°C until it was not viscous but of a fluid character, followed by a centrifugation step at 18,000 rpm for 30 minutes, 4°C. To purify the fusion protein, the according resin was added to the supernatant, which contains the soluble fusion protein, and rotated at 4°C for 2 to 3 hours. For GST fusions, Glutathione Sepharose 4B (GE Healthcare, 17-075601) and for MBP fusions, Amylose resin (BioLabs E8021L) were used. Each of the resin solutions were washed in PBS-2%TritonX-100 (T-PBS). For storage of the proteins on beads, 250µl beads baid volume were used (proteins bound to resin was stored at -20°C in 1x PBS with 50% glycerol); and for final protein elutions, 500µl beads baid volume were used for binding. After the binding, the beads were washed once with 0.5% T-PBS, once with 0.1% T-PBS and twice with Wash Buffer (50mM TrisHCl, 150mM NaCl, 0.1% TritonX-100). For further experiments with tagged protein bound to beads, they were stored at -20°C in 1x PBS with 50% glycerol. For elution of the proteins off the beads, Elution Buffer (10mM TrisHCl, 30mM NaCl, 0.02% TritonX-100, plus 15mM L-Glutathione for GST tagged proteins or 15mM Maltose for MBP tagged proteins) was added as twice the volume of the resin bait volume. Each protein was eluted 3 times at 4°C on a rotating wheel, for 2 hours or overnight for the first and second elution and for 2 hours for the third elution, and stored at -20°C. For use of the protein as an antigen in the generation of antibody, the protein was dialysed against 1x PBS overnight and again for 10 hours in fresh 1x PBS. In the case of MBP-Plk4-T172E and MBP-Plk4-T172E-K43M; the proteins were eluted in kinase buffer (20mM Na-HEPES pH7.5, 100mM NaCl, 10mM $MgCl_2$, 10mM $MnCl_2$, 1mM DTT), supplemented with 15mM D-Maltose, and stored at -80°C in Plk4-Kinase Buffer supplemented with 50% glycerol. Concentrations were measured by spectrophotometry and quality was analysed by SDS-PAGE.

Table 2-6 Summary of expressed and purified proteins as of their first appearance in the chapters of this thesis.

Chapter 3	Chapter 4	Chapter 5
GST	MBP-Plk4-T172E	GST-Sas6
MBP	MBP-Plk4-T172E-K43M	GST-HsSas6
GST-Ana2	MBP-Sas6	GST-Dragon
Asl-GST	MBP-Ana2	
GST- Cep97	GST-Ana2-N (aa1-280)	
GST-CP110 (aa1-400)	GST-Ana2-C (aa281-420)	
GST-CP110 (aa360-570)	GST-Ana2-4D	
MBP-Plk4	GST-Ana2-4A	
GST-Rcd4	GST-Ana2-C-4A	
GST-Sas4	GST-Ana2-S318A	
	GST-Ana2-S365A	
	GST-Ana2-S370A	
	GST-Ana2-S373A	
	GST-Ana2-C-S318A	
	GST-Ana2-C-S365A	
	GST-Ana2-C-S370A	
	GST-Ana2-C-S373A	
	GST-Ana2-aa315-384 (STAN only)	
	GST-Ana2-aa305-394	
	GST-Ana2-aa295-404	
	GST-Ana2-aa315-420	

2.5.2 Lambda-phosphatase bandshift assay

The λ-phosphatase bandshift assay was used to analyse the kinase activity of purified MBP-Plk4-T172E by its migration on SDS-PAGE. MBP-Plk4-T173E was resuspended in λ-phosphatase buffer (1x NEBuffer, 1x $MnCl_2$ Buffer, up to with ddH_2O, all NEB, P0753) and half the sample was treated with exogenous λ-phosphatase (NEB, P0753) for 1 hour at 30°C, followed by adding 3x sample buffer containing 15%β-Mercaptoethanol and boiling of the sample at 96°C for 5 minutes. Samples were subjected to SDS-PAGE and compared to the migration of kinase dead MBP-Plk4-T172E-K43M.

2.5.3 Antibodies generation and purification

Protein expression, purification and elution for the production of antibodies was performed as previously described (section 2.5.1). Antibodies applied in this study: MBP-Ana2 (full length) and GST-Sas6-C (aa236-472). The concentrated protein (150µg for 4 to 6 injections) was send to IMBC - instituto de biologia molecular e cellular, Porto, Portugal; to be used as antigen to generate IgG immunoglobulins specific for the antigen in rat. The received rat serum was stored in 50% glycerol at -80°C and used for antibody purification. The purification of the antibodies was performed as an IgG purification on rProteinA : ProteinG Sepharose (GE Healthcare, 17-1279-01, 17-0618-01 respectively) and were done small scale with 200µl resin suspension and 1000µl serum. This method allowed purification of all the IgGs present in the serum. The principle for the purification of IgG, IgG fragments and subclasses, is the high affinity of proteinA and proteinG for the Fc region of polyclonal IgG-type antibodies. ProteinA and ProteinG are bacterial proteins from *Staphylococcus aureus* and *Streptococcus* respectively, which were coupled to sepharose and can be used to isolate IgGs from serum. ProteinA has five regions for the Fc region of IgG to bind. Additionally, the used rProteinA (recombinant protein A) has been engineered to include a C-terminal cysteine which enables a single-point coupling to sepharose, allowing an increased binding capacity. ProteinG is a cell surface protein from Group G streptococci and a type III Fc-receptor, which binds through a non-immune mechanism. Compared to ProteinA, it binds more strongly to several polyclonal IgGs. Therefore a mixture of 50% rProteinA : ProteinG was used for serum from rat (anti-Ana2 and anti-Sas6). For the purification of sheep serum (anti-Plk4) only ProteinG and for the purification of rabbit serum (anti-Asterless and anti-Ana2-N) only rProteinA was used.

For the purification, the serum was diluted 10 times with PBS and centrifuges for 10 minutes at 14.000 rpm, 4°C to remove aggregates. Then it was mixed with the resin for binding on a rotating wheel for 60 minutes at 4°C, followed by two wash steps with PBS-0.1%TritonX-100 and two rinses with 1x PBS. The elutant was 0.1M Glycine-HCL pH3, which was added to the resin, mixed for 10 to 20 seconds and then removed and neutralised with 1M Tris-HCl pH8. Each antibody was eluted up to 4 times to win the highest protein concentration. For long term storage, the antibodies were concentrated by dialysing against a 50% Glycerol-PBS solution at 4°C overnight.

2.6 *In vivo* assays and Mass spectrometry

2.6.1 *In vivo* ProteinA and GFP-trap purification from *Drosophila* cell culture

For the identification of protein complexes *in vivo*, a combination of the methods of cell culture, single step ProteinA affinity or GFP trap purification and Mass Spectrometry has proven to be successful in mitotic and cytokinetic complexes. The method is based on the tagging of a bait protein with two IgG binding domains of Protein A or GFP, followed by stable expression in *Drosophila* cell culture, and isolation of the tagged bait protein together with its interacting partners by a single affinity purification step. The isolated protein complexes were then analysed Mass Spectrometry.

The cells for Mass Spectrometry analysis were expanded to 6 or 8 cell culture flasks of 175cm^2, using Express Five® SFM (1x) cell culture medium (Gibco^{TM}, Thermo Fisher Scientific, 10486-025) supplemented with 2mM L-glutamine (Gibco^{TM}, Thermo Fisher Scientific, 25030), and 100 U/ml penicillin and 100µg/ml streptomycin (Gibco^{TM}, Thermo Fisher Scientific, 15140). The cells were grown at 25°C until confluent, followed by passage. Cells were treated with 25µM MG132 for up to 5 hours to inhibit proteasomal degradation. For proteins which express from a pMT promoter, 1mM $CuSO_4$ was added to the medium for 22 hours to induce expression of the protein. 50% of each cell line was additionally treated with 50nM okadaic acid for 9 to 16 hours to inhibit the protein phosphatase PP2A and keep proteins in their phosphorylated state.

2.6.1.1 ProteinA purifications

For ProteinA purifications, the cells were harvested in PBS, resuspended in cold extraction buffer (75mM Na-HEPES pH7.5, 150mM NaCl, 2mM $MgCl_2$, 0.1%NP-40, 5mM DTT, 2mM EGTA, 5% glycerol, 1 tablet complete protease inhibitor per 50 ml), homogenised on ice and centrifuged at 4°C to pre-clear the soluble material. The supernatant was transferred to new tubes and magnetic rIgG-Dynabeads M-270 Epoxy (Invitrogen^{TM}, Thermo Fisher Scientific, 143.02D) were added. The mixture was incubated on a slowly spinning wheel at 4°C for 2 hours, to allow the rabbit IgG to bind to the complexes associated with the ProteinA tagged bait. After incubation, the beads were washed 5 times with extraction buffer, followed by elution using an elutant (0.5M NH_4OH, 0.5mM EDTA). For the analysis of the proteins, the eluted protein samples were desiccated to a volume of 100µl and an aliquot was taken for analysis using the SilverQuest™ Silver Staining Kit (Novex^{TM}, Thermo Fisher Scientific, LC6070). The proteins were then precipitated in small volumes with Acetone, dried in a speedvac centrifuge (Eppendorf, Concentrator 5301) and send for gel-free mass spectrometry analysis (Mass Spectrometry Laboratory, Institute of Biochemistry and Biophysisc, Warsaw, Poland).

The following purifications by Cunha-Ferreira, Dzhindzhev, Psternak, Schneider* and Weiskopf were reanalysed in chapter 3 and 5: pMT-Ana2-PrA*, pAct5-PrA-Ana2+pMT-Plk4*, Act5-PrA-Asl, Act5-Asl-PrA, Act5-Asl(aa531-994)-PrA, pMT-PrA-Cep97, pMT-Cep97-PrA, pMT-PrA-CP110, pMT-CP110-PrA, Act5-PrA-Plk4, pMT-PrA-Plk4, pMT-Rcd4-PrA, pMT-Sas4-PrA, pMT-PrA-Sas6. Additional purifications were performed but did not yield centrosomal duplication proteins in complex with the bait*: pAct5-PrA-Ana1, pAct5-Ana1-PrA, pAct5-PrA-Ana2, Act5-Ana2-PrA+pMT-Plk4, pAct5-PrA-Bld10, pAct5-PrA-Sas6. The constructs and cell lines were kindly provided by Dr. Dzhindzhev.

2.6.1.2 GFP-trap purifications

The GFP-trap purifications were performed in the cold room at 4°C and all reagents were kept at 4°C if not otherwise stated. The confluently grown *Drosophila* cells in 6x175cm^2 flasks (Corning®, 431079) were harvested with a cell scraper and centrifuged at room temperature and 900g for 5 minutes, followed by a 1x PBS wash and combining of all the cells into one 50ml falkon tube (Greiner Bio-One, 227261). The cells were then resuspended in 8ml Lysis Buffer 1 (20mM Tris pH7.5, 150mM NaCl, 2mM $MgCl_2$, 1mM DTT, 0.1% NP-40, 5% glycerol, 1x EDTA-free complete protease inhibitor cocktail (PIC, Roche) and 1mM PMSF (for samples other than tagged Sas6 purifications)) and homogenized at power 6 for 5-6 times for 30 seconds with breaks of 15 seconds (Fisherbrand PowerGen 125, FB70300). The lysate was clarified at 10,000 rpm for 15 minutes at 4°C. In the meantime the GFP-trap agarose bead suspension (ChromoTek, gta) was pre-equilibrated: 120µl of beads were added to 10ml LB1 and gently mixed 4-6 times, followed by centrifugation at a maximum of 2400g for 3 minutes at 4°C with a low deceleration speed and removal of the final supernatant. The supernatant of the cell lysate was then mixed with the GFP-trap beads and incubated on a rotating wheel (15-20 rpm) for 2-3 hours at 4°C. Thereafter, the beads were centrifuged at a maximum of 2400g for 3 minutes at 4°C with a low deceleration speed and the supernatant was removed. The beads were then washed twice in 10ml cold LB1 at 20rpm for 10 minutes, at 4°C; followed by transfer of the beads to a new pre-chilled Falcon tube and two wash steps in 10ml LB2 (same as LB1 but without PMSF and PIC). Beads were then transferred to a 1.5ml Eppendorf tube, adjusted to 1ml with LB2 and send for mass spectrometry. The protein complexes were mixed with 1x Laemmli sample buffer and analysed by Western Blotting.

The GFP-trap purifications from *Drosophila* cell culture stably expressing pMT-Dragon-GFP or pUb-GFP-Dragon (kindly provided by Miss Chu) were performed and analysed. Additionally, the purifications of pMT-PrA-Sas6 by Dr. Dzhindzhev was reanalysed.

2.6.2 Large scale collection and *in vivo* GFP-trap purification from *Drosophila* syncytial embryos

2.6.2.1 Large scale *Drosophila* embryo collection

For the large scale collection of 0-4 hours old syncytial *Drosophila* embryos that express poly-Ubiquitin-GFP-Dragon (flies kindly provided by Miss Chu), the flies were expanded to 9 large maintenance bottles and transferred into 2 large population cages (Genesee Scientific, FS59-104) for the collection of 1g of fresh embryos for GFP-trap purification. The population cages were kept at a 12/12 hours reversed light/dark cycles, with a room temperature of 25°C and a room humidity of 70%. On day 1 (morning), 2 chippy trays with grape juice agar and yeast paste were added to each cage, and replaced every 12 hours for a period of 48 hours. This stimulates the flies to the food-rich environment, which avoids eggs retainment and hence, synchronised egg laying. On day 3 (morning), a final change of chippy trays with yeast paste was added to the population cages for one hour to finalise full synchronisation. Thereafter new chippy trays with small amounts of yeast paste were added and replaced every 4 hours. The embryos were collected from the chippy trays with fine brushes and washed in mesh sieves with dH_2O, followed by a quick drying step with a paper towel pressed against the underneath of the sieve. For dechorionation, the embryos were transferred into a small beaker with 60ml 50% bleach (Kemtec) for 3-5 minutes, which was gently swirled manually. The dechorionated embryos were transferred into a small mesh sieve, washed with water, then wash buffer (0.7%NaCl+0.01% TritonX-100), to remove the vitelline membrane, and transferred into 2ml tubes and briefly centrifuged for collection. For long term storage, the decorionated embryos were frozen in liquid nitrogen.

2.6.2.2 *In vivo* GFP-trap purification from *Drosophila* syncytial embryos

1g of fresh *Drosophila* syncytial embryos (0-4 hours) expressing poly-Ubq-GFP-CG33052 were homogenised with a Dounce tissue grinder (Wheaton) in 10ml Extraction Buffer (EB: 20mM Tris-HCl pH7.5, 150mM NaCl, 2mM $MgCl_2$, 0.5mM Na-EGTA pH8, 1mM DTT (dithiothreitol), 0.1%NP-40, 5% glycerol, 1mM PMSF (phenylmethanesulfonyl fluoride), EDTA-free complete protease inhibitor cocktail (Roche)) at 4°C. 10ml of EB were then added to the sample, which was then vortexed for 10 seconds and passed through a needle and pre-chilled syringe three times, followed by a centrifugation step at 5000g for 20 minutes at 4°C. The supernatant was carefully transferred to a new tube, avoiding to remove any white fatty matter with it, and mixed with pre-equilibrated GFP-trap agarose beads (50-100µl per sample, gently mix in 5ml EB in 15ml conical tubes, sediment beads at 500g for 3 minutes at 4°C) for 30-150 minutes, at 18 rpm on a spinning wheel at 4°C. Thereafter, the beads were washed four times in 10ml Wash Buffer (same as EB) for 5 minutes each, at 4°C; sedimented and transferred to a new 15ml conical tube, washed two times in 10ml Final Wash Buffer (FWB: 20mM Tris-HCl pH7.5, 150mM NaCl, 2mM $MgCl_2$, 0.5mM Na-EGTA pH8, 1mM DTT) by gently rotating for 10 minutes at 4°C; again sedimented, transferred and twice washed with FWB; and finally all buffer was removed, and beads were stored at 4°C until on-beads tryptic digestion and mass spectrometry analysis.

The purifications of pUb-Sas6-GFP from *Drosophila* syncytial embryos by Dr. Dzhindzhev were reanalysed; these purifications were performed with normal NaCl concentration or with a high 440mM NaCl concentration and plus/minus okadaic acid.

2.6.3 Mass spectrometry and Phospho-peptide/residue mapping

The Mass Spectrometry data was generated by Dr. Dubski at the Mass Spectrometry Laboratory, Institute of Biochemistry and Biophysics, Pawinskiego 5a, 02-106, Warszawa, Poland. GST-Ana2 protein was phosphorylated by active Plk4 *in vitro* and ProteinA-Ana2 was phosphorylated by co-expressed non-degradable Plk4ND in *Drosophila* cell culture (*in vivo*). The protein samples were digested with trypsin (Promega V5111) and the peptide mixtures were analysed by LC–MS/MS (high-performance liquid chromatography tandem mass spectrometry) using Nano-Acquity (Waters) LC system and Orbitrap Velos mass spectrometer (Thermo Electron Corp.). The raw data was then analysed by Mascot Distiller followed by Mascot Search (Matrix Science) against the FlyBase database. The values of Mascot scores for individual proteins (‘Protein score’) and ‘number of identified peptides’ were analysed as a measure of ability for certain baits to co-purify with the prey protein. The Mascot score is a statistical score that represents how well the experimental data matches the database sequence (FlyBase). A 95% confidence level is required to identify a positive protein. The final Mascot score is generated from the summed scores of peptide masses and peptide fragment ion masses for the individual peptides that match a given protein.

2.7 Yeast-2-Hybrid – testing for direct interactions in an *in vivo* system

For the Yeast-2-Hybrid assay, each protein sequence was cloned into the vector pGBT9 and pGAD424 and then co-transfected into the yeast strain AH109. The method is based on the activation of the GAL promotor by its transcription factor, which is split into Binding Domain (BD) and Activation Domain (AD). The bait plasmid (pGBT9) contains the GAL4 DNA-Binding Domain (BD) and the prey plasmid (pGAD424) contains the GAL4-Activation Domain (AD). When proteins cloned into these plasmids interact directly with each other, they bring the BD and AD together, allowing for GAL promotor transcription and translation, which leads to colonies that grow on X-α-GAL to turn blue (colonies turn blue after up to 6 days at 30°C when a protein interaction occurs). If the co-transformation has been successful but the proteins do not interact with each other, the yeast can grow on the selection plates, which select for -Leu (pGD424) and –Trp (pGBT9), but they stay white and do not turn blue. If a transformation has not been successful with neither or only one of the plasmids, then the yeast strain cannot grow on the selection media.

For the co-transformation, the overnight culture of AH109 is diluted in 330ml YPD medium with OD600 = 0.3, then grown until OD600 = 0.6. The cells are centrifuged at RT, 1000g, 5 minutes, resuspended in 1x TE, centrifuged and resuspended in 1.5ml 1x TE/ 1x LiAc. 100µl of competent cells are added to 0.1µg plasmid DNA 1 + 0.1µg plasmid DNA 2 + 0.1mg carrier DNA and mixed by vortexing. 600µl of PEG/LiAc solution are added and the tube is vortexed for 10 seconds. The cells then incubate at 30°C, 220 rpm for 30 minutes. 70µl of DMSO is added to the cells and gently inverted, followed by a heat shock for 15 minutes at 42°C and 2 minutes on ice. Then the cells are resuspended in 1x TE, 100µl are plated on dropout media containing X-α-GAL and the plates are incubated at 30°C for up to 6 days.

Table 2-7 List of proteins that were cloned into pGAD424 or pBGT9 vectors. The vectors carry a GAL4-AD (activation domain) or GAL4-BD (binding domain) respectively; including plasmids used as positive and negative controls. The plasmids were used in yeast-2-hybrid interaction studies.

Vector	Domain	Proteins	Control
pGAD424	GAL4-AD	Asl, Ana2, Bld10, Cep97, CP110, Plk4, Rcd4, Sas4, Sas6, Polo and Spd2	-
pBGT9	GAL4-BD	Ana2, Bld10, CP110, Sas4 and Sas6	-
pGAD424	GAL4-AD		negative
pBGT9	GAL4-BD		negative
pGAD424	GAL4-AD	Mis12	positive
pBGT9	GAL4-BD	Nnf1a	positive
pGAD424	GAL4-AD	Nnf1a	positive
pBGT9	GAL4-BD	Mis12	positive

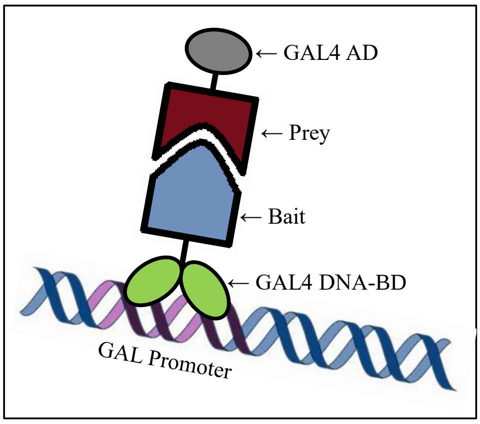

Figure 2-1 Schematic diagram of the GAL promotor activation in the yeast-2-hybrid system. Binding of bait and prey protein bring together the GAL4-AD and GAL4-BD which forms the transcription factor for the GAL promotor.

2.8 *In vitro* binding assays

2.8.1 *In vitro* binding assay

For the analysis of *in vitro* protein-protein-interactions, the methods of *in vitro* transcription – translation (IVTT), followed by binding assays and pull-downs were performed.

The method is divided into the production of two different sets of reagents, ^{35}S-Methionine-labelled proteins and tagged protein immobilised on resin (section 2.5.1). Every protein to analyse was amplified from cDNA in T7 containing promotors or from PCR products that carry the T7 promoter sequence 5’-GAATTAATACGACTCACTATAGGG-3’, the Kozak sequence 5’- AGAGCCGCCACC-3’, the start codon for protein transcription and the protein coding sequence. Alternatively, proteins were amplified from the pHY22 vector which contains a T7 promotor followed by the start codon and protein sequence. For the transcription-translation reaction, the TnT® T7 Quick Coupled Transcription/Translation System kit (Promega, L1170) was used. It contains a TnT® T7 Quick Master Mix, to which radioactively labelled ^{35}S-Methionine (Perkin Elmer, NEG709A001MC), RNasin Plus RNase Inhibitor (Promega, N2611), T7 TNT PCR Enhancer, protease inhibitor cocktail and the cDNA, PCR product or pHY22 vector with the protein sequence were added. The reaction of *in vitro* transcription/translation reaction was performed in a volume of 50µl, at 30°C for 30 to 120 minutes. The synthesised and radioactively labelled proteins were then used for binding assays. The cDNAs of *Drosophila* centriole duplication proteins were sourced from the BDGP Gold Collection, *Drosophila* Genomics Resource Center. The human GoRab variant 3 was sourced from Source Bioscience, followed by PCR to amplify att sequence overhangs and include a STOP codon after the protein sequence for Gateway® cloning into pDEST42 (C-terminal His tag). The human GoRab variant 1 was generated by PCR from a U2OS cDNA cell library, which was kindly provided by Dr. Lipinszki.

For the binding assay, each tagged protein on beads (bait) was mixed with each radioactively labelled protein (prey) in individual reactions in 800µl Binding Buffer (50mM

Hepes pH7.5, 1mM EGTA, 1mM $MgCl_2$, 1mM DTT, 100mM NaCl, 0.1%Triton X-100, 1x Protease Inhibitor, 0.5mg/ml BSA). The mixture rotated on a spinning wheel for 30-60 minutes at RT, followed by 3x5 minutes washes in Wash Buffer (50mM Hepes pH7.5, 1mM EGTA, 1mM $MgCl_2$, 1mM DTT, 100mM NaCl, 0.1%Triton X-100), to remove the radioactively labelled proteins that were not directly bound to the protein on beads. The resins were transferred into new tubes and 3xsample buffer containing 15%β-Mercaptoethanol was added. To analyse if interaction occurred between 2 proteins, the resin samples were subjected to SDS-PAGE followed by Western Blot or the drying of the SDS-PAGE, exposure to hypersensitive film (Kodak BioMax MS film, 8222648) at -80°C and autoradiography. The resulting exposure signals were categorised into: no interaction (-), weak interaction (+), interaction (++) and strong interaction (+++). Visually compared were the 'input versus negative control' signal, which in turn support the comparison of the 'interaction versus input' and 'interaction versus negative control' signal, to categorise the analysed interaction.

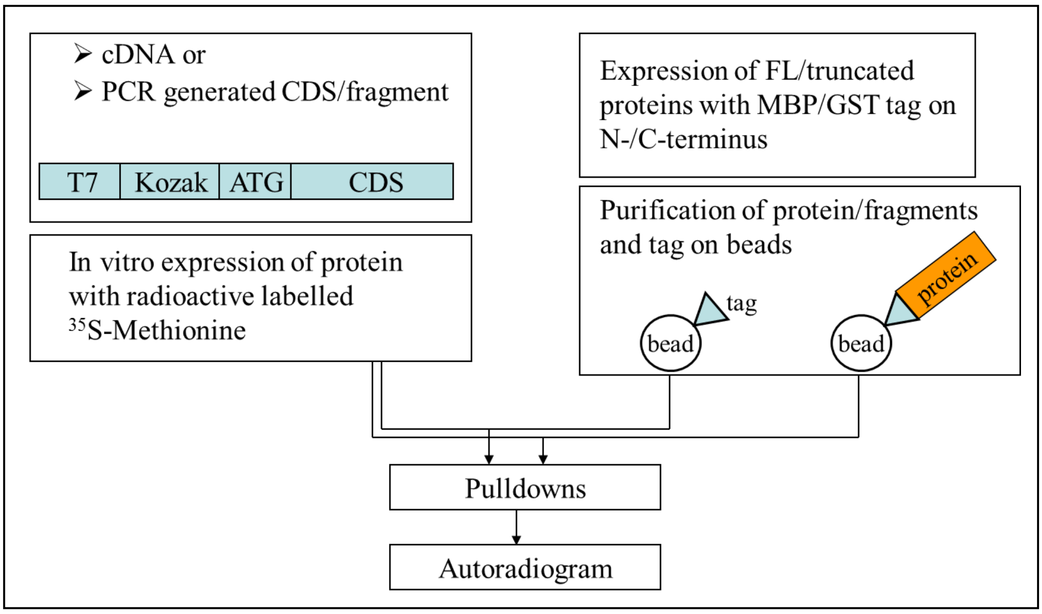

Figure 2-2 Schematic method of testing for direct protein interactions by *in vitro* binding assay. Two reagents were generated. Firstly, ^{35}S-Methionine labelled proteins from cDNA or PCR products by *in vitro* transcription-translation reaction (IVTT). And secondly, GST or MBP tagged protein, which was expressed and purified from *E. coli*, and stored on resin. For the binding assay or pulldown, two proteins were tested for their ability to interact directly. Therefore, one ^{35}S-Methionine labelled protein and one tagged protein to be tested for direct interaction were incubated together in binding buffer. After washes of the resin, it was subjected to SDS page and analysed by autoradiography.

Table 2-8 Summary of proteins that were generated by IVTT reaction. ^{35}S-Methionine labelled proteins used in this study (arranged as of their first appearance by chapter).

Chapter 3	Chapter 4	Chapter 5
Ana1	Sas6 (pHY22)	Dragon
Ana2	Sas6-aa1-180	Sas6-aa1-402
Ana3 Exon 1 (aa1-1146)	Sas6-aa181-408	Sas6-aa1-392
Ana3 Exon 2 (aa1146-1978)	Sas6-aa1-408	Dragon-aa1-171
Asterless	Sas6-aa181-472	Dragonaa172-339
Bld10	Sas6-aa221-472	Dragon-aa1-113
Cep97	Sas6-aa261-472	Dragon-aa114-243
CP110	Sas6-aa266-472	Dragon-aa244-339
Plk4	Sas6-aa271-472	Dragon-aa191-318
Rcd4	Sas6-aa276-472	Dragon∆aa219-244
Sas4	Sas6-aa291-472	Dragon∆aa244-259
Sas6	Sas6-aa295-472	Dragon∆aa286-320
Cnn	Sas6-aa341-472	Dragon∆aa303-320
D-Plp-N (aa1-1603)	Sas6-aa351-472	Dragon∆aa220-318
D-Plp-C (aa1604-2727)	Sas6-aa361-472	Dragon∆aa220-286
Polo	Sas6-aa371-472	Dragon∆aa260-286
Spd2	Sas6-aa381-472	Dragon∆aa260-266
	Sas6-aa1-462	Dragon∆aa267-281
	Sas6-aa1-452	Dragon∆aa282-286
	Sas6-aa1-442	GoRab variant 1
	Sas6-aa1-437	GoRab variant 3
	Sas6-aa1-432	
	Sas6-aa1-427	
	Sas6-aa1-422	
	Sas6-aa1-414	
	Sas6-aa1-412	

2.8.2 *In vitro* Plk4 kinase assay (MBP-Plk4-T172E phosphorylation assay using ^{32}P-γ-ATP)

To analyse if a protein is phosphorylated by active MBP-Plk4-T173E kinase a phosphorylation reactions was performed. The protein kinase or kinase dead (typically 4-10µg) was added to a reaction mix of 20-50µl, which contained Kinase Buffer (20mM Hepes, 100mM NaCl, 10mM MgCl2, 10mM MnCl2, 1mM DTT), 2.5mM ^{32}P-γ-ATP, 5-10µM cold ATP, tagged proteins bound to resin, ddH_2O. For non-radioactive kinase assays, 250µM cold ATP was used instead. The mix was incubated at 30°C for 45 minutes, followed by removal of the supernatant, adding 3x sample buffer containing 15%β-Mercaptoethanol and boiling of the sample at 96°C for 5 minutes. Samples were subjected to SDS-PAGE for protein separation, followed by drying of the SDS-PAGE, direct exposure to hypersensitive film (Kodak BioMax MS film, 8222648) at -80°C and autoradiography.

2.8.3 *In vitro* binding assay of Sas6 with pre-treated Ana2

To study the *in vitro* interaction of Ana2 and Sas6 in chapter 4, it is necessary to pre-phosphorylate Ana2 with active Plk4 kinase; including the necessary controls. For this, 4-5µg of GST-Ana2/GST on resin were gently mixed in Kinase Buffer (20mM Na-HEPES pH 7.5, 100mM NaCl, 10mM $MgCl_2$, 10mM $MnCl_2$, 1mM DTT) with 250µM ATP; and ~4.5µg of active or kinase dead MBP-Plk4, and incubated at 30°C for 60 minutes, with a gentle mix every 3 to 5 minutes. After the incubation time, 400µl ice-cold Binding Buffer (50mM Na-HEPES pH 7.5, 100mM NaCl, 2mM $MgCl_2$, 1mM EGTA, 1mM DTT, 0.1%Triton-X100, 1.1 tablets of PhosStop/10ml BB, 1 tablet of PIC/35 ml BB, 100nM okadaic acid, 0.5mg/ml BSA) and ^{35}S-Methionine-labelled Sas6 were added to the reaction, and the samples were incubated for 2 hours at 15 rpm on a rotating wheel at 4°C. Adding PhosStop (Roche, 04906837001) gives a complete protection of proteins against a broad range of phosphatases according to manufacturer. The samples were then centrifuged at 1200 rpm for 3 minutes at 4°C, the supernatant was removed and the beads washed three times with 800µl Wash Buffer 1 (as Binding Buffer but without BSA) for 5 minutes at 4°C. The beads were then transferred into new chilled tubes and washed with 1ml Wash Buffer 1, followed by two washes with Wash Buffer 2 (same as WB1 but contains 10mM NaCl and 0.2%Triton-X100). Finally, 3x sample buffer containing 15%β-Mercaptoethanol were added and the samples boiled at 96°C for 5 minutes, followed by analysis on SDS-PAGE, drying of the gels and direct exposure to hypersensitive film (Kodak BioMax MS film, 8222648) at -80°C and autoradiography.

2.9 *Drosophila* cell culture and Human U2OS cell culture experiments

2.9.1 Cell cultures

Drosophila cell cultures were grown in Express Five SFM medium (Gibco^{TM}, Thermo Fisher Scientific, 10486-025) supplemented with 2mM L-glutamine (Gibco^{TM}, Thermo Fisher Scientific, 25030-024) and Pen Strep (Gibco^{TM}, Thermo Fisher Scientific, 15140-122). To generate stable cell lines, FuGENE HD Transfection Reagent (Promega, E2311) was used and procedures were performed as for transient transfection described in section 2.9.2, with the addition that 0.5µg of ‘helper’ plasmid carrying a Blasticidin resistance (pCoBlast) were added. The antibiotic selection started 48hours post-transfection with 20µg/ml Blasticidin. After 1 to 2 days the cells with antibiotic resistance start dividing, and once they are confluent, they were split and kept under 20µg/ml Blasticidin treatment for 6 to 8 passages until stably expression was reached. For localisation studies, *Drosophila* cell lines stably expressing Act5-myc-Dragon, poly-Ubiquitin-Dragon-GFP and poly-Ubiquitin-GFP-DragonΔ^{IM} were generated.

2.9.2 Co-IP experiment

Drosophila cells were transiently co-transfected with poly-Ubiquitin-GFP, poly-Ubiquitin-GFP-Dragon or poly-Ubiquitin-GFP-Dragon$^{\Delta IM}$ and Act5-6xmyc-Sas6, followed by GFP immunoprecipitated after 24-36 hours with 50nM okadaic acid (Calbiochem, 459620) in the lysis buffer, and subsequent Western Blot analysis. For the transient transfection $4.5x10^6$ cells were seeded in each well of a 6 well plate (Corning, 3516) and topped to 2ml with Express Five® SFM medium (Gibco^{TM}, Thermo Fisher Scientific, 10486-025), after 2 hours a mix of 3µg of vectors DNA in 100µl nuclease-free water and 15µl FuGENE® HD Transfection Reagent (Promega, E2311) was incubated for 15 minutes and then added dropwise to the cells. The input samples of all three transient transfection confirmed the presence of Sas6 by anti-myc antibody staining (anti-myc 9E10, 1:6000, mouse), GFP/GFP-Dragon/GFP-Dragon$^{\Delta IM}$ by anti-GFP antibody staining (anti-GFP, 1:2000, rabbit) and as a control anti-α-tubulin (anti-α-tubulin DM1A, 1:2000, mouse). Secondary antibodies from Jackson ImmunoResearch were used at a 1:333 dilution (Table 2-5).

In collaboration with Dr. Lipinszki, *Drosophila* cells were transiently co-transfected with Actin5C-promoter-driven constructs encoding 3xFLAG-Ana2 (WT or 4A), Sas6-6xMyc or Plk4 (ND or NDKD) for 22 hours. Cells were treated with 25µM MG132 (Sigma-Aldrich, 133407-82-6) for 2.5hours before harvest. For the immunoprecipitation, the supernatants were mixed with anti-FLAGM2 magnetic beads (Sigma) for 3 hours at 4°C. After several washes proteins were eluted with 150 µg/ml 3xFLAG peptide, mixed with 3x sample buffer and subjected to SDS-PAGE followed by Western Blotting. Proteins were detected using the antibodies anti-Plk4 (1:2000, sheep), anti-FLAG (clone M2, 1:20,000, mouse), anti-myc (clone 9E10, 1:6000, mouse) and anti-α-tubulin (clone DM1A, 1:2000, mouse). Secondary antibodies from Jackson ImmunoResearch were used at a 1:333 dilution (Table 2-5).

2.9.3 RNAi – RNA interference

RNAi was performed using TransFast^{TM} transfection reagent (Promega, E2431). In the morning 1.5x10^{6} cells were transferred into wells of 6 well plates (Corning, 3516) with 2 to 4ml Express Five SFM medium (Gibco^{TM}, Thermo Fisher Scientific, 10486025) and transfection was performed 4 hours after. To prepare the transfection mix, 25µg of dsRNA were diluted in 1ml Express Five SFM medium, 20µl TransFast^{TM} transfection reagent was added and the whole mix was briefly vortexed, followed by 15 minutes incubation in which the complexes form. The medium was removed from the cells, which had attached to the bottom of the well, and the transfection mix was gently aspired in drops over the cells. The cells were incubated with the transfection mix for exactly 60 minutes at 25°C, after which 3ml of Express Five SFM medium was added. The cells remained in the transfection-medium-mix for 2 or 4 days, after which 500,000 to 800,000 cells per ml culture were transferred onto ConA coated cover slides for methanol fixation and Histo-Immuno-Staining. Additionally, $1.5\text{x}10^{6}$ cells were transferred for a second round of knock down by RNAi and the above protocol was followed repeatedly for further rounds of knock down. In collaboration with Dr. Dzhindzhev, the *Drosophila* cell lines stably expressing pAct5-Ana2-WT, pAct5-Ana2-4A and pAct5-Ana2-4D were used in RNAi experiments. Additionally, RNAi experiments were performed on wild-type *Drosophila* cells and cells expressing poly-Ubiquitin-GFP-Dragon or poly-Ubiquitin-GFP-Dragon$^{\Delta IM}$.

Table 2-9 Summary of oligonucleotide primers used to generate dsRNA. Listed are the name of the primer, FW primer (FW), reverse primer (RV) and the primer sequence 5' to 3'. Red: T7 promoter sequence; CDS (coding sequence); UTR (untranslated region). For efficient dsRNA-based silencing of endogenous Ana2, a 225 bp-long hybrid DNA template containing a combination of T7 promoter sequence (red), Ana2's 5'UTR (black directly downstream of red T7 promoter sequence), 15 first nucleotides of the Ana2 CDS (blue), 15 last nucleotides of the Ana2 CDS (green) and Ana2's 3'UTR (black downstream of green), was generated by Overlap Extension PCR.

Name	FW or RV	Primer sequence 5' to 3'
Rcd4	FW	GAATTAATACGACTCACTATAGGGAGAATGCCTCACAAACGTAGGAACCGAGTAC
	RV	GAATTAATACGACTCACTATAGGGAGACTAGTTGTATGTTCTCCTATATGCGCCG
Dragon CDS	FW	GAATTAATACGACTCACTATAGGGAGAATGACTGAGAAATTCAATGGTTTTA
	RV	GAATTAATACGACTCACTATAGGGAGAGCGGCGATGCTGTTCGAAGTCCTTC
Dragon 3'UTR	FW	GAATTAATACGACTCACTATAGGGAGAACACGTAACACGTGTAAATTCAACTTC
	RV	GAATTAATACGACTCACTATAGGGAGACACATAACATATACATATTTTATTTG
Dragon 5'UTR	FW	GAATTAATACGACTCACTATAGGGAGAACTCCACTCGTTCTGTTTGCATTTG
	RV	GAATTAATACGACTCACTATAGGGAGATGGTGTTTAACTTAGGGATAATTAGC
GST	FW	TAATACGACTCACTATAGGGAGAAAGGTGATAAATGGCGAAACAAAA
	RV	TAATACGACTCACTATAGGGAGACAACATCAAGAGCGTCATACAACA
Asterless	FW	TAATACGACTCACTATAGGGAGAATGAACACGCCAGGTATAAG
	RV	TAATACGACTCACTATAGGGAGATATTGGAGCACGTCTCTTT
Plk4	FW	TAATACGACTCACTATAGGGAGAATACGGGAGGAATTTAAGCAAGTC
	RV	TAATACGACTCACTATAGGGAGATTATAACGCGTCGGAAGCAGTCT
Ana2 CDS	FW	GAATTAATACGACTCACTATAGGGAGAATGTTTGTTCCCGAAACGGAGG
	RV	GAATTAATACGACTCACTATAGGGAGACAGAGCCGCCAGATCACTCTTA
Ana2 UTR		GAATTAATACGACTCACTATAGGGAGACAGATTCTCCCGCTCGAATTTAATTTAATCGGCAAATATAAACAAATACGCTCCAAATGTTTGTTCCCGAACCGAAGCTGTTGTGAAAGCATGTACAATGTTCGTTTTGTTATTTATGCATATGTCTATTTGCGATTTAAGTGGAAATATATTTCAATACACGGAAAAAAATCTCCCTATAGTGAGTCGTATTAATTC

2.9.4 siRNA in U2OS cells

U2OS cells were maintained in growth medium DMEM (1X) + GlutaMAX^{TM}-I (Gibco® Thermo Fisher Scientific, 31966-021) with antibiotics and FBS (Gibco® Thermo Fisher Scientific, 10500) at 37°C, 5% CO_2, in a humidified incubator; and were passaged after trypsination from the flask with 0.05% Trypsin-EDTA (1X) (Gibco® Thermo Fisher Scientific, 25300-054). For the siRNA experiment (Figure 2-3), $1x10^5$ cells were plated in 2ml of growth medium without antibiotics per well of a 6-well plate (Corning, 3516) on day 1, to reach 30-50% confluence before starting the siRNA experiment. On day 2, firstly, 125µl Opti-MEM® Medium I (Gibco® Thermo Fisher Scientific, 31985-047) and 7.5µl Lipofectamine RNAiMAX reagent (invitrogen^{TM} Thermo Fisher Scientific, 13778-030), and secondly, 125µl Opti-MEM® Medium I (Gibco® Thermo Fisher Scientific, 31985-047) and 25pmol siRNA were each mixed and incubated for 3 minutes at RT. The diluted siRNA was then added to the diluted Lipofectamine RNAiMAX reagent, mixed by pipetting, and incubated for 10 minutes at RT. In the meantime, the medium of the U2OS cells was replaced with medium without antibiotics for 10 minutes, followed by adding the siRNA-lipid complex mix to the cells. On day 3 (24 hours after transfection), the media was replaced with fresh complete media and 4µM Aphidicolin and 1.5mM Hydroxyurea were added to induce S-phase arrest of the cells. The cells were then fixed to sterile and 1x PBS-washed cover slides 72 hours after siRNA transfection by cold methanol. GoRab was depleted via three target siRNAs (Silencer® Select siRNAs, 4392420, IDs: s40927, s40928, s40929), and GFP siRNA (Silencer® Select siRNA, Ambion^{TM}, Thermo Fisher scientific, AM4626) was used as a negative control. The cells were stained with anti-γ-tubulin (1:250, mouse, Sigma, T6557) and secondary antibody AlexaFluor® 594 donkey anti-mouse (1:333, Thermo Fisher Scientific, A21203) for centrosomes. When U2OS cells are blocked in S-phase by Aphidicolin and Hydroxyurea, DNA duplication and therefore cell division was prohibited, but centriole duplication still occurred as normal. This leads to an increase in the number of centrosomes within each cell under control conditions.

Table 2-10 Summary of the three GoRab Silencer® Select siRNAs. Listed are the sense and antisense strand siRNAs of the GoRab Silencer® used.

GoRab siRNA	sense	antisense
ID s40927	CAGAGACCAUGAAACUAAATT	UUUAGUUUCAUGGUCUCUGCC
ID s40928	CCAUGAUGGUCACAACAAUTT	AUUGUUGUGACCAUCAUGGGA
ID s40929	CAGCAAAGCUAGAUAUACATT	UGUAUAUCUAGCUUUGCUGCA

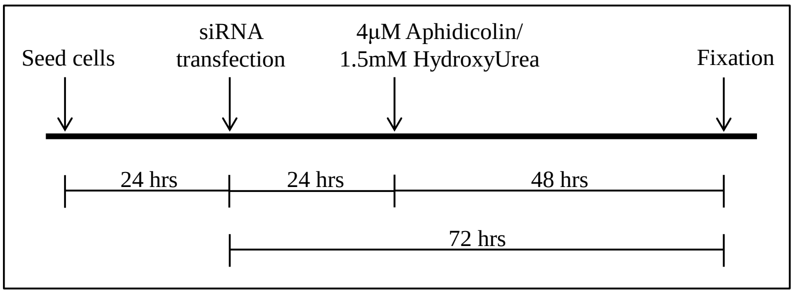

Figure 2-3 Time line of treatment of U2Os cells to study centrosome numbers after GFP and GoRab siRNA. U2Os cells were seeded at time point zero; siRNA transfection was performed 24 hours after; followed by arrest of cells in S-phase from 24 hours later by adding 4µM Aphidicolin and 1.5mM HydroxyUrea to the cell culture; and final fixation of cells 48 hours later.

2.9.5 Standard error and t-test

2.9.5.1 Standard error

The standard error was calculated for experiments were centrosomes were counted. Normally, three data points were generated; for all *Drosophila* cells 3 times 200 different cells were counted and for U2OS cells 3 times 100 different cells were counted. Initially, the Sample Standard Deviation was calculated by the square root of the Variance, which is the squared differences from the Mean divided by the ’number of data points minus 1’, with the Mean being the average of the data points. From there the Standard Error was calculated by dividing the Standard Deviation by the square root of the ‘number of data points’.

Data set: a, b, c

Mean: $M = (a+b+c) / n$ (n=population)

Sample Standard Deviation: $\sigma = \sqrt{}\ [((a-M)^2 + (b-M)^2 + (c-M)^2) / (n-1)]$

Standard Error: $SE = \sigma / \sqrt{n}$

2.9.5.2 t-test

For statistical analysis the paired t-test was used. It compares the population means of two correlated samples. Samples are classes as significant if $p<0.05$; and are categorised into statistically significant with $p<0.05$ (*) or $p<0.01$ (**) and statistically highly significant with $p<0.001$ (***).

2.10 Alignments and predictions

2.10.1 Protein sequence alignments

For the alignment of protein sequences to study their homology/orthology, protein sequences were acquired from http://www.flybase.org and alignments were performed with Clustal Omega [284] on http://www.ebi.ac.uk/Tools/msa/clustalo/.

2.10.2 Predicted secondary structure

For proteins of unknown secondary structure prediction softwares were used to indicate for potential secondary structure characteristics from protein sequences. Used were ‘psipred’ [285] and ‘coils server’ [286] on http://bioinf.cs.ucl.ac.uk/psipred/ and http://www.ch.embnet.org/software/COILS_form.html respectively. The resulting ‘windows number’ in the latter were described in [286]; in short the higher the window number, the better the distinction between coiled-coil and other regions.

2.10.3 Phosphorylation sites prediction

Generic phosphorylation site predictions were generated with the NetPhos 2.0 server on http://www.cbs.dtu.dk/services/NetPhos/. It generates neural network predictions for serine, threonine and tyrosine phosphorylation sites as was published in [287]. Blotted are ‘Phosphorylation potential’ against the sequence position. A residue is predicted not to be phosphorylated if its ‘phosphorylation potential’ lies below the threshold.

Chapter 3

Physical interaction screen to elucidate protein interactions governing centriole duplication

3 Physical interaction screen to elucidate protein interactions governing centriole duplication

3.1 Introduction

Two genome wide dsRNAi screens in *Drosophila melanogaster* cell culture identified a total of eighteen proteins required for centriole duplication. Out of these, eleven, Asterless (Asl), Ana1, Ana2, Ana3, Bld10, Cep97, CP110, Plk4, Rcd4, Sas4 and Sas6 showed specific centriole localisation and are therefore likely to be directly involved in the process [131,288]. Many of these individual proteins are currently investigated and their role in centriole biogenesis is becoming clearer. However, still very little is known about the precise molecular mechanisms and the physical and functional interplay of these proteins in the pathway as a whole. It has been shown that the core proteins identified in *C. elegans* show similarities in their assembly and function in other systems, suggesting that the relationship between the centriole duplication proteins is conserved [90,289–292]. It is believed that Polo like kinase 4 (Plk4) is the functional homologue of Zyg-1 in insects and vertebrates, and that it is the key regulator of centriole duplication [83–85].

In this chapter I wished to study and identify the physical interactions between the proteins Asl, Ana1, Ana2, Ana3, Bld10, Cep97, CP110, Plk4, Rcd4, Sas4 and Sas6 and how they act together to control centriole duplication. For this purpose, I have generated antibodies against most of these proteins and I have performed *in vivo* and *in vitro* assays to test for direct and indirect interactions between these proteins. It is my aim to analyse the relationship of the proteins involved in the complex centriole duplication network. For this purpose, I firstly analysed mass spectrometry data of the ProteinA purifications generated in our group by Cunha-Ferreira, Dr. Dzhindzhev, Psternak, Schneider and Weiskopf and generated further purifications from *Drosophila* cells expressing proteins of the centriole duplication process (section 3.2.1), followed by an *in vitro* interaction screen to supplement the *in vivo* findings by identifying direct protein-protein interactions (section 3.2.2) and applying the additional method of yeast-2-hybrid interaction (section 3.2.3).

3.2 Results

3.2.1 An *in vivo* protein interaction network of centriole duplication proteins designed from studies by ProteinA affinity purification

The tight regulation of centriole duplication is important for the maintenance of genomic stability, but only little is known about its molecular regulation. Therefore, my aim is to determine and map the physical interactions within the centriole duplication protein network using both *in vivo* and *in vitro* approaches. In this chapter I revisit ProteinA affinity purifications undertaken in our group; carry out and analyse additional ProteinA purifications of centriole duplication proteins; and create an interaction network considering the localisation of these proteins at the centrosome (Figure 3-1). To achieve single step affinity purifications, I expanded cell lines each expressing a centrosomal protein fused to ProteinA. I used IgG-coated resin to purify the expressed tagged protein and other endogenous proteins bound to it.

3.2.1.1 Plk4 – a master regulator forms complexes with the majority of proteins involved in centriolar duplication *in vivo*

Plk4 is described as the master kinase in centriole duplication and so it was of interest to identify its partners and substrates. Therefore, I focused on re-analysing previous ProteinA affinity purifications of ProteinA-tagged Plk4 purified from cultured cells and analysed by mass spectrometry, performed by K. Weiskopf and Dr. Dzhindzhev (complete lists in Appendix A). Of the possible Plk4 interactors, Asterless was the most striking showing a high Mascot score when co-purified with Plk4, indicating that peptides derived from Asterless were abundant in the purification (Table 3-1A). This is significant because genetic analysis shows that overexpression or depletion of Asterless results in similar phenotypes to overexpression and depletion of Plk4 [92]. In reciprocal purifications of Asterless tagged with ProteinA, Plk4 was also found as an interacting partner (Table 3-1B). Asterless was shown to recruit Plk4 to the centriole [92]. In addition to Plk4, Sas4 was also identified as a binding partner of Asterless. This suggests that Asterless is required for centriole duplication to form a scaffold that binds Plk4 and Sas4 [92,293,294]. Such a scaffold would bring Plk4 close to Sas4 or other centriolar proteins, to allow for their phosphorylation by Plk4. The purifications of Plk4 tagged to ProteinA also identified centriolar proteins (Table 3-1 A). Components of zone 1: Bld10 and Ana2; components of zone 2: Ana1, Sas4 and Spd2; components of zone 3: Asterless and D-Plp; components of zone 4: Cnn and Spd2, and in zone 5: CP110. The localisation of Ana3, also found in the purification, remains unknown in the centrosome (Figure 3-1, locations according to [24,30]). The localisation of these proteins might be important for the characterisation of the precise role of Plk4 at the centrosome and in identifying its substrates. As Asterless is known to recruit Plk4 directly, I also re-analysed affinity purifications of Asterless from cultured *Drosophila* cells, to identify potential additional interactors of the Asterless scaffold [92]. This identified Ana1, Bld10, D-Plp, Sas4, Spd2 and Plk4 (Table 3-1B). In summary, these purifications identify the proteins Ana1, Bld10, D-Plp, Sas4 and Spd2 in complex with Plk4 and Asterless. On the other hand, only Ana2, Ana3, Cnn and CP110 are specific in complex with Plk4 but not with Asterless.

Table 3-1 Mass spectrometry data from purifications of Plk4 (A) and Asterless (B) confirms centriole duplication proteins. ProteinA tagged Plk4 and Asterless were expressed and purified from *Drosophila* cell culture, followed by gel-free mass spectrometry analysis. The tables show the Mascot ‘score’ and ‘number of peptides’ of each according centriolar duplication and maturation protein identified in the purification data. OA, okadaic acid. MG132 treatment to inhibit proteasomal degradation. Complete lists in Appendix A.

A) Plk4 purifications

CG #	Score	# of peptides	Full name
Act5-PrA-Plk4			
CG7186	3411	118	Plk4
CG2919	636	25	Asterless
CG33957	460	19	D-Plp
CG4832	257	9	Cnn
CG17081	147	5	Bld10
CG10061	126	2	Sas4
CG6631	95	2	Ana1
CG14617	69	2	CP110
CG17286	53	1	Spd2
pMT-PrA-Plk4 (MG132)			
CG7186	8544	205	Plk4
CG2919	3542	148	Asterless
CG33957	468	13	D-Plp
CG4832	176	4	Cnn
CG6631	160	4	Ana1
CG17081	143	3	Bld10
CG10061	53	2	Sas4
pMT-PrA-Plk4+OA (MG132)			
CG33957	4029	116	D-Plp
CG7186	3011	111	Plk4
CG2919	1778	53	Asterless
CG6631	1776	55	Ana1
CG17081	1107	33	Bld10
CG4832	927	22	Cnn
CG10061	409	19	Sas4
CG13162	175	3	Ana3
CG8262	134	2	Ana2

B) Asterless purifications

CG #	Score	# of peptides	Full name
Act5-PrA-Asl			
CG2919	2736	138	Asterless
CG33957	772	29	D-Plp
CG6631	229	11	Ana1
CG17081	123	5	Bld10
CG17286	97	3	Spd2
CG7186	49	2	Plk4
CG10061	52	1	Sas4
Act5-Asl-PrA			
CG2919	10717	465	Asterless
CG33957	798	24	D-Plp
CG6631	628	26	Ana1
CG7186	224	9	Plk4
CG17081	174	6	Bld10
CG17286	87	4	Spd2
CG10061	71	1	Sas4
Act5-Asl (531-994)-PrA			
CG33957	542	13	D-Plp
CG7186	512	20	Plk4
CG2919	432	41	Asterless
CG17081	188	4	Bld10
CG6631	69	3	Ana1
CG10061	38	1	Sas4

3.2.1.2 *In vivo* studies of the centriole duplication proteins Ana2, Asterless, Cep97, CP110, Plk4, Rcd4 and Sas4 suggests a protein network

Additional ProteinA affinity purifications and mass spectrometry studies were then performed with Ana1, Ana2, Bld10, Cep97, CP110, Rcd4, Sas4 and Sas6, to search for candidates for their interacting proteins. The affinity purified complexes were analysed via gel free mass spectrometry. In the majority of cases, proteins were tagged with ProteinA on both their N- and C-terminus, to exclude possible interference of the affinity tag with binding. The affinity purifications of Ana1, Bld10 and Sas6 tagged to ProteinA did not identify any candidates involved in centriole duplication. However, the following proteins were found complexed to other centriole proteins: 1.) Ana2 purification identified Ana1, Plk4, Polo and Sas4; 2.) Sas4 purification identified Ana2, D-Plp and Polo; 3.) Rcd4 purification identified Ana2 and Ana3; 4.) Cep97 purification identified Ana2, CP110, D-Plp and Polo; and 5.) CP110 purification identified Cep97, Cnn, D-Plp and Polo (Table 3-2).

Interestingly, Ana2 was identified in complex with Sas4 and Plk4, and in the reciprocal ProteinA purifications the proteins Sas4 and Plk4 were identified in complex with Ana2, which strengthens the confidence of a potential interaction of Ana2 with Sas4 and Plk4 (Table 3-1, Table 3-2).

It is also noticeable that treatment of the *Drosophila* cells expressing Sas4 with okadaic acid seems to stabilise Polo in complex, as it was not identified when the cells were untreated. Thus Polo’s association with Sas4 might be phospho-dependent.

Similarly, only when cultured *Drosophila* cells expressing Cep97 were treated with okadaic acid, was CP110 found in the complex. This suggests that CP110 complexes with Cep97 in a phosphorylation-dependent manner.

Based upon these interactions I have constructed an interaction network between these proteins positioned at their known sites within the 3D structure of the centrioles as described by 3D-SIM (Figure 3-1) [24,30].

Table 3-2 Mass spectrometry data of centriole duplication proteins purified from *Drosophila* cell culture expressing ProteinA tagged Ana2, Sas4, Rcd4, Cep97 and CP110. Shown are the Mascot ‘score’ and ‘number of peptides’ identified of centriolar duplication and maturation proteins that were analysed in the purifications by mass spectrometry. OA, okadaic acid. MG132 treatment to inhibit proteasomal degradation. Complete lists in Appendix A.

CG #	Score	# of peptides	Full name
pMT-Ana2-PrA (MG132)			
CG8262	4562	80	Ana2
CG10061	24	1	Sas4
pMT-Ana2-PrA+OA (MG132)			
CG8262	11127	177	Ana2
CG6631	24	1	Ana1
pAct5-PrA-Ana2 + pMT-Plk4 +OA			
CG8262	7098	138	Ana2
CG12306	41	1	Polo
CG7186	32	1	Plk4

CG #	Score	# of peptides	Full name
pMT-Sas4-PrA (MG132)			
CG10061	39977	1290	Sas4
pMT-Sas4-PrA+OA			
CG10061	24851	848	Sas4
CG12306	281	9	Polo
CG33957	132	2	D-Plp
CG8262	123	2	Ana2

CG #	Score	# of peptides	Full name
pMT-Rcd4-PrA (MG132)			
CG17295	698	32	Rcd4
CG13162	199	8	Ana3
CG8262	70	1	Ana2
pMT-Rcd4-PrA+OA (MG132)			
CG17295	438	17	Rcd4
CG13162	207	8	Ana3

CG #	Score	# of peptides	Full name
pMT-PrA-Cep97+OA (MG132)			
CG3980	1465	50	Cep97
CG14617	178	5	CP110
CG33957	44	1	D-Plp
pMT-Cep97-PrA (MG132)			
CG3980	7109	208	Cep97
CG8262	235	3	Ana2
CG12306	41	1	Polo
pMT-Cep97-PrA+OA (MG132)			
CG3980	16796	437	Cep97
CG14617	330	11	CP110
CG12306	31	1	Polo

CG #	Score	# of peptides	Full name
pMT-PrA-CP110 (MG132)			
CG14617	2046	46	CP110
CG33957	148	5	D-Plp
CG12306	56	1	Polo
pMT-PrA-CP110+OA (MG132)			
CG14617	1506	33	CP110
CG4832	19	1	Cnn
pMT-CP110-PrA+OA (MG132)			
CG14617	2607	72	CP110
CG12306	104	5	Polo
CG3980	84	3	Cep97

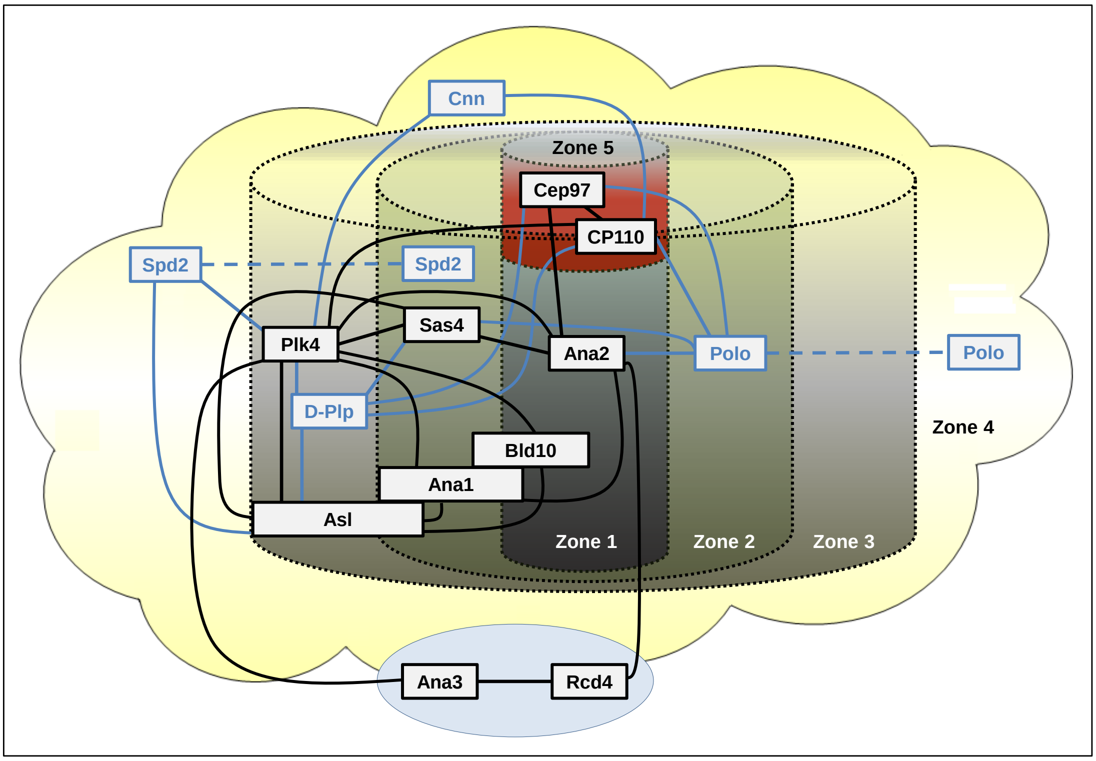

Figure 3-1 *In vivo* connections of centriolar duplication and maturation proteins and their localisation within the centrosome. (mass spectrometry data from Cunha-Ferreira, Dzhindzhev, Psternak, Schneider and Weiskopf; localisation studies from Fu [24,30]). Localisation of Ana3 and Rcd4 is unknown. Polo and Spd2 are localised in zone 2 and 4. Black lines connect proteins involved in centriole duplication. Blue lines connect to proteins involved in centriole maturation. Asl interaction with Plk4 and Sas4 was shown in [92].

As the localisation of Rcd4 within the centrosome had not been described, I depleted the protein by RNAi in cultured *Drosophila* cells. Cells were fixed and stained to reveal the centrosome marker D-Plp. This clearly showed that the knock down of Rcd4 over a 16 day interval resulted in a reduction of the number of centrosomes (Figure 3-2; 52.5% +/-2.5% of cells lost their centrosomes). The effect of Rcd4 depletion was less efficient than the positive control, depletion of Asterless, which causes loss of almost all centrosomes after 16 days of RNAi (90.8% +/-0.3%) but significantly greater than control GST RNAi (9.6% +/-1.8%). This confirms the findings of Dobbelaere *et al*. [131] that Rcd4 is required for centriole duplication.

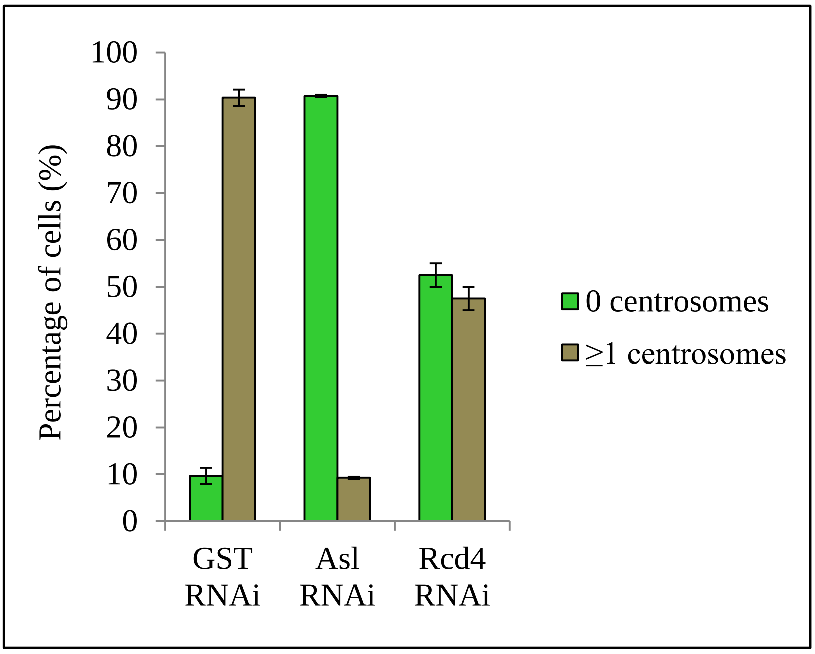

Figure 3-2 Effect of Rcd4 depletion on centrosome numbers in *Drosophila* cell culture. Rcd4 RNAi, Asterless RNAi (positive control) and GST RNAi (negative control) for 16 days with knock down every 4 days. High loss of centrosomes after Rcd4 and Asterless depletion. 3x200 cells; error bars represent standard error.

3.2.2 *In vitro* protein interaction assays confirm and expand interactions between centriole duplication proteins identified *in vivo*

To attempt to determine which of the above interactions might be direct I chose to carry out *in vitro* interaction assays. To this end, I asked whether the eleven centriolar duplication proteins (Ana1, Ana2, Ana3, Asl, Bld10, Cep97, CP110, Rcd4, Sas4, Sas6 and Plk4) and the pericentriolar proteins Cnn, D-Plp, Polo and Spd2, involved in the centrosome maturation process, would interact. For this study, I generated one putative partner that was ^{35}S-Methionine-labelled by coupled transcription-translation reactions and the other partner expressed as a fusion in *E. coli* (section 2.8.1, section 2.5.1). The binding complex was subjected to SDS-PAGE, followed by autoradiography. I simultaneously analysed a negative control (the tag alone bound to resin) and 1% input of the total radioactively labelled protein. I successfully expressed and purified eight tagged full length proteins (Ana2, Asl, Bld10, Cep97, Rcd4, Sas4, Sas6 and Plk4), and two fragments of CP110 (aa1-400 and aa360-570) for which the pENTR clones were kindly shared with me by Dr. Fu. I was not successful in my cloning strategy for Ana3. Moreover Ana1 and CP110 (aa571-666) could not be expressed successfully. I compared the autoradiographic signals for the protein interactions with the input and the corresponding negative control, and categorised the strength of the signal as: no interaction (-), weak interaction (+), interaction (++) and strong interaction (+++), with “d” indicating, that the strongest signal was observed as degraded protein (individual autoradiographic signals in Appendix B). I excluded tagged Sas6 and tagged Bld10 from the analyses, as these proteins exhibited strong non-specific binding to other proteins, most likely due to aberrant folding of Sas6 and Bld10. I was still able to analyse the reciprocal experiment following the binding properties of ^{35}S-Methionine labelled Sas6 and Bld10. All interactions are summarised in Table 3-3 [24,30]. The strongest direct protein interactions observed *in vitro* (+++) are highlighted in blue in Table 3-3. These are also indicated in relation to the localisation of the potential partner proteins within the centrosome in Figure 3-3; where black connecting lines highlight protein interactions that were also found *in vivo* (section 3.2.1); red connecting lines highlight strong protein interactions identified only *in vitro*. Good *in vitro* protein interactions (++) that verify *in vivo* protein interactions are highlighted in green in Figure 3-3.

In summary, the *in vitro* analyses of direct protein interactions suggest that some proteins found in complex *in vivo* correspond to direct interactions, namely Ana2 with Sas4, Ana2 with Plk4, CP110 with Polo, Asl with Plk4, Asl with Spd2 as well as Asl with Sas4 [92]. Additional interactions were only identified *in vitro*. These include CP110, which localises in the cap of the centriole (zone 5) that interacts strongly with Sas4 (zone 2) and vice versa *in vitro*. Additionally, CP110 is also linked to Ana3 (zone 1), Sas6 (zone 1) and Ana1 (mainly zone 2) by an *in vitro* interaction; and Sas4 (zone 2) is linked to Ana1 (mainly zone 2) and Rcd4 by direct *in vitro* interaction. Figure 3-3 also highlights potential protein interactions in green that were identified as a good interaction *in vitro* (++) and were also found associated in complex *in vivo*. These include interactions of Plk4 with Ana3, Bld10, CP110, D-Plp and Sas4; Ana2 with Cep97, Polo and Rcd4; Sas4 with D-Plp, Plk4 and Polo; CP110 with Cep97 and Cnn; Rcd4 with Ana3; and Cep97 with Ana2, Polo and CP110 (Table 3-1, Table 3-2, Figure 3-3). The assays also revealed strong interactions of Ana2, Rcd4 and CP110 with themselves but should be studied more carefully in future.

Table 3-3 Direct interaction levels of centriolar proteins using *in vitro* binding assays. Binding assays of radioactively labelled protein and tagged full length protein. Signals were categorised into no interaction (-), weak interaction (+), good interaction (++) and strong interaction (+++, blue background), with “d” indicating degraded protein size. The zones relate to the different layers of centrioles as described in [24,30]; ? indicates unknown protein localisation in the centrosome. GST-CP110 1/3 (aa1-400), GST-CP110 2/3 (aa360-570), D-Plp-N (aa1-1603), D-Plp-C (aa1604-2727). Individual autoradiographic signals in Appendix B.

			tagged protein							
		Zone	**GST-Ana2**	**Asl-GST**	**GST-Cep97**	**GST-CP110 1/3**	**GST-CP110 2/3**	**MBP-Plk4**	**GST-Rcd4**	**GST-Sas4**
^{35}S-Methionine labelled protein	**Ana1**	2	-	+	+	(+)	+++	(+)	+d	+++
	Ana2	1	+++	-	++	+	++	++	+	++
	Ana3 Exon1	?	(+)	(+)	+	(+)	++	++	+	(+)
	Ana3 Exon2	?	++	++	++	+++	+++	++	++	++
	Asl	3	+	++	++	++	++	+++	++	++
	Bld10	1	+	+	+	(+)	++	++	-	++
	Cep97	5	++	++	+	-	++	+	(+)	++
	CP110	5	++	++	++	+	+++	++	++	+++
	Plk4	3	+++	+++	(+)d	(+)d	(+)d	++	- d	++d
	Rcd4	?	++	++	++	++	++	++	+++	+++
	Sas4	2	+++	+++	++	+++	++	++	++	++
	Sas6	1	(+)	(+)	+	+	+++	(+)	+	++
	Cnn	3, 4	(+)	-	+	-	++	-	(+)	+
	D-Plp-N	3	-	+	+	(+)	(+)	++	-	++
	D-Plp-C	3	-	-	+	-	-	-	-	-
	Polo	2, 4	++	++	++	++	+++	-	++	++
	Spd2	2, 4	++	+++	++	-	++	-	(+)	-

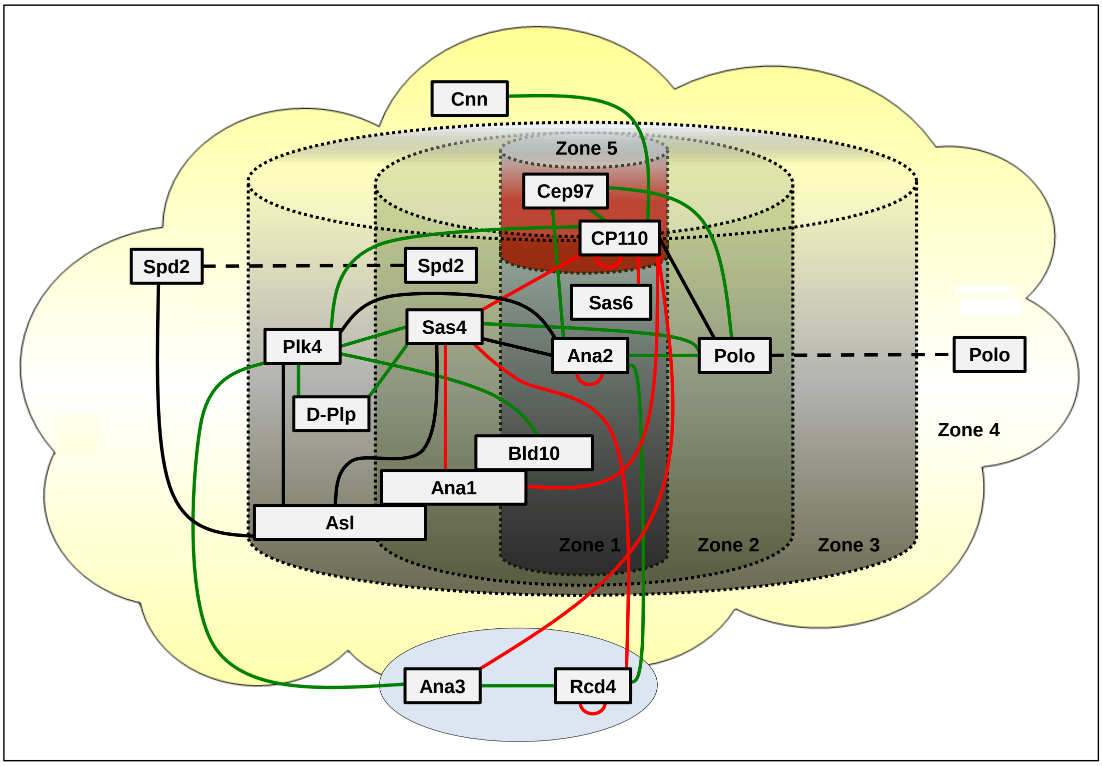

Figure 3-3 The protein network of centriole duplication after *in vivo* and *in vitro* interaction studies. Black connections stand for protein complexes analysed *in vivo* and confirmed as strong interactions *in vitro* (+++). Green lines stand for *in vivo* complexes confirmed as a good interaction *in vitro* (++). Red lines represent interactions only detected *in vitro* but with a strong autographic signal (+++).

3.2.3 Confirmatory studies using the Yeast-2-Hybrid Assay

The *in vivo* and *in vitro* analyses of complexes that I have described each have their advantages and disadvantages. The advantages of the *in vitro* method are its high sensitivity and its detection of direct interactions. On the other hand, the *in vivo* method detects proteins which form complexes between proteins that are correctly folded due to post-translational modifications. The *in vitro* method has the drawback that some protein interactions could only be observed in one direction but not reciprocally; for example: bacterially expressed Plk4 interacted well with ^{35}S-Methionine-labelled Rcd4 whereas bacterially expressed Rcd4 did not interact with ^{35}S-Methionine-labelled Plk4. The *in vivo* method is much less sensitive than in the *in vitro* approach. Thus certain interactions could only be detected *in vitro* but were not represented in complexes present *in vivo*. This could represent inaccessibility of a complex or formation of a complex at a specific time during the centriole duplication cycle. The yeast-2-hybrid system combines elements of the *in vitro* and *in vivo* methods, as it tests for direct protein-protein interactions but is performed within a eukaryotic cell and allows for post-translational protein modifications. I therefore applied the yeast-2-hybrid system in an attempt to confirm or deny protein interactions that were detected in only one of the previously applied methods. Methodically, the yeast-2-hybrid system is based on the activation of the GAL promotor by its transcription factor, which is split into a Binding Domain (BD) and an Activation Domain (AD). Each protein is tagged with these domains individually. Hence, when two proteins interact directly, they bring the AD and BD together, forming the functional transcription factor and activating the GAL4 transcription (section 2.7). The use of X-α-GAL gives a visual indication (colonies turn blue after up to 6 days at 30°C when a protein interaction occurs), if the two proteins interact directly and activate the GAL promotor. For the yeast-2-hybrid analysis, I generated 11 proteins in pGAD424 tagged with the GAL4 AD (Ana2, Asl, Bld10, Cep97, CP110, Plk4, Rcd4, Sas4, Sas6, Polo and Spd2), five proteins in pBGT9 tagged with the GAL4 BD (Ana2, Bld10, CP110, Sas4 and Sas6), two negative controls (AD-only, BD-only), and as positive controls I used BD-tagged Nnf1a and AD-tagged Mis12, and vice versa. Mis12 and Nnf1a are two interacting proteins in the Mis12 complex of the kinetochore [295]. All constructs were tested for autoactivation of the GAL promotor, of which only BD-Asl tested positive for autoactivation. Hence, only AD-Asl was used for interaction studies of Asterless.

My hybrid screen focused on centriolar proteins that localise to zone 1 and zone 2 of the centrosome and identified protein-protein interactions (highlighted in blue in Table 3-4). These confirm protein interactions found *in vitro* and in *in vivo* complexes (***), confirm protein interactions only found *in vitro* (a equals strong interaction (+++); b equals good interaction (++)), and suggest additional protein interactions (blue filled cells only). These interactions are summarised in relation to their localisation within the centrosome in Figure 3-4. Interestingly, the yeast-2-hybrid method confirms the interactions of Ana2 with Plk4, Sas4 and Polo, as previously described by the *in vitro* and *in vivo* tests (section 3.2.1, section 3.2.2). These are highlighted by black connection lines in Figure 3-4. The yeast-2-hybrid also confirms strong protein interactions (+++) observed *in vitro* of CP110 and Sas6, and the strong interaction of CP110 and Ana2 with themselves (marked ‘a’ in Table 3-4), and additionally confirming some good protein interactions observed *in vitro* (++) of Sas4 with itself, Sas6 with Sas4, and Spd2 with Ana2, Cep97 and CP110 (marked ‘b’ in Figure 3-4). The yeast-2-hybrid method also identified additional protein interactions which were not described in section 3.2.1 and 3.2.2. These include Sas6 with Ana2, Ana2 with Bld10, Sas6 with itself, Sas6 with Polo and Spd2, and Bld10 with Spd2 which are highlighted in orange in Figure 3-4.

Table 3-4 Confirmation of protein interactions found *in vivo* and/or *in vitro* applying the yeast-2-hybrid system. pGBT9 containing the GAL4-BD. pGAD424 containing the GAL4-AD. Blue highlighted boxes: observed protein interactions applying the yeast-2-hybrid method. White boxes: no protein interactions observed by yeast-2-hybrid. Additional symbols *** for interactions previously detected *in vivo* and *in vitro* (as good (++) or strong (+++) interactions); ‘a’ for interactions previously detected as strong interactions *in vitro* only (+++); ‘b’ for interactions previously detected as good interactions *in vitro* only (++).

		pGBT9					
		Ana2	Bld10	CP110	Sas4	Sas6	Spd2
pGAD424	Ana2	▨ a	▨		▨ ***	▨	▨ b
	Asl						
	Bld10	▨					▨
	Cep97						▨ b
	CP110			▨ a		▨ a	▨ b
	Plk4	▨ ***					
	Rcd4						
	Sas4	▨ ***			▨ b		
	Sas6	▨			▨ b	▨	▨
	Polo	▨ ***				▨	
	Spd2			▨ b			

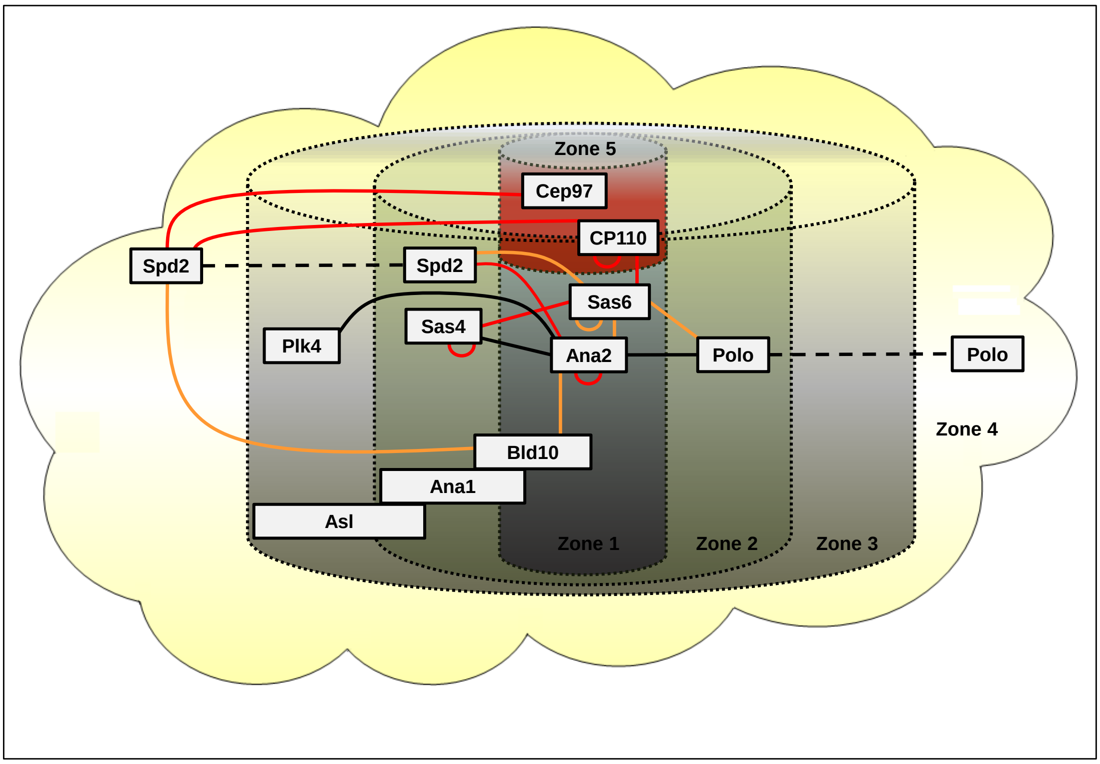

Figure 3-4 Diagram summarising the protein interactions detected by yeast-2-hybrid and confirming protein interactions identified by *in vivo* and *in vitro* methods. Black lines confirm proteins found in complex *in vivo* and as direct protein interactions *in vitro* (strong and good protein interactions). Red lines confirm interactions previously detected by strong or good *in vitro* interaction only. Orange lines indicate protein interactions newly detected by yeast-2-hybrid or previously identified as a (very) weak *in vitro* interaction.

3.3 Discussion

The studies I report in this chapter suggest that Plk4, master regulator of centriole duplication, directly or indirectly interacts with and regulates proteins localised in complex present *in vivo* within every zone of the centrosome. Additional ProteinA affinity purifications indicate a complex network of interacting proteins that participate in centriole duplication and centrosome maturation proteins (Figure 3-1). The *in vitro* interaction studies I carried out to identify direct protein-protein interactions gave some suggestions on functionally important interactions. It was previously shown that Asterless functions as a scaffold to recruit Plk4 and Sas4 to the daughter centriole, with the Asterless/Plk4 interaction being necessary for centriole duplication [92]. Significantly, Plk4 localises in the outer layer of the centrosome (zone 3) and Sas4 localises in the inner layer (zone 2), which goes in line with the recent discovery that their interacting protein partner Asterless localises mainly to zone 3 but also partially to zone 2 [30]. I was able to demonstrate these interactions as direct protein interactions *in vitro*. Plk4 interacts strongly with Asterless and vice versa; additionally, Asterless interacts with Sas4 and vice versa in the performed binding assays (Table 3-3). Hence, the *in vitro* method appears reproducible and reliable, and sheds further light on the finding of interactions *in vivo*. As seen in Figure 3-1, Plk4's partners are present in every zone of the centrosome, implying potentially diverse regulatory roles. Alternatively the large number of centriole duplication proteins purifying with Plk4 could indicate direct or indirect interactions occurring in the cytoplasm prior to incorporation into the centriole; for example Bld10 localises to zone 1 in the centriole but its interaction with Plk4 has not previously been described. At the time these *in vivo* analyses were carried out, neither direct substrates of Plk4 nor the timing of their interactions were known. Recently, it was discovered that Ana2 is a substrate of Plk4 and must be phosphorylated by Plk4 to allow for interaction and recruitment of Sas6 to the site of procentriole formation (Chapter 4) [296]. Significantly, Ana2 and Plk4 were detected in the reciprocal *in vivo* purifications (Table 3-1, Table 3-2) but with a low Mascot score and a low 'number of peptides'. The reason for this is not clear but could be explained if the interactions of the kinase with its substrates are only transitory. The interaction of Plk4 and Ana2 was confirmed as a direct interaction *in vitro* and additionally confirmed by the yeast-2-hybrid method.

Plk4 localises in zone 3 of the centrosome together with D-Plp and Asterless. The high Mascot scores of D-Plp in the Plk4 and Asterless purifications suggest a robust complex of these proteins. D-Plp is found predominantly on the mother centriole for most of the duplication cycle. D-Plp's C-terminus is localised at the centriole wall, from where it radiates outwards into the matrix, D-Plp could be a possible candidate for the recruitment of Asterless to the centriole [24,27]. Although recently it was shown that Bld10, Ana1 and Asterless are recruited sequentially in the centriole-to-centrosome conversion, that Asterless and Ana1 interact with each other, and that depletion of Ana1 leads to failure of Asterless and D-Plp localisation to the metaphase daughter centriole [30]. This suggests that D-Plp might be recruited to the centriole upstream of Asterless. Additionally, D-Plp has been shown to interact with Sas4 during PCM recruitment but its role in centriole duplication still needs to be investigated further [137,297].

On the other hand, in *C. elegans*, it was shown that Sas4 is recruited to the centriole by Sas5 (the Ana2 homologue) [53,91]. In accord with this I observed an interaction of Sas4 and Ana2 *in vivo*, *in vitro* and by yeast-2-hybrid, suggesting the possibility of a similar role of the Sas4/Ana2 interaction in *Drosophila*.

Of additional interest is the observation that Sas4 interacts directly with Cep97, CP110 and D-Plp *in vitro* but I identified only Cep97 and CP110 in complex with D-Plp *in vivo*. Sas4 has been associated with the process of PCM recruitment [11,20,25]. And a link to the cartwheel is supported by Sas4's interaction with proteins in zone 1 (Ana2) and zone 3 (Asterless, D-Plp) of the centrosome. In human cell culture, overexpression of CPAP (Sas4 homologue) leads to increased centriole length by enhanced accumulation of centriolar tubulin [38–40]. Elongated centrioles have also been observed after depletion of CP110, suggesting that CPAP and CP110 have antagonistic functions during centriole elongation and control centriole length [39], and Cep97 and CP110 function in cilia formation and length regulation [79,81]. On the other hand, in *Drosophila*, CP110 seems to restrict centriole length in a microtubule-depolymerising kinesin-like protein 10A (KLP10A) dependent manner [80,82].

Spd2 was also found in complex with Plk4 and Asterless, a finding of interest, as Spd2 exhibits a dual-localisation in zone 2 of the centrosome during interphase and mitosis, but additionally localises in zone 4 (PCM) after the onset of mitosis. This is also the case for Polo, which localises in zone 2 of the centrosome during interphase but also largely localises to zone 4 from metaphase onwards, where it is required for PCM recruitment [24]. In contrast to Spd2, Polo was also identified in complex with centriole duplication proteins that are in the core of the centrosome in zone 1, 2 and 5 (Ana2; Sas4; and Cep97 and CP110 respectively). This was confirmed by *in vitro* interaction studies, and the yeast-2-hybrid method confirmed the Polo and Ana2 interaction. Polo was only identified in the Sas4 purification when the cells were treated with okadaic acid, suggesting a potential phosphorylation-dependency of the Sas4/Polo interaction.

The connection between Ana3 and Rcd4 is of interest, as pilot experiments have linked Rcd4 to zone 1 or zone 5 by structured illumination microscopy on cultured cells expressing GFP-tagged Rcd4 (data not shown; cell lines by Mr Meghini; microscopy by Dr. Tzolovsky). The initial data suggests that Rcd4 recruitment to the centriole starts in interphase and reaches similar protein levels as Sas6 in metaphase (data not shown). Further studies will conclude the localisation of Rcd4 and give suggestions for Ana3 localisation.

The yeast-2-hybrid method confirms *in vitro* findings of potential self-interactions of Ana2, CP110 and Sas4. This accounts with the homodimerisation potential of Sas6 with itself, which has since been described in structural studies but was not detected in previous *in vivo* nor *in vitro* analyses [63,69]. Most interestingly, the interaction of Ana2/Sas6 was found using yeast-2-hybrid but not by *in vivo* and *in vitro* approaches. Significantly, at the time of the experiments, it was known that the interaction of *C. elegans* Sas5 and Sas6 is necessary in centriole duplication [53] but we showed only later that they also interact in *Drosophila* but in a manner dependent on Plk4 phosphorylation of Ana2 (Chapter 4) [296]. This was also confirmed in human cell culture for STIL and Sas6 [95,299,300]. The interaction of Ana2 and Bld10 was only detected by yeast-2-hybrid but not by *in vivo* or *in vitro* binding tests. Both proteins localise to zone 1 of the centriole and could possibly contribute to the formation or stability of the 9-fold symmetry of the cartwheel/centriole. Further studies need to confirm or dismiss the interaction of Bld10 and Ana2.

In conclusion, the studies I describe in this chapter have analysed proteins of centriole duplication and maturation that form complexes *in vivo* and were shown to interact directly by *in vitro* binding assays. Proteins that were found in complexes *in vivo* but did not interact *in vitro* might be connected indirectly. On the other hand, strong interactions found *in vitro* but that were not reflected in *in vivo* complexes could represent transient interactions in the centriole duplication cycle. The additional application of the yeast-2-hybrid method combines the advantages of testing for direct protein interactions in a system that allows for post-translational modifications. It confirmed protein interactions that were identified both *in vivo* and *in vitro*, and also protein interactions that were identified by the more sensitive *in vitro* approach only.

In summary, the application of *in vivo*, *in vitro* and yeast-2-hybrid methods in a screen to identify interactions of centriole duplication proteins has proven to be a guide to further studies rather than providing totally reliable conclusions. Each method in itself can be a strong and reliable method but needs to be accompanied by additional and more specific evidence of functional interaction to be conclusive.

Chapter 4

Interaction of Ana2 and Sas6 – Mediated by Plk4 phosphorylation of Ana2 and enabling procentriole formation

4 Interaction of Ana2 and Sas6 – Mediated by Plk4 phosphorylation of Ana2 and enabling procentriole formation

4.1 Introduction

Five proteins have been described to be essential in the centriole duplication pathway in *C. elegans*; Spd2, Zyg-1, Sas6, Sas5 and Sas4 [16–20,22,23,72,301]. My attempt to define the direct protein interactions of the *Drosophila* homologues and further centriole duplication proteins (Chapter 3) did not give the expected understanding how these *Drosophila* centriole duplication proteins interact with each other. Thus they gave little insight into molecular mechanisms underlying centriole duplication. The similarities of the core proteins identified in *C. elegans* in their assembly and function in other systems indicates that interactions between centriole duplication proteins are conserved [90,289–292]. The *Drosophila* proteins Ana2 and Sas6 were of particular interest and here I focus on their interactions. Their *C. elegans* homologues, Sas5 and Sas6, are recruited together to the procentriole, after Spd2 mediates recruitment of Zyg-1 [114,302]. However, how *Drosophila* Ana2 and Sas6 might interact was not clear. The substrates of the master kinase of centriole duplication Plk4 were also unknown. As in *C. elegans*, Zyg-1 is recruited upstream of the Sas5-Sas6 complex, I asked whether Ana2 and Sas6 interact, if they are substrates of the Plk4 kinase and function together in the centriole duplication process.

4.2 Results

4.2.1 Plk4 directly interacts with and phosphorylates Ana2 but not the centriole cartwheel protein Sas6

The recruitment of centriole duplication proteins is well described in *C. elegans* with Spd2 recruiting Zyg-1, the Plk4 homologue, followed by recruitment of Sas5 and Sas6 to the nascent procentriole, and recruitment of Sas4 for microtubules assembly [53,91]. In *Drosophila melanogaster*, the protein recruitment hierarchy of centriole biogenesis is similar to *C. elegans* but with some differences. Rather than Spd2, Asterless (Asl), a protein not present in *C. elegans*, recruits Plk4, the Zyg-1 homologue to the procentriole [92]. In human cells, both Cep152 and Cep192, the homologues of Asterless and Spd2 respectively cooperate in Plk4-recruitment in centriole biogenesis [93]. One question still remaining is what ensures the timely and functional recruitment of the *Drosophila* homologues of Sas5 (Ana2), Sas6 and Sas4 to the pro-centriole, especially in the light of Plk4s' characterisation as the master kinase for centriole duplication. We know that Plk4 is recruited to the centriole by Asterless and that Asterless interacts with Sas4 [92]. But despite this knowledge, we do not know the critical substrates that are phosphorylated by Plk4 during centriole duplication.

4.2.1.1 Ana2 and Plk4 interact *in vitro* but neither shows binding with Sas6

To address the above questions, I first attempted to determine which centriole proteins interact with each other during centriole duplication in *Drosophila*. Therefore, I performed an *in vitro* interaction screen in which I expressed tagged centriole duplication proteins (with MBP or GST) in *E. coli* and purified them on resins to determine whether they would interact with individual ^{35}S-Methionine-labelled centriole duplication proteins produced in an *in vitro* transcription-translation system. This allowed me to directly test whether two proteins bind each other by combining a) protein bound to resin with b) ^{35}S-Methionine-labelled protein in an *in vitro* interaction assay (section 2.8.1). The resin was then washed and subjected to SDS-PAGE, directly followed by protein transfer onto nitrocellulose membrane and autoradiography at -80°C. Such experiments revealed that Plk4 and Ana2 interact directly with each other *in vitro* (Figure 4-1). The autoradiogram in Figure 4-1A shows 1% input of ^{35}S-Methionine labelled Ana2 (lane 1) and the analysed interaction complexes of MBP and MBP-Plk4 with ^{35}S-Methionine-labelled Ana2 (lane 2 and 3 respectively). ^{35}S-Methionine-labelled Ana2 does not interact with MBP alone. Therefore, the observed signal with MBP-Plk4 is due to direct interaction of Ana2 with Plk4. The reciprocal assay is shown in Figure 4-1B and confirms the observations from Figure 4-1A. The autoradiogram in Figure 4-1B shows 1% input of ^{35}S-Methionine-labelled Plk4 (lane 1) and the interaction complexes of GST and GST-Ana2 with ^{35}S-Methionine-labelled Plk4 (lane 2 and 3 respectively). Plk4 does not interact with GST but the detected signal of ^{35}S-Methionine-labelled Plk4 with GST-Ana2 confirms that Plk4 directly interacts with Ana2 *in vitro*.

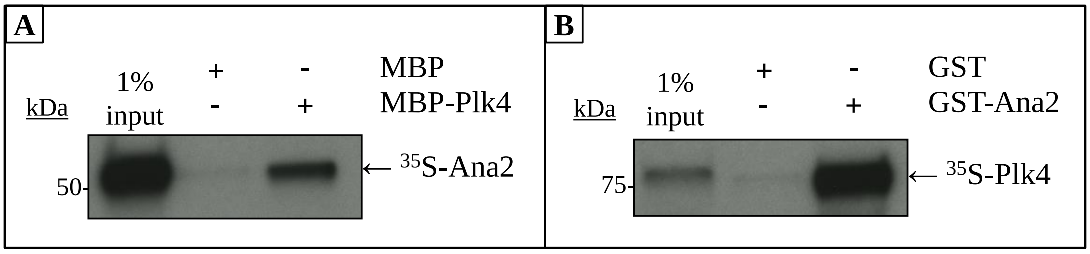

Figure 4-1 Ana2 and Plk4 protein interact directly *in vitro*. (A) MBP and MBP-Plk4 immobilised on resin were incubated with ^{35}S-Methionine-labelled Ana2 in an *in vitro* binding assay, subjected to SDS-PAGE and autoradiography. (B) GST and GST-Ana2 immobilised on resin were incubated with ^{35}S-Methionine-labelled Plk4 *in vitro*, subjected to SDS-PAGE and autoradiography. Autoradiograms show that Ana2 is found in complex with Plk4 (A) and Plk4 is found in complex with Ana2 (B).

The *in vitro* interaction assays shown in Figure 4-1 show that Plk4 and Ana2 interact directly with each other. It is known from *C. elegans*, that Sas5 and Sas6 are recruited to the centriole after Zyg-1 recruitment [53,91], with Ana2 and Sas6 being the respective homologues in *Drosophila*. This raises the question of whether *Drosophila* Sas6 can interact with Plk4 or Ana2. To address this, I applied the direct binding assay as described above using ^{35}S-Methionine-labelled Sas6 and MBP or MBP-Plk4 (Figure 4-2 A) and with GST or GST-Ana2 (Figure 4-2 B). I found no direct interaction of Sas6 with either of the two proteins, either with Plk4 or the negative control MBP (Figure 4-2A) or Ana2 or the negative control GST (Figure 4-2B).

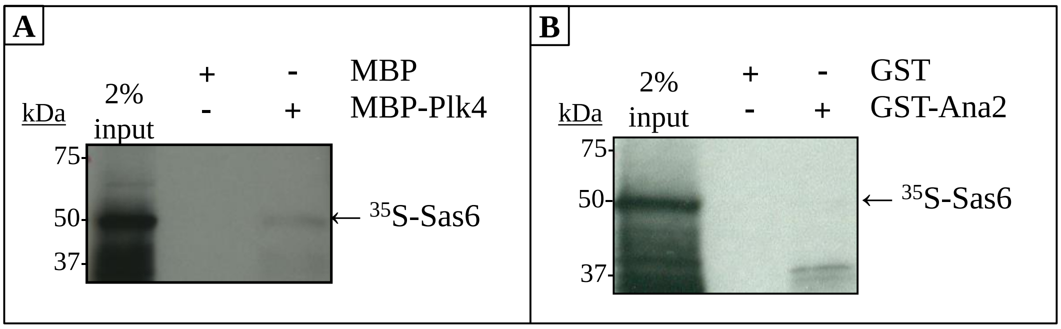

Figure 4-2 Plk4 and Ana2 proteins do not bind Sas6 directly *in vitro*. ^{35}S-Methionine-labelled Sas6 was incubated with MBP and MBP-Plk4 bound to resin (A) and GST and GST-Ana2 bound to resin (B). 2% ^{35}S-Methionine-labelled Sas6, as input, and the resin complexes were subjected to SDS-PAGE and autoradiography. The autoradiograms show that Sas6 was not associated with Plk4 (A) nor with Ana2 (B).

4.2.1.2 Plk4 phosphorylates itself and Ana2 *in vitro* but not Sas6

Initially, I expressed and purified MBP-Plk4-T172E-K43M and MBP-Plk4-T172E, the N-terminal MBP-tagged kinase dead and active form of Plk4 respectively. The expression constructs for MBP-Plk4-T172E-K43M and MBP-Plk4-T172E were generated by Dr. Dzhindzhev. MBP-Plk4-T172E carries a mutation at aa172 from T (Threonine) to E (Gutamic acid), located in the T-loop within the cryptic polo box of Plk4. MBP-Plk4-T172E-K43M carries an additional mutation at aa43 from K (Lysine) to M (Methionine), which is located in the kinase domain of Plk4 and corresponds to the kinase dead Plk4 version.

Plk4 is known to auto-phosphorylate in a self-regulatory fashion [107,109]. This auto-phosphorylation is also observed with MBP-Plk4, as a bandshift of the MBP-Plk4 protein can be observed when the protein is analysed on SDS-PAGE. To test if the purified batch of MBP-Plk4-T172E protein is an active Plk4 form and has phosphorylation ability, I incubated MBP-Plk4-T172E with lambda-phosphatase buffer and analysed its mobility on a SDS-PAGE in comparison to a) the active version treated with lambda phosphatase and b) the kinase dead version MBP-Plk4-T172E-K43M (Figure 4-3). A protein shift can be observed with MBP-Plk4-T172E treated with lambda phosphatase (lane 4) and MBP-Plk4-T172E-K43M (lane 1), confirming that MBP-Plk4-T172E is active and auto-phosphorylates. MBP-Plk4-T172E treated with lambda phosphatase (lane 4) has a similar mobility to kinase dead MBP-Plk4-T172E-K43M (lane 1). Thus the mobility shift between MBP-Plk4-T172E-K43M and MBP-Plk4-T172E results from auto-phosphorylation of the latter; and MBP-Plk4-T172E is an active form of Plk4 which was used in subsequent experiments.

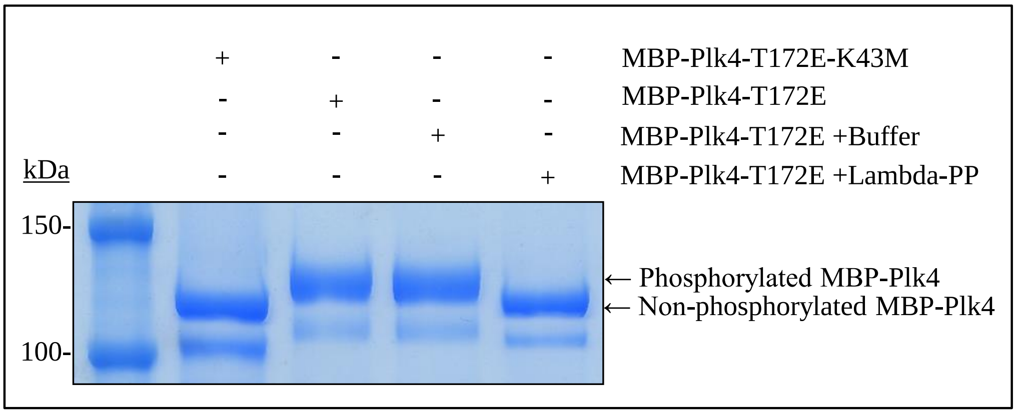

Figure 4-3 MBP-Plk4-T172E auto-phosphorylates but kinase dead MBP-Plk4-T172E-K43M does not. SDS-PAGE showing bandshift due to auto-phosphorylation of MBP-Plk4-T172E compared to the kinase dead MBP-Plk4-T172E-K43M. Bandshift and phosphorylation of MBP-Plk4-T172E is reverted to the level of kinase dead MBP-Plk4-T172E-K43M after treatment with lambda-phosphatase.

Experiments in *C. elegans* have shown that Sas5 (Ana2 homologue) and Sas6 are recruited to the procentriole after Zyg-1 (Plk4 homologue) [53,91]; that the recruitment of Sas6 to the procentriole is independent of Zyg-1 (Plk4 homologue); and that the kinase is necessary for the maintenance of Sas6 at the centriole which is achieved by Zyg-1 mediated phosphorylation of Sas6 at Ser123 [113]. To study whether Ana2 or Sas6 are substrates of Plk4 phosphorylation in centriole duplication, I applied a similar binding assay as above. I incubated active MBP-Plk4 kinase with several centriolar proteins, which were expressed in *E. coli* and purified onto resin before addition of ^{32}P-γ-ATP in kinase buffer. The proteins tested as potential substrates were MBP-Ana2 and MBP-Sas6; MBP was used as a negative control. After incubation, the resins were washed and subjected to SDS-PAGE; the gel was dried and exposed at -80°C. The autoradiograms showed that MBP-Ana2 but neither MBP nor MBP-Sas6 are Plk4 substrates.

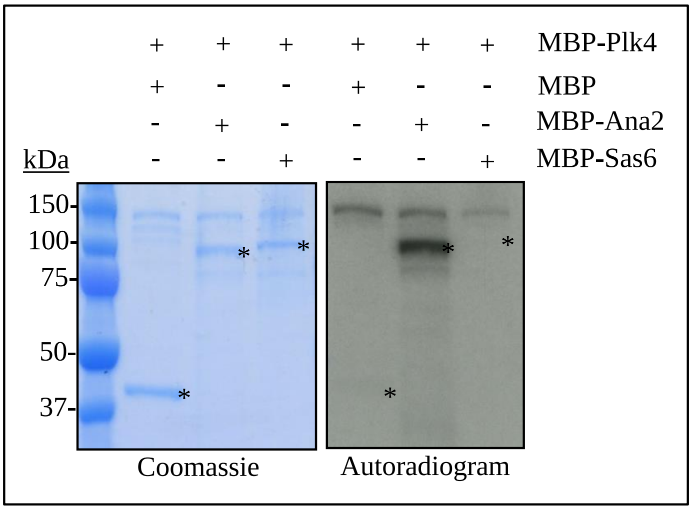

Figure 4-4 Active Plk4 phosphorylates Ana2 but not Sas6. Coomassie stained SDS-PAGE gel and correlating autoradiogram. SDS-PAGE shows MBP, MBP-Ana2 and MBP-Sas6, following incubation with active MBP-Plk4 and ^{32}P-γ-ATP. Autoradiogram shows radioactive signal only for MBP-Ana2, that was phosphorylated directly by active MBP-Plk4. MBP and MBP-Sas6 were not phosphorylated by active Plk4.

After showing that N-terminally MBP-tagged Ana2 is a substrate of Plk4 (Figure 4-4), I tested N-terminally GST-tagged Ana2 protein by *in vitro* phosphorylation assay (Figure 4-5), to confirm that GST-Ana2 can be phosphorylated by active Plk4. For this, I treated GST alone (negative control) or GST-Ana2 on resin, with either MBP-Plk4^{KD} (kinase dead Plk4) or active

MBP-Plk4, under addition of ^{32}P-γ-ATP. This revealed that only GST-Ana2 but not GST-alone was phosphorylated by the active form of Plk4 (Figure 4-5).

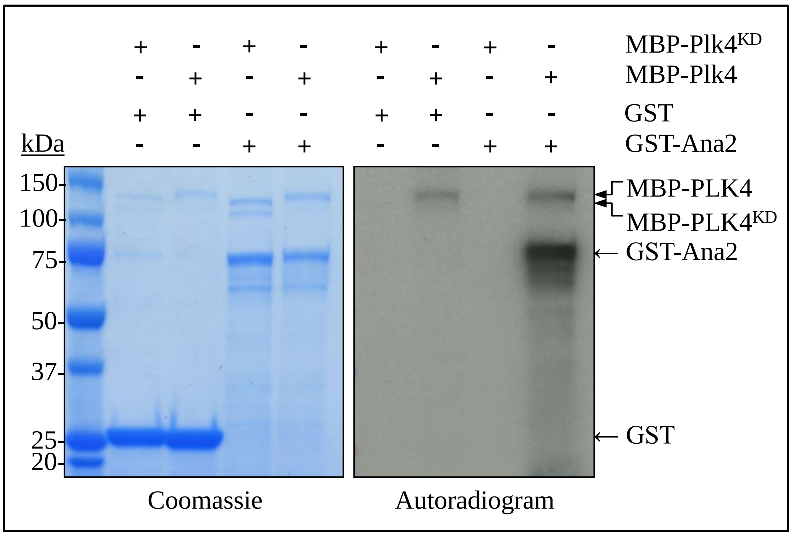

Figure 4-5 Ana2 is phosphorylated by Plk4. GST and GST-Ana2 bound to resin were treated with active MBP-Plk4 or kinase dead MBP-Plk4^{KD} in the presence of ^{32}P-ATP and then subjected to SDS-PAGE and autoradiography. Coomassie stained gel shows protein inputs and bandshift of GST-Ana2, treated with active MBP-Plk4. Bandshift of MBP-Plk4 due to phosphorylation state, as confirmed by ^{32}P signal in the autoradiogram.

4.2.2 Plk4 phosphorylates Ana2 at four main phosphorylation sites which are localised in the conserved Ana2-STAN motif

As shown in section 4.2.1.2, Ana2 is phosphorylated by active Plk4. To identify the Plk4-phosphorylation sites within Ana2, I generated Plk4 phosphorylated Ana2 *in vitro* (GST-Ana2 protein was phosphorylated by active Plk4) and Dr. Dzhindzhev generated Plk4 phosphorylated Ana2 *in vivo* (ProteinA-Ana2 was affinity purified from *Drosophila* cell culture expressing non-degradable Plk4ND), and both samples were analysed by phospho-peptide mapping by mass spectrometry by Dr. Dubski. Table 4-1 summarises the frequency of particular phospho-peptides detected *in vivo* or *in vitro*. This identified two tryptic peptides which are highly present in the *in vitro* and *in vivo* samples; namely S318, and the grouped S365, S370 and S373. Significantly, the identified phosphorylated peptides are within the conserved STAN motif of Ana2 (Figure 4-6, Figure 4-7). Other tryptic peptides, which were phosphorylated by Plk4, were also identified by phospho-peptide mapping by mass spectrometry of Ana2 phosphorylated *in vitro* and/or *in vivo* but at a lesser spectral count (Table 4–1). Several of these were previously reported as phosphorylated in *Drosophila* Kc 167 cells in a phospho-proteome analysis [303].

Figure 4-6 shows the schematic localisation of the identified Plk4 phosphorylation sites within Ana2 in red, the predicted coiled-coil region in green and the conserved STAN motif in blue. The four main Serine residues that are phosphorylated by Plk4 (S318, S365, S370, S373) lie within the conserved Ana2-STAN motif. And all four Serine residues are conserved as Serine/Threonine sites in the STAN motif throughout the analysed species *Homo sapiens*, *Gallus gallus*, *Xenopus laevis*, *Danio rerio*, and *Drosophila melanogaster* (Figure 4-7).

Having determined that full length Ana2 is phosphorylated by Plk4 throughout its sequence, with the C-terminal residues S318, S365, S370 and S373 in the conserved STAN motif being particularly prominent sites, I wished to test the separated N- and C-terminal parts as substrates. I generated two constructs splitting Ana2 to cover aa1-280 and aa281-420. In collaboration with Dr. Dzhindzhev, we then performed an *in vitro* kinase assay using the generated GST-tagged Ana2 fragments bound to resin (GST-Ana2-N, residues 1-280aa and GST-Ana2-C, residues 281-420aa) and treated them with active MBP-Plk4 kinase and ^{32}P-γ-ATP. This indicated that active MBP-Plk4 is able to phosphorylate both GST-Ana2 fragments, GST-Ana2-N and GST-Ana2-C (Figure 4-8). Significantly, the phosphorylation efficiency of GST-Ana2-C is ~2.5 times higher than the GST-Ana2-N fragment.

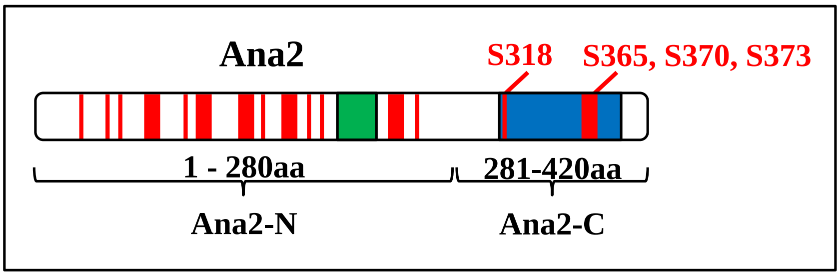

Figure 4-6 Localisation of the Plk4 phosphorylation sites within Ana2 identified by phospho-peptide mapping by mass spectrometry and listed in Table 4-1. Schematic of Ana2 showing the Plk4 phosphorylation sites (red), predicted coiled-coil domain (green) and the conserved STAN motif (blue). The four main Serines phosphorylated by Plk4 *in vitro* and *in vivo* are S318, S365, S370 and S373, which localise within the conserved STAN motif of Ana2.

Table 4-1 Plk4 phosphorylates Ana2 predominantly at residues S318, S365, S370 and S373 within the STAN motif *in vitro* and *in vivo* as identified by phospho-peptide mapping by mass spectrometry. GST-Ana2 was phosphorylated by MBP-Plk4 *in vitro* and *in vivo* ProteinA-Ana2 was affinity purified from *Drosophila* cell culture co-expressing PrA-Ana2 and non-degradable Plk4ND. Each sample was subjected to phospho-peptide mapping by mass spectrometry. The table summarises the number of times a particular phospho-peptide was detected from the *in vitro* and *in vivo* samples. Two tryptic peptides were preferentially phosphorylated, S318 and S365-373 (consisting of S365, S370 and S373).

	Total number of spectral counts	
Position	*In vitro*	*In vivo*
T69	10	10
S84	13	70
T89	11	0
S98-105	2	15
S119	7	8
T124-125	16	0
S150-153	28	24
T159	62	0
T164	16	0
S177	23	16
S184	2	3
S234	1	3
S237-242	71	9
S318	120	1
S365-373	378	70

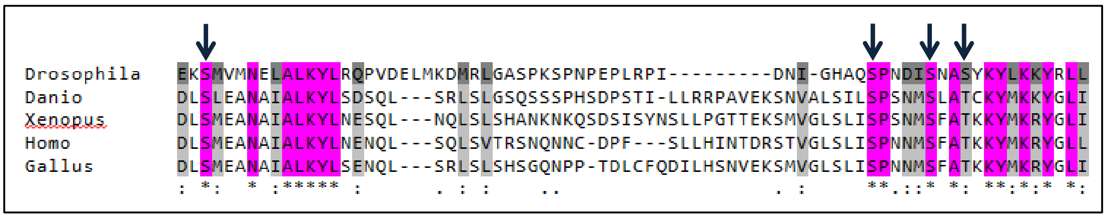

Figure 4-7 Alignment of orthologue Ana2 STAN motif sequences highlighting the four conserved Serines phosphorylated by Plk4. Analysis of Ana2/STIL STAN motif sequences of five species; *Drosophila melanogaster*, *Danio rerio*, *Xenopus laevis*, *Homo sapiens* and *Gallus gallus*. Arrows highlighting the Plk4 phosphorylation sites identified in *Drosophila melanogaster*, S318, S365, S370 and S373. Alignment was generated with Clustal Omega [284].

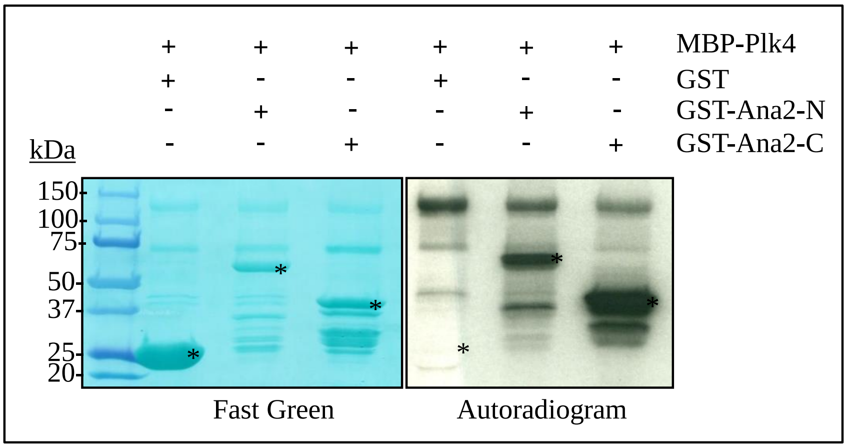

Figure 4-8 MBP-Plk4 phosphorylates Ana2-N (aa1-280) and Ana2-C (aa281-420) *in vitro*. In the presence of ^{32}P-γ-ATP, GST, GST-Ana2-N and GST-Ana2-C were treated with active MBP-Plk4 in a phosphorylation assay, subjected to SDS-PAGE and autoradiography. GST-Ana2-N and GST-Ana2-C show phosphorylation by MBP-Plk4.

4.2.3 Non-phosphorylatable Ana2 leads to loss of centrosomes; phospho-mimicking Ana2 rescues centriole duplication

4.2.3.1 Ana2 is efficiently depleted by dsRNA against Ana2 CDS and Ana2 UTR

Ana2 is a conserved protein, with the most striking region of homology being a predicted coiled-coil region in the central part of the protein and the conserved STAN motif in the C-terminal part (aa315-384). Ana2 and its homologues (Sas5 in *C. elegans*, STIL in *Homo sapiens*) are essential for centriole duplication. I wished to be able to deplete endogenous Ana2 from cultured cells in such a way that I could then express mutant forms of Ana2 in its place. To test the efficiency, I depleted endogenous Ana2 using dsRNA against its UTRs, and asked if I could transfect cells with a rescue construct lacking UTR elements. Depletion of Ana2 with dsRNA against its *CDS* or *UTR* and control RNAi was performed over 12 days with 3 dsRNA treatments every 4 days in collaboration with Dr. Dzhindzhev. Cells were fixed and stained to reveal the centrosome marker D-Plp. I then analysed the cells by automated fluorescent microscopy to determine centrosome numbers after depletion of Ana2 or control-GST (Figure 4-9). Over a time course of 4, 8 and 12 days *GST* RNAi treated cells showed a constant proportion of cells without centrosomes of less than 10%, which is comparable to wild-type *Drosophila* cell culture. Therefore, GST RNAi does not affect centriole duplication. In contrast, depletion of Ana2 using dsRNA against the CDS, led to an increasing percentage of cells without centrosomes; from 27.2% +/- 2.6% on day 4, to 67.7% +/- 4% on day 8, and 94.3% +/- 0.9% on day 12. When Ana2 was depleted via its UTR regions, the percentage of cells without centrosome increased significantly over the analysed time course; from 24% +/- 2.1% on day 4, to 38.5% +/- 3.3% on day 8, and 67.7% +/- 3.5% on day 12. Therefore, depletion of Ana2, either by its CDS or its UTR, results in loss of centrosomes. Ana2 dsRNA directed against the CDS is more effective in preventing centriole duplication than dsRNA against the UTR. Nevertheless, the effect of dsRNA against Ana2's

UTR is substantial (67.7% +/- 3.5% of cells without centrosomes on day 12) compared to the negative GST control (9% +/- 1% of cells without centrosomes on day 12).

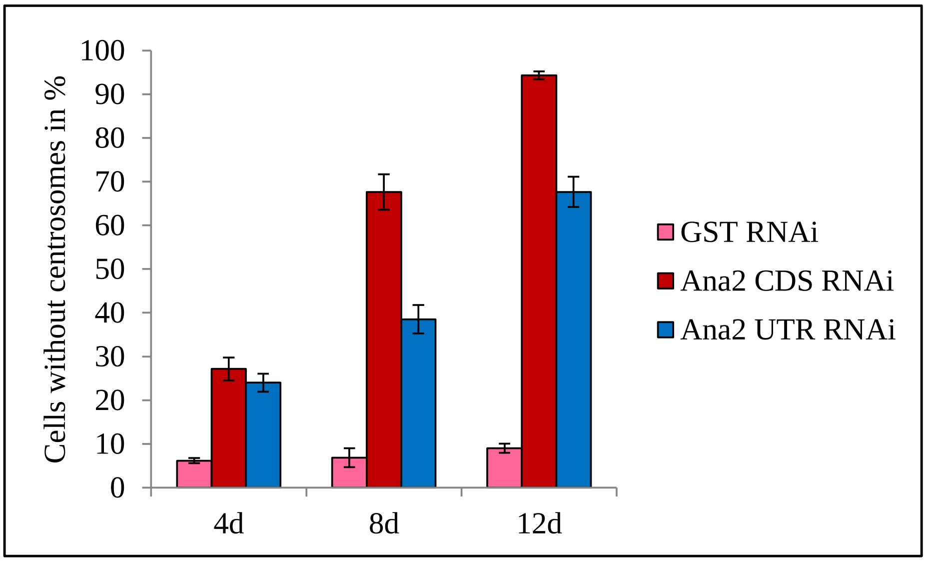

Figure 4-9 Depletion of Ana2 using dsRNA against Ana2 CDS or Ana2 UTRs leads to loss of centrosomes. Cultured *Drosophila* cells were depleted of Ana2 by RNAi with dsRNA against Ana2 CDS or dsRNA against Ana2 UTRs, with GST dsRNA as negative control. Centrosome numbers were scored after each round of RNAi on day 4, day 8 and day 12. Loss of Ana2 causes loss of centrosomes. 3x200 cells; error bars represent standard error.

4.2.3.2 Rescue of Ana2 depletion by Ana2-4D but not Ana2-4A

To test the biological significance of the four Plk4-phosphorylation sites in the STAN motif of Ana2, I performed rescue experiments, to study the effect of Ana2-4A and Ana2-4D on centrosome numbers after depletion of endogenous Ana2 in *Drosophila* cell culture. Ana2-4A and Ana2-4D carry mutations at the four identified Plk4-phosphorylation sites S318, S365, S370, and S373; with S to A (Serine to Alanine) mutations for the non-phosphorylatable Ana2-4A and S to D (Serine to Aspartic acid) mutations for the phospho-mimicking Ana2-4D respectively. In collaboration with Dr. Dzhindzhev, stable cell lines expressing pAct5-Ana2-WT, pAct5-Ana2-4A and pAct5-Ana2-4D, were depleted of endogenous Ana2 by RNAi with dsRNA against Ana2 UTR (versus negative control dsRNA

GST) for 12 days with a depletion round every four days. Cells were fixed and stained to reveal the centrosome markers D-Plp and Asl. DNA was stained with DAPI. Cells were analysed by automated microscopy, to analyse the percentage of cells without centrosomes (Figure 4-10, Figure 4-11). All three cell lines were treated with dsRNA against GST or Ana2 UTR for 12 days respectively, resulting in cells without centrosomes at 4.8% +/- 0.4% versus 11.5% +/- 1% for Ana2-WT expressing cells, 20.8% +/- 0.9% versus 83.5% +/- 0.3% for Ana2-4A expressing cells, and 9.3 % +/- 0.2% versus 22.7% +/- 2.7% for Ana2-4D expressing cells after GST RNAi versus Ana2 UTR RNAi (Figure 4-10). The expression of Ana2-WT and the phospho-mimicking Ana2-4D rescue the depletion of endogenous Ana2 and therefore can fully substitute for the endogenous protein. On the contrary, expression of the transgenic non-phosphorylatable Ana2-4A fails to rescue centrosome numbers, as the percentage of cells without centrosomes is higher after depletion of endogenous Ana2 versus the negative control of GST dsRNA. Additionally, the stable expression of Ana2-4A had a dominant-negative effect on centrosome numbers, with an increase of cells lacking centrosomes in 20.8% +/- 0.9% of cells, compared to 4.8% +/- 0.4% in Ana2-WT expressing cells after control-RNAi (dsRNA GST). Figure 4-11 shows a representative image of cells for each of the three cell lines after depletion of endogenous Ana2 for three rounds over 12 days. In cells expressing Ana2-WT and Ana2-4D, both centrosomal markers D-Plp and Asterless co-localise at the centrosomes whereas the signals for D-Plp and Asterless are greatly lost in the majority of cells expressing Ana2-4A, suggesting loss of centrosomes. Thus, depletion of endogenous Ana2 by its UTR can be rescued by Ana2-WT or Ana2-4D, but not by Ana2-4A. Therefore, the four identified Plk4 phosphorylation sites in the STAN motif of Ana2 (conserved S318, S365, S370, and S373) are functionally necessary to rescue the depletion of endogenous Ana2 and therefore important for centriole duplication.

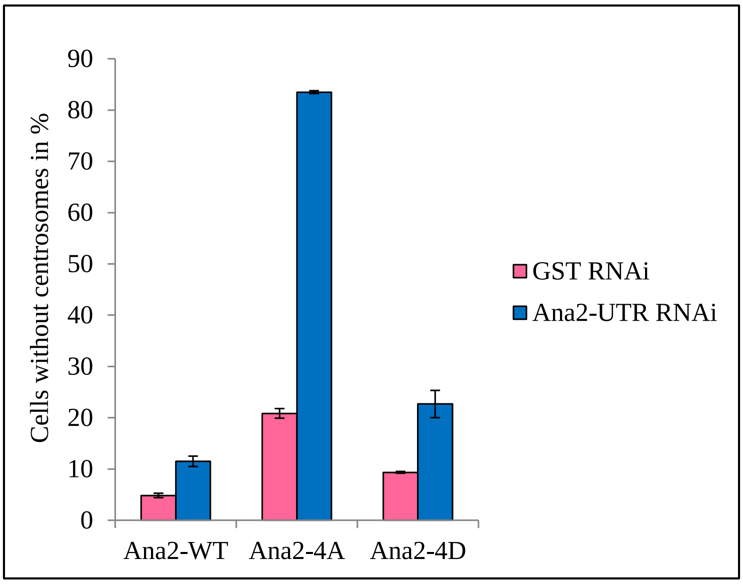

Figure 4-10 Ana2-WT or Ana2-4D but not Ana2-4A rescue the depletion of endogenous Ana2. Endogenous Ana2 was depleted from *Drosophila* cell cultures overexpressing pAct5c-Ana2-WT, pAct5c-Ana2-4A or pAct5c-Ana2-4D for 3 rounds of dsRNA treatment targeting Ana2 UTRs or control GST. Cells with zero centrosomes were counted on day 12. Error bars represent standard error; 3x200 cells counted.

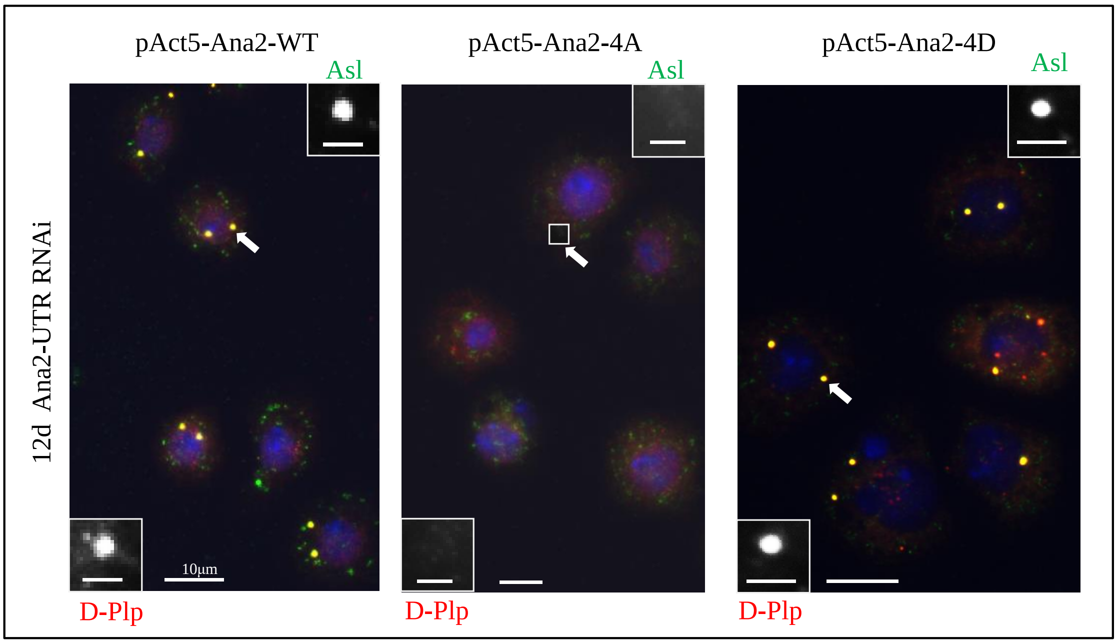

Figure 4-11 Centrosomal markers D-Plp (red) and Asterless (green), after 12 days of Ana2-UTR RNAi in *Drosophila* cell lines overexpressing Ana2-WT, Ana2-4A or Ana2-4D. Insets show enlarged centrosomes from one pole highlighted by arrows in monochrome for D-Plp and Asterless staining; insets scale bar represent 2µm. DNA was stained with DAPI. Main figure scale bars represent 10µm.

4.2.4 Ana2 can interact with Sas6 after it is phosphorylated by Plk4 *in vitro*

Sas5 and Sas6, the *C. elegans* homologues of *Drosophila* Ana2 and Sas6 respectively, are simultaneously recruited to the procentriole in *C. elegans* [53,91]. This raised the question of whether *Drosophila* Ana2 and Sas6 interact with each other. My *in vitro* and *in vivo* studies of direct protein binding (section 4.2.1.1) and mass spectrometry analyses of affinity purified Sas6 or Ana2 from *Drosophila* cell cultures (section 3.2.1.2), did not indicate any interaction between Ana2 and Sas6. However, the finding that Plk4 phosphorylates Ana2 but not Sas6 (section 4.2.2) raised the hypothesis, that in *Drosophila*, Plk4 phosphorylation of Ana2 might be essential for the interaction of Ana2 and Sas6. To analyse this hypothesis, I developed an efficient *in vitro* binding assay to test interactions of Sas6 with pre-phosphorylated Ana2. The final protocol, which was used for the following pre-phosphorylation-binding assays, was established by Dr. Lipinszki (section 2.8.3).

GST-tagged Ana2 and the non-phosphorylatable GST-tagged Ana2-4A were purified from *E. coli* onto resin and treated with active Plk4 (MBP-Plk4) or kinase-dead Plk4 (MBP-Plk4^{KD}) in a phosphorylation assay. Each pre-treated Ana2, Ana2-4A and GST sample (either with active Plk4 or kinase-dead Plk4) was then incubated with ^{35}S-Methionine-labelled Sas6 protein in binding assays, followed by multiple washes of the resin and analysis of the resulting complexes on SDS-PAGE (section 2.8.1). The wash steps remove any free ^{35}S-Methionine-labelled Sas6 from the resin. The SDS-PAGE was then dried and exposed. The resulting autoradiogram shows a signal from ^{35}S-Methionine-labelled Sas6 if it directly bound to a protein on resin (GST, GST-Ana2-WT, GST-Ana2-4A) (left panel of Figure 4-15). Only Plk4-phosphorylated Ana2 binds Sas6 directly *in vitro*, as seen by the detected ^{35}S-Methionine-labelled Sas6 signal in the autoradiogram. Importantly, there is no direct interaction between Ana2 and Sas6, when Ana2 was treated with kinase dead Plk4 (MBP-Plk4^{KD}), confirming the necessity of Plk4-mediated phosphorylation of Ana2, in such that it can interact with Sas6. GST does not interact with Sas6, either when treated with active or kinase dead Plk4. We also found that Ana2-4A, which cannot be phosphorylated by Plk4, cannot interact with Sas6. This indicates that the phosphorylation of Ana2 by Plk4 is necessary to allow Ana2 to interact with Sas6.

The above findings raised the question of whether Plk4 also regulates this interaction of Ana2 with Sas6 *in vivo*. In collaboration with Dr. Lipinszki, Co-IP studies on extracts of *Drosophila* cells confirmed that Ana2 interacts with Sas6, when it is phosphorylated by Plk4 (Figure 4-12). Transiently transfected *Drosophila* cell cultures co-expressing FLAG-Ana2-WT or FLAG-Ana2-4A with firstly, Sas6-Myc and secondly, non-degradable Plk4 ($Plk4^{ND}$) or kinase dead non-degradable Plk4 ($Plk4^{ND\text{-}KD}$) were FLAG immunoprecipitated, followed by SDS-PAGE and Western Blot analyses. Additionally, inputs were subjected to SDS-PAGE and Western Blot analyses. The input samples confirmed the presence of $Plk4^{ND}$ and $Plk4^{ND\text{-}KD}$ by anti-Plk4 antibody staining, Ana2 and Ana2-4D by-FLAG antibody staining, Sas6 by anti-Myc antibody staining and as a control anti-α-tubulin. The Western Blot analyses of the FLAG-IPs of the four samples confirm the presence of Ana2 and Ana2-4D in all the samples by anti-FLAG antibody staining. Sas6 was identified only in the FLAG-IP purification co-expressing FLAG-Ana2 with Sas6-Myc and non-degradable $Plk4^{ND}$. Hence, Sas6 is able to interact only with Ana2-WT and when Ana2 is phosphorylated by Plk4 *in vivo*. This confirms our previous *in vitro* observations.

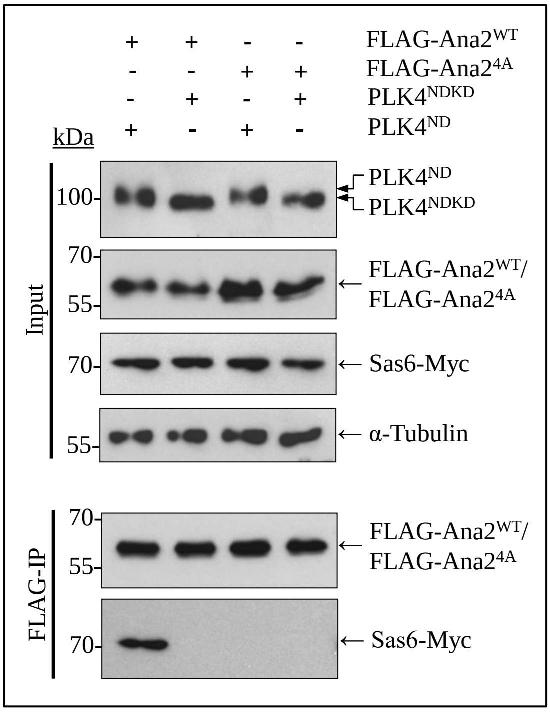

Figure 4-12 Plk4 phosphorylation of Ana2 triggers direct interaction of Ana2 and Sas6 *in vivo*. *Drosophila* cell cultures transiently overexpressing FLAG-Ana2-WT or the four Serine substitution mutant FLAG-Ana2-4A with Sas6-Myc and either the non-degradable degron mutant Plk4ND or the non-degradable kinase dead degron Plk4^{ND-KD} were subjected to FLAG-immunoprecipitation. Inputs of the *Drosophila* cell cultures and the FLAG-immunorecipitations were analysed by SDS-PAGE and Western blotting to reveal the indicated antigens. Experiment and image by Dr. Lipinszki [296].

4.2.4.1 The C-terminus of Ana 2 is nessessary for interaction with Sas6 *in vitro*

In section 4.2.4, I show that Sas6 directly binds Ana2 that was phosphorylated by Plk4, with the four main phosphorylation sites located within the Ana2-C-terminus (Figure 4-6). I wished to explore the possibilities if firstly, Sas6 binds only the Plk4-phosphorylated Ana2-C-terminus, or if secondly, Sas6 binds the Ana2-N-terminus, made accessable due to a confirmation change in Ana2 upon its phosphorylation by Plk4. To answer this question, I tested if Sas6 can directly bind Ana2-N-terminus (aa1-280) or Ana2-C-terminus (aa281-420), after treatment with active or kinase dead Plk4 (Figure 4-13). Together both Ana2 fragments cover the full length of the Ana2 sequence, with GST-Ana2-C containing only the four identified Plk4-phosphorylated Serine residues of the conserved STAN motif (S318, S365, S370, S373). The phosphorylation-binding-assays (section 2.8.3) confirm that after treatment with active Plk4, the Ana2-C-terminus but not Ana2-N-terminus interacts directly with Sas6. Treatment with kinase-dead Plk4 does not lead to their interaction. Plk4-phosphorylated Ana2-WT and Ana2-C-terminus bind Sas6 equally efficient, determined by equal Sas6 signals on the autoradiogram. In collaboration with Dr. Dzhindzhev, the phosphorylation assay of GST-Ana2-C-WT and GST-Ana2-C-4A treated with active MBP-Plk4 and ^{32}P-γ-ATP confirms that Ana2-C-terminus is phosphorylated by active Plk4 (Figure 4-14). Thus, the Plk4-phosphorylated Ana2-C-terminus is efficient and sufficient for direct interaction with Sas6.

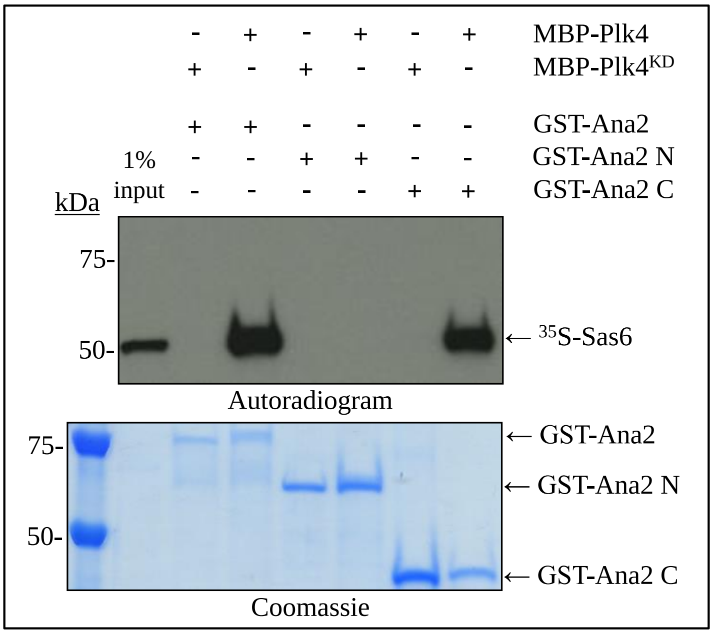

Figure 4-13 Plk4-phosphorylated Ana2-C (aa281-420) interacts directly with Sas6. GST-Ana2, GST-Ana2-N and GST-Ana2-C were treated with active or kinase dead Plk4 (MBP-Plk4 and MBP-Plk4^{KD} respectively) and incubated with ^{35}S-Methionine-labelled Sas6. The complexes were subjected to SDS-PAGE and autoradiography. SDS-PAGE shows comparable protein levels loaded of each protein sample. The respective autoradiogram shows 1% input of ^{35}S-Methionine-labelled Sas6 and interaction of GST-Ana2 and GST-Ana2-C with ^{35}S-Methionine-labelled Sas6 in a Plk4-phosphorylation dependent manner. GST-Ana2-N does not interact with ^{35}S-Methionine-labelled Sas6, independent of treatment with Plk4.

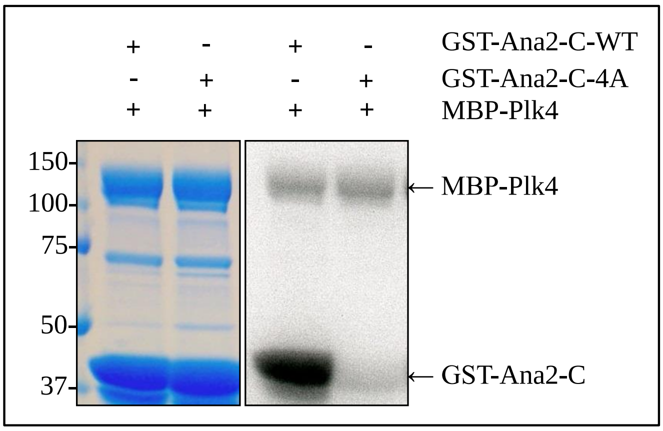

Figure 4-14 Plk4 phosphorylates GST-Ana2-C (aa281-420) at the four conserved Serines of Ana2-STAN motif. GST-Ana2-C (aa281-420) and GST-Ana2-C-4A (S318A, S365A, S370A, S373A) were incubated with active MBP-Plk4 and ^{32}P-γ-ATP, then subjected to SDS-PAGE and autoradiography. GST-Ana2-C is phosphorylated by MBP-Plk4. The Serine to Alanine substitution mutant (GST-Ana2-C-4A) is not phosphorylated by Plk4. The four conserved Serine residues in Ana2-STAN in the Ana2-C are necessary for phosphorylation by Plk4.

4.2.5 Plk4 phosphorylation of the four conserved Serines S318, S365, S370 and S373 within the Ana2-STAN motif are necessary for its interaction with Sas6

In section 4.2.4, I showed that Sas6 interacts with Ana2, when Ana2 is phosphorylated by Plk4. On the other hand, Ana2-4A, which has its four main Plk4 phosphorylation Serine residues S318, S365, S370 and S373 mutated to Alanine, cannot be phosphorylated. This raises the question of which of the four Serine residues contributes mainly to the Plk4-mediated phosphorylation of Ana2, that permits this interaction. To address this, I generated, expressed and purified Ana2 with S(erine) to A(lanine) mutations for each individual Serine residue identified as Plk4 phosphorylation residues in the conserved Ana2 STAN motif (section 4.2.4.1), generating GST-Ana2-S318A, GST-Ana2-S365A, GST-Ana2-S370A, and GST-Ana2-S373A. These fusion proteins were bound to resin and subjected to active Plk4 (MBP-Plk4) or kinase dead Plk4 (MBP-Plk4^{KD}) before incubation with ^{35}S-Methionine-labelled Sas6 (section 2.8.3). The samples were then washed and analysed on SDS-PAGE, followed by autoradiography of the dried gels (Figure 4-15). The autoradiogram shows reduced ^{35}S-Methionine-Sas6 binding with each of the Ana2 single-site mutation proteins, when treated with active Plk4, compared to the interaction with Plk4-phosphorylated Ana2-WT protein. The strongest reduction of the binding of ^{35}S-Methionine-labelled Sas6 to Ana2 can be seen when S373 or S370 are mutated to Alanine, with the latter showing the greatest effect. Control binding assays using kinase dead Plk4 show weak background binding of ^{35}S-Methionine-labelled Sas6 to the Ana2 single-site mutation proteins evident in long exposures.

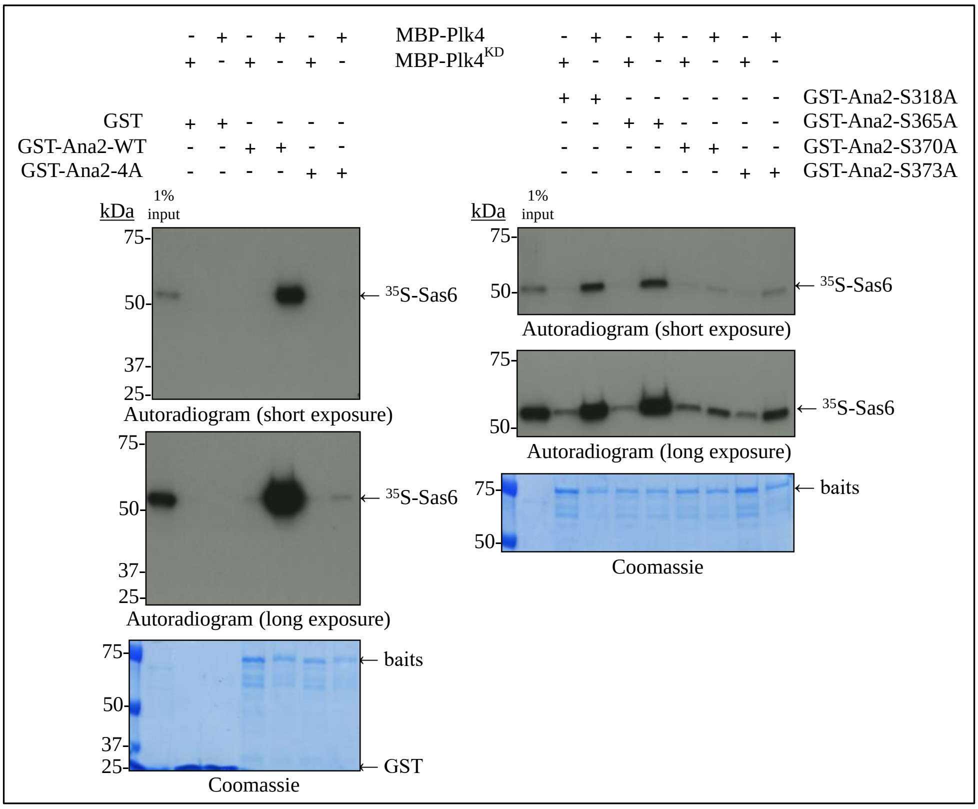

Figure 4-15 Plk-4 mediated phosphorylation of four conserved Serines within the Ana2-STAN motif is essential for its interaction with Sas6. Alanine substitution mutation of all four conserved Serines within the Ana2-STAN motif is necessary to abolish the Plk4-mediated interaction of Ana2 with Sas6. Individual Serine to Alanine substitutions do not fully abolish the interaction. S370A results in the greatest reduction of Sas6 binding to Ana2. GST, GST-Ana2-4A and individual Serine to Alanine mutation GST-Ana2 proteins (GST-Ana2-S318A, GST-Ana2-S365A, GST-Ana2-S370A, GST-Ana2-S373A) were treated with active or kinase dead Plk4 MBP-Plk4 and MBP-Plk4^{KD} respectively, followed by incubation with ^{35}S-Methionine-labelled Sas6. Complexes were subjected to SDS-PAGE and autoradiography.

In summary, mutations of individual Serine residues in the conserved STAN motif of Ana2 do not abolish the interaction of Sas6 with phosphorylated Ana2 although mutation of S370 has a significant effect. Together our findings point to the importance of phosphorylation of the four conserved Serine residues in the Ana2-STAN motif for interaction with Sas6 and thus the centriole duplication pathway.

4.2.5.1 Plk4-phosphorylation of all four conserved Serine residues in the STAN motif contribute to the direct interaction of Ana2-C and Sas6

The data provided in section 4.2.5 shows that Plk4-phosphorylation of all four conserved Serine residues in the Ana2-STAN motif, rather than a single site, are necessary for efficient direct interaction with Sas6. In section 4.2.4 and 4.2.4.1 I show that full-length Ana2 and Ana2-C-terminus, both Plk4-phosphorylated, bind Sas6 with equal efficiency. Therefore, I wanted to test if single mutations of the four conserved Serine residues in Ana2-C-terminus behave like their single mutations in full-length Ana2 or if the absence of Ana2-N-terminus might affect interaction with Sas6. I introduced single (S)erine to non-phosphorylatable A(lanine) mutations at S318A, S365A, S370A and S373A in Ana2-C-terminus. Each mutation lowers the efficiency of Ana2-C to bind Sas6 but no single mutation abolishes the interaction with Sas6 completely (Figure 4-16, right panel). The mutation of S373A and particularly S370A reduce the level of Sas6 binding to Plk4-phosphorylated Ana2-C the greatest. The interaction between Ana2-C-terminus and Sas6 can still be seen when only the three most C-terminal of the four Serine residues are mutated to non-phosphorylatable A(lanine) in Ana2-C-3A (S365A, S370A, and S373A). Thus, the findings for Ana2-C are in line with the findings for full-length Ana2 that all four conserved phosphorylation sites in Ana2-STAN contribute to the interaction of Ana2-C/Ana2 with Sas6, but S370 contributes the greatest.

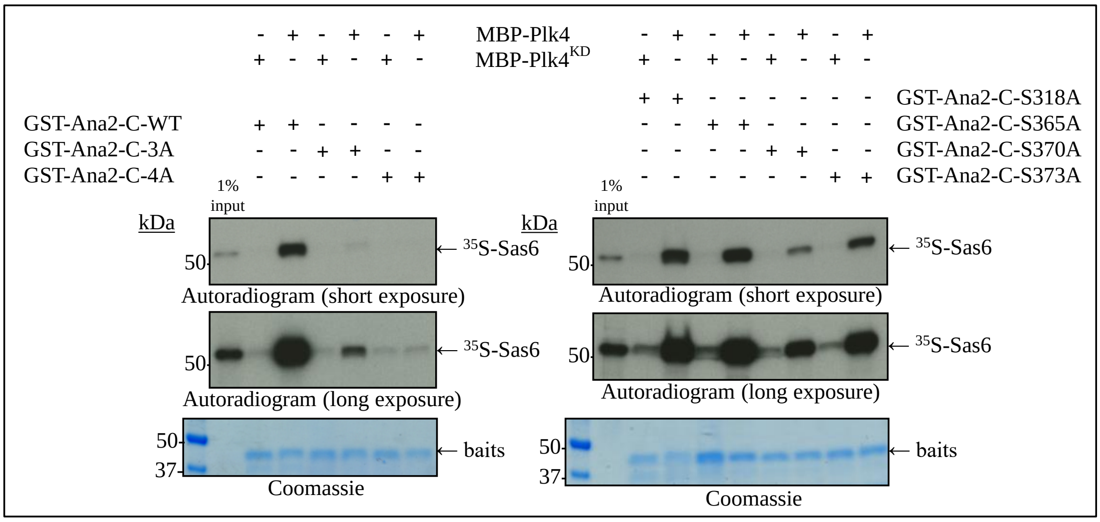

Figure 4-16 Plk-4 mediated phosphorylation of all four conserved Serines within the Ana2-STAN motif is essential for the interaction of GST-Ana2-C-terminus (aa281-420) with Sas6. GST-Ana2-C, GST-Ana2-C-3A, GST-Ana2-C-4A and individual Serine to Alanine mutation GST-Ana2-C proteins (GST-Ana2-C-S318A, GST-Ana2-C-S365A, GST-Ana2-C-S370A, GST-Ana2-C-S373A) were treated with active or kinase dead Plk4 (MBP-Plk4 and MBP-Plk4^{KD} respectively), followed by binding assay with ^{35}S-Methionine-labelled Sas6. Complexes were subjected to SDS-PAGE and autoradiography. Coomassie stainings show protein inputs of GST-Ana2-C constructs on residue. Autoradiogram (left) show abolished interaction between Sas6 and Ana2-C-4A only. Ana2-C-3A alone (S365A, S370A, S373A, left) and individual Ana2-C mutants (right) cannot fully inhibit interaction with Sas6. Importantly, S370A resulting in the greatest reduction of Sas6 binding to Ana2-C. The Alanine substitution mutation of all four conserved Serines within the Ana2-STAN motif is necessary to abolish the Plk4-mediated interaction of Ana2-C with Sas6.

4.2.6 Ana2-4A does not bind Sas6 but Ana2-4D does

As shown in section 4.2.3.2, Ana2-4A causes loss of centrosomes in the absense of wild-type Ana2 and expression of Ana2-4D and Ana2-WT rescues the loss of centrosomes. Ana2, phosphorylated by Plk4, interacts with Sas6 *in vitro* and *in vivo* (section 4.2.4). Non-phosphorylatable Ana2-4A does not interact with Sas6 *in vitro* and phosphorylation of all four Serine residues (S318, S365, S370, S373) is necessary for interaction of Ana2 with Sas6 (section 4.2.4 and 4.2.5). Together, this raises the hypothesis that the observed loss of centrosomes in Ana2-4A expressing cells (section 4.2.3.2) results from lack of interaction of

Ana2 with Sas6, due to the non-phosphorylation of the Ana2-STAN motif by Plk4. Therefore, I analysed if the phosphomimick Ana2-4D can interact with Sas6 *in vitro* or if the interaction of Ana2 and Sas6 is otherwise dependent on Plk4 and not alone dependent on the Ana2-STAN motif phosphorylation by Plk4. To this end, I used GST-alone, GST-Ana2, GST-Ana2-4A and GST-Ana2-4D that I treated with active MBP-Plk4 or kinase dead MBP-Plk4^{KD} and then subjected to a binding assay with ^{35}S-Methionine-labelled Sas6 (section 2.8.3). This showed that GST-Ana2 interacts strongly with Sas6 only after treatment with active Plk4 but shows weak background binding for the GST-Ana2 treated with kinase dead Plk4. GST-Ana2-4A does not interact with Sas6 (independent of treatment with active or kinase dead Plk) (Figure 4-17). On the other hand, GST-Ana2-4D which phosphomimicks the phosphorylation of the Ana2-STAN motif by Plk4, shows a strong interaction with ^{35}S-Methionine-labelled Sas6 independent of treatment with active or kinase dead Plk4. Thus the four conserved Serines in the Ana2-STAN motif must be phosphorylated by Plk4 to allow for the specific interaction of Sas6 with Ana2.

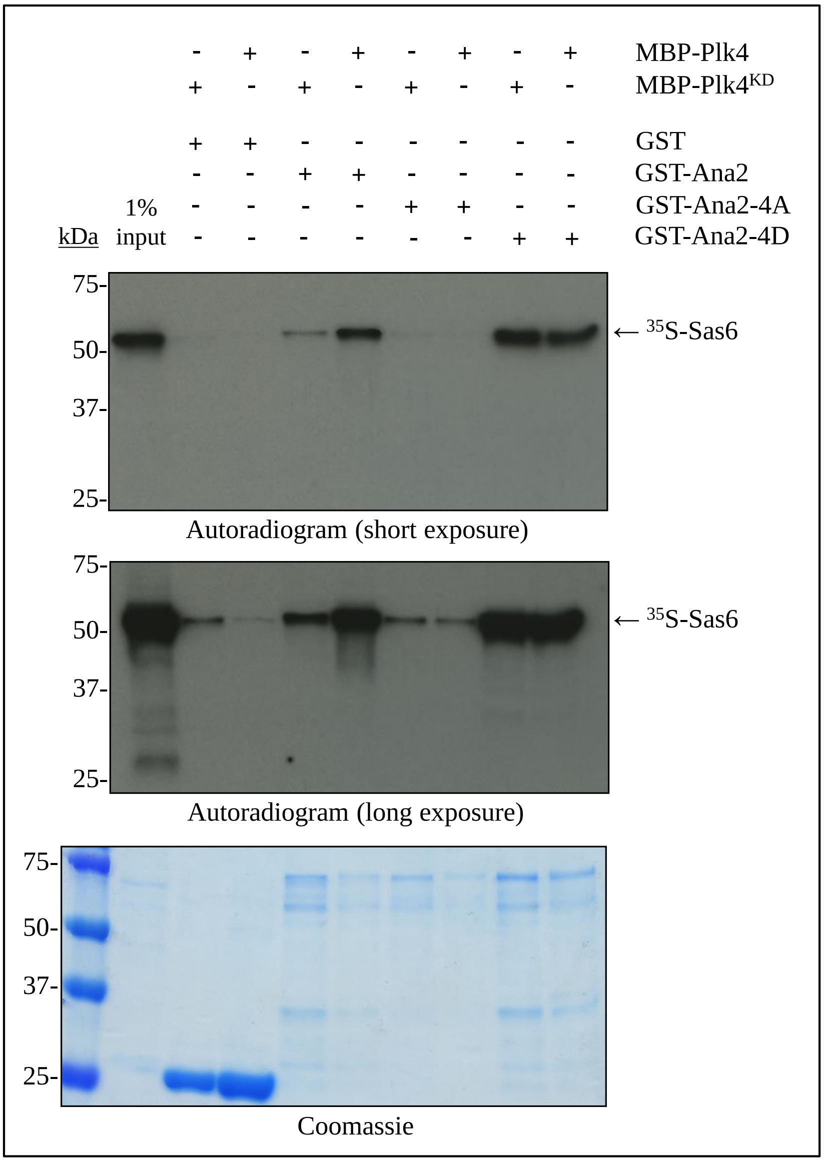

Figure 4-17 Ana2-4D interacts with Sas6 independently of Plk4 treatment *in vitro*. GST, GST-Ana2, GST-Ana2-4A and GST-Ana2-4D were treated with active or kinase dead Plk4 (MBP-Plk4 and MBP-Plk4^{KD} respectively) and incubated with ^{35}S-Methionine-labelled Sas6. The complexes were subjected to SDS-PAGE and autoradiography. Interaction of Sas6 with Ana2 is dependent on phosphorylation of the four conserved Serines within the Ana2-STAN motif, with Serine to Alanine mutations (non-phosphorylatable mutant) abolishing interaction, and Serine to Aspartic acid mutations (phospho-mimicking mutant) exhibiting interaction independent of pre-Plk4-treatment of Ana2.

4.2.7 Selective regulation of Ana2 binding by Plk4 phosphorylation

The interaction of Sas6 and Ana2 early on in the assembly of the new daughter centriole during centriole duplication is conserved. In *C. elegans* Spd2 recruits Zyg-1 and then Sas5 and Sas6 assemble to the forming procentriole [53,91]. However other screens have identified further proteins involved in the assembly of the daughter centriole, suggesting that other protein interactions might be regulated by Plk4 mediated phosphorylation.

This led me to test whether further centriole duplication proteins interact with Ana2 downstream of its phosphorylation by Plk4. I tested whether Ana1, Bld10, Rcd4 and Sas4 proteins, that are known to be involved in centriole duplication [131,288], might preferentially interact with Plk4-phosphorylated Ana2 (Figure 4-18). I treated GST-Ana2-WT with active or kinase dead Plk4, followed by incubation with ^{35}S-Methionine-labelled protein Ana1, Bld10, Rcd4, Sas4 and Sas6. The complexes were then analysed by SDS-PAGE and autoradiography (Figure 4-18). I found that Ana2 interacts with Sas4 independent of whether treated with active or kinase dead Plk4. Similarly, interaction of Bld10 occurred with phosphorylated and non-phosphorylated Ana2 but the interaction increases significantly when Ana2 is phosphorylated by Plk4. Rcd4 and Ana1 do not show any interaction with phosphorylated or non-phosphorylated Ana2. And as previously shown, Plk4-phosphorylated Ana2 interacts with Sas6 (section 4.2.4). These results show and strengthen the finding of the importance and specificity of the phosphorylation of Ana2 to fully trigger its interaction with Sas6.

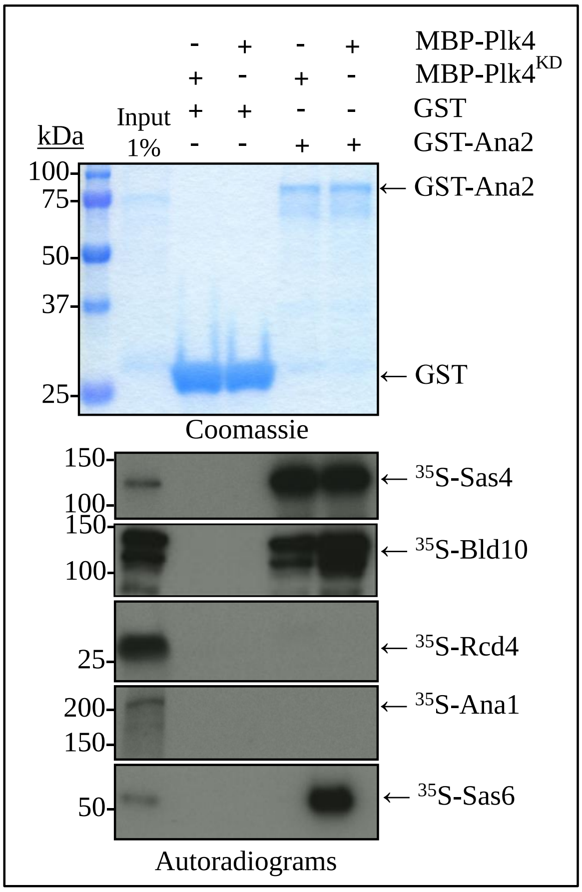

Figure 4-18 Interactions of different centriolar proteins with Ana2 following Plk4-phosphorylation of Ana2. GST-Ana2 was treated with active or kinase dead Plk4 (MBP-Plk4 and MBP-Plk4^{KD} respectively) and incubated with ^{35}S-Methionine-labelled Sas4, Bld10, Rcd4, Ana1 or Sas6. The complexes were subjected to SDS-PAGE and autoradiography. SDS-PAGE shows representative protein inputs of GST and GST-Ana2. Sas6 interacts with pre-phosphorylated Ana2 (MBP-Plk4 treated) but does not interact with Ana2 when treated with kinase dead Plk4 (MBP-Plk4^{KD}). Sas4 interacts with Ana2 independently of its phosphorylation state. Bld10 shows interaction with Ana2 but Plk4-mdiated phosphorylation of Ana2 increases the interaction. Rcd4 and Ana1 do not show interaction with Ana2, independent of treatment with active or kinase dead Plk4.

4.2.8 Physical interaction of Ana2 and Sas6

4.2.8.1 Plk4-mediated phosphorylation of the conserved Ana2-STAN motif is sufficient for binding of Sas6 to Ana2 *in vitro*

After I determined that the C-terminal Ana2-fragment (aa281-420), which contains the STAN motif and is phosphorylated by Plk4, is sufficient to bind Sas6, I wished to determine the smallest Ana2 region necessary for interaction with Sas6. As we know the signifiance of the STAN motif for Plk4-phosphorylation and as the STAN motif is conserved between species, I focused on this C-terminal Ana2 region. Therefore I generated Ana2-fragments which contain the STAN motif only (aa315-384), and constructs with additional sequence upstream and/or dowstream of the STAN motif (Figure 4-19). The Ana2-STAN constructs I made were: Ana2 aa315-384 (STAN only), Ana2 aa305-394, Ana2 aa295-404 and Ana2 aa315-420 (Figure 4-19), and Ana2 full length and Ana2-C (aa281-420) as controls. I expressed and purified the Ana2-STAN protein samples onto resin (section 2.5.1) and performed Plk4 phosphorylation assays, using active or kinase dead Plk4, followed by binding assays with ^{35}S-Methionine-labelled Sas6 (section 2.8.3). Figure 4-20 shows the coomassie stainings and autoradiograms of the binding assays of ^{35}S-Methionine-labelled Sas6 with the analysed Ana2 fragments, Ana2-FL and Ana2-C as controls. Significantly, when the Ana2 constructs are treated with kinase dead Plk4, none of them interact with ^{35}S-Methionine-labelled Sas6. On the other hand, when these Ana2 constructs are treated with active Plk4 kinase, all interacted with ^{35}S-Methionine-labelled Sas6 but with different efficiencies. Similar binding of ^{35}S-Methionine-labelled Sas6, as observed with Ana2-WT and Ana2-C can be seen for Ana2-STAN (aa315-384) and Ana2-aa315-420. The further two Ana2-STAN constructs analysed (aa295-404 and aa305-394) did not interact as strongly with ^{35}S-Methionine-labelled Sas6. In summary, the Ana2-STAN motif alone interacts as efficiently as Ana2-C with ^{35}S-Methionine-labelled Sas6 when phosphorylated by Plk4.

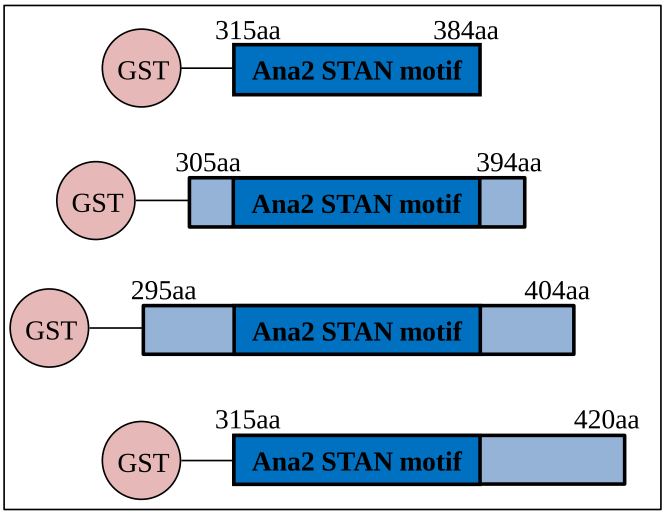

Figure 4-19 Schematic summary of Ana2-STAN constructs analysed for interaction with Sas6. Four N-terminal GST-tagged Ana2 constructs were generated: the first containing the Ana2-STAN motif only (aa315-384); the second including 10 additional amino acids upstream and downstream of the Ana2-STAN motif (aa305-394); the third including 20 additional amino acids upstream and downstream of the Ana2-SAN motif (aa295-404); and the fourth including the C-terminal part of Ana2 sequence after the STAN motif (aa315-420).

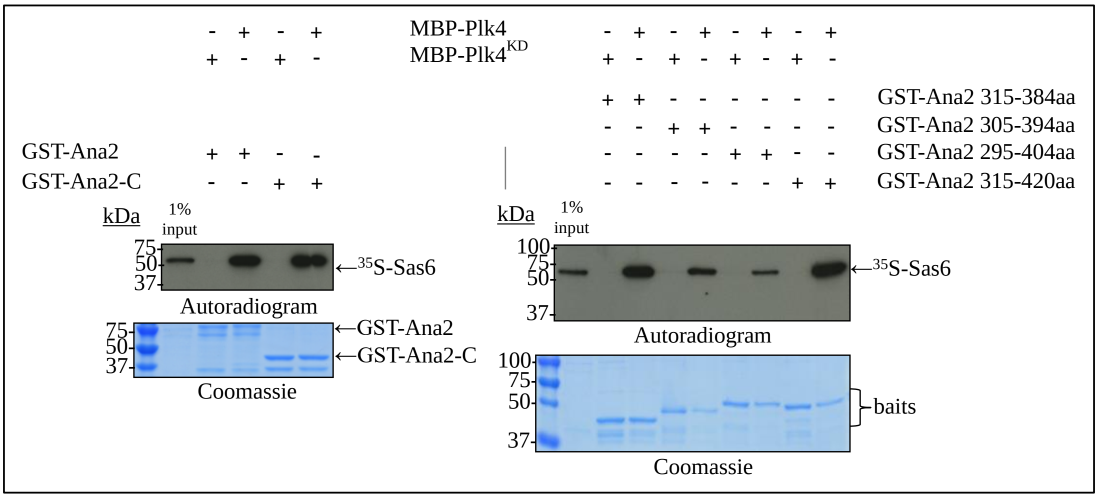

Figure 4-20 Plk4-phosphorylated Ana2-STAN motif is sufficient to interact with Sas6. GST-Ana2, GST-Ana2-C and the four GST-Ana2 constructs summarised in Figure 4-19 were treated with active or kinase dead Plk4 (MBP-Plk4 and MBP-Plk4^{KD} respectively) and incubated with ^{35}S-Methionine-labelled Sas6. Complexes were subjected to SDS-PAGE and autoradiography. Coomassie stainings show bait protein amounts. Autoradiograms show interaction of ^{35}S-Methionine-labelled Sas6 with all phosphorylated Ana2 constructs. GST-Ana2-STAN-only (aa315-384) being the smallest construct interacting as efficiently as GST-Ana2 full-length with Sas6.

4.2.8.2 The aa276-432 coiled-coil segment of Sas6 interacts with Ana2 that has been phosphorylated by Plk4

From section 4.2.8.1, we know that the C-terminal STAN motif of Ana2 is the smallest Ana2 domain which, after it has been phosphorylated by Plk4, interacts with Sas6. But what is the reciprocal domain within Sas6 that interacts with Ana2? To answer this question I generated Sas6 constructs representing the N-terminal head domain of Sas6 (aa1-180), the majority of the predicted coiled-coil domain of Sas6 (aa181-408), a construct combining these two regions (aa1-408), and a construct representing the whole coiled-coil domain with its most C-terminal unstructured region (aa181-472). The generation of the unstructured C-terminus alone or with additional amino acids from the most C-terminal part of the coiled-coil domain (aa421-472) was not possible, due to the small fragment size of 64aa and the size limitations of the *in vitro* transcription-translation system.

In collaboration with Dr. Lipinszki, these constructs were subjected to binding assays with ^{35}S-Methionine-labelled Ana2 that showed only one constructs was able to interact with Ana2, namely Sas6 aa181-472, which represents the whole coiled-coil and C-terminal unstructured domain of Sas6. Thus, the Sas6 N-terminal head domain alone and the Sas6 head domain together with the majority of the coiled-coil domain (aa1-180 and aa1-408 respectively) do not interact with Ana2. This raises the question of which specific region of Sas6 is necessary for interaction with Ana2. From the initial interaction assays it appeared possible that the regions of Sas6 which may interact with Ana2 are: the whole coiled-coil region, a C-terminal part of the coiled-coil region, the unstructured Sas6-C-terminus, or indeed the unstructured Sas6-C-terminus together with the whole coiled-coil region or together with a C-terminal fragment of the coiled-coil region. To distinguish these possibilities, I generated constructs of Sas6 protein fragments for *in vitro* transcription-translation, which were truncated N-terminal of the identified Sas6 fragment that interacts with phosphorylated Ana2 (Sas6 aa181-472) or C-terminal of full-length Sas6. Figure 4-21 summarises the constructs I generated and their ability to interact with Plk4-phosphorylated Ana2; dark blue represents a strong interaction, light blue a good interaction and yellow no interaction. I generated ^{35}S-Methionine-labelled Sas6 protein fragments by *in vitro* transcription-translation reactions and carried out binding assays with GST-Ana2 (pre-treated with active or kinase dead Plk4). I then subjected the complexes to SDS-PAGE and exposed dried gels to autoradiography. The constructs with N-terminal truncations were Sas6: aa221-472, aa261-472, aa266-472, aa271-472, aa276-472, aa291-472, aa295-472, aa341-472, aa351-472, aa361-472, aa371-472 and aa381-472. The smallest Sas6 construct that shows good interaction with phosphorylated Ana2 is Sas6 aa276-472 (Figure 4-22). The additional constructs analysed were truncated from the C-terminus of full-length Sas6: aa1-462, aa1-452, aa1-442, aa1-437, aa1-432, aa1-427, aa1-422, aa1-414, and aa1-412. The most truncated Sas6 fragment still showing good interaction with phosphorylated Ana2 was Sas6 aa1-432 (Figure 4-23). In summary, these findings show that Sas6 aa1-432 and Sas6 aa276-472 are the most C- and N-terminal truncated Sas6 fragments respectively, that interact with phosphorylated Ana2 (Figure 4-22, Figure 4-23). This experiment defines the Sas6 domain directly interacting with phosphorylated Ana2 *in vitro* as aa276-432 (Figure 4-21, Figure 4-24). From structural Sas6 protein predictions, this suggests, that it is the C-terminal part of the coiled-coil domain of Sas6 that interacts with Plk4-phosphorylated Ana2.

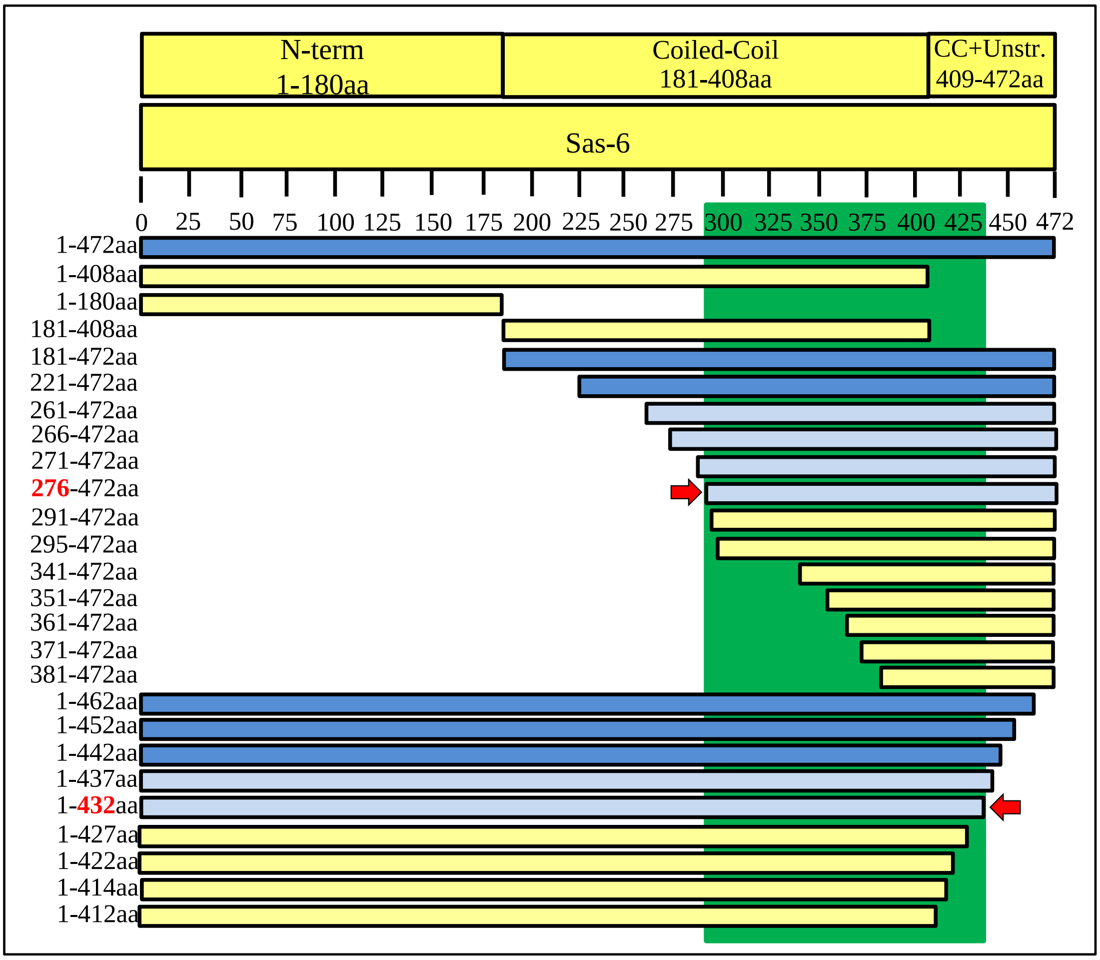

Figure 4-21 Schematic overview of Sas6 constructs, which were studied in an *in vitro* screen for interaction with Plk4-phosphorylated Ana2, determines Sas6 aa276-432 as the most N- and C-terminal truncated region interacting with Ana2. GST-Ana2 was treated with active or kinase dead Plk4 (MBP-Plk4 or MP-Plk4^{KD} respectively) and incubated with *in vitro* transcribed and translated ^{35}S-Methionine-labelled Sas6 constructs summarised. Complexes were subjected to SDS-PAGE and autoradiography. Green background highlights the smallest Sas6 region directly interacting with Plk4-phosphorylated Ana2 *in vitro*. Sas6 constructs and their individual interaction with Plk4-phosphorylated Ana2 are visualised in yellow (no interaction), light blue (good interaction) and darker blue strong interaction). Red arrows indicating the most N- and C-terminal truncated Sas6 constructs still interacting efficiently with Plk4-phosphorylated Ana2.

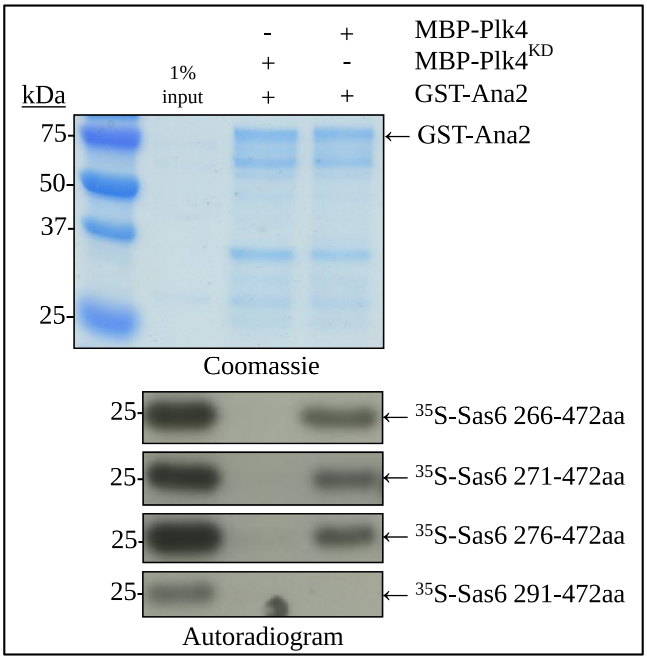

Figure 4-22 Most N-terminal truncated Sas6 construct interacting with Plk4-phosphorylated Ana2 defined as Sas6 aa276-472. GST-Ana2 was treated in a phosphorylation assay with active MBP-Plk4 or kinase dead MBP-Plk4^{KD} and incubated with different ^{35}S-Methionine-labelled Sas6 constructs truncated from the N-terminus in direct binding assays *in vitro*. Complexes were subjected to SDS-PAGE and autoradiography. The Coomassie stained gel shows GST-Ana2 inputs. The autoradiograms show four of the analysed Sas6 constructs, including the smallest (Sas6 aa276-472) and two larger Sas6 fragments (Sas6 aa271-472 and aa266-472) that interact with Plk4-phosphorylated Ana2, and a smaller Sas6 construct (Sas6 aa291-472) that does not interact with Ana2. Summary of all analysed Sas6 constructs in Figure 4-21.

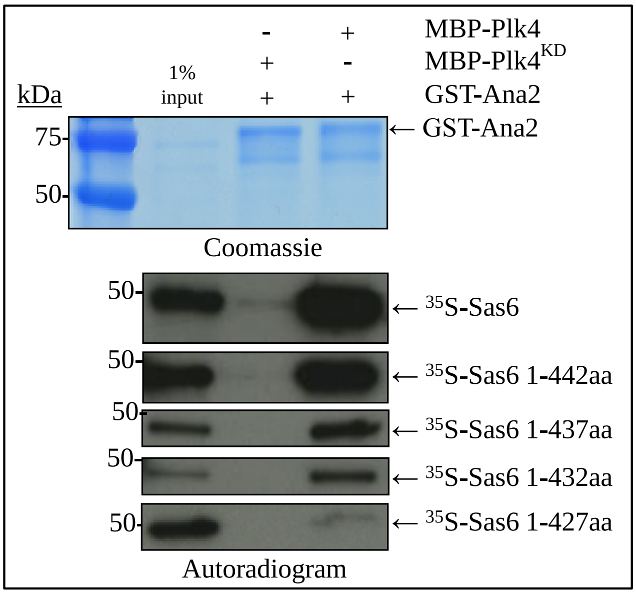

Figure 4-23 Sas6 construct most truncated from the C-terminus and still interacting with Plk4-phosphorylated Ana2 is Sas6 aa1-432. GST-Ana2 was treated with active MBP-Plk4 or kinase dead MBP-Plk4^{KD} in a phosphorylation assay, and incubated with different ^{35}S-Methionine-labelled Sas6 constructs truncated from the C-terminus in *in vitro* binding assays. Complexes were subjected to SDS-PAGE and autoradiography. Coomassie shows GST-Ana2 protein inputs. Autoradiograms show four of the analysed Sas6 constructs in comparison to full-length Sas6 interacting with Plk4-phosphorylated Ana2. Sas6 aa1-427 lacking interaction with Ana2, and Sas6 aa1-432 and larger fragments (aa1-437, aa1-442) interacting with Plk4-phosphorylated Ana2. Summary of all analysed Sas6 constructs in Figure 4-21.

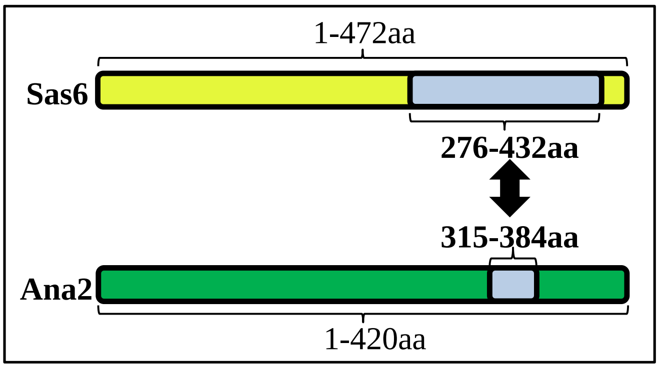

Figure 4-24 Summary of the findings of *in vitro* interaction studies: The Plk4-phosphorylated Ana2-STAN motif (blue, aa315-384) directly interacts with the Sas6 region aa276-432 (blue).

4.3 Discussion

This chapter focuses on the protein kinase Plk4 and the centriole duplication proteins Ana2 and Sas6. It elucidates their interaction, phosphorylation, dependencies, and strikingly describes their function in the initial steps of procentriole formation. The performed work results in the major centriole duplication related finding, that Plk4-mediated phosphorylation of the conserved STAN motif in Ana2 triggers its interaction with the cartwheel protein Sas6 and enables procentriole formation in *Drosophila*. This new knowledge is one further piece towards understanding the puzzle of the timely link of centriole duplication to only once per cell cycle in order to maintain correct centrosome numbers.

Initial protein interaction studies show that bacterial expressed and purified Plk4 and Ana2 interact directly with the ^{35}S-Methionine-labelled counter protein, expressed in an *in vitro* transcription-translation system, in *in vitro* interaction assays (section 4.2.1.1, Figure 4-1). In contrast, the cartwheel protein Sas6 does not interact with Plk4 or Ana2 in direct *in vitro* interaction assays (section 4.2.1.1, Figure 4-2). Plk4 is described as the master kinase of centriole duplication, as its overexpression induces centriole duplication in cell culture and *de novo* centriole formation in *Drosophila* unfertilized eggs, and depletion of Plk4 causes loss of centrosomes [83–85,96,289]. Plk4 is recruited to the centriole by Asterless [92] but little is known about Plk4 and its substrates in the centriole duplication process. It is known from *C. elegans*, that Sas5 and Sas6 are recruited to the centriole after the recruitment of Zyg-1 [53,91], the Plk4 homologue. This suggests that the *Drosophila* homologues Ana2 and Sas6 might be recruited in a similar timely manner. The finding in section 4.2.1.1, that Plk4 and Ana2 interact directly with each other *in vitro* supports this idea. In *C. elegans*, Sas5 and Sas6 are recruited simultaneously and co-dependently to form the central tube, which then further enlarges with the recruitment of Sas4. But the exact molecular mechanism of the Sas5 and Sas6 interaction is still not fully understood. It is suggested that the C-terminal Sas5 domain (aa390-404) interact with a narrow region in the Sas6 coiled-coil domain (aa275-288) [302]. And additionally, that the N-terminal domain of Ana2 (aa82-260) forms a tetramer, which then connects four Sas6 homodimers in two neighbouring rings of the central tube [304] (Figure 4-25). Importantly, the direct and phosphorylation-independent interaction of Zyg-1 with the Sas6 coiled-coil domain results in the recruitment of the Sas6-Sas5 complex to the mother centriole [15]. Both these findings from *C. elegans* differ to the findings observed and described here, where *Drosophila* Sas6 does not directly interact with Plk4 or Ana2 *in vitro* (section 4.2.1.1, Figure 4-2).

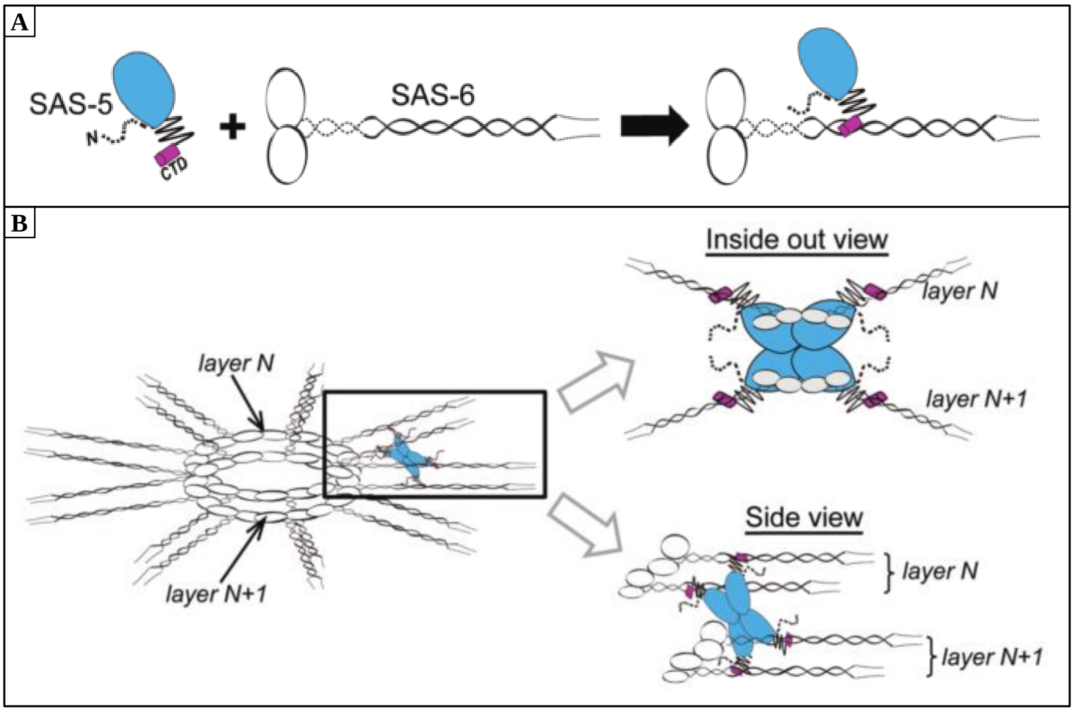

Figure 4-25 Schematic model how *C. elegans* Sas5 and Sas6 might interact to form the central hub of the centriole. (A) shows a Sas5 molecule interact with a central region of a Sas6 homodimer. Figure from [304] and as previously reported in [302]. (B) shows a model how tetrameric Sas5 could interact with two Sas6 homodimers from two neighbouring rings each in the central hub assembly of *C. elegans*. Figure reproduced with permission from [304].

The analyses of centriole duplication proteins and their possible role as phosphorylation substrates of Plk4 go in line with the direct interaction results. Two versions of Plk4 are used in the performed phosphorylation assays, firstly, an active form of Plk4 (MBP-Plk4-T172E), which has auto-phosphorylation activity, and secondly a kinase dead form of Plk4 (MBP-

Plk4-T172E-K43M). The phosphorylation activity of MBP-Plk4-T172E was shown by bandshift on SDS-PAGE due to auto-phosphorylation of the protein in comparison to the kinase dead Plk4 form (section 4.2.1.2, Figure 4-3). Additionally, treatment of active Plk4 with lambda-phosphatase, which releases phosphate groups from phosphorylated Serine, Threonine and Tyrosine residues, reverses the bandshift to the motility seen by kinase dead Plk4, confirming that MBP-Plk4-T172E is active and can phosphorylate (section 4.2.1.2, Figure 4-3). Phosphorylation assays with N-terminal MBP-tagged Ana2 and Sas6 (section 4.2.1.2, Figure 4-4) and N-terminal GST-tagged Ana2 (section 4.2.1.2, Figure 4-5) show that Plk4 phosphorylates MBP- and GST-N-terminal tagged Ana2 but not MBP-Sas6. The finding of Ana2 phosphorylation by Plk4 but the lack of Sas6 phosphorylation by Plk4 is incomparable to findings in *C. elegans* and human cells. In *C. elegans*, the Plk4 homologue Zyg-1 recruits Sas6 in a phosphorylation-independent manner, which in turn is in a pre-formed complex with Sas5, the Ana2 homologue [15]. However, it was previously described that Sas6 is phosphorylated by Zyg-1 at S123, and that this phosphorylation is crucial for centriole formation *in vivo* and it ensures the maintenance of Sas6 at the procentriole [113]. On the other hand, two publications show that the Serine/Threonine protein phosphatase 2A (PP2A) regulates Sas5 recruitment to the centriole. It is suggested that phosphorylation of Sas5 inhibits its recruitment to the procentriole [119] or that phosphorylation of Sas5 promotes its destruction [305]. However, neither publication show evidence for which kinase phosphorylates Sas5 in the first instance. It was suggested that Zyg-1 kinase regulates Sas5 association with the centrioles because *zyg-1* mutant embryos show normal cytoplasmic levels of Sas5 but lack centriolar localisation of Sas5 [72]. In summary, the *C. elegans* Sas5-Sas6-complex is positively regulated by a combination of PP2A dephosphorylating Sas5 and the Zyg-1 kinase phosphorylating Sas6. Presumably this is also the order of events, as PP2A does not localise to the centriole whereas Zyg-1 does. Additionally, at the time of my experiments, there had been no published evidence about the Plk4 phosphorylation of STIL or Sas6, the human homologues of Ana2 and Sas6. In summary, the phosphorylation of *Drosophila* Ana2 by Plk4 but on the other hand the lack of Sas6 phosphorylation by Plk4 is an intriguing new observation.

It is important to understand the phosphorylation of Ana2 by Plk4 and the potential role of this phosphorylation in centriole duplication, thus all Plk4 phosphorylation sites were identified by phospho-peptide mapping by mass spectrometry (section 4.2.2, Table 4‑1). Samples for analyses were either purified ProteinA-Ana2 from cultured *Drosophila* cells co-expressing non-degradable Plk4 or *in vitro* phosphorylated GST-Ana2 protein. The highest spectral counts identified *in vitro* and *in vivo* were S318 and S365/S370/S373. Further but weaker Plk4-phosphorylation sites are present in Ana2-N-terminus (section 4.2.2, Figure 4-6). The dominance of phosphorylation sites in the Ana2-C-terminus (aa281-420) is confirmed by the phosphorylation assay (section 4.2.2, Figure 4-8), which shows a stronger phosphorylation signal for C-terminal Ana2 than for N-terminal Ana2 (aa1-280). The significance of the phosphorylation of Ana2 in its C-terminal part suggests an evolutionary conserved region within Ana2. Ana2 does not exhibit a strong sequence homology between species and only recently has *Drosophila* Ana2 been identified as the functional orthologue of *C. elegans* Sas5 [116] and of human STIL. This is despite STIL having been described in connection with T-cell acute lymphoblastic leukaemia as early as 1991 [306] and more recently as being defective in primary microcephaly [307]. Structural similarities between Sas5, Ana2 and STIL exist; all proteins have a predicted central coiled-coil domain, a TIM motif at the most C-terminus (aa407-420 in *Drosophila*) [117] and most significantly a STAN motif localised in their C-terminal regions. A homology alignment of the STAN motif regions of different species confirms the high significance of the identified Plk4 phosphorylation sites S318, S365, S370 and S/T373 in Figure 4-7, as they are conserved between species. Due to the high spectral count of the four Serine sites in *Drosophila* Ana2 (section 4.2.2, Table 4‑1), the visually high Plk4-phosphorylation of Ana2-C-terminus compared to Ana2-N-terminus *in vitro* (section 4.2.2, Figure 4-8), and the conservation of these sites throughout different species (section 4.2.2, Figure 4-7), my focus was upon the further characterisation of Ana2 and its Plk4-phosphorylation on S318, S365, S370 and S373 to determine their functional role in centriole duplication.

The role of Ana2/Sas5/STIL in centriole duplication, structure and centrosome numbers is of great interest and its role is starting to emerge. The importance of Ana2 in centriole duplication is confirmed in section 4.2.3.1 (Figure 4-9) because its depletion via RNA-interference in cultured *Drosophila* cells leads to loss of centrosomes. The experiment shows the effect on centrosome numbers after depletion of Ana2 protein by two different dsRNAs against coding sequence (CDS) of Ana2 and the untranslated regions (UTR) of Ana2. After three rounds of depletion for 4 days each, the cells show a significant loss of centrosomes compared to the negative control (GST RNAi), with approximately 94.3% and 67.7% of cells lacking centrosomes after *Ana2 CDS* RNAi and *Ana2 UTR* RNAi respectively. The described inability to duplicate centrioles after Ana2 depletion was also observed in *C. elegans* [23] and human cells [41,117,118], after depletion of Sas5 and STIL respectively. Interestingly, the loss of centrosomes after Sas5 and STIL depletion is comparable to the observed loss of centrosomes after depletion of Plk4 and Sas6 [85,288]. Additionally, inactivation of Sas5 in *C. elegans* causes failure of centrosome duplication at the two-cell stage embryos [308], which is also the observed phenotype in embryos deprived of Zyg-1 [22] or Sas4 [16,20]. Taken together, this confirms the importance of Ana2 in centriole duplication.

Additionally, the results in Figure 4-9 show that Ana2 can be efficiently depleted by its UTR regions. In turn, this allows the specific targeting of endogenous Ana2 in cells expressing transgenic Ana2, with the latter not carrying UTR sequences. This method was applied in section 4.2.3.2, where cultured *Drosophila* cells expressing transient Ana2-4A or Ana2-4D were depleted of endogenous Ana2 by *UTR* RNAi in rescue experiments. Ana2-4A and Ana2-4D carry mutations at aa318, aa365, aa370 and aa373, with a Serine to Alanine mutation or a Serine to Aspartic acid mutation respectively, and represent non-Plk4-phosphorylatable and phospho-mimicking Ana2 constructs respectively. They were used to analyse the importance of the Plk4 phosphorylation of Ana2 at these residues (identified in section 4.2.2, Table 4–1) for centrosome numbers and therefore for centrosome duplication. The expression of transgenic Ana2-4D mutant rescues centrosome numbers after the depletion of endogenous Ana2 with a weak negative effect compared to cells treated with control GST RNAi (section 4.2.3.2, Figure 4-10 and Figure 4-11). This result is similar to that observed in cells expressing transgenic Ana2-WT after depletion of endogenous Ana2 (section 4.2.3.2, Figure 4-10 and Figure 4-11). On the other hand, cells expressing the transgenic Ana2-4A mutant were not able to rescue centrosome numbers after depletion of endogenous Ana2, as approximately 83.5% of cells exhibit no centrosomes after three rounds of RNAi (section 4.2.3.2, Figure 4-10 and Figure 4-11). The centrosomes were immune-stained using specific antibodies against D-Plp and Asterless, and centrosomes were counted. Cell lines expressing Ana2-WT and Ana2-4D, showed centrosomal co-localisation of Asterless and D-Plp after the depletion of endogenous Ana2 (section 4.2.3.2, Figure 4-11). Whereas cells that expressed transgenic Ana2-4A lacked centrosomal signals of Asterless and D-Plp (section 4.2.3.2, Figure 4-11). In summary, Ana2-4A, the transgenic construct that cannot be phosphorylated by Plk4 at residues aa318, aa365, aa370 and aa373, cannot support centriole duplication. Whereas Ana2-4D, which mimicks Plk4-phosphorylation, rescues centrosome numbers. In summary, the kinase activity of Plk4 in phosphorylating the four Serine residues in Ana2 (S318, S365, S370, S373) is important in the regulation of centriole duplication.

But how does the Plk4-phosphorylation of Ana2 affect centriole duplication? Is Ana2 phosphorylation directly necessary for its recruitment to the centrosome? Or does it change the accessibility of Ana2 protein for recruitment? And what function does the interaction of Plk4 and Ana2 serve compared to Ana2 phosphorylation? After all, Zyg-1 is recruited by Spd2 as the first protein to the procentriole in *C. elegans* [53,91], and it was observed in *Drosophila* that Plk4 is recruited by Asterless [92], and in human cells by the homologues of Spd2 and Asterless (Cep192 and Cep152 respectively) [93,294,309]. This raises the question of whether the phosphorylation of Ana2 in fact triggers a more downstream process in centriole duplication? In *C. elegans*, Sas5 and Sas6, the Ana2 and Sas6 homologues, form a Sas5-Sas6 complex before being recruited to the procentriole [114]. Therefore, I developed in collaboration with Dr. Lipinszki a phosphorylation and binding assay that enables the direct interaction of Sas6 with Plk4-phosphorylated Ana2 to be tested *in vitro* (section 2.8.3). The difficulties in designing this assay lay in the generation of protein reagents that can be used in combination but without unspecific binding; and to sustain the Plk4-phosphorylation state of Ana2, but still allow for direct protein interaction assays/pull-downs and washes. The finalised *in vitro* phosphorylation-binding-assay was then applied to treat GST-Ana2 and GST-Ana2-4A (on resin) with active MBP-Plk4 or kinase-dead MBP-Plk4^{KD}, followed by a direct binding assay with ^{35}S-Methionine-labelled Sas6 protein (section 4.2.4, Figure 4-15 left panel). Excitingly, this identified Sas6 as a direct binding partner of Plk4-phosphorylated Ana2 *in vitro*. This observation is highly significant in the understanding of the role of Ana2 in the *Drosophila* centriole duplication process. I previously showed that Sas6 does not interact directly with Ana2 in a direct binding assay *in vitro* (section 4.2.1.1, Figure 4-2). Moreover, the treatment of GST-Ana2 with kinase-dead Plk4, and GST-Ana2-4A with active and kinase-dead Plk4 in phosphorylation-binding-assays resulted in no interaction of Sas6 with Ana2. Thus, the phosphorylation of GST-Ana2 at S318, S365, S370 and S373 by active Plk4 triggers the interaction of Sas6 with Ana2. A potential physical interaction of Ana2 with Plk4 is not the trigger, as Ana2-4A does not interact with Sas6 independent of treatment with active or kinase-dead Plk4. Thus, the interaction of Sas6 and Ana2 is dependent on Plk4-phosphorylation of the four Ana2 Serine residues S318, S365, S370, and S373.

There are multiple hypotheses of how Plk4-phosphorylation of full-length Ana2 permits for its interaction with Sas6. Firstly, the phosphorylation state of the four conserved Serine residues in the Ana2-STAN motif might directly allow Sas6 to bind a region containing these phosphorylation sites. Secondly, phosphorylation of the Ana2-STAN motif might cause a conformational change which makes a more N-terminal Ana2-region accessible for Sas6 to bind. Thirdly, as seen in Table 4-1 and Figure 4-8, the N-terminal region of Ana2 is lightly phosphorylated by Plk4, which could contribute to Sas6 binding to Ana2-C-terminus. Therefore, I wished to know which region of Ana2 interacts with Sas6; and treated N-terminal Ana2 (aa1-280) and C-terminal Ana2 (aa281-420) with active and kinase-dead Plk4 and tested for their direct interaction with Sas6 *in vitro* (section 4.2.4.1, Figure 4-13). Significantly, only the Plk4-phosphorylated Ana2 C-terminal region was able to bind Sas6 directly, as seen for Plk4-phosphorylated full-length Ana2 (Figure 4-15 left panel). The N-terminal part of Ana2 does not appear to contribute to the interaction with Sas6, as it does not interact with Sas6 nor does its absence reduce the efficiency of the Plk4-phosphorylated C-terminal part of Ana2 to interact with Sas6.

That the interaction of Plk4-phosphorylated Ana2 and Sas6 is not an artefact observed only *in vitro* is suggested by the complementary co-immunoprecipitation of the two parts from extracts of living cells (section 4.2.4, Figure 4-12, in collaboration with Dr. Lipinszki). Two versions of Ana2 (FLAG-Ana2-WT and FLAG-Ana2-4A) were stably co-expressed with non-degradable or non-degradable kinase-dead Plk4, and transiently expressed Sas6-Myc. FLAG-co-immunoprecipitation revealed that only Plk4-phosphorylated Ana2 was able to interact with Sas6 protein, as observed *in vitro*. This strongly confirms the *in vitro* findings and highlights how important Plk4-mediated phosphorylation of Ana2 is for the very specific and triggered interaction with the cartwheel protein Sas6 and therefore for centriole duplication as a whole. The significance of the above finding is surprising, as nothing similar has been described for their homologues. In *C. elegans*, Sas5 and Sas6 are suggested to be present as individual oligomers, which change confirmation when they form a hetero-Sas5-Sas6-complex and that the interaction between Sas5 and Sas6 is based on synergistic hydrophobic and electrostatic interactions [302].

After identifying that the specific four Serine residues (S318, S365, S370, S373) in the Ana2 STAN motif must be phosphorylated by Plk4 to trigger interaction with Sas6, it raises the question of the importance of each individual Serine residues for Ana2-Sas6 interaction. Is the phosphorylation of a single site efficient to trigger the specific interaction? Or is phosphorylation of all four Serine residues required? The analyses of Sas6’s interaction with four individual Ana2 mutant constructs, each carrying a Serine to Alanine mutation at each of the four conserved Serine residues, suggests that all four Serine residues must be phosphorylated by Plk4 to enable a strong interaction of phosphorylated Ana2 with Sas6 (section 4.2.5, Figure 4-15). Significantly, none of the four analysed Ana2 constructs were able to interact as strongly as Ana2-WT with Sas6 but neither did any of the point mutations fully abolish interaction of Ana2 with Sas6. However, the mutation of Ana2-S370A reduces the interaction with Sas6 to a greater extent than the other Ana2 mutants, suggesting that

Plk4-phosphorylation of S370 is of particular significance for the interaction of Ana2 with Sas6. Nevertheless the loss of any one of the four Plk4-phosphorylation sites within the Ana2 STAN motif reduces its efficiency to interact with Sas6; and the interaction does not depend upon any single phosphorylation site.

Similarly, the C-terminal part of Ana2 (aa281-420) binds as efficiently to Sas6 as full-length protein (section 4.2.5.1, Figure 4-16). Significantly, also a triple mutant of Ana2-C-3A, which only retains the phosphorylatable S318 but carries Serine to Alanine mutations for aa365, aa370 and aa373, does not prevent binding of Sas6 fully (section 4.2.5.1, Figure 4-16). But Plk4-phosphorylated Ana2-C-3A shows a more significantly reduced interaction with Sas6 than any of the four individual Serine mutants of Ana2-C. All four conserved Serine residues in the Ana2-STAN motif must be phosphorylated by Plk4 to trigger efficient interaction with Sas6 and mutation in any one reduces but does not abolish binding.

Reciprocally I showed that the Ana2-4D mutant, which mimicks phosphorylation of Ana2 at S318D, S365D, S370D and S373D, interacts with Sas6 independently of treatment with active or kinase dead Plk4 (section 4.2.6, Figure 4-17). The strength of interaction is comparable to the interaction of Plk4-phosphorylated Ana2-WT with Sas6 accounting for the ability of Ana2-4D to rescue centriole duplication after depletion of endogenous Ana2 in *Drosophila* cell culture with similar efficiency as transgenic Ana2-WT (section 4.2.3.2, Figure 4-10 and Figure 4-11). That a phospho-mimicking Ana2 mutant (Ana2-4D) interacts with Sas6 confirms the findings that the four Serine residues in the Ana2-STAN motif are crucial and that their phosphorylation by Plk4 is the trigger for the interaction of Ana2 with the cartwheel protein Sas6.

The identification of a specific phosphorylation mechanism by which Sas6 is recruited raises the question whether Ana2-phosphorylation is also necessary to trigger further downstream interactions with other centrosomal proteins. To address this, I generated ^{35}S-Methionine-labelled proteins known to be found at centrioles, namely Sas4, Bld10, Rcd4 and Ana1 (section 4.2.7, Figure 4-18). The latter two do not interact with Ana2, not in Ana2's Plk4-phosphorylated nor non-phosphorylated state, whereas Sas4 interacts strongly with Ana2, and Bld10 increases its interaction when Ana2 is Plk4-phosphorylated.

Rcd4 is a protein identified in a genome-wide RNAi screen for centrosome defects, which localises to the centrosome and was categorised as functioning in centriole duplication and/or efficient PCM recruitment [131]. The *Drosophila* protein does not have any known homologues and to date, there have not been any further published studies on Rcd4.

Ana1 represents one of the three Ana proteins suggested to be involved in centriole duplication. So far, the research undertaken on the protein is limited. But it is known that Bld10, Ana1 and Asterless are recruited sequentially in the centriole-to-centrosome conversion [30] and that after depletion of Plk4, Ana1 no longer localises to the centrosome. Additionally, Ana1 depletion leads to a highly reduced signal of Sas6 at the spindle poles [310]. This suggests, that Plk4 is required for Ana1 recruitment to centrioles and that Ana1 acts downstream of Plk4. Conversely, Ana1 is recruited to the centriole upstream of Sas6. But Sas6 does not seem required for Ana1 recruitment to centrioles but might play a role in the maintenance of Ana1 at the centriole.

Sas4, a centriole protein essential for microtubule recruitment, interacts strongly with Ana2 independently of Plk4-phosphorylation. That Sas4 interacts with Ana2, regardless of Ana2's phosphorylation state, is in line with the interaction of CPAP and STIL, the human orthologues of Sas4 and Ana2 respectivelly. The analysis of their crystal structure defined their interaction interface to be the STAN motif of STIL and the C-terminal G-box of CPAP, and significantly, mutations within this interface disturbs centriole duplication *in vivo* [41,42,44]. Depletion of STIL interfered with CPAP recruitment to the procentriole and centriole elongation, but reciprocal, depletion of CPAP did not affect targeting of STIL to the centriole, suggesting that STIL recruitment to the centriole occurs upstream and is independent of CPAP [41]. Significantly, overexpression of Sas4 causes rapid *de novo* formation of centriole-like structures in approximately 60% of unfertilized *Drosophila* eggs, which normally do not have centrioles [96]. Moreover, overexpression of Sas4 does not lead to extra centriole-like structures in brain cells nor spermatocytes [96]. The major role of Sas4 at the centriole is in recruitment and/or maintenance of microtubules, as depletion of *C. elegans* Sas4 prevents these processes [53]. Moreover CPAP overexpression causes very long centrioles [38,39]. More research needs to be undertaken to further understand how Sas4 and Ana2 interact with each other and how this affects centriole duplication in *Drosophila*.

Interestingly, Bld10, which is known to maintain centriole structure but is not essential for centriole duplication in *Drosophila* [65], interacts with non-phosphorylated Ana2 but this interaction is stronger when Ana2 is Plk4-phosphorylated. The strength of interaction of the latter is comparable to the interaction strength of Sas6 with Plk4-phosphorylated Ana2. Bld10 protein is conserved amongst organisms that have centrioles, and has homologues in *C. elegans* and human cells; Bld10p and Cep135 respectively [32]. Bld10p and Cep135 are essential for centriole formation in *Paramecium*, *Tetrahymena* and human cells but not so in *Drosophila* [43,65,73,311,312]. *Drosophila* mutants that lack Bld10 assemble cartwheels and centrioles, although the cartwheel appears to be wider and unstable [32,64–66]. In contrast, *Chlamydomonas* Bld10 forms the distal part of the cartwheel spoke and contributes to their proper length [62]. Additionally, Bld10p/Bld10/Cep135 are microtubule-binding proteins [43,68], which suggests they might nucleate and/or stabilize microtubules at the transition zone of cartwheel spokes to microtubules. Details of the molecular interaction of Ana2 and Bld10 and its function is currently unknown but it is possible to speculate that Ana2 might recruit Bld10 to the centriole or that Ana2 could stabilise the cartwheel and microtubules via Bld10. The increase in binding of Bld10 to phosphorylated Ana2 could be a mechanism that times Bld10’s association with the centriole or to license Bld10 to interact with other proteins of the cartwheel or centriole.

Structural homology studies of Ana2/STIL reveal that the protein has two conserved C-terminal motifs: the STAN motif and the TIM motif at the very C-terminus [117], with the latter being truncated in microcephaly patients [307]. The C-terminal part of Ana2 contains both of these motifs. However, my studies subsequently showed that the STAN motif alone is efficient for phospho-dependent binding to Sas6 which does not depend on the TIM motif (Figure 4-20). This is in line with observations of microcephaly mutants of STIL, which lack the C-terminal TIM motif and cannot be degraded but remain a normal STIL function [307]. It also confirms the high importance of the Ana2-STAN motif in cartwheel assembly and centriole biogenesis.

My phosphorylation and binding assays show that Sas6 aa276-432 is the smallest region able to interact with Ana2 (section 4.2.8.2). We do not know the structure of the entire protein Sas6. However, crystallographic studies of Sas6 homologues have elucidated the 3D structure of the N-terminal head domain and the N-terminal part of the coiled-coil domain [63,69,74,75]. These studies show that Sas6 has an N-terminal head domain, which forms the inner cartwheel hub and a coiled-coil domain which dimerises to form the cartwheel spokes, and an unstructured C-terminal end. However, the structure of the whole coiled-coil domain and particularly the C-terminal region, which could be part of the cartwheel spokes that connect microtubules, is not known. It is intriguing that this C-terminal region of Sas6 interacts with Ana2-STAN, as it localises Ana2 function to the outer cartwheel region. This is significant in the light of observations in human cells, where STIL interacts directly with CPAP, and in the case of STIL or Sas6 depletion where CPAP fails to localise to the nascent procentriole [41]. The identification of the interacting regions between Ana2 and Sas6 needs further analysis at atomic resolution, to determine the precise structural interaction and how this might affect centriole duplication. This presents a big challenge. To show this, it will be necessary to overcome lack of solubility of the proteins and fragments of the proteins for crystallisation trials; and their stoichiometry, as we know that both proteins form homodimers giving the potential for change in stoichiometry when the proteins interact. To fully understand precisely how Ana2 and Sas6 interact, it will be necessary to overcome these difficulties to gain further insight.

Chapter 5

The novel direct interaction and centrosome localisation of Dragon (CG33052) with the cartwheel protein Sas6

5 The novel direct interaction and centrosome localisation of Dragon (CG33052) with the cartwheel protein Sas6

5.1 Introduction

In this chapter I will explore the interactions of Sas6 with a second protein that we have called Dragon (CG33052) that to date has not been studied in *Drosophila*.

We identified the *Drosophila* homologue Dragon as a partner of the centrosomal protein Sas6 following its affinity purification from *Drosophila* cell culture. My objective in this chapter was to understand its interaction with centriolar proteins and its potential role in centriole duplication. Specifically, I wanted to determine if there is a direct protein-protein interaction between Dragon and the centrosomal cartwheel protein Sas6. If so, what are the structural and interaction characteristics of this potential interaction, where does Dragon localise, and what effect does depletion of Dragon have on centrosome numbers?

5.2 Results

5.2.1 Identification of Dragon, a Golgi protein in complex with the centrosomal protein Sas6

5.2.1.1 *In vivo* purifications of Sas6 reveal the novel Golgi protein Dragon in complex

As part of a study of the interactions made by centrosomal proteins, different centrosomal proteins were purified from *Drosophila* cell culture and *Drosophila* syncytial embryos, and subjected to mass spectrometry analyses. My particular interest was in Sas6, which is known to form the inner hub and cartwheel structure of centrioles and is one of the first proteins detected at the site of daughter centriole formation on the mother centriole. In chapter 4, I show phosphorylation of Ana2 by Plk4 at its STAN motif triggers direct interaction of Ana2 with Sas6 and recruitment to the site of procentriole formation. In the analyses of Sas6 assosiated proteins purified from *Drosophila* cell culture and syncytial embryos, we repeatedly observed the previously uncharacterised protein CG33052 in *Drosophila*. From here onwards CG33052 will be refered to as Dragon. Table 5-1 summarises the Mascot ’scores‘ and ’number of peptides‘ identified by mass spectrometry for Sas6 and Dragon, purified from cultured *Drosophila* cells and *Drosophila* syncytial embryos (complete lists in Appendix C). *Drosophila* cells were stably transformed with pMT-PrA-Sas6 and expression of PrA-Sas6 was induced with 1mM $CuSO_4$ for 22 hours. As indicated, cells were treated with 25µM MG132 for up to 5 hours to inhibit proteasomal degradation and/or 50nM okadaic acid for 9 to 16 hours to inhibit protein phosphatases. Sas6 was also expressed constitutively in *Drosophila* syncitial embryos (aged 0-4 hours) derived from *poly-Ub-Sas6-GFP* expressing flies. During the purification of Sas6, high NaCl (440mM) concentrations and 50nM okadaic acid were included in the elution and wash buffer, as indicated (Table 5-1B).

The Sas6 bait exhibited high Mascot ‘scores‘ and large ‘number of identified peptides‘ in all analysed samples, suggesting successful enrichment of Sas6 protein from *Drosophila* cell cultures and embryos. The samples from cultured *Drosophila* cells consistently revealed Dragon in complex with the bait protein Sas6. Dragon was present with high Mascot scores in the purifications from syncytial embryos, independently of whether okadiac acid treatment was given. A high 440mM NaCl concentration in the elution and wash buffer led to lower Mascot scores of Dragon compared to the samples treated with the usual 150mM NaCl concentration. Control purifications of PrA or GFP expressed alone do not identify Dragon. Purification of Dragon with consistantly high scores when Sas6 was purified from either *Drosophila* cell culture or syncytial embryos suggests that Dragon is a true member of a complex with the centrosomal protein Sas6 *in vivo*.

Table 5-1 Sas6 protein purification and mass spectrometry analyses from *Drosophila* cell culture and *Drosophila* syncytial embryos reveal Dragon protein in a complex with Sas6. Sas6 protein was purified from *Drosophila* cell culture expressing pMT-PrA-Sas6 (treated with and without okadaic acid), and from *Drosophila* syncytial embryos expressing poly-Ubiquitin-Sas6-GFP (treated with and without okadaic acid, high salt equals 440mM), followed by mass spectrometry. The tables summarise the presence of Sas6 and Dragon in complex and their according number of peptides in the samples (*purifications in student projects). OA: okadaic acid. Complete lists in Appendix C.

A *Drosophila* cell culture

Protein	Score	# of peptides
pMT-PrA-Sas6; MG132*		
Sas6	4576	281
Dragon	69	5
pMT-PrA-Sas6; OA and MG132*		
Sas6	4606	280
Dragon	55	2

B *Drosophila* syncytial embryos

Protein	Score	# of peptides
pUb-Sas6-GFP; 0-4h*		
Sas6	13751	272
Dragon	6514	105
pUb-Sas6-GFP; 0-4h, high salt*		
Sas6	5900	123
Dragon	1641	27
pUb-Sas6-GFP; 0-4h, high salt and OA*		
Sas6	4677	131
Dragon	1380	27

5.2.1.2 *In vivo* purifications of Dragon confirm Sas6 in complex

To further confirm that Sas6 and Dragon form in complex *in vivo*, I performed the reciprocal experiment; to analyse whether GFP-tagged Dragon co-purifies with Sas6. To this end, I established cell lines for inducible Dragon-GFP and constitutively expressed GFP-Dragon, and affinity purified these proteins from *Drosophila*. Dragon protein purified from *Drosophila* cell culture was analysed by mass spectrometry (complete lists in Appendix C). All samples showed high bait Mascot scores for Dragon between 16669 to 61897 (253 to 766 peptides), giving a high protein coverage of 62 to 74%. Sas6 protein was identified as the only centriole duplication protein by mass spectrometry in all analysed purifications (Table 5-2A). But co-purified Sas6 seems to be positively affected or stabilised if the Dragon bait is constitutively expressed rather than induced, Dragon is N-terminally tagged rather than C-terminally and the cells were treated with okadaic acid. Significantly, Sas6 was identified as the top scoring protein and the only centriole duplication protein purified with Dragon from syncytial *Drosophila* embryos (Table 5-2B). Though common contaminants were Heat shock protein cognate 4 CG4264 and Elongation factor 1α48D CG8280 (for full list see Appendix C), which are often found in control purifications. The GFP-trap binding was performed for 2.5 hours to allow for efficient purification of Dragon protein in complexes, including potentially less represented complexes within the sample. Mass spectrometry identified the bait Dragon with a score of 2764 (50 peptides, giving a protein coverage of 71%). On the other hand, Sas6 was identified in complex with Dragon at a score of 752 (18 peptides, 44% protein coverage). Thus, confirming that Dragon and Sas6 co-purify in complex *in vivo* from cultured *Drosophila* cells as well as directly from *Drosophila* syncytial embryos.

Table 5-2 Purifications of Dragon reveal it is in complex with Sas6 *in vivo*. Dragon protein, purified from A) *Drosophila* cell culture expressing poly-Ubiquitin-GFP-Dragon or pMT-Dragon-GFP (treated with and without okadaic acid) and B) from *Drosophila* syncytial embryos expressing poly-Ubiquitin-GFP-Dragon. Mass spectrometry reveals that Sas6 is in complex with Dragon. Number of peptides and the peptide coverage for Dragon and Sas6 are indicated for each sample. Complete lists in Appendix C.

A *Drosophila* cell culture

Protein	Score	# of peptides	Coverage
pUb-GFP-Dragon			
Dragon	18036	290	63%
Sas6	159	4	10%
pUb-GFP-Dragon; OA			
Dragon	61897	766	66%
Sas6	1961	37	37%
pMT-Dragon-GFP; 0.5mM $CuSO_4$ 24h			
Dragon	16669	253	62%
Sas6	90	2	5%
pMT-Dragon-GFP 0.5mM $CuSO_4$ 24h, 100nM OA 2h			
Dragon	24140	337	74%
Sas6	223	7	10%

B *Drosophila* syncytial embryos

Protein	Score	# of peptides	Coverage
pUb-GFP-Dragon; 2.5hrs binding			
Dragon	2764	50	71%
Sas6	752	18	44%

5.2.1.3 *In vivo* purifications of Dragon confirm COPI subunits in complex

In addition to the centrosomal cartwheel protein Sas6 in complex with Dragon (section 5.2.1.2), the majority of the subunits of the Golgi COPI proteins were present in Dragon purifications from *Drosophila* cell culture (Table 5-3). The subunits αCOP, β'COP and εCOP of the cage-like subcomplex of COPI and the subunits γCOP and βCOP of the adaptor subcomplex of COPI were present in all samples. The εCOP subunit of the cage-like subcomplex was present in all purifications but one. Hence, all three subunits of the cage-like subcomplex (α-β'-ε-COPs) are present in the Dragon purifications. On the other hand, the subunits δCOP and ζCOP were not identified. Thus, only two out of the four subunits of the adaptor subcomplex of COPI are present in Dragon purifications. No COPI subunits were found in GFP control purifications or in complex with purified Sas6. Thus COPI subunits appear to associate specifically with the Dragon bait. Additionally, CtBP (C-terminal binding protein), which was suggested to function as a transcriptional co-repressor [313–317], was highly represented in complex with Dragon in all four Dragon purifications from *Drosophila* cell cultures and apparently in higher quantity in cells treated with okadaic acid. This suggests that the inhibition of dephosphorylation by PP2A stabilises CtBP in complex with Dragon.

Table 5-3 Purifications and mass spectrometry analyses reveal subunits of COPI and CtBP in complex with Dragon. Dragon protein, purified from *Drosophila* cell culture expressing poly-Ubiquitin-GFP-Dragon or pMT-Dragon-GFP (treated with (+OA) and without okadaic acid), followed by mass spectrometry show CtBP and five out of seven known COPI subunits in complex with Dragon. Highlighted in pink are the COPI subunits forming the cage-like subcomplex (α-β'-ε-COPs), and in blue the COPI subunits forming the adaptor subcomplex (γ-β-δ-ζ-COPs). When present in the purification sample, the Mascot 'scores' and 'number of peptides' are stated for Dragon, CtBP and each subunit of COPI.

	pUb-GFP-Dragon		**pUb-GFP-Dragon +OA**		**pMT-Dragon-GFP**		**pMT-Dragon-GFP +OA**	
Symbol	Score	# of peptides	Score	# of peptides	Score	# of peptides	Score	# of peptides
Dragon	18036	290	61897	766	16669	253	24140	337
αCOP	1106	26	606	13	72	2	329	11
β'COP	322	8	212	3	336	4	441	6
βCOP	1263	19	582	9	259	4	590	12
γCOP	1792	29	1171	22	109	3	488	8
δCOP	-		-		-		-	
εCOP	96	2	92	2	-		138	1
ζCOP	-		-		-		-	
CtBP	655	11	3502	47	768	22	2262	40

5.2.2 Localisation of Dragon at the centrosome and Golgi

5.2.2.1 Dragon co-localises to the centrosome with Sas6

The human counterpart of Dragon is the protein GoRab that is reported to function at the Golgi and its vesicles [202,214–216]. Thus the purification of Dragon in complex with the centrosomal protein Sas6 from *Drosophila* was unexpected. I therefore asked whether Dragon localises with Sas6 at the centrosome. Therefore, I performed immune localisation studies to determine whether Dragon-GFP or myc-Dragon, stably expressed in cultured *Drosophila* cells, would allocate with the centrosomal marker D-Plp. This revealed co-localisation of D-Plp with GFP- and myc-Dragon at the centrosome (Figure 5-1), and also GFP- and myc-Dragon at the Golgi structure (this is further explored in section 5.2.2.2). I then set out to determine the position of Dragon related to Sas6 at the centrosome by structured illumination microscopy in collaboration with Dr. Tzolovsky. *Drosophila* wild-type cells were stained with antibodies against Dragon, Sas6 and D-Plp, followed by imaging and analysis. These images confirmed that Dragon localises to the centrosome and more specifically to zone 1 with the centrosomal cartwheel protein Sas6 within the D-Plp ring (Figure 5-2). D-Plp allows the mother and daughter centriole to be distinguished. D-Plp forms a ring-like structure at the centrosome during the whole cell cycle, and the daughter centriole matures by recruiting D-Plp in a ‘horn’-like pattern which develops into a ring-like structure by meta-/anaphase. Sas6 and Dragon co-localise to the inner space of the D-Plp ring (zone 1), corresponding to the mother centriole, throughout the whole cell cycle. Sas6 and Dragon also co-localise as a single dot at the site of procentriole formation. Thus, Sas6 and Dragon co-localise throughout centriole assembly, maturation and separation, and hence are present on both mother and daughter centriole throughout the whole cycle (Figure 5-2). This suggests a simultaneous rather than a sequential recruitment of Sas6 and Dragon.

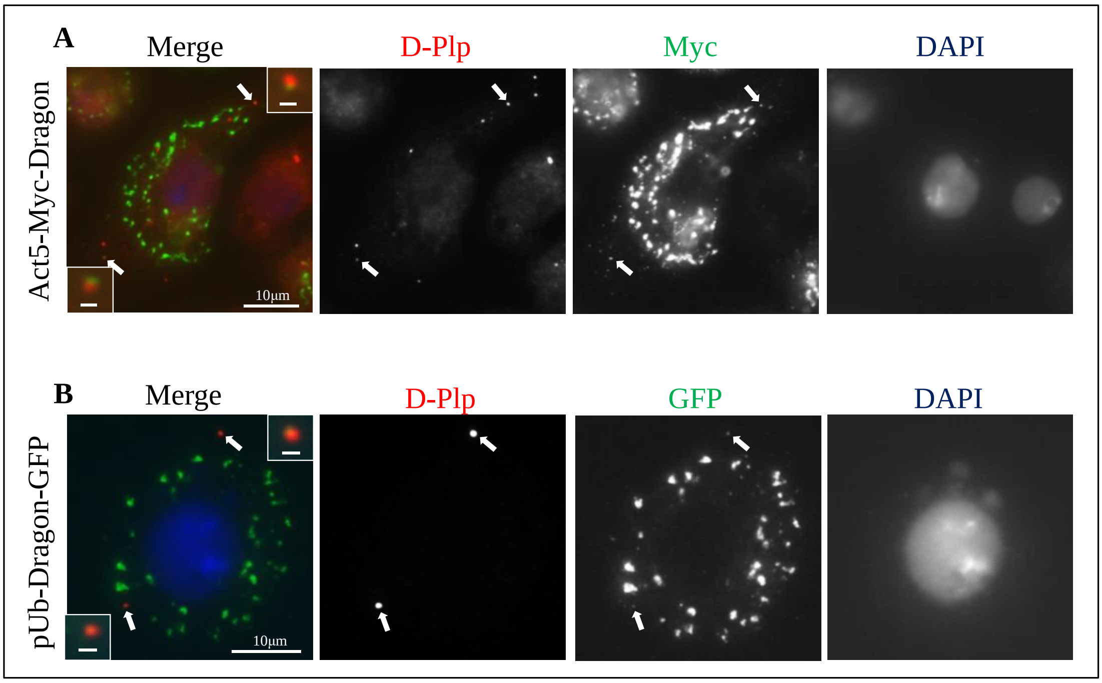

Figure 5-1 Dragon localises to centrosomes in *Drosophila* cell culture. Micrographs show centrosomes revealed by D-Plp and Myc/GFP co-staining in the two *Drosophila* cell lines expressing Act5-Myc-Dragon or pUb-Dragon-GFP; insets show D-Plp and Myc/GFP co-localisation from each pole (indicated by white arrows). Additionally, Myc/GFP stainings reveal Golgi localisation of Dragon in both cell lines (as further explained in Figure 5-3). DNA is stained with DAPI (blue). Scale bars represent 10µm for main image and 1µm for insets.

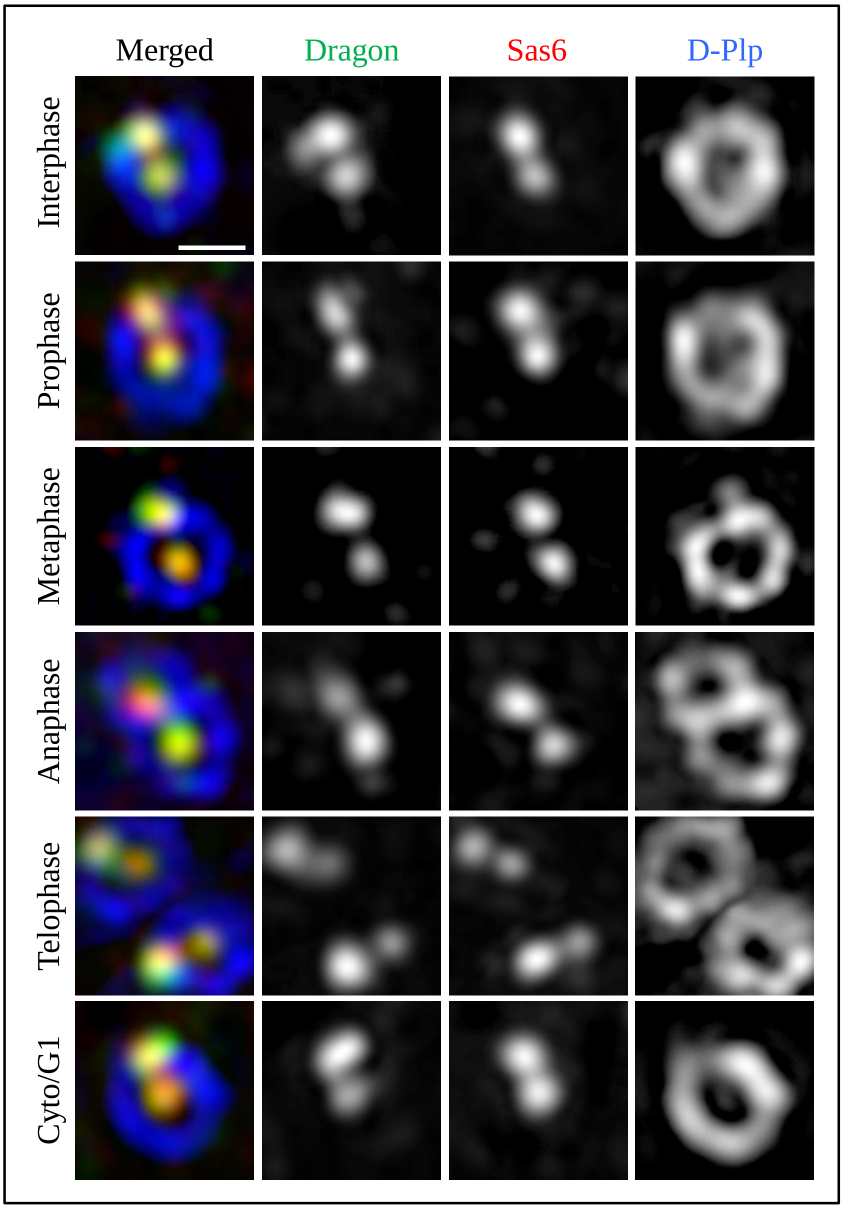

Figure 5-2 Localisation of endogenous Dragon (green) relative to centrosomal Sas6 (red) and D-Plp (blue) throughout the cell cycle. Structured illumination microscopy of endogenous Dragon, Sas6 and D-Plp throughout cell cycle stages in wild type *Drosophila* cell culture. Dragon and Sas6 co-localise at the centre of the D-Plp ring at the mother centriole throughout the cell cycle, as well as at the site of procentriole formation and daughter centriole at the periphery of the D-Plp ring. Scale bar 0.25μm. Microscopy and images by Dr. Tzolovsky.

5.2.2.2 Dragon protein localises to the *trans*-Golgi but not the *cis*-Golgi in *Drosophila* cell culture

As the human homologue of Dragon, GoRab, was reported as a *trans*-Golgi protein [202] I wanted to determine whether *Drosophila* Dragon was also a Golgi protein. In collaboration with Miss Chu I studied *Drosophila* cell culture stably expressing FLAG-Dragon to reveal the FLAG-tag, Golgin-245, GM130 and DAPI, to localise Dragon, the *trans*-Golgi, the *cis*-Golgi and DNA respectively (Figure 5-3) [318,319]. This identified Dragon at the Golgi, where it co-localises with the *trans*-Golgi marker Golgin-245 but not with the *cis*-Golgi marker GM130. Interestingly, this is similar to observations in human cell culture, where the Dragon homologue GoRab co-localises with the *trans*-Golgi protein Rab6 but not with the *cis*-Golgi matrix marker GM130 [202]. Thus Dragon has a dual localisation within cultured *Drosophila* cells; at the *trans*-Golgi and co-localised with Sas6 at the core of the centriole.

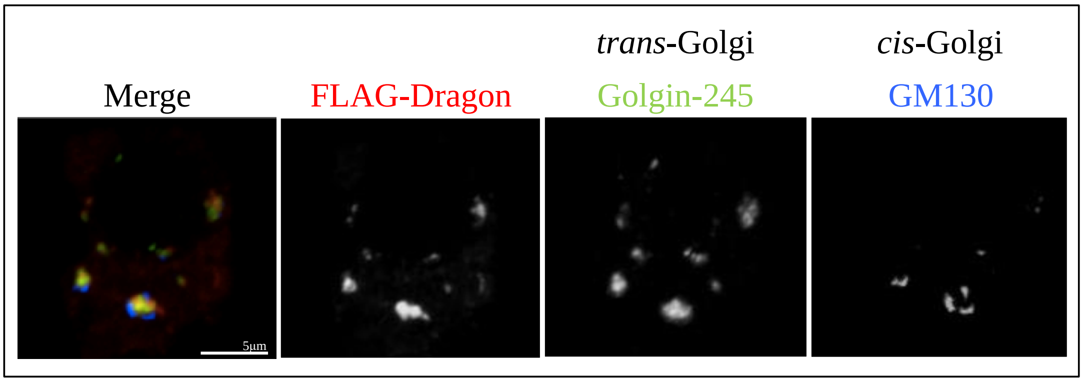

Figure 5-3 Localisation of Dragon to the *trans*-Golgi. Cultured *Drosophila* cells stained to reveal FLAG (Dragon, red), Golgin-245 (green) and GM130 (blue). Dragon co-localises to the *trans*-Golgi with Golgin-245 but not to the *cis*-Golgi with GM130. Scale bar 5µm. Microscopy and images by Miss Chu.

5.2.3 Depletion of Dragon in *Drosophila* cell culture causes loss of centrosomes but Golgi structures are not affected

5.2.3.1 Depletion of Dragon in *Drosophila* cell culture affects centriole duplication and causes loss of centrosomes

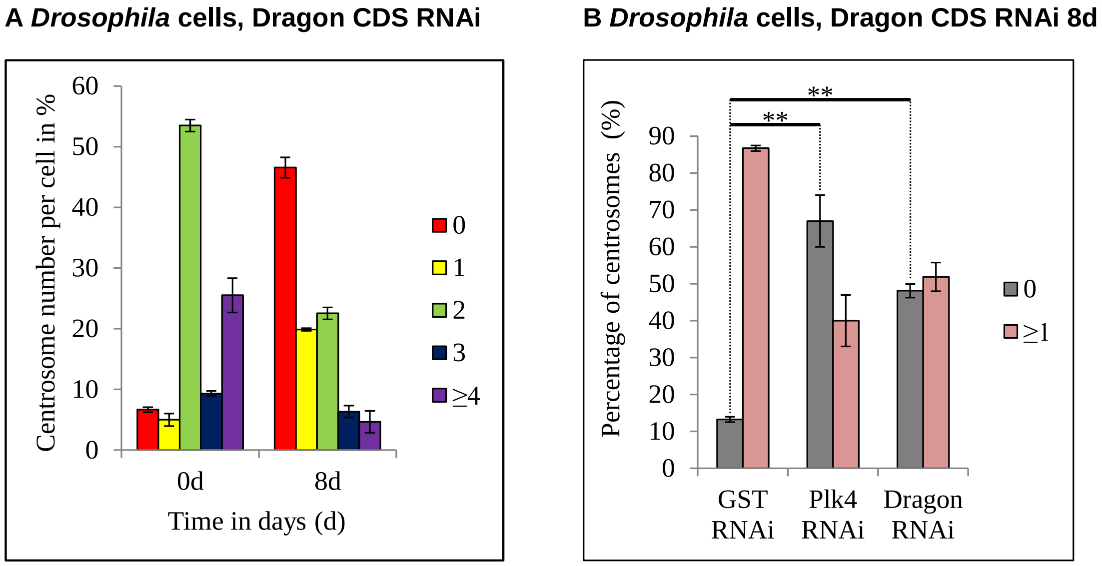

A *Drosophila* cells, Dragon CDS RNAi

B *Drosophila* cells, Dragon CDS RNAi 8d

Figure 5-4 Depletion of Dragon by RNAi causes loss of centrosomes in cultured *Drosophila* cells after eight days. A) Numbers of centrosomes per cell are colour coded in the key. (B) Number of cells with zero or with greater and equal than one centrosome per cell after treatment with Dragon dsRNA, GST dsRNA and Plk4 dsRNA. Error bars represent standard error; 3x200 cells counted; significance was calculated by t-test.

As Dragon co-purified and co-localised with Sas6, I wanted to determine whether depletion of Dragon also affected centriole duplication. Therefore, I used RNAi to deplete Dragon from wild-type *Drosophila* cell culture, to study the effect on centrosome numbers. As positive and negative controls, I depleted Plk4 and GST. I performed two 4 day rounds of RNAi and analysed centrosome numbers on day 8. I found that Dragon depletion over this 8 day interval led to loss of centrosomes (Figure 5-4A). The proportion of cells with no centrosomes increased from 6.7% to 46.6%; and with a single centrosome per cell, from 5% to 19.9% after Dragon depletion. This was accompanied by a corresponding decrease in cells with two centrosomes (from 53.5% to 22.5%); three centrosomes (from 9.3% to 6.3%); and four or more centrosomes (from 25.5% to 4.7%). Dragon depletion was not as effective as Plk4 depletion (46.6% versus 72.2% of cells without centrosomes, Figure 5-4B) but nevertheless suggests a role for Dragon in centriole duplication.

5.2.3.2 Depletion of Dragon does not affect the structure of the Golgi suggesting an alternative role of Dragon at the Golgi

As Dragon co-localises with Golgin-245 at the *trans*-Golgi (section 5.2.2.1) it raised the question whether the Golgi organisation was affected following Dragon depletion by RNAi. Therefore pilot experiments were performed in collaboration with Miss Chu. Cultured *Drosophila* cells were treated with dsRNA against Dragon, Sas6, GFP (negative control), and Plk4 (positive control) for three days. Cells were fixed and stained with antibodies against firstly, D-Plp, Dragon and GM130 for *cis*-Golgi or secondly, against D-Plp, GM130 and Golgin-245 for *trans*-Golgi. These pilot experiments (data not shown) suggest that after control GFP RNAi; D-Plp localised to centrosomes, and Dragon adjacent to the *cis*-Golgi (GM130). After Sas6 or Plk4 RNAi; the centrosomal D-Plp signal was lost, but Dragon and GM130 remained localised at the Golgi. Dragon RNAi led to reduced or absent D-Plp signals at centrosomes, and loss of Dragon from the Golgi, but localisation of GM130 to the *cis*-Golgi and Golgin-245 to the trans-Golgi appeared unaffected by Dragon depletion. Thus, the pilot experiments suggest that depletion of centrosomal proteins Sas6 and Plk4 lead to loss of centrosomes without affecting the localisation of Dragon to the Golgi structure. Additionally, it is suggested that the depletion of Dragon led to loss of centrosomes and loss of Dragon from Golgi. However, the localisation of GM130 and therefore the *cis*-Golgi structure, and Golgin-245 and therefore the trans-Golgi structure do not seem to be structurally affected.

5.2.4 Direct interaction of Dragon and Sas6 confirmed by *in vitro* assays - Identification of binding domains between Dragon and Sas6 *in vitro*

5.2.4.1 The full-length proteins Dragon and Sas6 interact directly with each other *in vitro*

After determining that Dragon and Sas6 exist in a complex *in vivo*; that they co-localise at the centrosome; and that depletion of Dragon protein from *Drosophila* cell culture causes loss of centrosomes, I wished to determine whether Dragon and Sas6 directly interact with each other.

To this end I first expressed full-length GST-tagged Sas6, full-length GST-Dragon and GST-alone in *E. coli*. I purified all of the proteins by binding to Glutathione Sepharose 4B resin via their GST tag (section 2.5.1). Secondly, I synthesised radioactively (^{35}S-Methionine) labelled Sas6 and Dragon protein in coupled transcription-translation reactions. The reactions were performed using the Promega kit TnT® T7 Quick Coupled Transcription/Translation System which contains T7 polymerase and rabbit reticulocyte lysate. For the *in vitro* binding assays, I individually incubated GST-tagged protein or GST-alone bound to resin with ^{35}S-Methionine-labelled protein in binding buffer and at room temperature (section 2.8.1). After allowing a period for binding, I washed the resin samples multiple times and subjected them to SDS-PAGE, transferred the separated proteins to nitrocellulose membrane and exposed them at -80°C using enhancer film. The signal detected on the autoradiogram shows if and to a certain extent how well the ^{35}S-Methionine-labelled protein binds to the protein on resin.

I first analysed whether GST-Dragon immobilised on resin would bind ^{35}S-Methionine-labelled Sas6 protein directly (Figure 5-5A) and secondly, if GST-Sas6 immobilised on resin would bind ^{35}S-Methionine-labelled Dragon protein directly (Figure 5-5B). As a negative control, I used GST-alone bound to resin. ^{35}S-Methionine-labelled Sas6 does not bind to GST alone (lane 2) but shows a strong binding with GST-Dragon. In the reciprocal experimental set up of the *in vitro* binding assays, GST-Sas6 bound to ^{35}S-Methionine-labelled Dragon whereas GST-alone did not (Figure 5-5B).

In summary, the *in* vitro transcription-translation system and binding assay, which contains only the two proteins of interest confirms that Dragon and Sas6 protein bind each other directly *in vitro*, accounting for the co-purification of Sas6 and Dragon in complex from cultured *Drosophila* cells and *Drosophila* syncytial embryos.

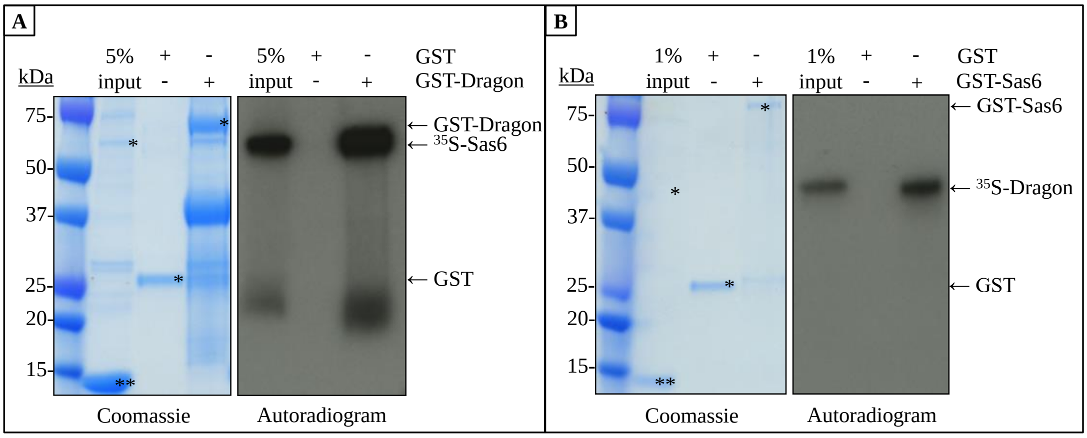

Figure 5-5 Sas6 and Dragon interact directly *in vitro*. (A) GST-Dragon was incubated with ^{35}S-Methionine-labelled Sas6 and (B) GST-Sas6 was incubated with ^{35}S-Methionine-labelled Dragon. The complexes were subjected to SDS-PAGE and autoradiography. Both interaction assays confirm that Sas6 and Dragon interact directly with each other *in vitro*. GST (negative control) did not exhibit any interaction with ^{35}S-Methionine-labelled Dragon nor ^{35}S-Methionine-labelled Sas6. * indicates protein sample loaded; ** indicates reticulocyte lysate residue.

5.2.4.2 The C-terminal region of Sas6 binds directly to Dragon *in vitro*

After I identified full-length Dragon and Sas6 as directly interacting proteins *in vitro*, I wanted to further understand which regions of the proteins were required for the direct protein-protein interaction.

To analyse which region within Sas6 interacts with Dragon *in vitro*, I generated vectors containing fragments of Sas6 downstream of a T7 promotor, to generate protein fragments of Sas6 with the Promega TnT® T7 Quick Coupled Transcription/Translation System for radioactive labelling. I then performed binding assays with these ^{35}S-Methionine-labelled Sas6 fragments and GST-Dragon (full-length) bound to resin (section 2.8.1). The Sas6 fragments I tested in this way are summarised in Figure 5-6 and Figure 5-7.

The first series of Sas6 fragments were designed according to the predicted secondary structure of Sas6 (Figure 5-9). These Sas6 fragments represented the N-terminal head-domain of Sas6 (N, aa1-180); the majority of the coiled-coil domain (CC, aa181-408); the N-terminal head- and majority of the coiled-coil domain together (NC, aa1-408); and the coiled-coiled domain with the unstructured most C-terminal part (CC+C, aa181-472). I carried out binding assays with each of these ^{35}S-Methionine-labelled Sas6 fragments and GST-Dragon before carrying out SDS-PAGE and protein transfer onto nitrocellulose membrane for autoradiography. I observed direct interaction of Dragon only with the Sas6 fragment containing the coiled-coiled and unstructured C-terminal region (CC+C, aa181-472). None of the other analysed Sas6 fragments interacted with Dragon (Figure 5-6, Figure 5-7A).

We know from structural studies that the N-terminal head domain of Sas6 forms the ‘inner hub’ of the centriole cartwheel and that the N-terminal part of the coiled-coiled domain of Sas6 molecules dimerise and form the cartwheel spokes of the centrioles (Figure 1-8, Figure 1-7). My above described analysis suggests that a region at the C-terminal part of the Sas6 coiled-coil domain and adjacent upstream sequence is important for interaction with Dragon. The coiled-coil region alone (CC) and the N-terminus are not sufficient for binding to Dragon. This suggests an interaction of Dragon with Sas6 in its so far uncharacterised C-terminal coiled-coil region.

To further narrow down the region of Sas6 necessary for binding Dragon, I generated additional Sas6 fragments from within the fragment aa181-472. These constructs are stepwise truncations from the N- or C-terminus of the Sas6 aa181-472 fragment (Figure 5-6). Each of these Sas6 fragments was labelled with ^{35}S-Methionine by coupled transcription-translation reaction and tested for its ability to bind GST-Dragon immobilised on resin. The most C-terminal truncated Sas6 construct analysed that still exhibits direct binding with Dragon is the Sas6 fragment aa1-462 (Figure 5-6, Figure 5-7C). Sas6 fragments smaller, including aa1-452, do not bind Dragon. Hence, the very C-terminal 10aa of Sas6, which represent the unstructured C-terminus of the protein according to secondary structure prediction in Figure 5-9, are not essential for binding with Dragon. Removal of N-terminal sequence from Sas6 did not prevent interaction with Dragon until residue 351 (construct aa351-472; Figure 5-6, Figure 5-7B).

Taken together, Sas6 protein fragments aa1-462 and aa351-472 are respectively the most C- and N-terminal truncated protein fragments which are still able to directly interact with Dragon *in vitro*. Thus the Sas6 protein region 351-462aa is necessary for interaction with Dragon. Interestingly, this region of Sas6 shows conservation between species (Figure 5-8).

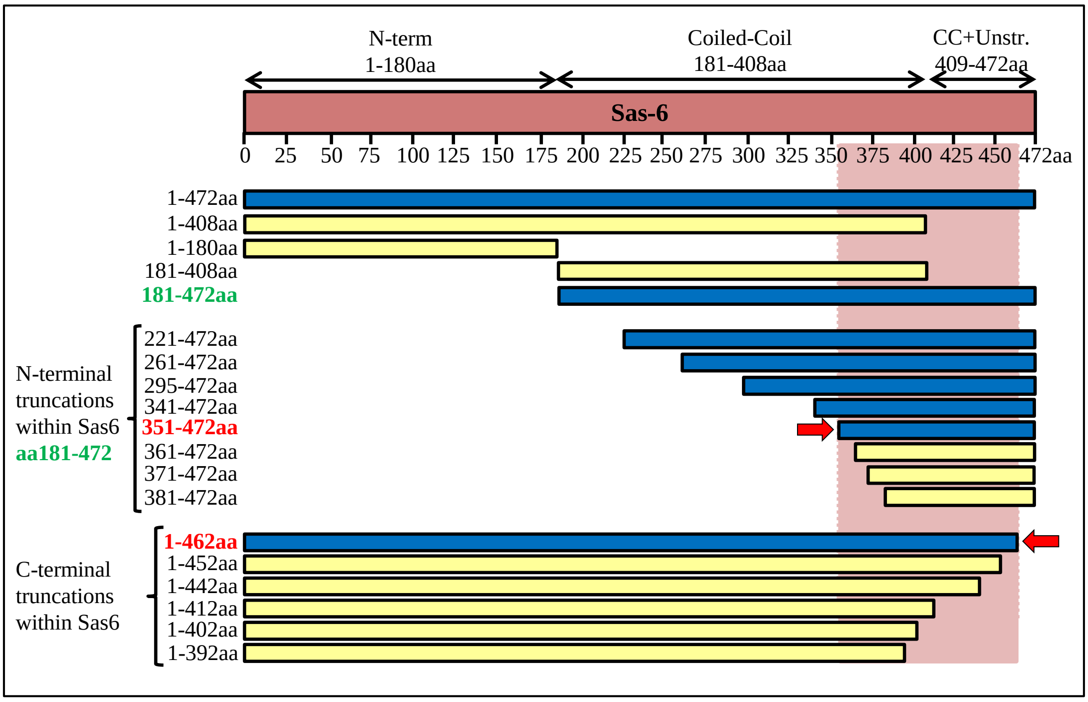

Figure 5-6 Schematic diagram of interactions of Sas6 protein fragments with Dragon *in vitro*. Sas6 fragments are shown relative to secondary structure features of Sas6 (N-term, coiled-coil, C-terminal coiled-coil and unstructured region). 19 Sas6 fragments were analysed corresponding to the indicated numbers of amino acids. Blue, Sas6 fragments that interact with Dragon *in vitro*. Yellow, Sas6 fragments that do not interact with Dragon *in vitro*. Units of the interacting region are identified by red arrows and pink shading.

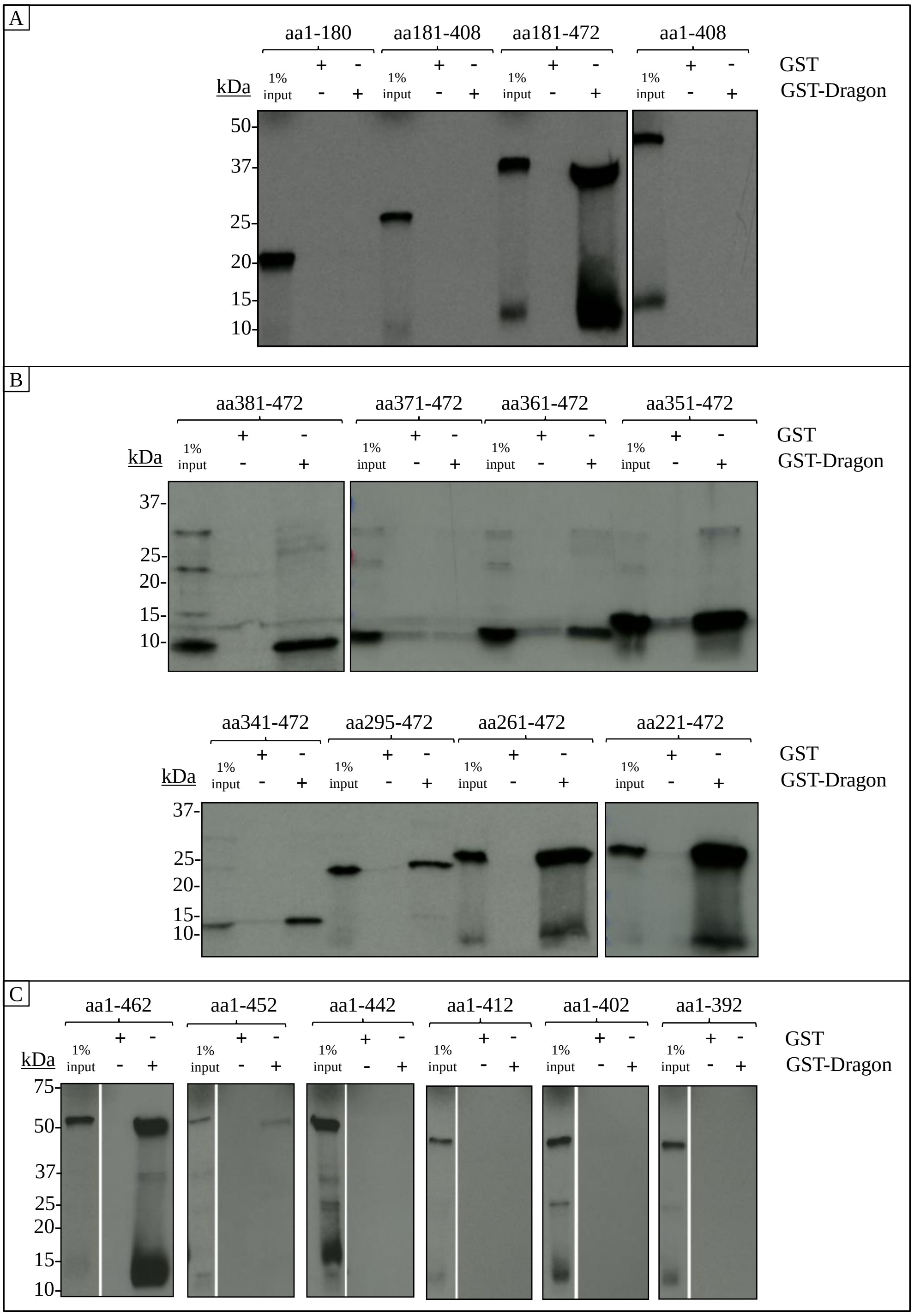

Figure 5-7 Autoradiograms of Sas6 fragments and their interaction with full-length Dragon. (A) Sas6 segment aa181-472 interacts with Dragon. (B) Testing for the smallest Sas6 fragment with stepwise N-terminal truncations within aa181-472 that interacts with Dragon reveals aa351-472. (C) Testing for the most C-terminal truncation within Sas6 that allows for interaction with Dragon reveals aa1-462. Complementary to Figure 5-6. Shown is 1% input of ^{35}S-Methionine-labelled Sas6 constructs and their interaction with GST (negative control) or GST-Dragon. Autoradiograms in (C) were cropped from the same exposure, original film in Appendix D.

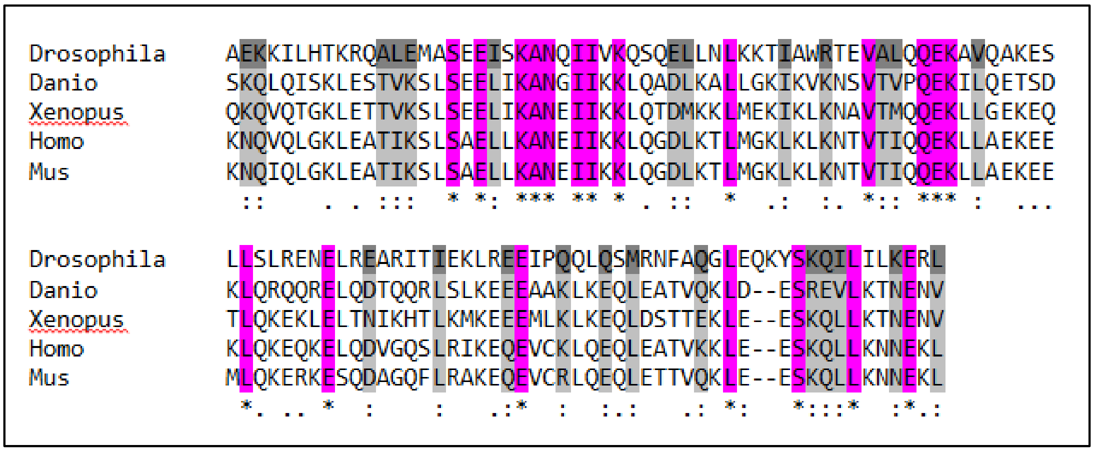

```
Drosophila      AEKKILHTKRQALEMASEEISKANQIIVKQSQELLNLKKTIAWRTEVALQQEKAVQAKES
Danio           SKQLQISKLESTVKSLSEELIKANGIIKKLQADLKALLGKIKVKNSVTVPQEKILQETSD
Xenopus         QKQVQTGKLETTVKSLSEELIKANEIIKKLQTDMKKLMEKIKLKNAVTMQQEKLLGEKEQ
Homo            KNQVQLGKLEATIKSLSAELLKANEIIKKLQGDLKTLMGKLKLKNTVTIQQEKLLAEKEE
Mus             KNQIQLGKLEATIKSLSAELLKANEIIKKLQGDLKTLMGKLKLKNTVTIQQEKLLAEKEE
                 ::    . . :::  * *: *** ** * . ::  *  .:  :. *:: *** :  ...

Drosophila      LLSLRENELREARITIEKLREEIPQQLQSMRNFAQGLEQKYSKQILILKERL
Danio           KLQRQQRELQDTQQRLSLKEEEAAKLKEQLEATVQKLD--ESREVLKTNENV
Xenopus         TLQKEKLELTNIKHTLKMKEEEMLKLKEQLDSTTEKLE--ESKQLLKTNENV
Homo            KLQKEQKELQDVGQSLRIKEQEVCKLQEQLEATVKKLE--ESKQLLKNNEKL
Mus             MLQKERKESQDAGQFLRAKEQEVCRLQEQLETTVQKLE--ESKQLLKNNEKL
                 *. .. *  :    :   .:*  :  :.:   .: *:   *:::*  :*.:
```

Figure 5-8 Alignment of the Dragon interacting region of *Drosophila melanogaster* Sas6 (aa351-462) shows that it is highly conserved. The five aligned species are: *Drosophila melanogaster*, *Danio rerio*, *Xenopus laevis*, *Homo sapiens* and *Mus musculus*. Pink background highlights amino acids conserved between species; grey background highlights similar amino acid groups between species, with dark grey background highlighting the amino acid for *Drosophila melanogaster*. Alignment generated with Clustal Omega [284].

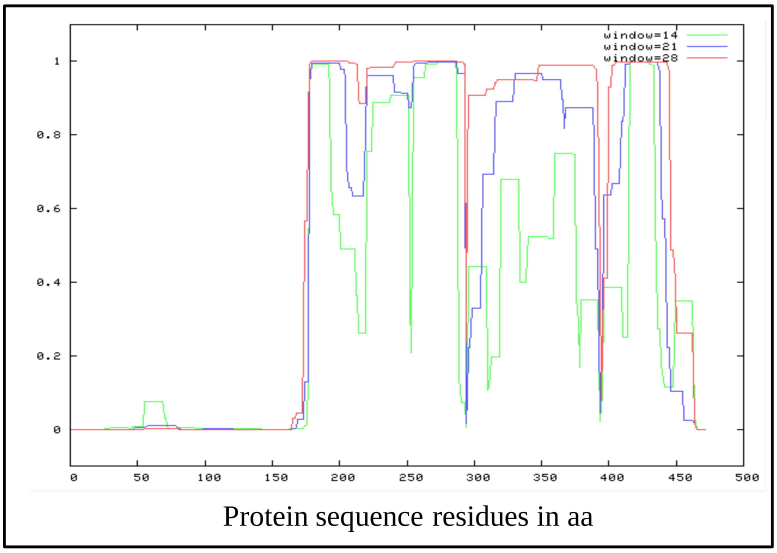

Figure 5-9 Secondary structure prediction shows that Dragon-interacting domain of Sas6 (aa351-462) is the C-terminal part of a predicted coiled-coil domain. Sas6 full-length secondary structure prediction shows the N-terminal head domain between residues 1 and 180, followed by a predicted coiled-coil domain and a small C-terminal unstructured region. Windows described in [286]; the higher the window number, the better is the distinction between coiled-coil and other regions. Analysing software: coils server [286].

5.2.4.3 The C-terminal coiled-coiled region of Dragon interacts directly with Sas6 *in vitro*

After I identified the Sas6 region aa351-462 within its coiled-coiled domain to interact directly with Dragon *in vitro*, I wanted to determine which part of Dragon binds directly to Sas6. To this end I constructed recombinant DNAs containing a T7 promotor and fragments of the Dragon DNA sequence, which I used to generate ^{35}S-Methionine-labelled Dragon protein fragments by coupled transcription-translation. I divided the Dragon protein fragments into N- and C-terminal parts (aa1-171 and aa172-339 respectively), and approximate thirds (aa1-113, aa114-243 and aa244-339 respectively) (Figure 5-10). I then performed binding assays with these ^{35}S-Methionine-labelled Dragon protein fragments and GST-Sas6 immobilised on resin (section 2.8.1). The fragments aa1-113, aa1-171 and aa114-243 did not interact with Sas6 whereas the fragment aa172-339 bound efficiently. The smaller C-terminal Dragon fragment, aa244-339, interacted with Sas6 but more weakly. I then expressed a Dragon fragment, aa191-318, designed to cover the predicted C-terminal coiled-coil domain of the protein (Figure 5-12). This fragment of Dragon (aa191-318) interacted with Sas6 as efficiently as full-length Dragon (Figure 5-11). This coiled-coil region of Dragon exhibits a high homology with *Danio rerio*, *Mus musculus* and *Homo sapiens*, *Xenopus (Silurana) tropicalis* and *Chrysemys picta bellii* (Figure 5-13).

In summary, the *in vitro* binding assays identified aa191-318 of Dragon as the binding domain for Sas6 protein, which corresponds to a predicted and conserved coiled-coil domain. I also showed that the aa351-462 segment of Sas6 interacts directly with Dragon (Figure 5-14).

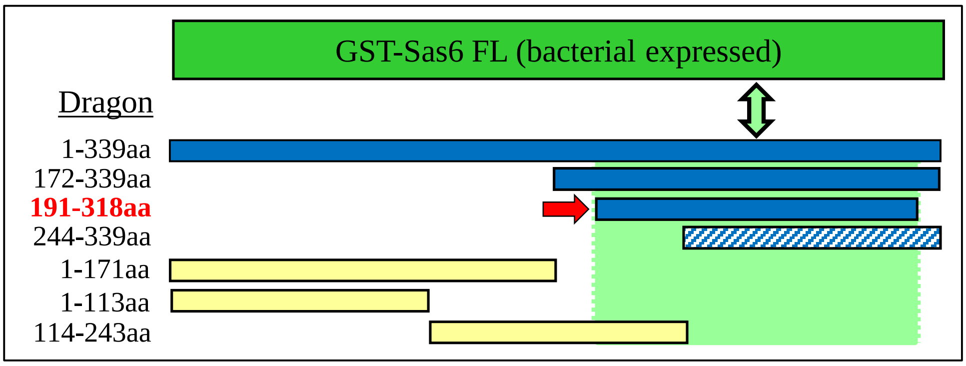

Figure 5-10 Schematic image of Dragon protein fragments that were tested for direct interaction with full-length Sas6 *in vitro*. The binding assays identified the C-terminal Dragon aa191-318 domain as the smallest fragment to strongly interact with Sas6. Blue, interaction; blue stripes, weak interaction; yellow, no interaction of Dragon fragment and Sas6 *in vitro*.

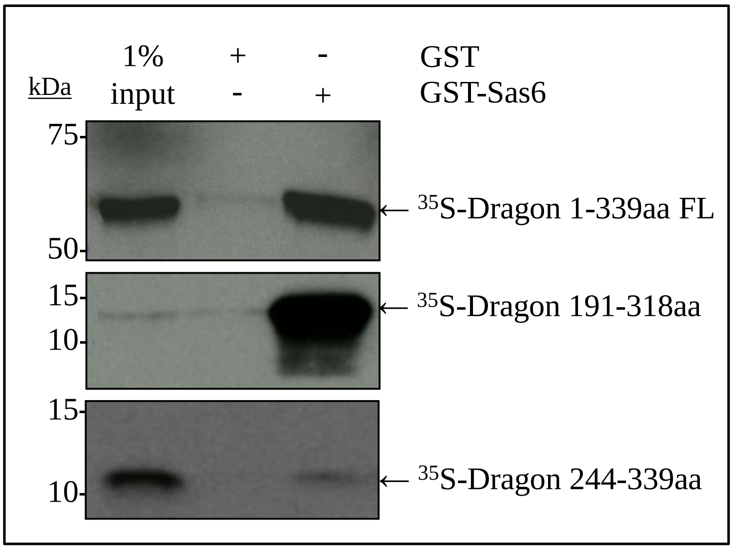

Figure 5-11 Autoradiograms showing binding of Sas6 with Dragon full-length and Dragon aa191-318. In contrast the comparably weak interaction with the smaller Dragon aa244-339 fragment. GST and GST-Sas6 immobilised on resin were incubated with ^{35}S-Methionine-labelled Dragon full length (aa1-339), aa191-318 or aa244-339. 1% input of the ^{35}S-Methionine-labelled Dragon constructs and the resin complexes were then subjected to SDS-PAGE and autoradiography. Complementary to Figure 5-10.

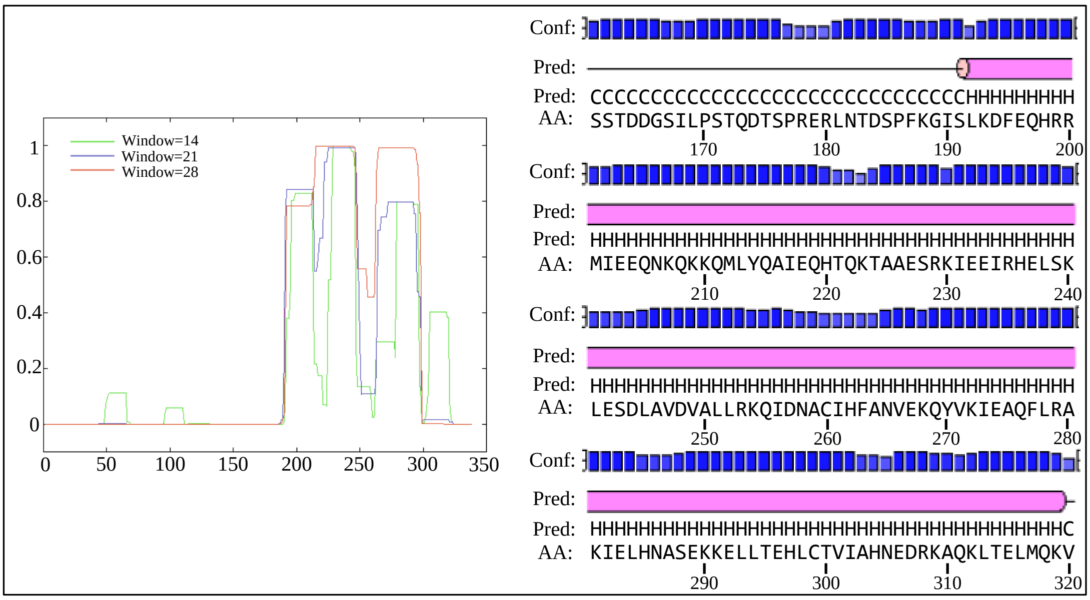

Figure 5-12 Secondary structure prediction of Dragon aa191-318, identified as interacting directly with Sas6 *in vitro*. This region of Dragon is predicted to be the main coiled-coil structure (right, pink) within the protein. Analysing software: coils server (left) [286] and Psipred (right) [285].

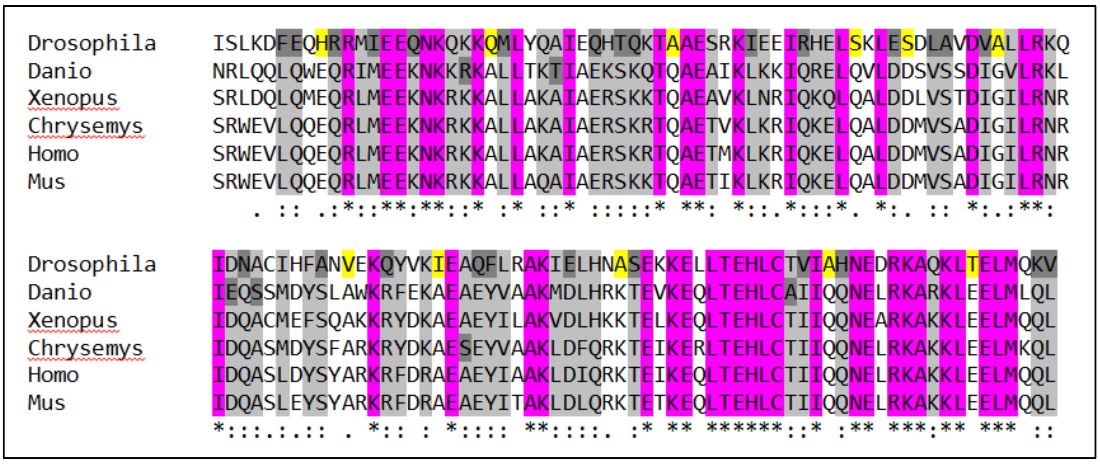

```
Drosophila    ISLKDFEQHRRMIEEQNKQKKQMLYQAIEQHTQKTAAESRKIEEIRHELSKLESDLAVDVALLRKQ
Danio         NRLQQLQWEQRIMEEKNKKRKALLTKTIAEKSKQTQAEAIKLKKIQRELQVLDDSVSSDIGVLRKL
Xenopus       SRLDQLQMEQRLMEEKNKRKKALLAKAIAERSKKTQAEAVKLNRIQKQLQALDDLVSTDIGILRNR
Chrysemys     SRWEVLQQEQRLMEEKNKRKKALLAKAIAERSKRTQAETVKLKRIQKELQALDDMVSADIGILRNR
Homo          SRWEVLQQEQRLMEEKNKRKKALLAKAIAERSKRTQAETMKLKRIQKELQALDDMVSADIGILRNR
Mus           SRWEVLQQEQRLMEEKNKRKKALLAQAIAERSKKTQAETIKLKRIQKELQALDDMVSADIGILRNR
                 . :: .:*::**:**::* :* ::* :::::* **: *::.*:::*. *:. :: *:.:**:

Drosophila    IDNACIHFANVEKQYVKIEAQFLRAKIELHNASEKKELLTEHLCTVIAHNEDRKAQKLTELMQKV
Danio         IEQSSMDYSLAWKRFEKAEAEYVAAKMDLHRKTEVKEQLTEHLCAIIQQNELRKARKLEELMLQL
Xenopus       IDQACMEFSQAKKRYDKAEAEYILAKVDLHKKTELKEQLTEHLCTIIQQNEARKAKKLEELMQQL
Chrysemys     IDQASMDYSFARKRYDKAESEYVAAKLDFQRKTEIKERLTEHLCTIIQQNELRKAKKLEELMKQL
Homo          IDQASLDYSYARKRFDRAEAEYIAAKLDIQRKTEIKEQLTEHLCTIIQQNELRKAKKLEELMQQL
Mus           IDQASLEYSYARKRFDRAEAEYITAKLDLQRKTETKEQLTEHLCTIIQQNELRKAKKLEELMQQL
              *:::.:.:: . *:: : *:::: **::::. :* ** ******::* :** ***:** *** ::
```

Figure 5-13 Alignment of *Drosophila melanogaster* Dragon aa190-320 with other species reveals conservation of the coiled-coil domain. The five aligned species are: *Drosophila melanogaster*, *Danio rerio*, *Xenopus laevis*, *Chrysemys picta bellii*, *Homo sapiens* and *Mus musculus*. Pink, amino acids conserved between all analysed species; grey, similar amino acid groups between species; dark grey, the single divergent amino acid within the analysed species; and yellow, a single divergent amino acid in *Drosophila* compared to all other analysed species. Alignment generated with Clustal Omega [284].

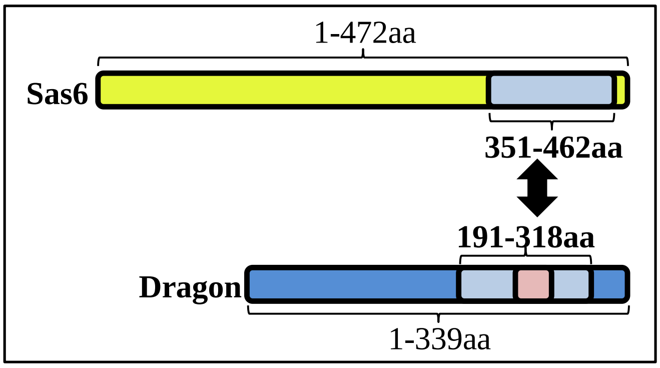

Figure 5-14 Summary figure of *in vitro* direct interaction assays. The C-terminal Sas6 aa351-462 (light blue) interacts directly with C-terminal Dragon aa191-318 (light blue) *in vitro*. Pink, Dragon interaction motif aa260-286 (as described in section 5.2.5).

5.2.4.4 Dragon interacts with itself *in vitro*

Sas6 molecules are known to dimerise via their coiled-coil regions and assemble into 9-fold cartwheel structures via their N-terminal head domains. This led me to consider whether Dragon, like Sas6, might oligomerise. I applied the *in vitro* direct binding assay used in previous sections to answer this question. I incubated full-length GST-Dragon bound to resin with full-length ^{35}S-Methionine-labelled Dragon in a binding assay, washed the resin to remove any unbound ^{35}S-Methionine-labelled Dragon, and subjected aliquots to SDS-PAGE and transferred the separated proteins onto nitrocellulose membrane for autoradiography. This showed that full-length Dragon molecules interact directly with each other. To characterise which region of Dragon enables oligomerisation, I carried out binding assays with the previously described ^{35}S-Methionine-labelled Dragon fragments and GST-Dragon (full-length) and GST-alone control (Figure 5-15). This revealed the C-terminal third of Dragon (aa244-339) as the smallest analysed Dragon fragment which can efficiently bind full-length Dragon directly (Figure 5-16). This region overlaps with the region that interacts with Sas6 (aa191-318; section 5.2.4.3). Significantly, the aa244-339 segment of Dragon was not able to bind Sas6 protein as efficient as aa191-318 (section 5.2.4.3). The analysis of the smallest protein region necessary for oligomerisation of Dragon still needs to be analysed further.

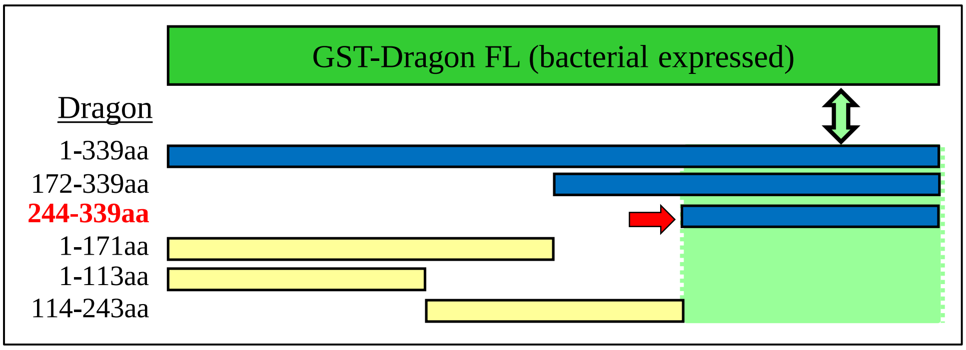

Figure 5-15 *In vitro* interaction analysis shows that Dragon interacts with itself at its C-terminus. Five Dragon fragments representing thirds and halves of the protein show that Dragon C-terminus is important for potential oligomerisation, with the most narrow analysed fragment covering aa244-339.

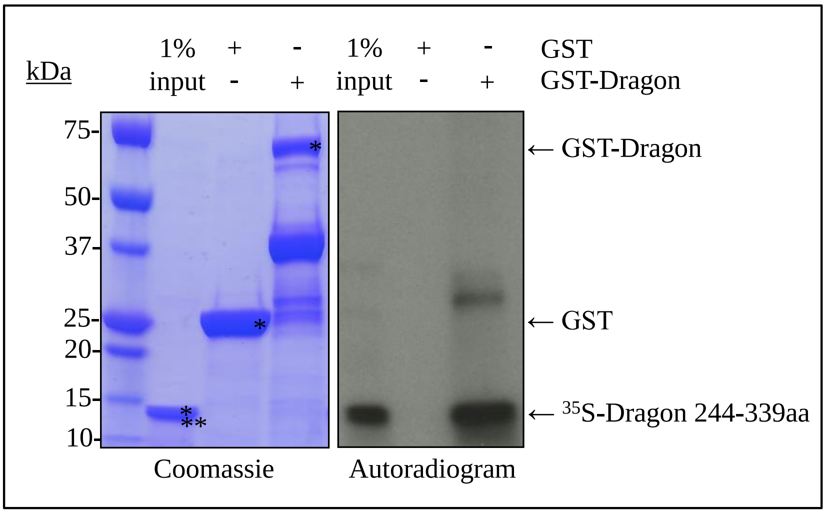

Figure 5-16 Dragon C-terminus (aa244-339) interacts with Dragon full-length *in vitro*. Protein coomassie gel and autoradiography show that ^{35}S-Methionine-labelled Dragon aa244-339 directly interacts with Dragon full-length protein. * protein sample loaded; ** reticulocyte lysate residue.

5.2.5 Identification of the interaction motif (IM) in Dragons’ C-terminal binding domain which is essential for interaction with Sas6

5.2.5.1 *In vitro* direct interaction screen of Dragon mutants, to identify a Dragon interaction motif necessary for the binding of Sas6

In section 5.2.4.3, I described a region of 128aa within the C-terminus of Dragon aa191-318 as able to bind Sas6. To narrow down the binding region I made small deletions within the conserved binding domain (Dragon aa191-318) by site-directed mutagenesis of grouped conserved amino acids. These mutants are summarised in Figure 5-17. These mutant constructs were used to generate ^{35}S-Methionine-labelled proteins *in vitro* that were used in binding assays with GST-Sas6. The outcome of these experiments is summarised in Figure 5-17. It can be seen that the smallest deletion which abolishes Dragon’s binding to Sas6 is aa260-286. Interestingly, three independent and smaller deletions within the region of Dragon (aa260-266, aa267-281 and aa282-286) are still able to bind Sas6 (Figure 5-18). Two further but larger deletion mutants, which include the 260-286aa deletion, also abolish binding of Sas6, namely deletions aa220-286 and aa220-318. This confirms the importance of aa260-286 of Dragon, in its interaction with Sas6. All other tested Dragon-mutants that carry a deletion outside of aa260-286 bind Sas6 efficiently *in vitro*.

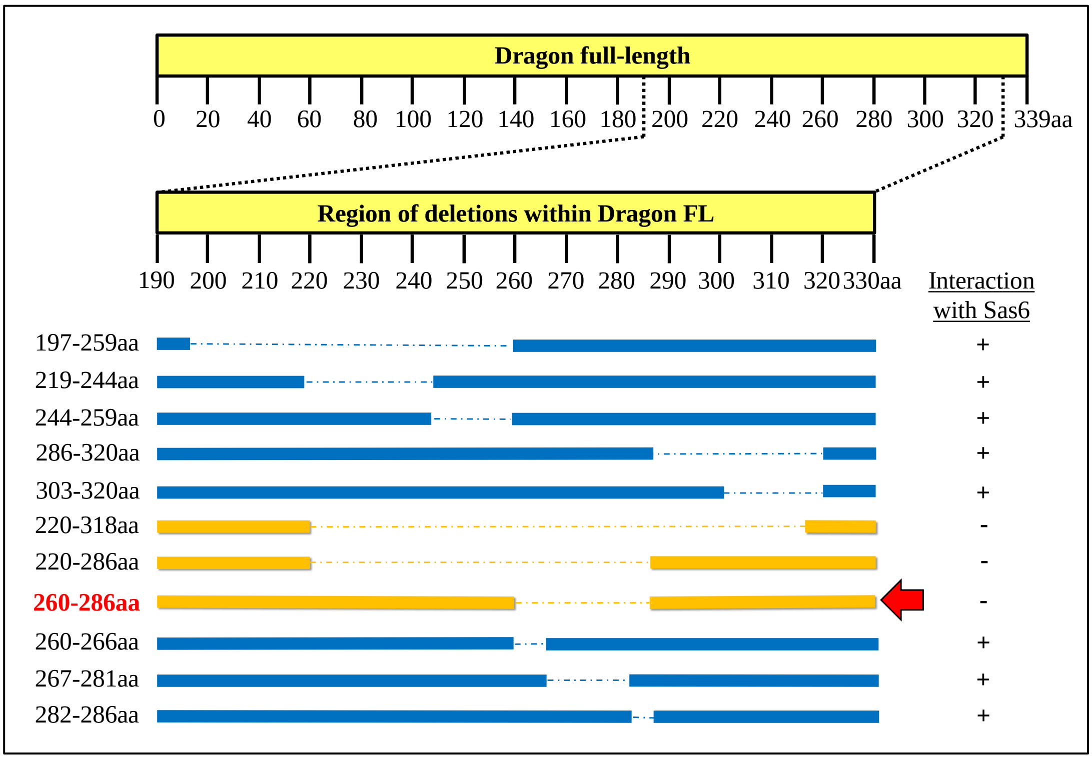

Figure 5-17 Dragon deletion mutants used to identify interaction motif (IM) for binding to Sas6 as aa260-286. 11 Dragon mutants were generated in full-length Dragon protein by site-directed mutagenesis, with deletions indicated. ^{35}S-Methionine-labelled mutant proteins were used in direct *in vitro* interaction assays with Sas6. +, *in vitro* interaction of Sas6 with Dragon mutant. -, no *in vitro* interaction of Sas6 with Dragon mutant.

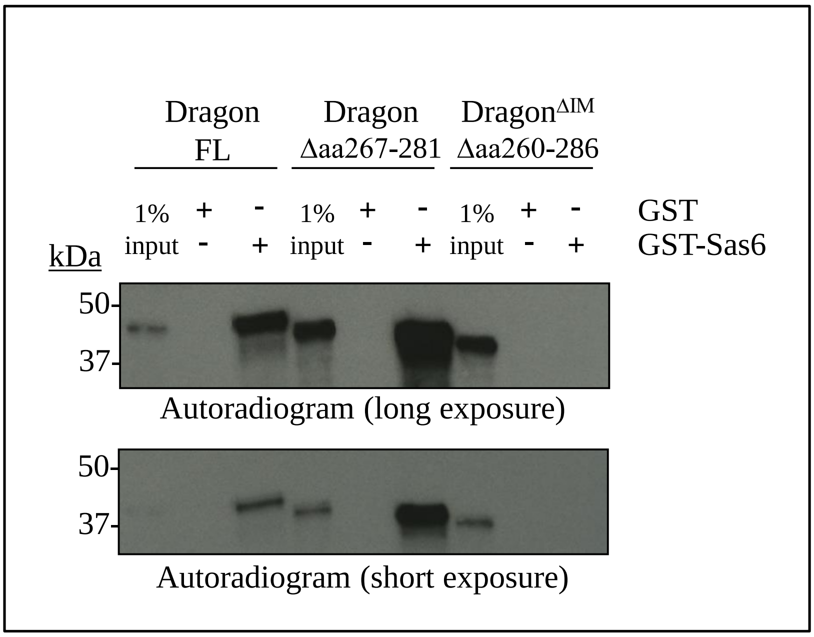

Figure 5-18 The mutant Dragon$^{\Delta IM}$ (DragonΔaa260-286) is unable to interact with Sas6 *in vitro*. Autoradiography of Sas6 interaction with ^{35}S-Methionine-labelled Dragon FL, DragonΔaa267-281 and Dragon$^{\Delta IM}$ (Δaa260-286); confirming interaction of the full-length proteins Sas6 and Dragon but that deletion of aa260-286 within Dragon abolishes this interaction. A smaller deletion in DragonΔaa267-281 still allows for interaction with Sas6. Short and long exposures confirm the lost direct interaction between Dragon$^{\Delta IM}$ and Sas6.

5.2.5.2 Purification of GFP-Dragon constructs from *Drosophila* cell culture, transiently transfected with Sas6 and Dragon variants, confirms that the Dragon-IM region is essential for interaction with Sas6 *in vivo*

Having identified a Dragon deletion (Δaa260-286) that fails to bind Sas6, I wished to determine the consequences of expressing this protein *in vivo*. Therefore, I transiently transfected *Drosophila* cell culture with myc-Sas6 and GFP; myc-Sas6 and GFP-Dragon; and myc-Sas6 and GFP-Dragon$^{\Delta IM}$ and performed GFP-purifications with extracts of each of the three transiently transfected cell culture samples. I then determined by Western Blotting and antibody staining, which Dragon construct could interact with Sas6 (Figure 5-19). I used antibodies against GFP, myc and α-tubulin to detect GFP/GFP-Dragon/GFP-Dragon$^{\Delta IM}$, myc-

Sas6 and α-tubulin (control) respectively. Figure 5-19 shows the according Western Blots of the GFP-purifications and inputs/cell lysates. The inputs confirm that each combination of transient transfection was efficient, as anti-GFP detects GFP, GFP-Dragon and GFP-Dragon$^{\Delta IM}$, anti-myc detects myc-Sas6, and α-tubulin is detected in all three samples. The Western Blots of the GFP-purifications confirm that GFP, GFP-Dragon and GFP-Dragon$^{\Delta IM}$ are present in the respective cell samples. Significantly, I could only detect myc-Sas6 associated with GFP-Dragon. I could not detect myc-Sas6 with GFP only or with GFP-Dragon$^{\Delta IM}$. Thus the deletion of aa260-286 in otherwise full-length Dragon abolishes the interaction with Sas6 *in vivo*, confirming my *in vitro* findings.

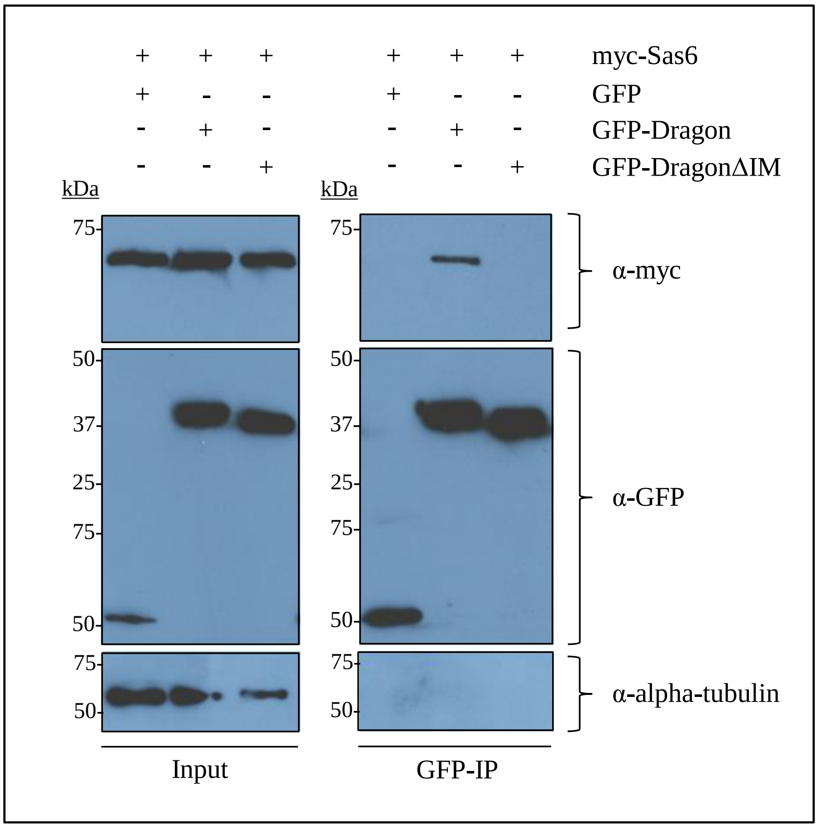

Figure 5-19 Co-IP confirms *in vivo* that Dragon$^{\Delta IM}$ cannot interact with Sas6. *Drosophila* cell cultures were transiently transfected with myc-Sas6 and GFP-Dragon$^{\Delta IM}$, GFP-Dragon or GFP, followed by GFP-IP. Western Blot and anti-myc staining shows loss of interaction between Sas6 and GFP-Dragon$^{\Delta IM}$, whereas interaction occurs between Sas6 and Dragon. Anti-GFP stains for GFP, GFP-Dragon and GFP-Dragon$^{\Delta IM}$. Anti-α-tubulin control and anti-myc signals detected in the input samples.

5.2.5.3 GFP-Dragon$^{\Delta IM}$ and its effect on centrosome numbers compared to GFP-Dragon and *Drosophila* WT cells

I then wished to determine whether the Dragon$^{\Delta IM}$ mutant could rescue loss of centriole depletion resulting from Dragon depletion (section 5.2.3.1). This experiment necessitated that I deplete Dragon efficiently with dsRNA against its UTR sequence so that I could utilise the mutant gene that does not carry the UTR sequences. To determine whether UTR mediated RNAi had similar effect on centriole duplication as observed with RNAi using Dragon CDS I carried out three 4 day rounds of RNAi directed against GST (control), Dragon CDS and Dragon UTRs (Figure 5-20). The loss of centrosomes was significant in a comparison between GST (control) and both Dragon depletions (CDS and UTRs). There is also a significant difference in cells without centrosomes when RNAi against Dragon CDS is compared to Dragon UTRs. But this difference is less significant compared to the GST control. Thus, depletion of Dragon by dsRNA CDS and UTRs are efficient and have a significant effect on centriole duplication, causing loss of centrosomes.

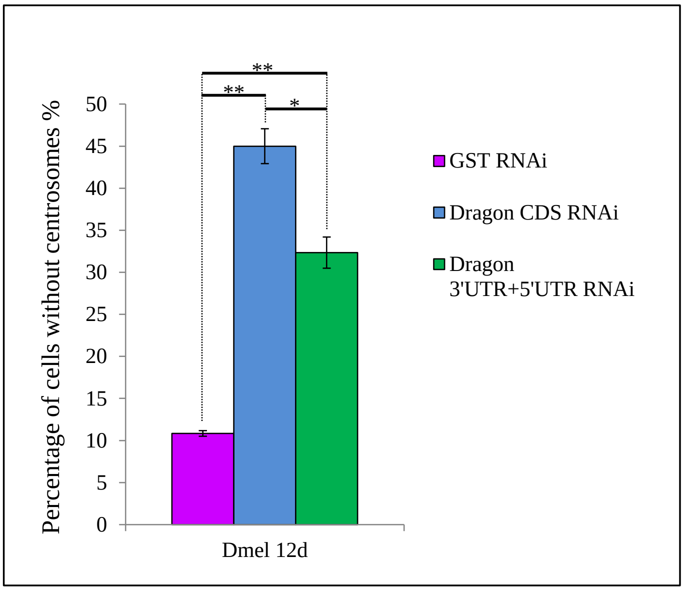

Figure 5-20 Depletion of Dragon using dsRNA against Dragon CDS or Dragon UTRs both lead to loss of centrosomes. *Drosophila* cell culture was depleted of Dragon by RNAi (dsRNA CDS or dsRNA UTRs) versus GST control RNAi. Centrosome numbers were scored on day 12, after three rounds of depletion. Error bars represent standard error; 3x200 cells counted; significance was calculated by t-test.

Having identified conditions for efficient depletion of Dragon by RNAi directed against its UTRs, I generated a cell line stably expressing GFP-Dragon$^{\Delta IM}$ from the constitutively active promotor poly-Ubiquitin. RNAi directed against Dragon UTR in control cells resulted in an increase of cells lacking centrosomes, from 13.3% to 26.7%. A similar result was seen for GFP-Dragon$^{\Delta IM}$ expressing cells where cells without centrosomes increase from 6.8% to 15.2%. But GFP-Dragon expressing cells show only a slight increase of cells without centrosomes, from 14.8% to 21.2%. The ratio of cells without centrosomes after GST RNAi versus Dragon UTRs RNAi is 1:2 in control cells, 1:2.2 in GFP-Dragon$^{\Delta IM}$ expressing cells, and 1:1.4 in cells expressing GFP-Dragon. Hence, Dragon$^{\Delta IM}$ fails to rescue the depletion of endogenous Dragon (Figure 5-21). The Western Blot in Figure 5-22 shows the complete depletion of endogenous Dragon after RNAi of Dragon UTRs and the expression of constitutively expressed GFP-Dragon and GFP-Dragon$^{\Delta IM}$.

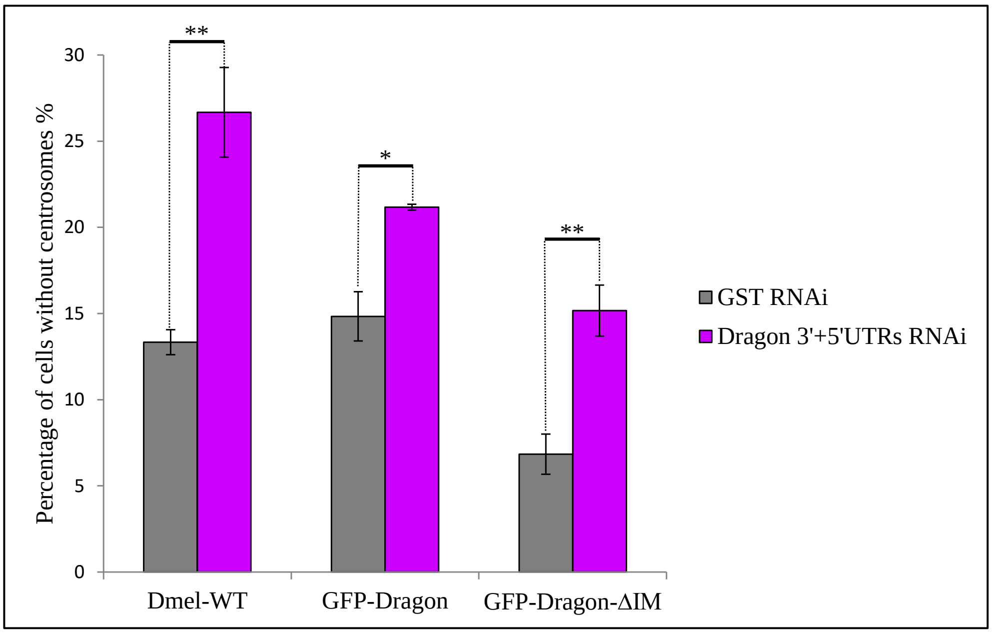

Figure 5-21 Expression of GFP-Dragon$^{\Delta IM}$ fails to rescue loss of centrosomes resulting from Dragon depletion. Cultured *Drosophila* cells stably expressing GFP-Dragon or GFP-Dragon$^{\Delta IM}$ were depleted of endogenous Dragon by dsRNA *Dragon UTRs* over two rounds of RNAi for eight days. Centrosome numbers were analysed after staining with the centrosomal marker D-Plp. *Drosophila* wild-type cells and GFP-Dragon$^{\Delta IM}$ expressing cells fail to rescue loss of centrosomes after depletion of endogenous Dragon. Cells expressing GFP-Dragon reveal a milder effect on loss of centrosomes. Error bars represent standard error; 3x200 cells counted; significance was calculated by t-test.

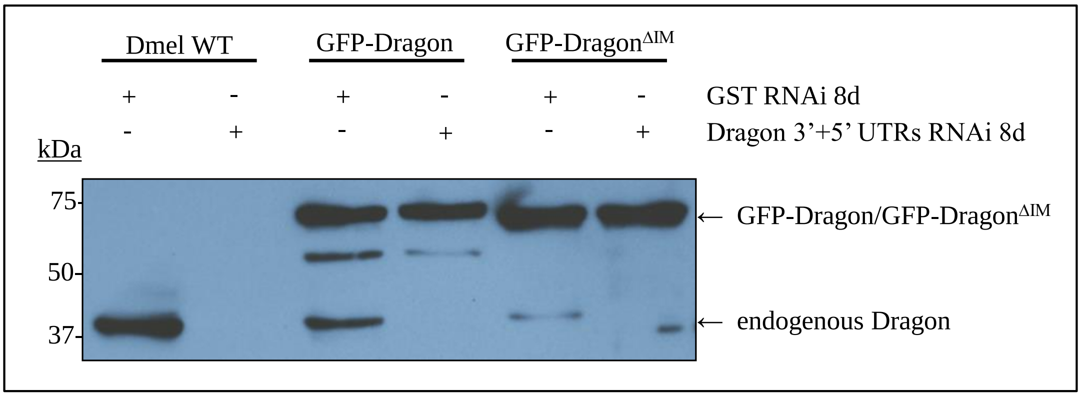

Figure 5-22 Endogenous Dragon is fully depleted from wild-type *Drosophila* cells and cells stably expressing GFP-Dragon or GFP-Dragon$^{\Delta IM}$ after two rounds of RNAi against Dragon UTRs over 8 days. Constitutively expressed GFP-Dragon and GFP-Dragon$^{\Delta IM}$, and endogenous Dragon are revealed by anti-DragonN antibody staining after Western Blot.

5.2.6 Study of the human homologues GoRab and HsSas6, in relation to the findings for *Drosophila* Dragon and Sas6

5.2.6.1 The human homologues GoRab and HsSas6 interact directly *in vitro*

As human cells have homologues for both proteins Dragon and Sas6, namely GoRab and HsSas6 respectively, I wished to analyse if these human homologues also interacted directly. The human homologue GoRab has two functional isoforms, variant 1 and variant 3. The first isoform represents the full-length protein (395aa) and the latter is a shorter version (247aa), which lacks the C-terminal extension of variant 1. When comparing these two variants with *Drosophila* Dragon by homology, it is evident, that only GoRab variant 1 contains the region homologous to *Drosophila* Dragon-IM (aa260-286) and the full *Drosophila* Sas6-binding domain (aa191-318). GoRab variant 3 contains only aa191-247, which corresponds to the N-terminal region of the *Drosophila* Dragon for Sas6 binding (aa191-246) upstream of *Drosophila* Dragon-IM (aa260-286) (Figure 5-23, Figure 5-24). To study if human GoRab and HsSas6 interact directly with each other, I expressed GST-HsSas6 in *E. coli* and bound it to Glutathione Sepharose 4B resin via the GST tag (section 2.5.1). I generated ^{35}S-Methionine-labelled GoRab variant 1 and variant 3 by coupled *in vitro* transcription-translation reaction. I then performed *in vitro* binding assays (section 2.8.3) with GST-HsSas6 and ^{35}S-Methionine-labelled GoRab variant 1 or variant 3, subjected the proteins to SDS-page and transferred the separated proteins onto nitrocellulose membrane for autoradiography. The autoradiograms show that GoRab variant 1 directly interacts with HsSas6 but not the negative control GST-alone (Figure 5-25A). In contrast, ^{35}S-Methionine-labelled GoRab variant 3 interacts similarly with the negative control GST and GST-HsSas6, indicative of background binding and not due to the interaction of ^{35}S-Methionine-labelled GoRab variant 3 with HsSas6.

In summary the human counterparts of Dragon and Sas6, GoRab variant 1 and HsSas6, also interact directly with each other *in vitro*. A second isoform of the human homologue, GoRab variant 3, which is a shorter C-terminal truncated isoform of variant 1, does not interact directly with HsSas6 *in vitro*.

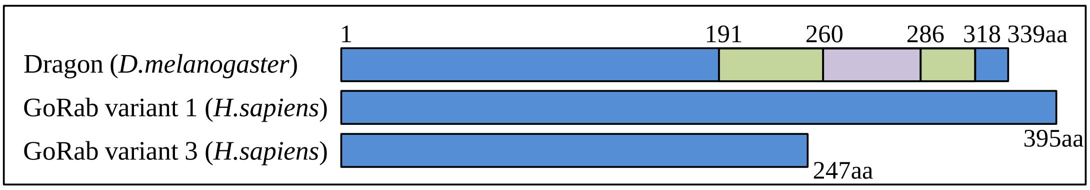

Figure 5-23 Homology between *Drosophila* Dragon and *Homo sapiens* GoRab variant 1 and variant 3. *Drosophila* Dragon aa191-318 (green) is the Sas6 binding domain identified by direct *in vitro* binding assays, and aa260-286 (purple) is the Dragon-IM that is necessary for Sas6 to bind Dragon. GoRab variant 1 includes the full and according homologous region of Dragon aa190-318, whereas GoRab variant 3 is a shorter isoform which only contains the most N-terminal homologous region and lacks the homologous Dragon-IM and the upstream sequence.

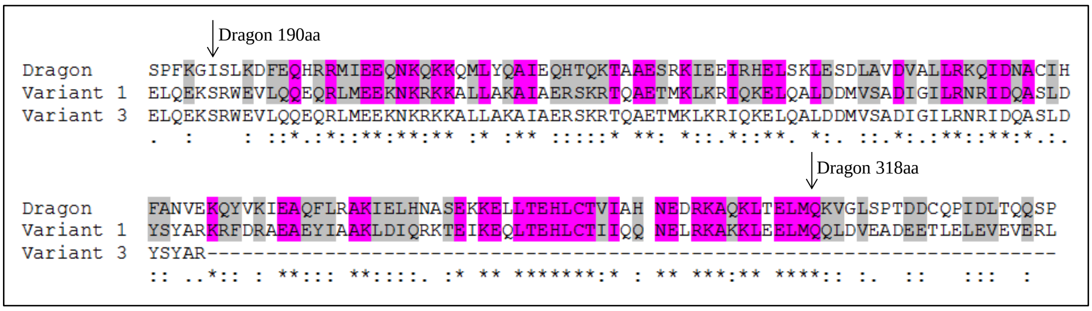

```
                 ↓Dragon 190aa
Dragon      SPFKGISLKDFEQHRRMIEEQNKQKKQMLYQAIEQHTQKTAAESRKIEEIRHELSKLESDLAVDVALLRKQIDNACIH
Variant 1   ELQEKSRWEVLQQEQRLMEEKNKRKKALLAKAIAERSKRTQAETMKLKRIQKELQALDDMVSADIGILRNRIDQASLD
Variant 3   ELQEKSRWEVLQQEQRLMEEKNKRKKALLAKAIAERSKRTQAETMKLKRIQKELQALDDMVSADIGILRNRIDQASLD
            .  :    : ::*.:*::**:**:** :* :** :::::* **: *::.*::**. *:. ::.*:.:**::**:*.:.
                                                                    ↓Dragon 318aa
Dragon      FANVEKQYVKIEAQFLRAKIELHNASEKKELLTEHLCTVIAH NEDRKAQKLTELMQKVGLSPTDDCQPIDLTQQSP
Variant 1   YSYARKRFDRAEAEYIAAKLDIQRKTEIKEQLTEHLCTIIQQ NELRKAKKLEELMQQLDVEADEETLELEVEVERL
Variant 3   YSYAR------------------------------------------------------------------------
            :: ..*:: : **::: **::::. :* ** *******:* : ** ***:** ****:: :.  ::   :::  :
```

Figure 5-24 Alignment of *Drosophila* Dragon aa185-338 and *Homo sapiens* GoRab variant 1 and variant 3. GoRab variant 1 and variant 3 share the same sequence of amino acids but differ in length. Highlighted are the same amino acids that are identical between Dragon and GoRab (pink) or similar (grey). Alignment generated with Clustal Omega [284].

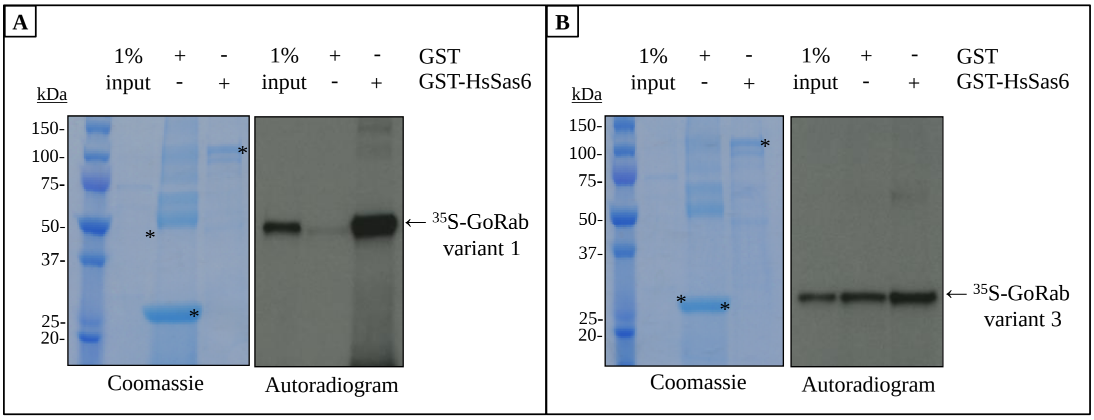

Figure 5-25 Only the long isoform of GoRab variant 1 directly interacts with HsSas6 *in vitro*, confirming findings for *Drosophila* Dragon and Sas6. ^{35}S-Methionine-labelled GoRab variant 1 and variant 3 were individually assessed for binding to HsSas6 *in vitro*. Coomassie stainings show protein inputs for GST and GST-HsSas6. Autoradiograms show direct interaction of GoRab variant 1 with HsSas6 but lacks specific interaction for GoRab variant 3 with HsSas6.

5.2.6.2 Centrosome numbers are reduced in U2OS cells following GoRab RNAi

After I determined that HsSas6 and GoRab variant 1 could interact directly with each other *in vitro* (section 5.2.6.1), I wished to know whether depletion of GoRab in human cell culture would reduce centrosome numbers, as observed after depletion of Dragon in *Drosophila* cell culture in section 5.2.3.1.

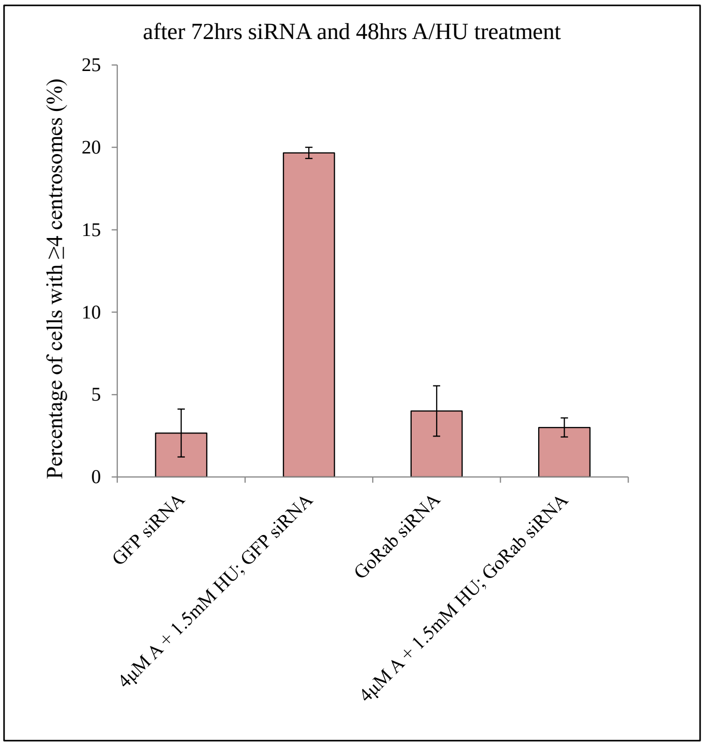

Figure 5-26 Depletion of GoRab in U2Os cells negatively affects centriole duplication. U2Os cells that are arrested in S-phase by Aphidicolin (A) and HydroxyUrea (HU) treatment and under control GFP siRNA conditions show a significant increase in cells with ≥4 centrosomes per cell. Treatment of U2Os cells with GoRab siRNA prevents an increase in cells with ≥4 centrosomes per cell, suggesting a negative effect on centriole duplication. Error bars represent standard error; 3x100 cells counted.

To address this question, I depleted GoRab via siRNA from U2OS cells and blocked the cells in S-phase 24 hours after transfection with Aphidicolin and Hydroxyurea before assessing centrosome numbers; GFP siRNA was used as a negative control (section 2.9.4). When U2OS cells are blocked in S-phase by Aphidicolin and Hydroxyurea, DNA duplication and therefore cell division is prohibited, but centriole duplication still occurs as normal leading to an increase in the number of centrosomes within each cell. Accordingly, cells treated with control RNAi and blocked in S-phase show an increase from 2.7% to 19.7% of cells having ≥4 centrosomes per cell. By contrast, U2OS cells treated with GoRab siRNA alone exhibited just 4% of cells with ≥4 centrosomes per cell, which is comparable to the 3% of U2OS cells showing ≥4 centrosomes per cell after treatment with GoRab siRNA and being blocked in S-phase. This shows that duplication of centrosomes in S-phase blocked U2OS cells is prevented after depletion of GoRab. Thus, the homologues Dragon and GoRab appear to have roles in centriole duplication in *Drosophila* and human cells respectively.

5.3 Discussion

5.3.1 Dragon and the centrosome

It is curious why purification of Sas6 from cultured cells do not show other centriole duplication proteins. But most interestingly, the uncharacterised Dragon was present in all Sas6 purifications (Table 5-1). Indeed, Dragon and Sas6 appear to be in complex *in vivo*, when either is overexpressed in *Drosophila* cell cultures, or in *Drosophila* syncytial embryos overexpressing Dragon (Table 5-1 and Table 5-2). The levels/'number of peptides' of Dragon were increased when purified Sas6 is constitutively expressed in *Drosophila* syncytial embryos compared to induced overexpression of Sas6 in *Drosophila* cell culture. On the other hand treatment with okadaic acid to inhibit dephosphorylation by PP2A and treatment with MG132 to inhibit proteasomal degradation did not seem to affect the ratio of Sas6:Dragon. Thus, Dragon seems to associate with Sas6 in a phosphorylation independent manner. On the other hand, the constitutive expression of Dragon results in a higher number of Sas6 peptides in complex compared to the induced expression of Dragon, which can be due to constitutive versus induced expression. Alternatively, complex formation could be affected by the tag on the N- or C-terminus of Dragon. It is possible that the GFP-tag at the C-terminus interferes with the ability of Sas6 to be in complex with Dragon.

Dragon localises with Sas6 to the mother and procentriole/daughter centriole (Figure 5-2). Its presence at procentriole formation could indicate that it supports the process of daughter centriole formation [296]. An indication for a potential structural role of Dragon at the centriole is its localisation not only at the procentriole/daughter centriole but that it also remains co-localised with Sas6 at the mother centriole. Additionally, depletion of Dragon causes loss of centrosomes (Figure 5-4). To further understand the recruitment of Sas6 and Dragon to the centriole, additional structural illumination microscopy needs to be performed to study the interdependency of Dragon and Sas6 at the centriole when one or the other protein is depleted. This will shed light on their recruitment hierarchy to the site of procentriole formation to determine whether this occurs sequentially, together, or interdependent, and the consequences of their depletion upon the centrosome structure.

5.3.2 Dragon and the Golgi

Dragon also localises to the Golgi (Figure 5-1), in accordance with previous observations with the human homologue GoRab [202]. Specifically it co-localises with Golgin-245 at the *trans*-Golgi (Figure 5-3), as was observed for the human homologue GoRab [202], and the GoRab interacting partner Rab6 [320]. Dragon's function at the *trans*-Golgi is not known but indications from mass spectrometry analyses of its complexes suggest a potential role in dependency to COPI. This is because five out of seven subunits of COPI were identified by mass spectrometry as co-purifying with Dragon from cultured *Drosophila* cells. Interestingly, COPI is one of three types of vesicles at the Golgi, in addition to COPII and clathrin-coated vesicles. These proteins are vesicle coat proteins with a diverse set of functions at the Golgi, representing division of the Golgi into three stages of maturation from the cisternal assembly stage to the carbohydrate synthesis stage and carrier formation (Figure 1-13) [321,322]. The three types of Golgi coat proteins function in direct protein and membrane trafficking, by selecting specific cargo proteins in different Golgi compartments. Proteins synthesized in the Endoplasmic Reticulum (ER) are selectively exported by COPII vesicles, which in turn then bud to form new *cis*-Golgi cisterna [323]. On the other hand, COPI vesicles function in the transfer of Golgi proteins between medial- and *trans*-Golgi cisternae, and additionally recycle proteins from the *cis*-Golgi to the ER [323–326]. The third vesicle type, clathrin-coated vesicles, are cargo carriers that form during cisterna disintegration at the *trans*-Golgi-network (TGN) and apparently recycle proteins from mature to newly formed TGN cisternae [327–329]. It is known that COPI protein forms two subcomplexes; the adaptor subcomplex made up of γ-β-δ-ζ-COPs and the cage-like subcomplex of α-β'-ε-COPs [330–334]. The mass spectrometry data shows that all subunits of the latter are present in the Dragon purifications from *Drosophila* cell culture (Table 5-3). Thus, suggesting a COPI specific function of Dragon at the Golgi.

That the subunits of COPI and COPII are not present in the Dragon complexes purified from *Drosophila* syncytial embryos most likely reflects the timing of the biosynthesis of the Golgi. The Golgi apparatus consists of small fragments in syncytial and gastrulating *Drosophila* embryos [335–338] but it mainly develops later to have small vesicles and tubules in early third-instar larvae (72 hours after fertilisation). Larger clusters of Golgi marked with GM130, p115, and Fringe appear in late third-instar larvae, and only at the pupa state do Golgi stacks appear (120 hours after fertilisation) [339,340]. Additional support for the hypothesis that *Drosophila* Dragon functions in the secretory pathway comes from the known interaction of the human homologue GoRab with Rab6 [202]. Rab6 functions in the recruitment of motor proteins and the retrograde transport from endosomes to the Golgi apparatus [341,342]. The absence of Rab proteins in complex with the purified Dragon from *Drosophila* cell culture is therefore surprising but may reflect the stability of this association. I was unable to reveal a function of Dragon at the Golgi because the attempted depletion of Dragon did not show any changes in the co-localisation with the *trans*-Golgi marker Golgin-245 or localisation of the *cis*-Golgi marker GM130 by fluorescent microscopy (data not shown, collaboration with Miss Chu). Several explanations are possible: either the RNAi was inefficient at depleting Dragon to a sufficient degree to see a Golgi phenotype; that the assay used was inadequate for deleting Dragon's Golgi function; or that indeed Dragon has no Golgi function. An interesting finding for more study is C-terminal binding protein (CtBP) that is present in complex with Dragon (Table 5-3). CtBP is required for the G2-mitotic checkpoint that leads to fission of the Golgi ribbon into separate Golgi stacks in mammalian cells [343], followed by further fragmentation and disassembly [344]. The specific function or the mechanism behind the disassembly of the mammalian Golgi is not understood but suggestions include that the process could be necessary for the correct division of the Golgi into the two daughter cells by the mitotic spindle during cell division [345] or that the Golgi disassembly might release proteins that are important for chromosome segregation or cytokinesis. Importantly and in contrast to mammalian Golgi, *Drosophila* Golgi stacks are not connected by a ribbon [183] and they do not fragment or disassemble [346]. But we know that Dragon exhibits dual localisation to the Golgi and the centrosome (section 5.2.2), and that the Golgi is associated with microtubules and the centrosome [184,345]. Initial pilot experiments of *in vitro* binding assay failed to indicate direct protein interaction of CtBP with Dragon or Sas6 (data not shown). Could therefore CtBP function be part of a signalling pathway linking the Golgi and the centrosome or cilia for centriole biogenesis or cilia absorption; for the progress of the cell into mitosis; or the correct division of the Golgi into the two daughter cells during cell division? These speculations also go hand in hand with the finding that the centrosomal Dragon signal increases in interphase and adjusts to the levels of its interacting partner Sas6 thereafter (Figure 5-2). Additionally, the mammalian homologue CtBP is targeted by Pak1 kinase [347], which is required for mitotic entry [348]; and the function of CtBP in mitotic entry could be conserved in *Drosophila*. Dragon's specific function at the Golgi was not the focus in this study and further studies need to be performed to understand its potential role in secretion and signalling pathways.

5.3.3 Physical interaction of Dragon and Sas6

My findings demonstrate that Dragon and Sas6 interact directly with each other *in vitro* (section 5.2.4.1). It is Sas6 fragments that contain the C-terminal region of the coiled-coil domain that interact with Dragon *in vitro* (schematic in Figure 5-6). Significantly, this region was not described previously. On the other hand, the N-terminal head domain of Sas6 form the cartwheel hub of centrioles, and the N-terminal regions of the coiled-coil domains of two Sas6 molecules dimerise and form a spoke of the centriole cartwheel. The most truncated protein fragments of Sas6 that still interact strongly with Dragon are the segments aa351-472 and Sas6 aa1-462 (Figure 5-6, Figure 5-7). The latter is potentially truncated by the majority of the predicted unstructured C-terminal domain of Sas6. Figure 5-9 suggests that the predicted coiled-coil domain ends around aa450 and a closer analysis of the homology alignment of Sas6 from multiple species in Figure 5-8 shows a two amino acids insertion (QK: Glutamine and Lysine respectively) only in *Drosophila* at aa449-450 and could potentially be the site of transition from coiled-coil to unstructured protein sequence. The homology alignment of Sas6 (Figure 5-8) shows conserved regions but it does not identify a specifically and highly conserved domain in the C-terminal region of the coiled-coil domain.

The structural features of *Drosophila* Dragon protein are uncharacterised. It has a predicted C-terminal coiled-coil domain (aa191-318, Figure 5-12) that interacts directly with Sas6 *in vitro* (Figure 5-10, Figure 5-11). Significantly, the C-terminal third fragment of Dragon (aa244-339), which is smaller and misses the N-terminal part of the coiled-coil domain, interacts only weakly with Sas6. This suggests a specific interaction of the whole coiled-coil domain of Dragon with Sas6. This notion is supported by the alignment studies of *Drosophila* Dragon aa190-320 with other species, which confirms that the coiled-coil domain is highly conserved between species (Figure 5-13). On the other hand, sequences N- and C-terminal to the coiled-coil region show almost no conserved residues, apart from a short 12 amino acid stretch in the N-terminus (aa5-16 in *Drosophila*, not shown). Thus, the coiled-coil domain is likely to play an important role that is conserved throughout species. The C-terminus of Dragon interacts with Sas6, making it likely that a C-terminally tagged Dragon is less efficient at interacting with Sas6, highlighting the importance of the accessibility of Dragon's C-terminally coiled-coil domain (section 5.2.4.3).

That Dragon interacts with C-terminal Sas6 suggests that it localises to the ends of the centriole cartwheel spokes. Potential functions could be stabilising the cartwheel endings; aiding and guiding Sas6 self-assembly abilities as a distance spacer between Sas6 cartwheel spokes; determining the 9-fold symmetry of the centriole; or supporting the transition zone between the cartwheel and microtubules. The specificity of Dragon interaction and co-localisation with Sas6 is intriguing as Dragon was not observed in other purifications of centriole duplication proteins. Preliminary attempts were made in collaboration with Dr. Gang Dong (Vienna) to address the stoichiometry of the Dragon and Sas6 interaction with the potential to purify an affinity complex for crystallisation trials. However the expression of Dragon resulted in low purification yields, and increasing concentrations led to aggregate formation. On the other hand, a smaller fragment of Dragon (aa172-339) proved unstable and degraded during purification. In summary, when Sas6 and Dragon are co-expressed, these problems of Dragon degradation and aggregation have not allowed to date for the measurement of exact binding affinities. Thus, it was not possible to advance further structural examination of Dragon or its interaction with Sas6. Further studies will be required to precisely characterise Dragon's structure and function at the centrosome.

A region of potential Dragon self-interaction was found in the Dragon C-terminal third (aa244-339) that overlaps with the region that interacts directly with Sas6 (section 5.2.4.4, Figure 5-10, Figure 5-15). The potential of competition between Dragon oligomerisation and its interaction with Sas6 presents regulatory possibilities that should be studied further.

Protein phosphorylation plays a critical role in centriole duplication. Hennies *et al.* highlight that GoRab protein has many predicted phosphorylation sites (Figure 5-27A) [202], but Dragon has potentially many fold more possibilities of potential phosphorylation (Figure 5-27B). Remarkably there are clusters of predicted phosphorylation sites at Dragon aa79-94 and aa113-191, which are located directly upstream of the Sas6 binding site (aa191-318). This further fuels the idea that the phosphorylation of Dragon by an unknown kinase might be necessary for its function at the centrosome or Golgi. To gain a better understanding of Dragon's function at both the centrosome and Golgi, it will be important to identify and characterise other interacting proteins of Dragon and the phosphodependence of their interactions. Additionally, this might further our understanding of the microtubule nucleation functions of the centrosome and the Golgi, and a potential link between the two processes.

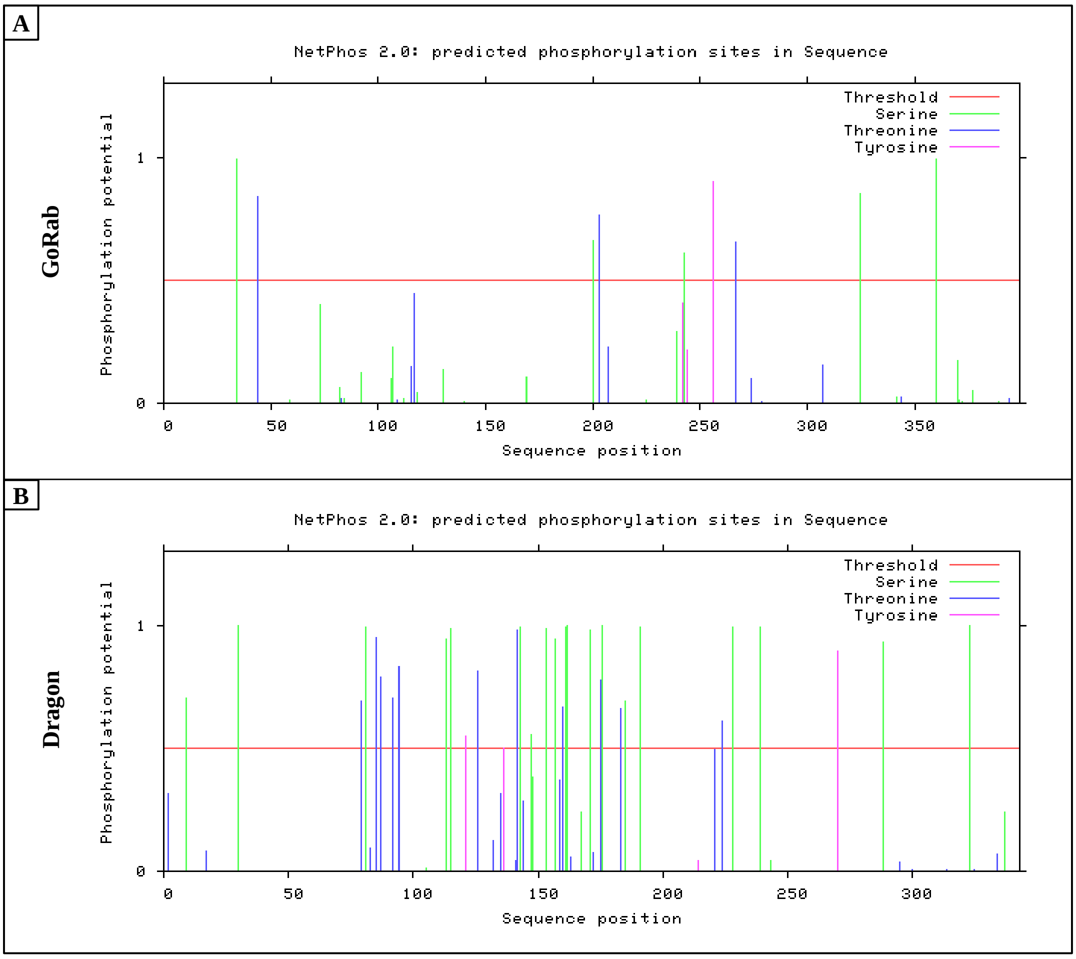

Figure 5-27 Predicted generic phosphorylation sites in the homologous GoRab (A) and Dragon (B). Analyses performed with NetPhos 2.0 Server [349] over the whole protein sequences of GoRab and Dragon. The sequence position of potential phosphorylation sites (in amino acids) are blotted against their phosphorylation potential (with 0 to 1 equalling ‘unlikely’ to ‘very likely’, and the threshold in red at 0.5). Pictured are predicted phosphorylation sites for Serine (green), Threonine (blue) and Tyrosine (pink). The closer the phosphorylation potential towards 1, the more ‘very likely’ is the predicted phosphorylation site a true phosphorylation site.

To study the cellular effect of loss of interaction between Dragon and Sas6 at the centrosome, I further analysed which smaller site in Dragon aa191-318 was essential for interaction with Sas6. A mutant that lacks the region aa260-286 cannot interact with Sas6 *in vitro* (section 5.2.5.1). This interaction motif (IM) could be the necessary site for direct protein-protein interaction between Dragon and Sas6 or it could function as a “spacer” within

Dragon that leads to a secondary structure formation of Dragon that allows for physical interaction with Sas6. If this “spacer” was deleted, as for the Dragon$^{\Delta IM}$ mutant, it could change the secondary structure of Dragon and consequently its physical and structural ability to bind Sas6. The Dragon$^{\Delta IM}$ mutant cannot rescue the loss of centrosomes after the depletion of endogenous Dragon (section 5.2.5.3). Whether the loss of centrosomes after loss of interaction between Dragon and Sas6 is directly due to failed co-recruitment of Dragon and Sas6 to the procentriole or a missing protein interaction at the centrosome itself requires further study by immune fluorescence and especially high resolution structured illumination microscopy. This will shed light on the dependency of the interaction of Dragon and Sas6 on recruitment and localisation of the two proteins to the centrosome. Both possibilities are likely and yet it is surprising that Dragon has not been described previously in screens for *Drosophila* centriole duplication proteins [131,288]. Therefore, it seems rather likely that Dragon supports centriole duplication structurally by interacting with the cartwheel protein Sas6.

5.3.4 The human homologue GoRab and centriole duplication

The human homologue of Dragon, GoRab, has been described in relation to the disease Gerodermia osteodysplastica but a centrosomal connection has not been published. But alignments of Dragon and GoRab from different species, including *Drosophila* and *Homo sapiens*, show that the C-terminal domain of *Drosophila* aa191-318 is highly conserved (Figure 5-13, Figure 5-24). The identification of the novel direct interaction of Sas6 and Dragon and its effects on centriole duplication when Dragon is depleted or cannot interact with Sas6 raises the question if this function is conserved in the human homologue GoRab (section 5.2.6). Two functional isoforms of GoRab are known, GoRab variant 1 and GoRab variant 3, which share the same amino acid sequence but variant 3 is truncated at the C-terminus (Figure 5-22). A closer analysis of the isoforms with the homology alignment reveals that GoRab variant 3 does not align to the full Dragon region that interacts with Sas6 (aa191-318); it only contains most of the N-terminal region downstream of Dragon-IM (aa260-286). On the other hand, GoRab variant 1 aligns along the whole *Drosophila* Dragon sequence. The study of these two GoRab isoforms and their direct interaction with HsSas6 *in vitro* shows that only GoRab variant 1 is able to directly interact with HsSas6. Thus, as observed in *Drosophila*, also the human homologous GoRab and HsSas6 interact directly *in vitro* and the highly conserved C-terminal domain is necessary to allow for this interaction. The conserved interaction between GoRab and HsSas6 raises the question of whether there is a conserved functional role in centriole duplication in human cell culture. Performed siRNA experiments on U2Os cells revealed that the depletion of GoRab protein does result in failure of centriole duplication (Figure 5-26). This is in line with loss of centrosomes observed after Dragon depletion in *Drosophila* cell culture and the failure of Dragon$^{\Delta IM}$ to rescue centriole duplication.

Together the data presented in this chapter indicated that the novel direct interaction of Dragon/GoRab with Sas6 has a significant function in centriole duplication. Dragon and Sas6 interact within their C-terminal protein domains and have potential functions for both centriole duplication and structure. The roles of Dragon at the Golgi are less certain and further research will be necessary to further understand the role and specific function of Dragon in vesicle trafficking.

Chapter 6

Final discussion

6 Final discussion

This thesis focuses how the core proteins of the centriole interact with each other as a network, with a specific focus on the structural and functional interaction of Sas6 with Ana2 and Sas6 with Dragon in the process of centriole duplication.

In Chapter 3 I studied the interactions of centriole duplication proteins identified by mass spectrometric analysis of protein complexes purified using affinity tagged centriole duplication proteins in cultured *Drosophila* cells (section 3.2.1). I also performed protein-protein binding assays *in vitro* to test for direct protein interactions (section 3.2.2) and studied direct protein interactions *in vivo* by yeast-2-hybrid assays (section 3.2.3). Together this allowed me to build a protein network of potentially interacting centriole duplication proteins in relation to their localisation within the five zones of the centrosome [24,30]. Each of these three methods can be strong and reliable but in my hands they have proven to be a guide for further studies rather than giving conclusive results.

In Chapter 4 I focused on the core centriole duplication proteins Ana2 and Sas6, which were identified as centriole duplication proteins in two genome wide dsRNAi screens in *D. melanogaster* cell culture [131,288]. Moreover Sas6 was shown to be a major component of the centriole cartwheel [63,69,74,75]. In summary, I show that Plk4 and Ana2 interact directly with each other but that neither shows direct interaction with Sas6 using *in vitro* binding assays (section 4.2.1). Similarly, Plk4 phosphorylates Ana2 but not Sas6 *in vitro* (section 4.2.1.1). Phospho-peptide mapping by mass spectrometry identified that the residues S318, S365, S370 and S373 in the conserved Ana2-STAN motif are phosphorylated by Plk4 (section 4.2.2). Importantly, an Ana2-4A mutant that cannot be phosphorylated by Plk4 leads to loss of centrosomes, which in turn can be rescued by the phospho-mimicking Ana2-4D mutant (section 4.2.3). This suggests an essential downstream event of Ana2 phosphorylation for centriole duplication. *In vitro* and *in vivo* studies showed that Plk4-phosphorylation of Ana2 mediates the interaction of the centriole cartwheel protein Sas6 with Ana2 (section 4.2.4). Structurally, the Plk4-phosphorylated Ana2-C-terminus is sufficient for the interaction with Sas6 (section 4.2.4.1); and specifically the four Serine residues within the Ana2-STAN motif (S318, S365, S370, S373) need to be phosphorylated by Plk4 for the interaction of Sas6 with Ana2-C-terminus to occur (section 4.2.5). Accordingly, the non-phosphorylatable Ana2-4A mutant does not interact with Sas6 *in vitro*, whereas the phospho-mimicking Ana2-4D does (section 4.2.6). Further *in vitro* interaction studies revealed that the Plk4-phosphorylated Ana2-STAN motif alone is sufficient for interaction with Sas6 and that the Sas6 aa276-432 coiled-coil segment is efficient in binding Ana2 (section 4.2.8).

In Chapter 5 I report the identification and initial characterisation of a novel protein Dragon (CG33052) that associates with centrosomes and the Golgi. Dragon was identified by mass spectrometry analysis of Sas6-complexes purified from cultured *Drosophila* cells (section 6.2.1.1). Reciprocal purifications of Dragon from cultured *Drosophila* cells identified the centrosomal cartwheel protein Sas6 and subunits of the Golgi COPI protein in complex with Dragon (section 6.2.1.2 and section 6.2.1.3). Dragon is a novel protein that exhibits dual localisation at the *trans*-Golgi and the centrosome in *Drosophila* cell culture. Dragon co-localises with the cartwheel protein Sas6 at the centriole throughout its duplication cycle (section 6.2.2). *In vitro* binding assays confirmed that Dragon interacts directly with Sas6 (section 6.2.4). Specifically, the segment of Sas6 between aa351-462 interacts directly with the conserved Dragon C-terminal coiled-coil domain (aa191-318) within which the sequence between aa260-286 is necessary for interaction with Sas6. The human homologues of Dragon and Sas6, GoRab variant 1 and HsSas6 respectively, also interact directly *in vitro* (section 6.2.6.1). Depletion of Dragon/GoRab causes loss of centrosomes in *Drosophila* cell culture and human U2Os cells (section 6.2.3 and section 6.2.6.2 respectively). Moreover a Dragon$^{\Delta IM}$ mutant that does not interact with Sas6 *in vitro* or *in vivo* fails to rescue centriole duplication in *Drosophila* cell culture (section 6.2.5). Thus Dragon appears necessary for centriole duplication. In contrast, the precise function of Dragon at the Golgi and potentially in secretory pathways is uncertain.

The relationship between Plk4, Ana2 and Sas6 and their role in procentriole formation was further characterised by examining loading dependencies *in vivo* using structured illumination microscopy to assess loading (expertise of Dr. Tzolovsky, RNAi by Dr. Dzhindzhev). These studies support the *in vitro* findings [296]. Together this establishes the loading dependencies of Ana2 and Sas6 and characterises their interaction in relation to their localisation at the centriole. In wild-type *Drosophila* cells, endogenous Sas6 and Ana2 localise to the mother and the daughter centriole as two independent dots throughout the cell cycle (the outer centriolar marker D-Plp allows mother and daughter centrioles to be distinguished; Figure 6-1). In interphase and prometaphase, Sas6 and Ana2 localise to the centre of the mother centriole and D-Plp ring, and to the daughter centriole which has yet to develop its D-Plp ring. The daughter centriole matures by recruiting D-Plp in a “horn” like pattern around the centriole and completes its ring structure by meta-/anaphase. This is followed by disengagement of the mother and daughter centriole in anaphase. In late ana-/telophase, each of the separated centrioles shows a new dot for Ana2 and Sas6 at the periphery of the mother D-Plp ring. This characterises the site of the nascent procentriole, which is already determined at telophase and not after cytokinesis in G_1, as previously believed.

Significantly, the depletion of Sas6 by RNAi does not have an effect on the above described centriole localisation of Ana2 in the majority of analysed *Drosophila* cells, with the majority of interphase cells exhibiting two dots of Ana2, of which one is in the centre and one on the periphery of the D-Plp ring, the mother centriole and the site of procentriole formation respectively (Figure 6-2). This suggests that Ana2 localises to the centriole independently of Sas6. Therefore, Ana2 maintenance at the mother centriole and Ana2 recruitment to the site of procentriole formation does not depend on Sas6. On the contrary, depletion of Ana2 or Plk4 by RNAi causes Sas6 to localise to a single dot at the mother centriole in the centre of the D-Plp ring. Localisation of Sas6 to a second dot at the periphery of the D-Plp ring and therefore to the site of procentriole formation does not occur in the majority of Ana2 depleted interphase cells (Figure 6-3A). Thus individually depleting Ana2 or Plk4 does not allow for Sas6 to be recruited to the site of procentriole formation but they do not interfere with maintenance of Sas6 at the mother centriole. In other words, the loading of Sas6 and consequential the formation of the procentriole are dependent on Ana2. The lack of Sas6 recruitment could be due to the lack of Plk4 or Ana2 protein after their depletion thus preventing potential physical interactions between Sas6 and Ana2.

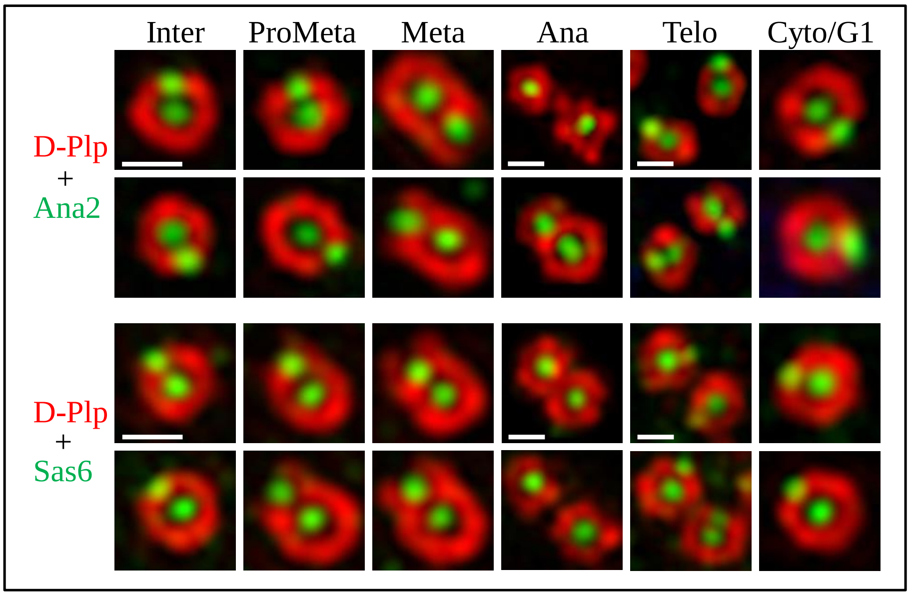

Figure 6-1 Localisation of endogenous Ana2 and Sas6 relative to D-Plp throughout the cell cycle. Structured illumination microscopy of endogenous Ana2, Sas6 and D-Plp throughout cell cycle stages in cultured *Drosophila* cells. Ana2 and Sas6 localise to the mother centriole at the centre of the D-Plp ring throughout the cell cycle. At mitotic entry, Ana2 and Sas6 localise as a second dot to the periphery of the D-Plp ring of the mother centriole, the site of procentriole formation. The second dot matures a D-Plp ring until meta-/anaphase, followed by disengagement of mother and daughter centriole. At late ana-/telophase, each of the two centrioles acquires a new dot of Ana2 and Sas6 at the new site of procentriole formation. Scale bar: 0.5µm. Images by Dr. Tzolovsky [296].

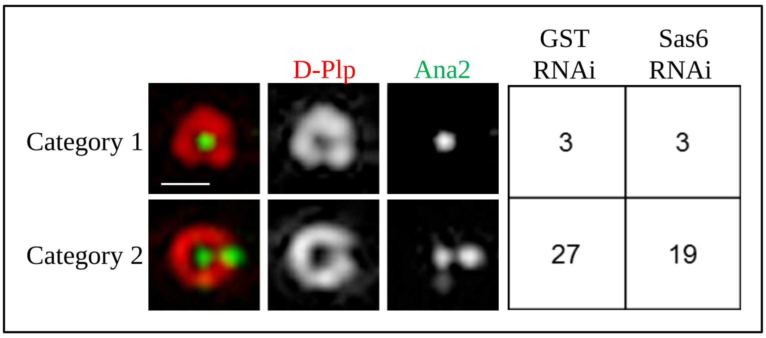

	GST RNAi	Sas6 RNAi
Category 1	3	3
Category 2	27	19

Figure 6-2 Ana2 localisation to the centriole is independent of Sas6. Structural illumination microscopy and categories of Ana2 in interphase *Drosophila* cells after Sas6 or control RNAi. Numbers on the right indicate how many centrioles were observed in each category. Ana2 localisation relative to the outer centriole marker D-Plp. The majority of cells exhibit a two dot localisation of Ana2 at the mother and procentriole. Scale bar: 0.5µm. Images by Dr. Tzolovsky [296].

Together with the described *in vitro* findings that Plk4 phosphorylates Ana2, to allow for Sas6 to interact with the phosphorylated Ana2 (section 4.2.4), this suggests that Sas6 localisation to the site of procentriole formation depends on the upstream event of Ana2 phosphorylation by Plk4. When endogenous Ana2 was depleted (by UTRs directed RNAi) from transgenic cells expressing Ana2-WT or Ana2-4A the majority of Ana2-WT cells exhibited the previously described double dot localisation of Ana2 and Sas6 to the centre and the periphery of the mother centriole D-Plp ring (Figure 6-1), whereas the majority of Ana2-4A expressing cells showed correct Ana2 localisation and the localisation of Sas6 is limited to the centre of the mother centrioles (Figure 6-4B). This resembles the findings of Sas6 localisation in wild-type *Drosophila* cells after RNAi of Ana2 or Plk4 (Figure 6-3). In summary, this confirms that the lack of Sas6 protein at the site of procentriole formation is due to the lack of Plk4-phosphorylated Ana2 and is therefore in line with the *in vitro* finding that Plk4-phosphorylation of Ana2 triggers its interaction with Sas6 (section 4.2.4). Additionally, this confirms that Ana2 is recruited to the centriole independently of its phosphorylation in the STAN motif by Plk4; and that Ana2 and Sas6 do not have to form a complex to allow for Ana2 recruitment to the centriole. This is in line with findings in human cells, where STIL and Sas6 have not been detected in a stable complex [117], nor using protein fragments in yeast-2-

hybrid assays [41]. This contrasts to Sas5 and Sas6 that form a complex and are recruited co-dependently to the procentriole in *C. elegans* [72].

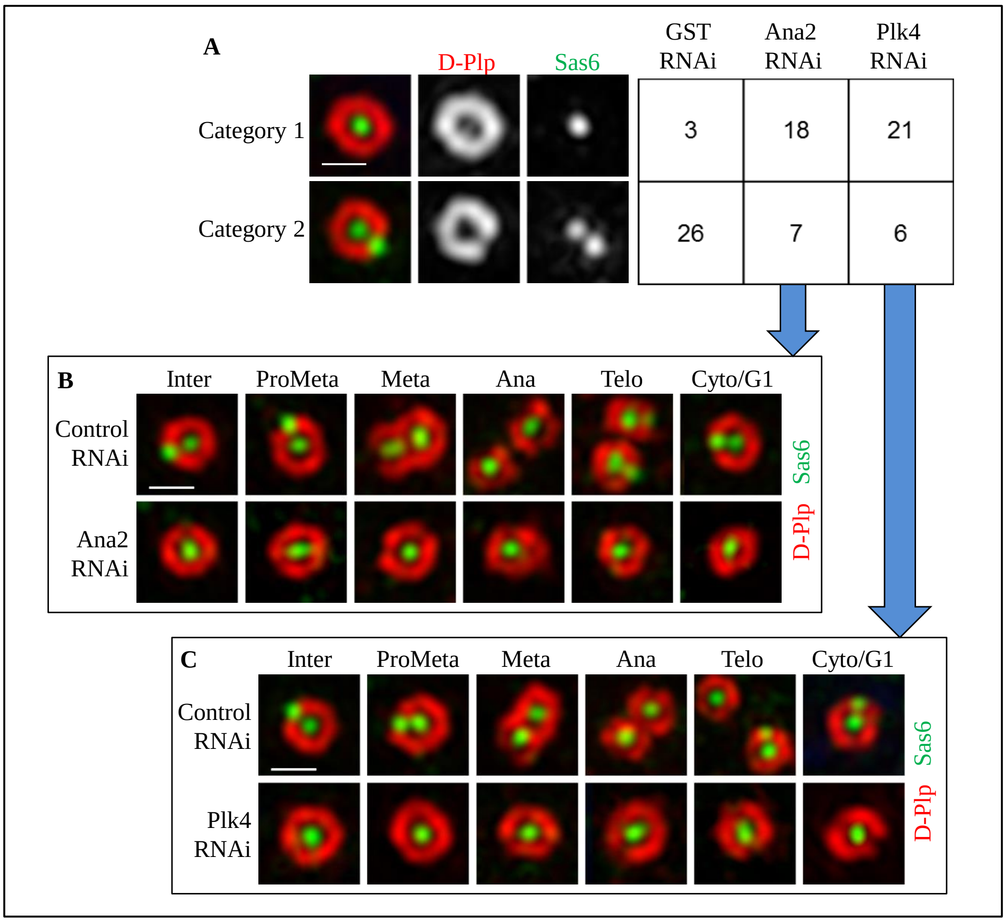

Figure 6-3 Ana2 and Plk4 are essential for centriolar loading of Sas6. Structured illumination microscopy of Sas6 and D-Plp in *Drosophila* cells after Ana2, Plk4 or control RNAi. Sas6 (green) localisation relative to the outer centriole marker D-Plp (red). (A) Categories of Sas6 localisation at the centriole as one or two dots and relative to number of times observed after Ana2, Plk4 or control RNAi. (B) Localisation of Sas6 relative to D-Plp throughout cell cycle stages after Ana2 or control RNAi. Cells depleted of endogenous Ana2 fail to load Sas6. (C) Localisation of Sas6 relative to D-Plp throughout cell cycle stages after Plk4 or control RNAi. Cells depleted of endogenous Plk4 or Ana2 fail to load Sas6. Scale bar: 0.5µm. Images by Dr. Tzolovsky [296].

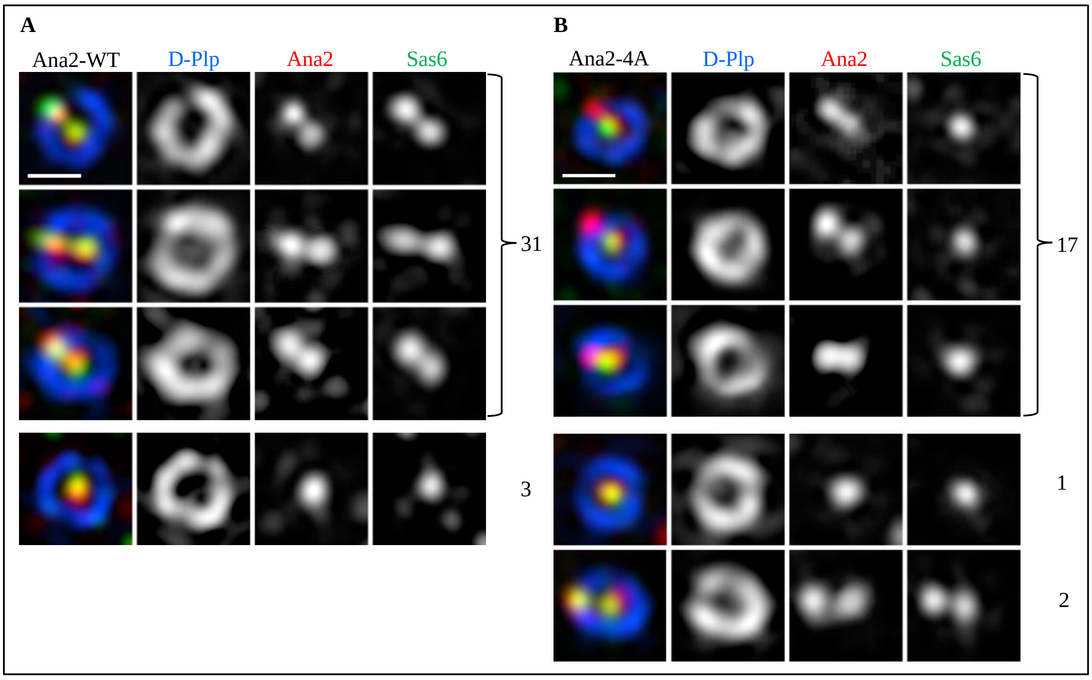

Figure 6-4 Plk4-mediated phosphorylation of S318, S365, S370 and S373 in the Ana2-STAN motif is essential for Sas6 recruitment to centrioles. Structured illumination microscopy of Ana2, Sas6 and D-Plp in interphase *Drosophila* cells expressing Ana2-WT (A) or Ana2-4A (B) after depletion of endogenous Ana2. Number of centrioles observed indicated on the right. (A) The majority of interphase cells expressing transgenic Ana2-WT exhibit co-localisation of Ana2 and Sas6 as two dots at the centre and the periphery of the D-Plp ring, the mother centriole and the site of procentriole initiation respectively. (B) The majority of interphase cells expressing transgenic Ana2-4A, a non-Plk4-phosphorylatable mutant at four Serine residues in the Ana2-STAN motif, which are essential for interaction with Sas6, has normal Ana2 localisation at the mother centriole and is recruited to the site of procentriole formation (two dots of Ana2, comparable to Ana2 localisation in Figure 6-4A). Sas6 only localises as one dot to the mother centriole and is not recruited to the site of procentriole formation. Scale bar: 0.5µm. Images by Dr. Tzolovsky [296].

It has also been suggested that the direct binding of Plk4 to STIL activates its kinase activity by promoting auto-phosphorylation of the activation loop in the kinase domain. This would provide a timely mechanism for Plk4 activity in centriole duplication because human Plk4 localises to the centriole throughout the cell cycle [26] whereas STIL only accumulates from late G_1-/early S-phase and is then degraded after anaphase onset in human cells [41,117,120]. Thus STIL could be a regulating protein for Plk4 and not only a target substrate. However, human Plk4 becomes localised to a single site of procentriole formation at the beginning of S-phase [93–95]. So far, it is only known that depletion of STIL prevents this localisation of Plk4 to a single site [95] but the precise molecular basis of this remains unknown. How Ana2/STIL is recruited and how Plk4 is activated at a single site in the process are questions that remain to be answered. I have shown that Plk4-phosphorylation of the Ana2 STAN motif is necessary to allow Sas6 to bind to the single site and initiate procentriole formation. Similar findings have been made in human cells, where STIL S1108 and S1116 are phosphorylated by Plk4 and these phosphorylations are necessary for efficient targeting of STIL and Sas6 binding to the centriole [300]. We have shown that Ana2 does not require Plk4 phosphorylation at its STAN motif for centriole localisation. However in human cells, it has been suggested by Moyer *et al.* that the efficient targeting of STIL depends on STAN-phosphorylation by Plk4 but the actual interaction between the two proteins does not [300]. On the other hand Kratz *et al.* suggested that Plk4-phosphorylation of STIL is not mandatory for its interaction with Plk4 nor its localisation to the centriole but it is required to allow centriole duplication [123]. Significantly, the residue S1116, identified in human cells [123,300] corresponds to *Drosophila* S370 [95,296], thus confirming the conserved importance of this Plk4-phosphorylation site within the STIL/Ana2-STAN motif for centriole duplication. Interestingly, it is not the loss of the STAN motif but the loss of the central coiled-coil domain of STIL that strongly reduces its localisation to the centriole, as this was observed to be necessary for interaction with Plk4 [95]. A significant difference between *Drosophila* and human cells is seen in the recruitment of Sas6. Whereas Sas6 is recruited directly to the site of procentriole formation in *Drosophila*, the human Sas6 homologue is transiently recruited to the lumen of the mother centriole in early S-phase and then relocates to the outer wall in a process dependent upon Plk4 and STIL. This is followed by cartwheel and procentriole assembly [350], and then the cartwheel structure is lost again during daughter-to-mother centriole transitions in mitosis [120]. This occurs with the loss of centrosomal STIL by Cdk1, followed by loss of Sas6 from the centriole [120]; suggesting that dephosphorylation of STIL could potentially cause dissociation of Sas6 from the centriole.

It is remarkable that Sas6 does not interact with non-phosphorylated Ana2 at all. Therefore, phosphorylation of Ana2 must be tightly regulated, to guarantee its phosphorylation only occurs when recruitment of Sas6 and procentriole formation must be initiated. It is known from *C. elegans* that Sas5 and Sas6 are present as homodimers, before an unknown process allows them to form a complex [15,114,302,304]. However, the structural differences in the organisation of the core centriole and the arrangement of Sas6 in the two species may indicate a requirement for different regulatory steps. Further structural and molecular information on Ana2 and Sas6 complexes is needed, to fully understand the difference between their recruitment to the site of procentriole formation in *C. elegans* and *Drosophila* that reflect the structural character of tube and cartwheel respectively. How the structural arrangement of Ana2 and Sas6 correlates on a molecular basis with the phosphorylation state of Ana2 still needs to be answered.

Together, my results demonstrate that Ana2 and Plk4 are interacting proteins and that Plk4-mediated phosphorylation of Ana2 brings about the interaction of Sas6 with Ana2. Structured illumination microscopy by Dr. Tzolovsky additionally shows that Ana2 localises to the procentriole independently of its phosphorylation state by Plk4 and that Sas6 is recruited to the procentriole only when Ana2 is phosphorylated by Plk4. These results further our understanding of the molecular and functional processes during centriole duplication. For further directions, it is of utmost interest how Ana2 is recruited to the centriole, how it localises to a single site for procentriole formation and what regulates its timely recruitment. It is of interest to understand the structural complex between Ana2 and Sas6 as this will further our understanding of the instructural arrangements during procentriole formation.

The identification of the uncharacterised protein Dragon; its co-localisation with Sas6 at the centriole; and the finding that Dragon and Sas6 interact directly with each other is of particular interest. Dragon’s human homologue GoRab localises to the *trans*-Golgi [202] and a null mutant has been identified in patients exhibiting gerodermia osteodysplastica [202].

Despite this knowledge the precise function of GoRab is unknown. Similarly, Dragon localises to the *trans*-Golgi and could function in signalling pathways as well as in connection with COPI transport vesicles because subunits of COPI were identified in complex with Dragon by mass spectrometry. However, the precise function of Dragon at the Golgi remains unknown. Dragon protein participates in centriole duplication because its depletion leads to loss of centrosomes. However, Dragon's precise molecular function at the centriole remains unknown. Additionally, I show that the conserved C-terminal coiled-coil domain of Dragon (aa191-318) interacts with the C-terminal part of the Sas6 coiled-coil domain (aa351-462). The latter region was not described in structural studies for the formation of the centriole cartwheel by Sas6. Thus Dragons could be important in the assembly of the procentriole or in the transition from the cartwheel assembly to interactions with microtubules. Dragon could structurally support the 9-fold symmetry of the centriole or directly connect proteins in the centriole assembly process. Importantly Dragon co-localises with Sas6 throughout the cell-cycle, suggesting it has a cartwheel related function or participates in another unidentified process that occurs with similar timing as Sas6 recruitment. From here onwards, studies of the interdependency between Dragon and Sas6 in their roles in centriole duplication and maturation need to be studied in greater detail. Additional structural knowledge of Dragon and Sas6 or their interacting regions in complex would lead to further understanding of the arrangement of these proteins at the centriole and what roles they might have on the cartwheel of the centriole as a whole in guaranty of 9-fold symmetry. Once these questions have been answered and we have more knowledge about the function of Dragon at the centriole, we can determine the relationship between the centriole and the Golgi mediated by Dragon or its isoforms. Additional studies of Dragon at *Drosophila* spermatocytes and the basal body of the sperm are needed to elucidate its function at these sites.

Bibliography

Bibliography

1. Archambault, V. & Glover, D. M. Polo-like kinases: conservation and divergence in their functions and regulation. *Nat Rev Mol Cell Biol* **10,** 265–275 (2009).

2. Carmena, M., Ruchaud, S. & Earnshaw, W. C. Making the Auroras glow: regulation of Aurora A and B kinase function by interacting proteins. *Curr. Opin. Cell Biol.* **21,** 796–805 (2009).

3. Khodjakov, A., Copenagle, L., Gordon, M. B., Compton, D. a. & Kapoor, T. M. Minus-end capture of preformed kinetochore fibers contributes to spindle morphogenesis. *J. Cell Biol.* **160,** 671–683 (2003).

4. Tulu, U., Fagerstrom, C., Ferenz, N. & Wadsworth, P. Molecular requirements for kinetochore-associated microtubule formation in mammalian cells. *Curr Biol* **16,** 536–541 (2006).

5. Li, X. & Nicklas, R. B. Mitotic forces control a cell-cycle checkpoint. *Nature* **373,** 630–2 (1995).

6. Nicklas, R. B. & Koch, C. A. Chromosome micromanipulation. 3. Spindle fiber tension and the reorientation of mal-oriented chromosomes. *J. Cell Biol.* **43,** 40–50 (1969).

7. Santaguida, S. & Musacchio, A. The life and miracles of kinetochores. *EMBO J.* **28,** 2511–31 (2009).

8. Lampson, M. A., Renduchitala, K., Khodjakov, A. & Kapoor, T. M. Correcting improper chromosome-spindle attachments during cell division. *Nature cell biology* **6,** 232–237 (2004).

9. Cimini, D., Wan, X., Hirel, C. B. & Salmon, E. D. Aurora kinase promotes turnover of kinetochore microtubules to reduce chromosome segregation errors. *Curr. Biol.* **16,** 1711–1718 (2006).

10. Pines, J. Mitosis: A matter of getting rid of the right protein at the right time. *Trends in Cell Biology* **16,** 55–63 (2006).

11. Musacchio, A. & Salmon, E. D. The spindle-assembly checkpoint in space and time. *Nature reviews. Molecular cell biology* **8,** 379–93 (2007). Reprinted by permission from Macmillan Publishers Ltd. DOI: 10.1038/nrm2163

12. Fawcett, D. W. & Porter, K. R. A study of the fine structure of ciliated epithelia. *J. Morphol.* **94,** 221–381 (1954).

13. De Harven Bernhard, W., E. & De Harven, E., Bernhard, W. Etude au microscope electronique du l’ultrastructure du centriole chez les vertebrates. *Zeitschrift fiir Zellforsch.* **45,** 378–398 (1956).

14. Bettencourt-Dias, M. & Glover, D. M. Centrosome biogenesis and function: centrosomics brings new understanding. *Nat Rev Mol Cell Biol* **8,** 451–463 (2007). Reprinted by permission from Macmillan Publishers Ltd. DOI: 10.1038/nrm2180

15. Lettman, M. M. *et al.* Direct binding of SAS-6 to ZYG-1 recruits SAS-6 to the mother centriole for cartwheel assembly. *Dev Cell* **25,** 284–298 (2013).

16. Kirkham, M., Müller-Reichert, T., Oegema, K., Grill, S. & Hyman, A. A. SAS-4 is a C. elegans centriolar protein that controls centrosome size. *Cell* **112,** 575–587 (2003).

17. Pelletier, L. *et al.* The Caenorhabditis elegans centrosomal protein SPD-2 is required for both pericentriolar material recruitment and centriole duplication. *Curr Biol* **14,** 863–873 (2004).

18. Dammermann, A. *et al.* Centriole assembly requires both centriolar and pericentriolar material proteins. *Dev Cell* **7,** 815–829 (2004).

19. Kemp, C. A., Kopish, K. R., Zipperlen, P., Ahringer, J. & O'Connell, K. F. Centrosome maturation and duplication in C. elegans require the coiled-coil protein SPD-2. *Dev Cell* **6,** 511–523 (2004).

20. Leidel, S. & Gönczy, P. SAS-4 is essential for centrosome duplication in C elegans and is recruited to daughter centrioles once per cell cycle. *Dev Cell* **4,** 431–439 (2003).

21. Leidel, S. & Gonczy, P. Centrosome duplication and nematodes: recent insights from an old relationship. *Dev Cell* **9,** 317–325 (2005).

22. O'Connell, K. F. *et al.* The C. elegans zyg-1 gene encodes a regulator of centrosome duplication with distinct maternal and paternal roles in the embryo. *Cell* **105,** 547–558 (2001).

23. Delattre, M. *et al.* Centriolar SAS-5 is required for centrosome duplication in C. elegans. *Nat Cell Biol* **6,** 656–664 (2004).

24. Fu, J. & Glover, D. M. Structured illumination of the interface between centriole and peri-centriolar material. *Open Biol* **2,** 120104 (2012). CC BY 3.0 DOI: 10.1098/rsob.120104

25. Sillibourne, J. E. *et al.* Assessing the localization of centrosomal proteins by PALM/STORM nanoscopy. *Cytoskelet.* **68,** 619–627 (2011).

26. Sonnen, K. F., Schermelleh, L., Leonhardt, H. & Nigg, E. A. 3D-structured illumination microscopy provides novel insight into architecture of human centrosomes. *Biol Open* **1,** 965–976 (2012).

27. Mennella, V. *et al.* Subdiffraction-resolution fluorescence microscopy reveals a domain of the centrosome critical for pericentriolar material organization. *Nat Cell Biol* **14,** 1159–1168 (2012).

28. Lawo, S., Hasegan, M., Gupta, G. D. & Pelletier, L. Subdiffraction imaging of centrosomes reveals higher-order organizational features of pericentriolar material. *Nat Cell Biol* **14,** 1148–1158 (2012).

29. Lau, L., Lee, Y. L., Sahl, S. J., Stearns, T. & Moerner, W. E. STED microscopy with optimized labeling density reveals 9-fold arrangement of a centriole protein. *Biophys. J.* **102,** 2926–2935 (2012).

30. Fu, J. *et al.* Conserved molecular interactions in centriole-to-centrosome conversion. *Nat. Cell Biol.* **18,** 87–99 (2016).

31. Carvalho-Santos, Z., Azimzadeh, J., Pereira-Leal, J. B. & Bettencourt-Dias, M. Evolution: Tracing the origins of centrioles, cilia, and flagella. *J Cell Biol* **194,** 165–175 (2011).

32. Carvalho-Santos, Z. *et al.* Stepwise evolution of the centriole-assembly pathway. *j Cell sci* **123,** 1414–1426 (2010).

33. Hodges, M. E., Scheumann, N., Wickstead, B., Langdale, J. A. & Gull, K. Reconstructing the evolutionary history of the centriole from protein components. *J Cell Sci* **123,** 1407–1413 (2010).

34. Bobinnec, Y. *et al.* Centriole disassembly in vivo and its effect on centrosome structure and function in vertebrate cells. *J. Cell Biol.* **143,** 1575–1589 (1998).

35. Li, S., Fernandez, J.-J., Marshall, W. F. & Agard, D. A. Three-dimensional structure of basal body triplet revealed by electron cryo-tomography. *EMBO J.* **31,** 552–562 (2012).

36. Guichard, P. *et al.* Native architecture of the centriole proximal region reveals features underlying its 9-fold radial symmetry. *Curr Biol* **23,** 1620–1628 (2013). DOI: 10.1016/j.cub.2013.06.061

37. Guichard, P., Chretien, D., Marco, S. & Tassin, A. M. Procentriole assembly revealed by cryo-electron tomography. *EMBO J* **29,** 1565–1572 (2010).

38. Kohlmaier, G. *et al.* Overly long centrioles and defective cell division upon excess of the SAS-4-related protein CPAP. *Curr. Biol.* **19,** 1012–1018 (2009).

39. Schmidt, T. I. *et al.* Control of centriole length by CPAP and CP110. *Curr Biol* **19,** 1005–1011 (2009).

40. Tang, C. J., Fu, R. H., Wu, K. S., Hsu, W. B. & Tang, T. K. CPAP is a cell-cycle regulated protein that controls centriole length. *Nat Cell Biol* **11,** 825–831 (2009).

41. Tang, C. J. *et al.* The human microcephaly protein STIL interacts with CPAP and is required for procentriole formation. *EMBO J* **30,** 4790–4804 (2011).

42. Cottee, M. A. *et al.* Crystal structures of the CPAP/STIL complex reveal its role in centriole assembly and human microcephaly. *Elife* e01071 (2013). doi:10.7554/eLife.01071.001 10.7554/eLife.01071.002

43. Lin, Y. C. *et al.* Human microcephaly protein CEP135 binds to hSAS-6 and CPAP, and is required for centriole assembly. *EMBO J* **32,** 1141–1154 (2013).

44. Hatzopoulos, G. N. *et al.* Structural analysis of the G-box domain of the microcephaly protein CPAP suggests a role in centriole architecture. *Structure* **21,** 2069–2077 (2013).

45. Shang, Y., Li, B. & Gorovsky, M. A. Tetrahymena thermophila contains a conventional gamma-tubulin that is differentially required for the maintenance of different microtubule-organizing centers. *J. Cell Biol.* **158,** 1195–1206 (2002).

46. Moritz, M., Braunfeld, M. B., Guénebaut, V., Heuser, J. & Agard, D. A. Structure of the gamma-tubulin ring complex: a template for microtubule nucleation. *Nat. Cell Biol.* **2,** 365–370 (2000).

47. Moritz, M., Braunfeld, M. B., Sedat, J. W., Alberts, B. & Agard, D. A. Microtubule nucleation by gamma-tubulin-containing rings in the centrosome. *Nature* **378,** 638–640 (1995).

48. Erickson, H. P. Gamma-tubulin nucleation: template or protofilament? *Nat. Cell Biol.* **2,** E93–E96 (2000).

49. Keating, T. J. & Borisy, G. G. Immunostructural evidence for the template mechanism of microtubule nucleation. *Nat. Cell Biol.* **2,** 352–357 (2000).

50. Paintrand, M., Moudjou, M., Delacroix, H. & Bornens, M. Centrosome organization and centriole architecture: their sensitivity to divalent cations. *J. Struct. Biol.* **108,** 107–128 (1992).

51. Guichard, P. *et al.* Cartwheel architecture of Trichonympha basal body. *Scienc.* **337,** 553 (2012). Reprinted with permission from AAAS. DOI: 10.1126/science.1222789

52. Gonczy, P. Towards a molecular architecture of centriole assembly. *Nat Rev Mol Cell Biol* **13,** 425–435 (2012). Reprinted by permission from Macmillan Publishers Ltd. DOI: 10.1038/nrm3373

53. Pelletier, L., O'Toole, E., Schwager, A., Hyman, A. A. & Muller-Reichert, T. Centriole assembly in Caenorhabditis elegans. *Nature* **444,** 619–623 (2006).

54. Strnad, P. *et al.* Regulated HsSAS-6 levels ensure formation of a single procentriole per centriole during the centrosome duplication cycle. *Dev Cell* **13,** 203–213 (2007).

55. Alvey, P. L. Do adult centrioles contain cartwheels and lie at right angles to each other? *Cell Biol. Int. Rep.* **10,** 589–598 (1986).

56. Gibbons, I. R. & Grimstone, a V. On flagellar structure in certain flagellates. *J. Biophys. Biochem. Cytol.* **7,** 697–716 (1960).

57. Mizukami, I. & Gall, J. Centriole replication. II. Sperm formation in the fern, Marsilea, and the cycad, Zamia. *J. Cell Biol.* **29,** 97–111 (1966).

58. Anderson, R. G. & Brenner, R. M. The formation of basal bodies (centrioles) in the Rhesus Monkey oviduct. *J. Cell Biol.* **50,** 10–34 (1971).

59. Perkins, F. O. Formation of centriole and centriole-like structures during meiosis and mitosis in Labyrinthula sp. (Rhizopodea, Labyrinthulida). An electron-microscope study. *J. Cell Sci.* **6,** 629–653 (1970).

60. Cavalier-Smith, T. Basal body and flagellar development during the vegetative cell cycle and the sexual cycle of Chlamydomonas reinhardii. *J. Cell Sci* **16,** 529–556 (1974).

61. Dippell, R. V. The development of basal bodies in paramecium. *Proc Natl Acad Sci USA.* **61,** 461–468 (1968).

62. Hiraki, M., Nakazawa, Y., Kamiya, R. & Hirono, M. Bld10p constitutes the cartwheel-spoke tip and stabilizes the 9-fold symmetry of the centriole. *Curr Biol* **17,** 1778–1783 (2007).

63. Van Breugel, M. *et al.* Structures of SAS-6 suggest its organization in centrioles. *Science* **331,** 1196–1199 (2011). Reprinted with permission from AAAS. DOI: 10.1126/science.1199325

64. Mottier-Pavie, V. & Megraw, T. L. Drosophila bld10 is a centriolar protein that regulates centriole, basal body, and motile cilium assembly. *Mol Biol Cell* **20,** 2605–2614 (2009).

65. Roque, H. *et al.* Drosophila Cep135/Bld10 maintains proper centriole structure but is dispensable for cartwheel formation. *J Cell Sci.* **125,** 5881–5886 (2012).

66. Blachon, S. *et al.* A proximal centriole-like structure is present in Drosophila spermatids and can serve as a model to study centriole duplication. *Genetics* **182,** 133–144 (2009).

67. Matsuura, K., Lefebvre, P. A., Kamiya, R. & Hirono, M. Bld10p, a novel protein essential for basal body assembly in Chlamydomonas: localization to the cartwheel, the first ninefold symmetrical structure appearing during assembly. *J Cell Biol* **165,** 663–671 (2004).

68. Carvalho-Santos, Z. *et al.* BLD10/CEP135 is a microtubule-associated protein that controls the formation of the flagellum central microtubule pair. *Dev Cell* **23,** 412–424 (2012).

69. Kitagawa, D. *et al.* Structural basis of the 9-fold symmetry of centrioles. *Cell* **144,** 364–375 (2011). CC BY 3.0 DOI: 10.1016/j.cell.2011.01.008

70. Nakazawa, Y., Hiraki, M., Kamiya, R. & Hirono, M. SAS-6 is a cartwheel protein that establishes the 9-fold symmetry of the centriole. *Curr Biol* **17,** 2169–2174 (2007).

71. Rodrigues-Martins, A. *et al.* DSas-6 organizes a tube-like centriole precursor, and its absence suggests modularity in centriole assembly. *Curr. Biol.* **17,** 1465–1472 (2007).

72. Leidel, S., Delattre, M., Cerutti, L., Baumer, K. & Gonczy, P. SAS-6 defines a protein family required for centrosome duplication in C. elegans and in human cells. *Nat Cell Biol* **7,** 115–125 (2005).

73. Kleylein-Sohn, J. *et al.* Plk4-induced centriole biogenesis in human cells. *Dev Cell* **13,** 190–202 (2007).

74. Cottee, M. A., Raff, J. W., Lea, S. M. & Roque, H. SAS-6 oligomerization: the key to the centriole? *Nat Chem Biol* **7,** 650–653 (2011).

75. Schuldt, A. Cytoskeleton: SAS-6 turns a cartwheel trick. *Nat Rev Mol Cell Biol* **12,** 137 (2011).

76. Geimer, S. & Melkonian, M. The ultrastructure of the Chlamydomonas reinhardtii basal apparatus: identification of an early marker of radial asymmetry inherent in the basal body. *J. Cell Sci* **117,** 2663–2674 (2004).

77. Marshall, W. F. Centriole assembly: the origin of nine-ness. *Curr. Biol.* **17,** R1057–9 (2007).

78. Hilbert, M. *et al.* Caenorhabditis elegans centriolar protein SAS-6 forms a spiral that is consistent with imparting a ninefold symmetry. *Proc Natl Acad Sci U S A* **110,** 11373–11378 (2013). CC By 3.0 DOI: 10.1073/pnas.1302721110

79. Tsang, W. Y. & Dynlacht, B. D. CP110 and its network of partners coordinately regulate cilia assembly. *Cilia* **2,** 9 (2013).

80. Franz, A., Roque, H., Saurya, S., Dobbelaere, J. & Raff, J. W. CP110 exhibits novel regulatory activities during centriole assembly in Drosophila. *J Cell Biol* **203,** 785–799 (2013).

81. Spektor, A., Tsang, W. Y., Khoo, D. & Dynlacht, B. D. Cep97 and CP110 suppress a cilia assembly program. *Cell* **130,** 678–690 (2007).

82. Delgehyr, N. *et al.* Klp10A, a microtubule-depolymerizing kinesin-13, cooperates with CP110 to control Drosophila centriole length. *Curr Biol* **22,** 502–509 (2012).

83. Bettencourt-Dias, M. *et al.* SAK/PLK4 is required for centriole duplication and flagella development. *Curr Biol* **15,** 2199–2207 (2005).

84. Habedanck, R., Stierhof, Y. D., Wilkinson, C. J. & Nigg, E. A. The Polo kinase Plk4 functions in centriole duplication. *Nat Cell Biol* **7,** 1140–1146 (2005).

85. Rodrigues-Martins, A., Riparbelli, M., Callaini, G., Glover, D. M. & Bettencourt-Dias, M. Revisiting the role of the mother centriole in centriole biogenesis. *Science* **316,** 1046–1050 (2007).

86. Jana, S. C., Bazan, J. F. & Bettencourt-Dias, M. Polo boxes come out of the crypt: a new view of PLK function and evolution. *Structure* **20,** 1801–1804 (2012).

87. Slevin, L. K. *et al.* The structure of the Plk4 cryptic polo box reveals two tandem polo boxes required for centriole duplication. *Structure* **20,** 1905–1917 (2012). DOI: 10.1016/j.str.2012.08.025

88. Lowery, D. M., Lim, D. & Yaffe, M. B. Structure and function of Polo-like kinases. *Oncogene* **24,** 248–259 (2005).

89. Bruinsma, W., Raaijmakers, J. A. & Medema, R. H. Switching Polo-like kinase-1 on and off in time and space. *Trends Biochem Sci* **37,** 534–542 (2012).

90. Avidor-Reiss, T. & Gopalakrishnan, J. Building a centriole. *Curr Opin Cell Biol* **25,** 72–77 (2013).

91. Delattre, M., Canard, C. & Gonczy, P. Sequential protein recruitment in C. elegans centriole formation. *Curr Biol* **16,** 1844–1849 (2006).

92. Dzhindzhev, N. S. *et al.* Asterless is a scaffold for the onset of centriole assembly. *Nature* **467,** 714–718 (2010).

93. Sonnen, K. F., Gabryjonczyk, A. M., Anselm, E., Stierhof, Y. D. & Nigg, E. A. Human Cep192 and Cep152 cooperate in Plk4 recruitment and centriole duplication. *J Cell Sci* **126,** 3223–3233 (2013).

94. Kim, T. S. *et al.* Hierarchical recruitment of Plk4 and regulation of centriole biogenesis by two centrosomal scaffolds, Cep192 and Cep152. *Proc Natl Acad Sci U S A* **110,** E4849–57 (2013).

95. Ohta, M. *et al.* Direct interaction of Plk4 with STIL ensures formation of a single procentriole per parental centriole. *Nat Commun* **24,** 5267 (2014).

96. Peel, N., Stevens, N. R., Basto, R. & Raff, J. W. Overexpressing centriole-replication proteins in vivo induces centriole overduplication and de novo formation. *Curr Biol* **17,** 834–843 (2007).

97. Nigg, E. A. & Stearns, T. The centrosome cycle: Centriole biogenesis, duplication and inherent asymmetries. *Nat Cell Biol* **13,** 1154–1160 (2011).

98. Eckerdt, F., Yamamoto, T. M., Lewellyn, A. L. & Maller, J. L. Identification of a polo-like kinase 4-dependent pathway for de novo centriole formation. *Curr Biol* **21,** 428–432 (2011).

99. Basto, R. *et al.* Centrosome amplification can initiate tumorigenesis in flies. *Cell* **133,** 1032–1042 (2008).

100. Ko, M. A. *et al.* Plk4 haploinsufficiency causes mitotic infidelity and carcinogenesis. *Nat Genet* **37,** 883–888 (2005).

101. Pihan, G. a., Wallace, J., Zhou, Y. & Doxsey, S. J. Centrosome abnormalities and chromosome instability occur together in pre-invasive carcinomas. *Cancer Res.* **63,** 1398–1404 (2003).

102. Brownlee, C. W., Klebba, J. E., Buster, D. W. & Rogers, G. C. The Protein Phosphatase 2A regulatory subunit Twins stabilizes Plk4 to induce centriole amplification. *J Cell Biol* **195,** 231–243 (2011).

103. Rogers, G. C., Rusan, N. M., Roberts, D. M., Peifer, M. & Rogers, S. L. The SCF Slimb ubiquitin ligase regulates Plk4/Sak levels to block centriole reduplication. *J Cell Biol* **184,** 225–239 (2009).

104. Guderian, G., Westendorf, J., Uldschmid, A. & Nigg, E. A. Plk4 trans-autophosphorylation regulates centriole number by controlling TrCP-mediated degradation. *J Cell Sci* **123,** 2163–2169 (2010).

105. Cunha-Ferreira, I. *et al.* The SCF/Slimb Ubiquitin Ligase Limits Centrosome Amplification through Degradation of SAK/PLK4. *Curr. Biol.* **19,** 43–49 (2009).

106. Klebba, J. E., Buster, D. W., McLamarrah, T. A., Rusan, N. M. & Rogers, G. C. Autoinhibition and relief mechanism for Polo-like kinase 4. *Proc Natl Acad Sci U S A* **112,** E657–66 (2015). CC BY 3.0 DOI: 10.1073/pnas.1417967112

107. Holland, A. J., Lan, W., Niessen, S., Hoover, H. & Cleveland, D. W. Polo-like kinase 4 kinase activity limits centrosome overduplication by autoregulating its own stability. *J Cell Biol* **188,** 191–198 (2010).

108. Klebba, J. E. *et al.* Polo-like kinase 4 autodestructs by generating its Slimb-binding phosphodegron. *Curr Biol* **23,** 2255–2261 (2013).

109. Cunha-Ferreira, I. *et al.* Regulation of autophosphorylation controls PLK4 self-destruction and centriole number. *Curr. Biol.* **23,** 2245–2254 (2013).

110. Holland, A. J. *et al.* Polo-like kinase 4 controls centriole duplication but does not directly regulate cytokinesis. *Mol Biol Cell* **23,** 1838–1845 (2012).

111. Holland, A. J. *et al.* The autoregulated instability of Polo-like kinase 4 limits centrosome duplication to once per cell cycle. *Genes Dev* **26,** 2684–2689 (2012).

112. Zeevaart, J. G. *et al.* Cullin 1 functions as a centrosomal suppressor of centriole multiplication by regulating polo-like kinase 4 protein levels. *Cancer Res* **69,** 6668–6675 (2009).

113. Kitagawa, D., Busso, C., Flückiger, I. & Gönczy, P. Phosphorylation of Sas-6 by Zyg-1 is critical for centriole formation in C. elegans embryos. *Dev. Cell* **17,** 900–907 (2009).

114. Stevens, N. R., Roque, H. & Raff, J. W. DSas-6 and Ana2 coassemble into tubules to promote centriole duplication and engagement. *Dev Cell* **19,** 913–919 (2010).

115. Puklowski, A. *et al.* The SCF-FBXW5 E3-ubiquitin ligase is regulated by PLK4 and targets HsSAS-6 to control centrosome duplication. *Nat Cell Biol* **13,** 1004–1009 (2011).

116. Stevens, N. R., Dobbelaere, J., Brunk, K., Franz, A. & Raff, J. W. Drosophila Ana2 is a conserved centriole duplication factor. *J Cell Biol* **188,** 313–323 (2010).

117. Arquint, C., Sonnen, K. F., Stierhof, Y. D. & Nigg, E. A. Cell-cycle-regulated expression of STIL controls centriole number in human cells. *J Cell Sci* **125,** 1342–1352 (2012).

118. Vulprecht, J. *et al.* STIL is required for centriole duplication in human cells. *J Cell Sci* **125,** 1353–1362 (2012).

119. Kitagawa, D. *et al.* PP2A phosphatase acts upon Sas-5 to ensure centriole formation in C. elegans embryos. *Dev. Cell* **20,** 550–562 (2011).

120. Arquint, C. & Nigg, E. A. STIL microcephaly mutations interfere with APC/C-mediated degradation and cause centriole amplification. *Curr Biol* **24,** 351–360 (2014).

121. Wong, C. & Stearns, T. Centrosome number is controlled by a centrosome-intrinsic block to reduplication. *Nat Cell Biol* **5,** 539–544 (2003).

122. Tsou, M. F. & Stearns, T. Mechanism limiting centrosome duplication to once per cell cycle. *Nature* **442,** 947–951 (2006).

123. Kratz, A.-S., Bärenz, F., Richter, K. T. & Hoffmann, I. Plk4-dependent phosphorylation of STIL is required for centriole duplication. *Biol. Open* **4,** 370–377 (2015).

124. Cottee, M. A. *et al.* The homo-oligomerisation of both Sas-6 and Ana2 is required for efficient centriole assembly in flies. *Elife* e07236 (2015). doi:10.7554/eLife.07236

125. Slevin, L. K., Romes, E. M., Dandulakis, M. G. & Slep, K. C. The mechanism of dynein light chain LC8-mediated oligomerization of the Ana2 centriole duplication factor. *J Biol Chem* **289,** 20727–20739 (2014).

126. Gould, R. R. & Borisy, G. G. The pericentriolar material in Chinese hamster ovary cells nucleates microtubule formation. *J. Cell Biol.* **73,** 601–615 (1977).

127. Robbins, E., Jentzsch, G. & Micali, A. The centriole cycle in synchronized HeLa cells. *J Cell Biol* **36,** 329–339 (1968).

128. Mennella, V., Agard, D. A., Huang, B. & Pelletier, L. Amorphous no more: Subdiffraction view of the pericentriolar material architecture. *Trends Cell Biol.* **24,** 188–197 (2014).

129. Sönnichsen, B. *et al.* Full-genome RNAi profiling of early embryogenesis in Caenorhabditis elegans. *Nature* **434,** 462–469 (2005).

130. Moutinho-Pereira, S. *et al.* Genes involved in centrosome-independent mitotic spindle assembly in Drosophila S2 cells. *Proc Natl Acad Sci U S A.* **110,** 19808–19813 (2013).

131. Dobbelaere, J. *et al.* A genome-wide RNAi screen to dissect centriole duplication and centrosome maturation in Drosophila. *PLoS Biol* **6,** e224 (2008).

132. Hutchins, J. R. a *et al.* Systematic analysis of human protein complexes identifies chromosome segregation proteins. *Science* **328,** 593–599 (2010).

133. Neumann, B. *et al.* Phenotypic profiling of the human genome by time-lapse microscopy reveals cell division genes. *Nature* **464,** 721–727 (2010).

134. Varmark, H. *et al.* Asterless is a centriolar protein required for centrosome function and embryo development in Drosophila. *Curr Biol* **17,** 1735–1745 (2007).

135. Conduit, P. T. & Raff, J. W. Cnn dynamics drive centrosome size asymmetry to ensure daughter centriole retention in Drosophila neuroblasts. *Curr Biol* **20,** 2187–2192 (2010).

136. Conduit, P. T. *et al.* Centrioles regulate centrosome size by controlling the rate of Cnn incorporation into the PCM. *Curr Biol* **20,** 2178–2186 (2010).

137. Gopalakrishnan, J. *et al.* Sas-4 provides a scaffold for cytoplasmic complexes and tethers them in a centrosome. *Nat Commun* **2,** 359 (2011).

138. Gopalakrishnan, J. *et al.* Tubulin nucleotide status controls Sas-4-dependent pericentriolar material recruitment. *Nat Cell Biol* **14,** 865–873 (2012).

139. Lee, K. & Rhee, K. PLK1 phosphorylation of pericentrin initiates centrosome maturation at the onset of mitosis. *J Cell Biol* **195,** 1093–1101 (2011).

140. Sunkel, C. E. & Glover, D. M. polo, a mitotic mutant of Drosophila displaying abnormal spindle poles. *J Cell Sci* **89,** 25–38 (1988).

141. Lane, H. A. & Nigg, E. A. Antibody microinjection reveals an essential role for human polo-like kinase 1 (Plk1) in the functional maturation of mitotic centrosomes. *J. Cell Biol.* **135,** 1701–1713 (1996).

142. Mahen, R., Jeyasekharan, A. D., Barry, N. P. & Venkitaraman, A. R. Continuous polo-like kinase 1 activity regulates diffusion to maintain centrosome self-organization during mitosis. *Proc. Natl. Acad. Sci. U. S. A.* **108,** 9310–9315 (2011).

143. Hannak, E., Kirkham, M., Hyman, A. A. & Oegema, K. Aurora-A kinase is required for centrosome maturation in Caenorhabditis elegans. *J Cell Biol* **155,** 1109–1116 (2001).

144. Giet, R. *et al.* Drosophila Aurora A kinase is required to localize D-TACC to centrosomes and to regulate astral microtubules. *J Cell Biol* **156,** 437–451 (2002).

145. Seki, A., Coppinger, J. a, Jang, C.-Y., Yates, J. R. & Fang, G. Bora and the kinase Aurora a cooperatively activate the kinase Plk1 and control mitotic entry. *Science* **320,** 1655–1658 (2008).

146. Macůrek, L. *et al.* Polo-like kinase-1 is activated by aurora A to promote checkpoint recovery. *Nature* **455,** 119–123 (2008).

147. Sumiyoshi, E., Sugimoto, A. & Yamamoto, M. Protein phosphatase 4 is required for centrosome maturation in mitosis and sperm meiosis in C. elegans. *J. Cell Sci.* **115,** 1403–1410 (2002).

148. Helps, N. R. *et al.* Protein phosphatase 4 is an essential enzyme required for organisation of microtubules at centrosomes in Drosophila embryos. *J. Cell Sci.* **111,** 1331–1340 (1998).

149. Han, X. *et al.* The role of protein phosphatase 4 in regulating microtubule severing in the Caenorhabditis elegans embryo. *Genetics* **181,** 933–943 (2009).

150. Schlaitz, A. L. *et al.* The C. elegans RSA complex localizes protein phosphatase 2A to centrosomes and regulates mitotic spindle assembly. *Cell* **128,** 115–127 (2007).

151. Sontag, E., Nunbhakdi-Craig, V., Bloom, G. S. & Mumby, M. C. A novel pool of protein phosphatase 2A is associated with microtubules and is regulated during the cell cycle. *J. Cell Biol.* **128,** 1131–1144 (1995).

152. Decker, M. *et al.* Limiting amounts of centrosome material set centrosome size in C. elegans embryos. *Curr Biol* **21,** 1259–1267 (2011).

153. Krueger, L. E., Wu, J. C., Tsou, M. F. B. & Rose, L. S. LET-99 inhibits lateral posterior pulling forces during asymmetric spindle elongation in C. elegans embryos. *J. Cell Biol.* **189,** 481–495 (2010).

154. Megraw, T. L., Kilaru, S., Turner, F. R. & Kaufman, T. C. The centrosome is a dynamic structure that ejects PCM flares. *J. Cell Sci.* **115,** 4707–4718 (2002).

155. Wang, W. J., Soni, R. K., Uryu, K. & Tsou, M. F. The conversion of centrioles to centrosomes: essential coupling of duplication with segregation. *J Cell Biol* **193,** 727–739 (2011).

156. Tsou, M. F. *et al.* Polo kinase and separase regulate the mitotic licensing of centriole duplication in human cells. *Dev Cell* **17,** 344–354 (2009).

157. Schockel, L., Mockel, M., Mayer, B., Boos, D. & Stemmann, O. Cleavage of cohesin rings coordinates the separation of centrioles and chromatids. *Nat Cell Biol* **13,** 966–972 (2011).

158. Wong, R. W. & Blobel, G. Cohesin subunit SMC1 associates with mitotic microtubules at the spindle pole. *Proc. Natl. Acad. Sci. U. S. A.* **105,** 15441–15445 (2008).

159. Gregson, H. C. *et al.* A potential role for human cohesin in mitotic spindle aster assembly. *J. Biol. Chem.* **276,** 47575–47582 (2001).

160. Kong, X. *et al.* Cohesin associates with spindle poles in a mitosis-specific manner and functions in spindle assembly in vertebrate cells. *Mol Biol Cell* **20,** 1289–1301 (2009).

161. Sumara, I. *et al.* The dissociation of cohesin from chromosomes in prophase is regulated by polo-like kinase. *Mol. Cell* **9,** 515–525 (2002).

162. Uhlmann, F., Lottspeich, F. & Nasmyth, K. Sister-chromatid separation at anaphase onset is promoted by cleavage of the cohesin subunit Scc1. *Nature* **400,** 37–42 (1999).

163. Piel, M., Meyer, P., Khodjakov, A., Rieder, C. L. & Bornens, M. The respective contributions of the mother and daughter centrioles to centrosome activity and behavior in vertebrate cells. *J. Cell Biol.* **149,** 317–329 (2000).

164. Stemmann, O., Zou, H., Gerber, S. A., Gygi, S. P. & Kirschner, M. W. Dual inhibition of sister chromatid separation at metaphase. *Cell* **107,** 715–726 (2001).

165. Matsuo, K. *et al.* Kendrin is a novel substrate for separase involved in the licensing of centriole duplication. *Curr Biol* **22,** 915–921 (2012).

166. Yang, J., Adamian, M. & Li, T. Rootletin interacts with C-Nap1 and may function as a physical linker between the pair of centrioles/basal bodies in cells. *Mol. Biol. Cell* **17,** 1033–1040 (2006).

167. Bahe, S., Stierhof, Y. D., Wilkinson, C. J., Leiss, F. & Nigg, E. A. Rootletin forms centriole-associated filaments and functions in centrosome cohesion. *J. Cell Biol.* **171,** 27–33 (2005).

168. Fry, A. M. *et al.* C-Nap1, a novel centrosomal coiled-coil protein and candidate substrate of the cell cycle-regulated protein kinase Nek2. *J. Cell Biol.* **141,** 1563–1574 (1998).

169. Mayor, T., Stierhof, Y. D., Tanaka, K., Fry, A. M. & Nigg, E. A. The centrosomal protein C-Nap1 is required for cell cycle-regulated centrosome cohesion. *J. Cell Biol.* **151,** 837–846 (2000).

170. Kim, K., Lee, S., Chang, J. & Rhee, K. A novel function of CEP135 as a platform protein of C-NAP1 for its centriolar localization. *Exp Cell Res* **314,** 3692–3700 (2008).

171. Mayor, T., Hacker, U., Stierhof, Y.-D. & Nigg, E. A. The mechanism regulating the dissociation of the centrosomal protein C-Nap1 from mitotic spindle poles. *J. Cell Sci.* **115,** 3275–3284 (2002).

172. Helps, N. R., Luo, X., Barker, H. M. & Cohen, P. T. NIMA-related kinase 2 (Nek2), a cell-cycle-regulated protein kinase localized to centrosomes, is complexed to protein phosphatase 1. *Biochem. J.* **349,** 509–518 (2000).

173. Fletcher, L., Cerniglia, G. J., Nigg, E. A., Yend, T. J. & Muschel, R. J. Inhibition of centrosome separation after DNA damage: a role for Nek2. *Radiation research* **162,** 128–135 (2004).

174. Faragher, A. J. & Fry, A. M. Nek2A kinase stimulates centrosome disjunction and is required for formation of bipolar mitotic spindles. *Mol. Biol. Cell* **14,** 2876–2889 (2003).

175. Mardin, B. R. *et al.* Components of the Hippo pathway cooperate with Nek2 kinase to regulate centrosome disjunction. *Nat. Cell Biol.* **12,** 1166–1176 (2010).

176. Bornens, M. Centrosome composition and microtubule anchoring mechanisms. *Curr Opin Cell Biol* **14,** 25–34 (2002).

177. Efimov, A. *et al.* Asymmetric CLASP-dependent nucleation of non-centrosomal microtubules at the trans-Golgi network. *Dev Cell* **12,** 917–930 (2007).

178. Kollman, J. M., Merdes, A., Mourey, L. & Agard, D. A. Microtubule nucleation by γ-tubulin complexes. *Nat Rev Mol Cell Biol* **12,** 709–721 (2011).

179. Preuss, D., Mulholland, J., Franzusoff, A., Segev, N. & Botsteint, D. Characterization of the Saccharomyces Golgi complex through the cell cycle by immunoelectron microscopy. *Mol. Biol. Cell* **3,** 789–803 (1992).

180. Henderson, G. P., Gan, L. & Jensen, G. J. 3-D ultrastructure of O. tauri: Electron cryotomography of an entire Eukaryotic cell. *PLoS One* **2,** (2007).

181. Mogelsvang, S., Gomez-Ospina, N., Soderholm, J., Glick, B. S. & Staehelin, L. A. Tomographic evidence for continuous turnover of Golgi cisternae in Pichia pastoris. *Mol. Biol. Cell* **14,** 2277–2291 (2003).

182. DaSilva, L. L. *et al.* Endoplasmic reticulum export sites and Golgi bodies behave as single mobile secretory units in plant cells. *Plant Cell* **16,** 1753–1771 (2004).

183. Kondylis, V. & Rabouille, C. The Golgi apparatus: lessons from Drosophila. *FEBS Lett* **583,** 3827–3838 (2009). DOI: 10.1016/j.febslet.2009.09.048

184. Rios, R. M. & Bornens, M. The Golgi apparatus at the cell centre. *Curr. Opin. Cell Biol.* **15,** 60–66 (2003).

185. Yadav, S. & Linstedt, A. D. Golgi positioning. *Cold Spring Harb Perspect Biol* **3,** (2011).

186. Hurtado, L. *et al.* Disconnecting the Golgi ribbon from the centrosome prevents directional cell migration and ciliogenesis. *J Cell Biol* **193,** 917–933 (2011).

187. Miller, P. M., Folkmann, A. W., Maia, A. R. R., Efimova, N. & Kaverina, I. Golgi-derived CLASP-dependent microtubules control Golgi organization and polarized trafficking in motile cells. *Nat Cell Biol* **11,** 1069–1080 (2009).

188. Yadav, S., Puthenveedu, M. A. & Linstedt, A. D. Golgin160 recruits the dynein motor to position the golgi apparatus. *Dev Cell* **23,** 153–165 (2012).

189. Wei, J.-H. & Seemann, J. Unraveling the Golgi ribbon. *Traffic* **11,** 1391–1400 (2010).

190. Sütterlin, C., Hsu, P., Mallabiabarrena, A. & Malhotra, V. Fragmentation and dispersal of the pericentriolar Golgi complex is required for entry into mitosis in mammalian cells. *Cell* **109,** 359–369 (2002).

191. Ríos, R. M., Sanchís, A., Tassin, A. M., Fedriani, C. & Bornens, M. GMAP-210 recruits γ-tubulin complexes to cis-Golgi membranes and is required for Golgi ribbon formation. *Cell* **118,** 323–335 (2004).

192. Infante, C., Ramos-Morales, F., Fedriani, C., Bornens, M. & Rios, R. M. Gmap-210, a cis-Golgi network-associated protein, is a minus end microtubule-binding protein. *J. Cell Biol.* **145,** 83–98 (1999).

193. Broekhuis, J. R., Rademakers, S., Burghoorn, J. & Jansen, G. SQL-1, homologue of the Golgi protein GMAP210, modulates intraflagellar transport in C. elegans. *J. Cell Sci.* **126,** 1785–95 (2013).

194. Follit, J. a. *et al.* The Golgin GMAP210/TRIP11 anchors IFT20 to the Golgi complex. *PLoS Genet.* **4,** (2008).

195. Maia, A. R. R. *et al.* Modulation of Golgi-associated microtubule nucleation throughout the cell cycle. *Cytoskeleton* **70,** 32–43 (2013).

196. Rivero, S., Cardenas, J., Bornens, M. & Rios, R. M. Microtubule nucleation at the cis-side of the Golgi apparatus requires AKAP450 and GM130. *EMBO J.* **28,** 1016–1028 (2009).

197. Roubin, R. *et al.* Myomegalin is necessary for the formation of centrosomal and Golgi-derived microtubules. *Biol Open* **2,** 238–250 (2013).

198. Wang, Z. *et al.* Conserved motif of CDK5RAP2 mediates its localization to centrosomes and the Golgi complex. *J Biol Chem* **285,** 22658–22665 (2010).

199. Sengupta, D., Truschel, S., Bachert, C. & Linstedt, A. D. Organelle tethering by a homotypic PDZ interaction underlies formation of the Golgi membrane network. *J. Cell Biol.* **186,** 41–55 (2009).

200. Puthenveedu, M. a, Bachert, C., Puri, S., Lanni, F. & Linstedt, A. D. GM130 and GRASP65-dependent lateral cisternal fusion allows uniform Golgi-enzyme distribution. *Nat. Cell Biol.* **8,** 238–248 (2006).

201. Millarte, V. & Farhan, H. The Golgi in cell migration: regulation by signal transduction and its implications for cancer cell metastasis. *Sci. World J.* **2012,** (2012).

202. Hennies, H. C. *et al.* Gerodermia osteodysplastica is caused by mutations in SCYL1BP1, a Rab-6 interacting golgin. *Nat Genet* **40,** 1410–1412 (2008).

203. Farquhar, M. G. & Palade, G. E. The Golgi apparatus (complex)-(1954-1981)-from artifact to center stage. *J. Cell Biol.* **91,** 77s–103s (1981).

204. Ruiz-May, E., Kim, S.-J., Brandizzi, F. & Rose, J. K. C. The secreted plant N-glycoproteome and associated secretory pathways. *Front. Plant Sci.* **3,** (2012).

205. Stanley, P. Golgi glycosylation. *Cold Spring Harb. Perspect. Biol.* **3,** (2011).

206. Dick, G., Akslen-Hoel, L. K., Grøndahl, F., Kjos, I. & Prydz, K. Proteoglycan synthesis and Golgi organization in polarized epithelial cells. *J. Histochem. Cytochem.* **60,** 926–35 (2012).

207. Al-Dosari, M. & Alkuraya, F. S. A novel missense mutation in SCYL1BP1 produces geroderma osteodysplastica phenotype indistinguishable from that caused by nullimorphic mutations. *Am J Med Genet A* **149A,** 2093–2098 (2009).

208. Gardeitchik, T. *et al.* Clinical and biochemical features guiding the diagnostics in neurometabolic cutis laxa. *Eur J Hum Genet* **22,** 888–895 (2014).

209. Noordam, C. *et al.* Decreased bone density and treatment in patients with autosomal recessive cutis laxa. *Acta Paediatr.* **98,** 490–494 (2009).

210. Boreux, G. Osteodysplasic geroderma of sex-linked heredity, a new clinical and genetic entity. *J Genet Hum. 1969* **17,** 137–178 (1969).

211. Rajab, A. *et al.* Geroderma osteodysplasticum hereditaria and wrinkly skin syndrome in 22 patients from Oman. *Am. J. Med. Genet. Part A* **146A,** 965–976 (2008).

212. Morava, E., Guillard, M., Lefeber, D. J. & Wevers, R. A. Autosomal recessive cutis laxa syndrome revisited. *Eur J Hum Genet* **17,** 1099–1110 (2009).

213. Hunter, A. G. Is geroderma osteodysplastica underdiagnosed? *J. Med. Genet.* **25,** 854–7 (1988).

214. Di, Y. *et al.* Cloning and characterization of a novel gene which encodes a protein interacting with the mitosis-associated kinase-like protein NTKL. *J Hum Genet* **48,** 315–321 (2003).

215. Burman, J. L., Hamlin, J. N. R. & McPherson, P. S. Scyl1 regulates golgi morphology. *PLoS One* **5,** (2010).

216. Burman, J. L. *et al.* Scyl1, mutated in a recessive form of spinocerebellar neurodegeneration, regulates COPI-mediated retrograde traffic. *J. Biol. Chem.* **283,** 22774–22786 (2008).

217. Conner, S. D. & Schmid, S. L. CVAK104 is a novel poly-L-lysine-stimulated kinase that targets the beta2-subunit of AP2. *J. Biol. Chem.* **280,** 21539–21544 (2005).

218. Gherzi, R., Bellini, C. & Bonioli, E. Altered response to stimuli of the AP-1/DNA binding activity in a syndrome of precocious ageing (geroderma osteodysplastica hereditaria). *Mech. Ageing Dev.* **100,** 169–175 (1998).

219. Yan, J., Di, Y., Shi, H., Rao, H. & Huo, K. Overexpression of SCYL1-BP1 stabilizes functional p53 by suppressing MDM2-mediated ubiquitination. *FEBS Lett* **584,** 4319–4324 (2010).

220. Prives, C. Signaling to p53: Breaking the MDM2-p53 circuit. *Cell* **95,** 5–8 (1998).

221. Yan, J. *et al.* A Newly Identified Pirh2 substrate SCYL1-BP1 can bind to MDM2 and accelerate MDM2 self-ubiquitination. *FEBS Lett.* **584,** 3275–3278 (2010).

222. Ma, J. *et al.* A second p53 binding site in the central domain of Mdm2 is essential for p53 ubiquitination. *Biochemistry* **45,** 9238–9245 (2006).

223. Papanikou, E. & Glick, B. S. Golgi compartmentation and identity. *Curr Opin Cell Biol* **29,** 74–81 (2014). DOI: 10.1016/j.ceb.2014.04.010

224. Satir, P. & Christensen, S. T. Overview of structure and function of mammalian cilia. *Annu. Rev. Physiol.* **69,** 377–400 (2007).

225. Wheatley, D. N., Wang, A. M. & Strugnell, G. E. Expression of primary cilia in mammalian cells. *Cell Biol. Int.* **20,** 73–81 (1996).

226. Pan, J., Wang, Q. & Snell, W. J. Cilium-generated signaling and cilia-related disorders. *Lab. Investig.* **85,** 452–463 (2005).

227. Schou, K. B., Pedersen, L. B. & Christensen, S. T. Ins and outs of GPCR signaling in primary cilia. *EMBO Rep.* **16,** 1099–1113 (2015).

228. Davenport, J. R. *et al.* Disruption of intraflagellar transport in adult mice leads to obesity and slow-onset cystic kidney disease. *Curr. Biol.* **17,** 1586–1594 (2007).

229. Berbari, N. F., Lewis, J. S., Bishop, G. A., Askwith, C. C. & Mykytyn, K. Bardet-Biedl syndrome proteins are required for the localization of G protein-coupled receptors to primary cilia. *Proc. Natl. Acad. Sci. U. S. A.* **105,** 4242–6 (2008).

230. Seo, S. *et al.* Requirement of Bardet-Biedl syndrome proteins for leptin receptor signaling. *Hum. Mol. Genet.* **18,** 1323–1331 (2009).

231. Wang, Z. *et al.* Adult type 3 adenylyl cyclase-deficient mice are obese. *PLoS One* **4,** (2009).

232. Marion, V. *et al.* Transient ciliogenesis involving Bardet-Biedl syndrome proteins is a fundamental characteristic of adipogenic differentiation. *Proc. Natl. Acad. Sci. U. S. A.* **106,** 1820–5 (2009).

233. Goetz, S. C. & Anderson, K. V. The primary cilium: a signalling centre during vertebrate development. *Nat. Rev. Genet.* **11,** 331–44 (2010).

234. Beales, P. L., Warner, A. M., Hitman, G. A., Thakker, R. & Flinter, F. A. Bardet-Biedl syndrome: a molecular and phenotypic study of 18 families. *J. Med. Genet.* **34,** 92–8 (1997).

235. Sorokin, S. Centrioles and the formation of rudimentary cilia by fibroblasts and smooth muscle cells. *J. Cell Biol.* **15,** 363–377 (1962).

236. Garcia-Gonzalo, F. R. & Reiter, J. F. Scoring a backstage pass: mechanisms of ciliogenesis and ciliary access. *J Cell Biol* **197,** 697–709 (2012).

237. Gilula, N. B. & Satir, P. the Ciliary Necklace. *J. Cell Biol.* **53,** 494–509 (1972).

238. Breslow, D. K. & Nachury, M. V. Primary cilia: How to keep the riff-raff in the plasma membrane. *Curr. Biol.* **21,** R434–R436 (2011).

239. Breslow, D. K., Koslover, E. F., Seydel, F., Spakowitz, A. J. & Nachury, M. V. An in vitro assay for entry into cilia reveals unique properties of the soluble diffusion barrier. *J. Cell Biol.* **203,** 129–47 (2013).

240. Vieira, O. V *et al.* FAPP2, cilium formation, and compartmentalization of the apical membrane in polarized Madin-Darby canine kidney (MDCK) cells. *Proc. Natl. Acad. Sci. U. S. A.* **103,** 18556–18561 (2006).

241. Ounjai, P. *et al.* Architectural insights into a ciliary partition. *Curr. Biol.* **23,** 339–344 (2013).

242. Rosenbaum, J. L. & Witman, G. B. Intraflagellar transport. *Nat. Rev. Mol. cell* **3,** 813–825 (2002).

243. Molla-Herman, A. *et al.* The ciliary pocket: an endocytic membrane domain at the base of primary and motile cilia. *J. Cell Sci.* **123,** 1785–1795 (2010).

244. Rohatgi, R. & Snell, W. J. The ciliary membrane. *Curr. Opin. Cell Biol.* **22,** 541–546 (2010).

245. Benmerah, A. The ciliary pocket. *Curr. Opin. Cell Biol.* **25,** 1–7 (2013). DOI: 10.1016/j.ceb.2012.10.011

246. Haller, K. & Fabry, S. Brefeldin A affects synthesis and integrity of a eukaryotic flagellum. *Biochem. Biophys. Res. Commun.* **242,** 597–601 (1998).

247. Deretic, D., Schmerl, S., Hargrave, P. A., Arendt, A. & McDowell, J. H. Regulation of sorting and post-Golgi trafficking of rhodopsin by its C-terminal sequence QVS(A)PA. *Proc. Natl. Acad. Sci. U. S. A.* **95,** 10620–10625 (1998).

248. Klemm, R. W. *et al.* Segregation of sphingolipids and sterols during formation of secretory vesicles at the trans-Golgi network. *J. Cell Biol.* **185,** 601–612 (2009).

249. Iomini, C., Babaev-Khaimov, V., Sassaroli, M. & Piperno, G. Protein particles in Chlamydomonas flagella undergo a transport cycle consisting of four phases. *J. Cell Biol.* **153,** 13–24 (2001).

250. Iomini, C., Li, L., Esparza, J. M. & Dutcher, S. K. Retrograde intraflagellar transport mutants identify complex A proteins with multiple genetic interactions in Chlamydomonas reinhardtii. *Genetics* **183,** 885–896 (2009).

251. Chen, D. *et al.* Multiple pathways differentially regulate global oxidative stress responses in fission yeast. *Mol. Biol. Cell* **19,** 308–317 (2008).

252. Filigheddu, N. *et al.* Ghrelin and des-acyl ghrelin promote differentiation and fusion of C2C12 skeletal muscle cells. *Mol. Biol. Cell* **18,** 986–994 (2007).

253. Deane, J. A., Cole, D. G., Seeley, E. S., Diener, D. R. & Rosenbaum, J. L. Localization of intraflagellar transport protein IFT52 identifies basal body transitional fibers as the docking site for IFT particles. *Curr. Biol.* **11,** 1586–1590 (2001).

254. Pazour, G. J., San Agustin, J. T., Follit, J. A., Rosenbaum, J. L. & Witman, G. B. Polycystin-2 localizes to kidney cilia and the ciliary level is elevated in orpk mice with polycystic kidney disease. *Curr. Biol.* **12,** 378–380 (2002).

255. Mencarelli, C., Mitchell, A., Leoncini, R., Rosenbaum, J. & Lupetti, P. Isolation of intraflagellar transport trains. *Cytoskeleton* **70,** 439–452 (2013).

256. Taschner, M., Bhogaraju, S. & Lorentzen, E. Architecture and function of IFT complex proteins in ciliogenesis. *Differentiation* **83,** 1–22 (2012).

257. Pedersen, L. B. & Rosenbaum, J. L. Intraflagellar transport (IFT) role in ciliary assembly, resorption and signalling. *Curr Top Dev Biol* **85,** 23–61 (2008).

258. Pigino, G. *et al.* Electron-tomographic analysis of intraflagellar transport particle trains in situ. *J. Cell Biol.* **187,** 135–148 (2009).

259. Eggenschwiler, J. T. & Anderson, K. V. Cilia and developmental signaling. *Annu. Rev. Cell Dev. Biol.* **23,** 345–73 (2007).

260. Kiprilov, E. N. *et al.* Human embryonic stem cells in culture possess primary cilia with hedgehog signaling machinery. *J. Cell Biol.* **180,** 897–904 (2008).

261. Masyuk, A. I. *et al.* Cholangiocyte cilia detect changes in luminal fluid flow and transmit them into intracellular Ca2+ and cAMP signaling anatoliy. *Gastroenterology* **131,** 911–920 (2006).

262. Wong, S. Y. & Reiter, J. The primary cilium: at the crossroad of mammalian hedgehog signaling. *Curr Top Dev Biol* **85,** 225–260 (2008).

263. Kaplan, O. I. *et al.* The AP-1 clathrin adaptor facilitates cilium formation and functions with RAB-8 in C. elegans ciliary membrane transport. *J. Cell Sci.* **123,** 3966–3977 (2010).

264. Moritz, O. L., Tam, B. M., Papermaster, D. S. & Nakayama, T. A functional rhodopsin-green fluorescent protein fusion protein localizes correctly in transgenic

Xenopus laevis retinal rods and is expressed in a time-dependent pattern. *J. Biol. Chem.* **276,** 28242–28251 (2001).

265. Schneider, L. *et al.* PDGFRalphaalpha signaling is regulated through the primary cilium in fibroblasts. *Curr. Biol.* **15,** 1861–1866 (2005).

266. Clement, C. *et al.* TGF-β signaling is associated with endocytosis at the pocket region of the primary cilium. *Cell Rep.* **3,** 1806–1814 (2013).

267. Corbit, K. C. *et al.* Vertebrate Smoothened functions at the primary cilium. *Nature* **437,** 1018–1021 (2005).

268. Corbit, K. C. *et al.* Kif3a constrains beta-catenin-dependent Wnt signalling through dual ciliary and non-ciliary mechanisms. *Nat. Cell Biol.* **10,** 70–76 (2008).

269. Hassounah, N. B. *et al.* Primary cilia are lost in preinvasive and invasive prostate cancer. *PLoS One* **8,** (2013).

270. Seeley, E. S., Carrière, C., Goetze, T. & Longnecker, D. S. Pancreatic cancer and precursor pancreatic intraepithelial neoplasia lesions are devoid of primary cilia. *Cancer Res.* **69,** 422–430 (2009).

271. Kim, J., Dabiri, S. & Seeley, E. S. Primary cilium depletion typifies cutaneous melanoma in situ and malignant melanoma. *PLoS One* **6,** (2011).

272. Schraml, P. *et al.* Sporadic clear cell renal cell carcinoma but not the papillary type is characterized by severely reduced frequency of primary cilia. *Mod. Pathol.* **22,** 31–36 (2009).

273. Yuan, K. *et al.* Primary cilia are decreased in breast cancer: analysis of a collection of human breast cancer cell lines and tissues. *J. Histochem. Cytochem.* **58,** 857–870 (2010).

274. Basten, S. G. & Giles, R. H. Functional aspects of primary cilia in signaling, cell cycle and tumorigenesis. *Cilia* **2,** 6 (2013).

275. Kuehn, E. W., Walz, G. & Benzing, T. Von Hippel-Lindau: A tumor suppressor links microtubules to ciliogenesis and cancer development. *Cancer Res.* **67,** 4537–4540 (2007).

276. Mans, D. A., Voest, E. E. & Giles, R. H. All along the watchtower: Is the cilium a tumor suppressor organelle? *Biochim. Biophys. Acta - Rev. Cancer* **1786,** 114–125 (2008).

277. Han, Y. *et al.* Dual and opposing roles of primary cilia in medulloblastoma development. *Nat Med* **15,** 1062–1065 (2009).

278. Michaud, E. J. & Yoder, B. K. The primary cilium in cell signaling and cancer. *Cancer Res.* **66,** 6463–6467 (2006).

279. Nielsen, S. K. *et al.* Characterization of primary cilia and Hedgehog signaling during development of the human pancreas and in human pancreatic duct cancer cell lines. *Dev. Dyn.* **237,** 2039–52 (2008).

280. Wong, S. Y. *et al.* Primary cilia can both mediate and suppress Hedgehog pathway–dependent tumorigenesis. *Nat Med* **15,** 1055–1061 (2009).

281. Plotnikova, O. V, Golemis, E. A. & Pugacheva, E. N. Cell cycle-dependent ciliogenesis and cancer. *Cancer Res* **68,** 2058–2061 (2008).

282. D'Avino, P. P. *et al.* Isolation of protein complexes involved in mitosis and cytokinesis from Drosophila cultured cells. *Methods Mol Biol.* **545,** 99–112 (2009).

283. Frangioni, J. V & Neel, B. G. Solubilization and purification of enzymatically active glutathione S-transferase (pGEX) fusion proteins. *Anal. Biochem.* **210,** 179–87 (1993).

284. Sievers, F. *et al.* Fast, scalable generation of high-quality protein multiple sequence alignments using Clustal Omega. *Mol. Syst. Biol.* **7,** 539 (2011).

285. Jones, D. Protein secondary structure prediction based on position-specific scoring matrices. *Journal of molecular biology* **292,** 195–202 (1999).

286. Lupas, A., Van Dyke, M. & Stock, J. Predicting coiled coils from protein sequences. *Science (New York, N.Y.)* **252,** 1162–1164 (1991).

287. Blom, N., Gammeltoft, S. & Brunak, S. Sequence and structure-based prediction of eukaryotic protein phosphorylation sites. *Journal of molecular biology* **294,** 1351–62 (1999).

288. Goshima, G. *et al.* Genes required for mitotic spindle assembly in Drosophila S2 cells. *Science* **316,** 417–421 (2007).

289. Brito, D. A., Gouveia, S. M. & Bettencourt-Dias, M. Deconstructing the centriole: structure and number control. *Curr Opin Cell Biol* **24,** 4–13 (2012).

290. Strnad, P. & Gonczy, P. Mechanisms of procentriole formation. *Trends Cell Biol* **18,** 389–396 (2008).

291. Nigg, E. A. & Raff, J. W. Centrioles, centrosomes, and cilia in health and disease. *Cell* **139,** 663–678 (2009).

292. Meraldi, P. & Nigg, E. A. The centrosome cycle. *FEBS Lett.* **521,** 9–13 (2002).

293. Cizmecioglu, O. *et al.* Cep152 acts as a scaffold for recruitment of Plk4 and CPAP to the centrosome. *J Cell Biol* **191,** 731–739 (2010).

294. Hatch, E. M., Kulukian, A., Holland, A. J., Cleveland, D. W. & Stearns, T. Cep152 interacts with Plk4 and is required for centriole duplication. *J Cell Biol* **191,** 721–729 (2010).

295. Richter, M. M. *et al.* Network of protein interactions within the Drosophila inner kinetochore. *Open Biol.* **6,** 150238 (2016).

296. Dzhindzhev, N. S. *et al.* Plk4 phosphorylates Ana2 to trigger Sas6 recruitment and procentriole formation. *Curr Biol* **24,** 2526–2532 (2014). CC BY 3.0 DOI: 10.1016/j.cub.2014.08.061

297. Martinez-Campos, M., Basto, R., Baker, J., Kernan, M. & Raff, J. W. The Drosophila pericentrin-like protein is essential for cilia/flagella function, but appears to be dispensable for mitosis. *J Cell Biol* **165,** 673–683 (2004).

298. Hsu, W. B. *et al.* Functional characterization of the microtubule-binding and -destabilizing domains of CPAP and d-SAS-4. *Exp Cell Res* **314,** 2591–2602 (2008).

299. Kim, M., Fong, C. S. & Tsou, M. F. B. Centriole duplication: When PLK4 meets Ana2/STIL. *Curr. Biol.* **24,** R1046–R1048 (2014).

300. Moyer, T. C., Clutario, K. M., Lambrus, B. G., Daggubati, V. & Holland, A. J. Binding of STIL to Plk4 activates kinase activity to promote centriole assembly. *J. Cell Biol.* **209,** 863–878 (2015).

301. Whitfield, Z. J., Chisholm, J., Hawley, R. S. & Orr-Weaver, T. L. A meiosis-specific form of the APC/C promotes the oocyte-to-embryo transition by decreasing levels of the Polo kinase inhibitor matrimony. *PLoS Biol* **11,** e1001648 (2013).

302. Qiao, R., Cabral, G., Lettman, M. M., Dammermann, A. & Dong, G. SAS-6 coiled-coil structure and interaction with SAS-5 suggest a regulatory mechanism in C. elegans centriole assembly. *EMBO J* **31,** 4334–4347 (2012).

303. Bodenmiller, B. *et al.* PhosphoPep--a phosphoproteome resource for systems biology research in Drosophila Kc167 cells. *Mol Syst Biol* **3,** 139 (2007).

304. Shimanovskaya, E., Qiao, R., Lesigang, J. & Dong, G. The SAS-5 N-terminal domain is a tetramer, with implications for centriole assembly in C. elegans. *Worm* **2,** e25214 (2013). CC BY 3.0 DOI: 10.4161/worm.25214

305. Song, M. H., Liu, Y., Anderson, D. E., Jahng, W. J. & O'Connell, K. F. Protein phosphatase 2A-SUR-6/B55 regulates centriole duplication in C. elegans by controlling the levels of centriole assembly factors. *Dev Cell* **20,** 563–571 (2011).

306. Aplan, P. D., Lombardi, D. P. & Kirsch, I. R. Structural characterization of SIL, a gene frequently disrupted in T-cell acute lymphoblastic leukemia. *Mol. cell Biol.* **11,** 5462–5469 (1991).

307. Kumar, A., Girimaji, S. C., Duvvari, M. R. & Blanton, S. H. Mutations in STIL, encoding a pericentriolar and centrosomal protein, cause primary microcephaly. *Am. J. Hum. Genet.* **84,** 286–290 (2009).

308. Schmutz, C. & Spang, A. Knockdown of the centrosomal component SAS-5 results in defects in nuclear morphology in Caenorhabditis elegans. *Eur J Cell Biol* **84,** 75–82 (2005).

309. Park, S. Y. *et al.* Molecular basis for unidirectional scaffold switching of human Plk4 in centriole biogenesis. *Nat Struct Mol Biol* **21,** 696–703 (2014).

310. Goshima, G. Assessment of mitotic spindle phenotypes in Drosophila S2 cells. *Methods Cell Biol.* **97,** 259–275 (2010).

311. Jerka-Dziadosz, M. *et al.* Basal body duplication in Paramecium: the key role of Bld10 in assembly and stability of the cartwheel. *Cytoskelet.* **67,** 161–171 (2010).

312. Bayless, B. A., Giddings Jr., T. H., Winey, M. & Pearson, C. G. Bld10/Cep135 stabilizes basal bodies to resist cilia-generated forces. *Mol Biol Cell* **23,** 4820–4832 (2012).

313. Boyd, J. M. *et al.* A region in the C-terminus of adenovirus 2/5 E1a protein is required for association with a cellular phosphoprotein and important for the negative modulation of T24-ras mediated transformation, tumorigenesis and metastasis. *EMBO J.* **12,** 469–78 (1993).

314. Schaeper, U. *et al.* Molecular cloning and characterization of a cellular phosphoprotein that interacts with a conserved C-terminal domain of adenovirus E1A involved in negative modulation of oncogenic transformation. *Proc. Natl. Acad. Sci. U. S. A.* **92,** 10467–71 (1995).

315. Sollerbrant, K., Chinnadurai, G. & Svensson, C. The CtBP binding domain in the adenovirus E1A protein controls CR1-dependent transactivation. *Nucleic Acids Res.* **24,** 2578–2584 (1996).

316. Nibu, Y., Zhang, H. & Levine, M. Interaction of short-range repressors with Drosophila CtBP in the embryo. *Science (New York, N.Y.)* **280,** 101–4 (1998).

317. Poortinga, G., Watanabe, M. & Susan, S. M. Drosophila CtBP: A Hairy-interacting protein required for embryonic segmentation and Hairy-mediated transcriptional repression. *EMBO J.* **17,** 2067–2078 (1998).

318. Fritzler, M. J., Hamel, J. C., Ochs, R. L. & Chan, E. K. L. Molecular characterization of two human autoantigens: unique cDNAs encoding 95- and 160-kD proteins of a putative family in the Golgi complex. *J. Exp. Med.* **178,** 49–62 (1993).

319. Nakamura, N. *et al.* Characterization of a cis-Golgi Matrix Protein, GM130. *J Cell Biol.* **131,** 1715–1726 (1995).

320. Fridmann-Sirkis, Y., Siniossoglou, S. & Pelham, H. R. B. TMF is a golgin that binds Rab6 and influences Golgi morphology. *BMC Cell Biol.* **5,** 18 (2004).

321. Glick, B. S., Elston, T. & Oster, G. A cisternal maturation mechanism can explain the asymmetry of the Golgi stack. *FEBS Lett.* **414,** 177–181 (1997).

322. Glick, B. S. & Nakano, A. Membrane traffic within the Golgi apparatus. *Annu Rev Cell Dev Biol* **25,** 113–132 (2009).

323. Barlowe, C. K. & Miller, E. A. Secretory protein biogenesis and traffic in the early secretory pathway. *Genetics* **193,** 383–410 (2013).

324. Donohoe, B. S., Kang, B.-H. & Staehelin, L. A. Identification and characterization of COPIa- and COPIb-type vesicle classes associated with plant and algal Golgi. *Proc. Natl. Acad. Sci. U. S. A.* **104,** 163–168 (2007).

325. Glick, B. S. & Malhotra, V. The curious status of the Golgi apparatus. *Cell* **95,** 883–889 (1998).

326. Popoff, V., Adolf, F., Brügge, B. & Wieland, F. COPI budding within the Golgi stack. *Cold Spring Harb. Perspect. Biol.* **3,** 1–19 (2011).

327. De Matteis, M. A. & Luini, A. Exiting the Golgi complex. *Nat. Rev. Mol. Cell Biol.* **9,** 273–284 (2008).

328. Valdivia, R. H., Baggott, D., Chuang, J. S. & Schekman, R. W. The yeast clathrin adaptor protein complex 1 is required for the efficient retention of a subset of late Golgi membrane proteins. *Dev. Cell* **2,** 283–294 (2002).

329. Viotti, C. *et al.* Endocytic and secretory traffic in Arabidopsis merge in the trans-Golgi network/early endosome, an independent and highly dynamic organelle. *Plant Cell* **22,** 1344–1357 (2010).

330. Schledzewski, K., Brinkmann, H. & Mendel, R. R. Phylogenetic analysis of components of the eukaryotic vesicle transport system reveals a common origin of adaptor protein complexes 1, 2, and 3 and the F subcomplex of the coatomer COPI. *J. Mol. Evol.* **48,** 770–778 (1999).

331. Yu, X., Breitman, M. & Goldberg, J. A Structure-based mechanism for Arf1-dependent recruitment of coatomer to membranes. *Cell* **148,** 530–542 (2012).

332. Lee, C. & Goldberg, J. Structure of coatomer cage proteins and the relationship among COPI, COPII, and clathrin vesicle coats. *Cell* **142,** 123–132 (2010).

333. Hsia, K.-C. & Hoelz, A. Crystal structure of alpha-COP in complex with epsilon-COP provides insight into the architecture of the COPI vesicular coat. *Proc. Natl. Acad. Sci. U. S. A.* **107,** 11271–6 (2010).

334. Faini, M. *et al.* The structures of COPI-coated vesicles reveal alternate coatomer conformations and interactions. *Science* **336,** 1451–1454 (2012).

335. Fullilove, S. L. & Jacobson, A. G. Nuclear elongation and cytokinesis in Drosophila montana. *Dev. Biol.* **26,** 560–577 (1971).

336. Ripoche, J., Link, B., Yucel, J. K., Tokuyasu, K. & Malhotra, V. Location of Golgi membranes with reference to dividing nuclei in syncytial Drosophila embryos. *Proc Natl Acad Sci U S A.* **91,** 1878–1882 (1994).

337. Stanley, H., Botas, J. & Malhotra, V. The mechanism of Golgi segregation during mitosis is cell type-specific. *Proc. Natl. Acad. o Sci. United States Am.* **94,** 14467–14470 (1997).

338. Mahowald, A. P., Goralski, T. J. & Caulton, J. H. In vitro activation of Drosophila eggs. *Dev. Biol.* **98,** 437–445 (1983).

339. Rabouille, C. *et al.* The Drosophila GMII gene encodes a Golgi alpha-mannosidase II. *J. Cell Sci.* **112,** 3319–3330 (1999).

340. Kondylis, V., Goulding, S. E., Dunne, J. C. & Rabouille, C. Biogenesis of Golgi stacks in imaginal discs of Drosophila melanogaster. *Mol Biol Cell* **12,** 2308–2327 (2001).

341. Grigoriev, I. *et al.* Rab6 regulates transport and targeting of exocytotic carriers. *Dev. Cell* **13,** 305–314 (2007).

342. Mallard, F. *et al.* Early/recycling endosomes-to-TGN transport involves two SNARE complexes and a Rab6 isoform. *J. Cell Biol.* **156,** 653–664 (2002).

343. Colanzi, A. *et al.* The Golgi mitotic checkpoint is controlled by BARS-dependent fission of the Golgi ribbon into separate stacks in G2. *EMBO J.* **26,** 2465–2476 (2007).

344. Shorter, J. & Warren, G. Golgi architecture and inheritance. *Annu Rev Cell Dev Biol* **18,** 379–420 (2002).

345. Shima, D. T., Cabrera-Poch, N., Pepperkok, R. & Warren, G. An ordered inheritance strategy for the Golgi apparatus: Visualization of mitotic disassembly reveals a role for the mitotic spindle. *J. Cell Biol.* **141,** 955–966 (1998).

346. Colanzi, A., Suetterlin, C. & Malhotra, V. Cell-cycle-specific Golgi fragmentation: How and why? *Curr. Opin. Cell Biol.* **15,** 462–467 (2003).

347. Barnes, C. J. *et al.* Functional inactivation of a transcriptional corepressor by a signaling kinase. *Nat. Struct. Biol.* **10,** 622–628 (2003).

348. Cotteret, S. & Chernoff, J. Pak GITs to Aurora-A. *Dev. Cell* **9,** 573–574 (2005).

349. Blom, N., Gammeltoft, S. & Brunak, S. Sequence and structure-based prediction of eukaryotic protein phosphorylation sites. *J. Mol. Biol.* **294,** 1351–62 (1999).

350. Fong, C. S., Kim, M., Yang, T. T., Liao, J. C. & Tsou, M. F. Sas-6 assembly templated by the lumen of cartwheel-less centrioles precedes centriole duplication. *Dev Cell* **30,** 238–245 (2014).

Appendix

Appendix

Appendix A: Mass spectrometry results from purifications of centriole duplication proteins from cultured *Drosophila* cells.

Tables show the full list of hits identified from the stated purification; indicating CG numbers, Mascot scores, Number of peptides (#pep), and the Full name of the protein if available. Tables are supplementary to Table 3-1 and Table 3-2.

A.1 Act5-PrA-Plk4 purification from *Drosophila* cells

CG #	Score	#pep	Full name
CG7186	3411	118	Plk4
CG9277	1532	55	beta-Tubulin at 56D
CG4264	1051	37	Heat shock protein cognate 4
CG3401	935	35	beta-Tubulin at 60D
CG1913	895	30	alpha-Tubulin at 84B
CG4821	808	29	Tequila
CG2919	636	25	Asterless
CG14025	538	15	Blastoderm-specific gene 25D
CG33957	460	19	cp309
CG4147	447	15	Heat shock protein cognate 3
CG7439	368	12	Argonaute 2
CG7808	358	8	Ribosomal protein S8
CG5502	352	11	Ribosomal protein L4
CG7490	337	13	Ribosomal protein LP0
CG9795	314	9	CG9795
CG6453	302	8	Glucosidase 2 β subunit
CG7123	298	6	Laminin B1
CG31022	288	8	prolyl-4-hydroxylase-alpha EFB
CG2199	280	6	CG2199
CG4087	279	7	Ribosomal protein LP1
CG16858	268	8	viking
CG3412	261	10	supernumerary limbs
CG13800	259	8	CG13800
CG4832	257	9	centrosomin
CG5436	251	8	Heat shock protein 68
CG3992	240	6	serpent
CG14792	233	7	stubarista
CG11100	232	5	Mes2
CG1119	230	7	Germ line transcription factor 1
CG6253	229	5	Ribosomal protein L14
CG2168	206	8	Ribosomal protein S3A
CG6759	200	5	cdc16
CG9212	200	6	Nipsnap
CG5504	200	4	lethal (2) tumorous imaginal discs
CG7283	196	4	Ribosomal protein L10Ab
CG7450	194	4	Cyclic-AMP response element binding protein A
CG5920	184	4	string of pearls
CG7434	181	5	Ribosomal protein L22
CG16983	180	6	skpA
CG15220	170	3	Replication protein A3
CG5119	168	7	polyA-binding protein
CG13624	165	3	Repressed by TOR
CG3195	162	4	Ribosomal protein L12
CG4897	159	7	Ribosomal protein L7
CG4164	155	3	CG4164
CG8615	155	3	Ribosomal protein L18
CG3751	154	4	Ribosomal protein S24
CG12101	153	5	Heat shock protein 60
CG16973	151	3	misshapen
CG33130	149	6	lethal (2) k07433
CG6143	148	1	Protein on ecdysone puffs
CG4918	148	4	Ribosomal protein LP2
CG9282	147	2	Ribosomal protein L24
CG17081	147	5	CG17081
CG11999	141	2	CG11999
CG6815	139	3	belphegor
CG10732	136	4	combover
CG8415	130	2	Ribosomal protein S23
CG8900	130	4	Ribosomal protein S18
CG7518	129	3	CG7518
CG10061	126	2	lethal (3) s2214
CG10944	125	4	Ribosomal protein S6
CG3836	125	4	stonewall
CG4337	124	3	mitochondrial single stranded DNA-binding protein
CG6509	124	4	Discs large 5
CG1524	123	4	Ribosomal protein S14a
CG6386	122	3	ballchen
CG6988	122	3	Protein disulfide isomerase
CG17383	120	2	jing interacting gene regulatory 1
CG8108	117	3	CG8108
CG10652	117	2	Ribosomal protein L30
CG2746	117	4	Ribosomal protein L19
CG31650	116	3	CG31650
CG4863	115	3	Ribosomal protein L3
CG6779	114	4	Ribosomal protein S3
CG31012	112	3	CIN85 and CD2AP orthologue
CG11276	112	5	Ribosomal protein S4
CG10377	109	3	Heterogeneous nuclear ribonucleoprotein at 27C
CG14999	108	4	Replication-factor-C 40kD subunit
CG10305	104	3	Ribosomal protein S26
CG12163	104	3	CG12163
CG8280	103	4	Elongation factor 1alpha48D
CG4463	100	2	Heat shock protein 23
CG8610	100	2	Cdc27
CG17489	99	3	Ribosomal protein L5
CG14648	98	3	lost
CG1821	98	3	Ribosomal protein L31
CG5654	95	2	ypsilon schachtel
CG6631	95	2	anastral spindle 1
CG9372	95	3	CG9372
CG11734	94	1	HERC2
CG9775	93	1	CG9775
CG6944	92	2	Lamin
CG1883	92	3	Ribosomal protein S7
CG3314	92	3	Ribosomal protein L7A
CG7622	92	2	Ribosomal protein L36
CG9484	91	2	hyperplastic discs
CG2508	90	3	cdc23
CG8715	90	2	lingerer
CG9198	88	1	shattered
CG31160	87	2	CG31160
CG3203	86	1	Ribosomal protein L17
CG3589	86	1	CG3589
CG17870	84	1	14-3-3zeta
CG12233	83	4	lethal (1) G0156
CG10811	82	1	Eukaryotic-initiation-factor-4G
CG3379	80	3	Histone H4 replacement
CG14476	79	1	Glucosidase 2 α subunit
CG15784	79	1	CG15784
CG7323	79	1	CG7323
CG8055	78	2	shrub
CG33956	78	1	kayak
CG10473	77	1	Acinus
CG6241	76	1	TATA box-binding protein-associated factor RNA polymerase I subunit B
CG7977	76	4	Ribosomal protein L23A
CG7726	75	1	Ribosomal protein L11
CG4399	75	1	enhanced adult sensory threshold
CG7111	73	2	Receptor of activated protein kinase C 1
CG6258	72	1	Replication factor C 38kD subunit
CG31992	71	1	gawky
CG10712	70	1	Chromator
CG2998	69	2	Ribosomal protein S28b
CG14617	69	2	CP110
CG17521	69	1	Qm

CG1341	69	1	Rpt1
CG3395	69	4	Ribosomal protein S9
CG6904	68	1	CG6904
CG12740	68	2	Ribosomal protein L28
CG11522	67	1	Ribosomal protein L6
CG1344	67	1	CG1344
CG3548	66	1	CG3548
CG17520	66	1	Casein kinase II alpha subunit
CG11271	65	1	Ribosomal protein S12
CG3917	65	1	gamma-tubulin ring protein 84
CG15437	65	1	modifier of rpr and grim, ubiquitously expressed
CG18001	64	1	Ribosomal protein L38
CG3008	64	1	CG3008
CG4145	64	2	Collagen type IV
CG8947	63	1	26-29kD-proteinase
CG14066	63	1	La related protein
CG3661	62	1	Ribosomal protein L23
CG8987	61	1	tamas
CG7863	61	1	dream
CG17437	61	1	will die slowly
CG32435	59	1	chromosome bows
CG1242	59	1	Heat shock protein 83
CG3361	57	2	martik
CG12775	57	1	Ribosomal protein L21
CG3061	57	1	CG3061
CG18495	56	1	Proteasome alpha6 subunit
CG6141	56	1	Ribosomal protein L9
CG5575	56	1	ken and barbie
CG3060	55	1	morula
CG15697	54	1	Ribosomal protein S30
CG5313	54	1	RfC3
CG10423	54	1	Ribosomal protein S27
CG7110	53	1	CG7110
CG3074	53	1	Secreted Wg-interacting molecule
CG17286	53	1	spindle defective 2
CG10289	52	1	CG10289
CG7337	52	1	CG7337
CG13780	51	1	PDGF- and VEGF-related factor 2
CG15442	51	1	Ribosomal protein L27A
CG4573	51	1	Glutamyl-tRNA synthetase, mitochondrial
CG6846	50	1	Ribosomal protein L26
CG2960	50	1	Ribosomal protein L40
CG4460	50	1	Heat shock protein 22
CG3422	49	1	Proteasome 28kD subunit 1
CG9641	49	1	CG9641
CG18572	49	1	rudimentary
CG5499	49	1	Histone H2A variant
CG7627	48	2	CG7627
CG5726	48	1	CG5726
CG3157	47	1	gamma-Tubulin at 23C
CG12179	47	1	CG12179
CG12052	47	1	longitudinals lacking
CG5827	47	1	Ribosomal protein L37A
CG9633	46	1	Replication Protein A 70
CG4046	46	1	Ribosomal protein S16
CG6831	46	1	rhea
CG5336	46	1	Ced-12
CG6742	46	1	centaurin beta 1A
CG17342	45	1	Lk6
CG12275	45	1	Ribosomal protein S10a
CG9273	45	1	Replication protein A2
CG18811	45	1	Caprin
CG8857	45	1	Ribosomal protein S11
CG5378	44	1	Rpn7
CG33087	44	1	LDL receptor protein 1
CG3647	44	1	shuttle craft
CG1399	44	1	Leucine-rich repeat
CG4759	44	1	Ribosomal protein L27
CG6692	44	1	Cysteine proteinase-1
CG32491	43	1	modifier of mdg4
CG12157	43	1	Translocase of outer membrane 40
CG1263	43	1	Ribosomal protein L8
CG5690	43	1	Centrobin
CG6439	43	2	CG6439
CG12437	42	1	raw
CG4785	42	1	Integrator 14

A.2 pMT-PrA-Plk4 +MG132 purification from *Drosophila* cells

CG #	Score	#pep	Full name
CG16901	48679	842	squid
CG1913	11462	224	α-Tubulin at 84B
CG9277	8869	252	β-Tubulin at 56D
CG7186	8544	205	Plk4
CG15792	4434	83	zipper
CG2919	3542	148	asterless
CG3401	1730	37	β-Tubulin at 60D
CG4264	1707	64	Heat shock protein cognate 4
CG7185	692	12	CG7185
CG4147	641	19	Heat shock protein cognate 3
CG5178	515	22	Actin 88F
CG5119	505	14	polyA-binding protein
CG4145	503	13	Collagen type IV
CG16858	500	11	viking
CG4027	494	21	Actin 5C
CG3201	470	12	Myosin light chain cytoplasmic
CG14648	470	17	growl
CG33957	468	13	cp309
CG4463	405	13	Heat shock protein 23
CG18743	402	14	Heat-shock-protein-70Ab
CG6450	398	9	lava lamp
CG5834	396	14	Hsp70Bbb
CG12101	389	9	Heat shock protein 60
CG8280	378	11	Elongation factor 1α48D
CG4183	365	13	Heat shock protein 26
CG5654	362	12	ypsilon schachtel
CG4466	327	8	Heat shock protein 27
CG31618	325	5	His2A:CG31618
CG7581	322	9	Bub3
CG9748	318	8	belle
CG7439	311	13	Argonaute 2
CG15784	308	4	CG15784
CG5436	296	11	Heat shock protein 68
CG10811	296	6	eukaryotic translation initiation factor 4G
CG1528	282	6	Coat Protein (coatomer) γ
CG10578	263	9	DnaJ-like-1
CG14066	259	4	La related protein
CG12233	249	7	lethal (1) G0156
CG1691	239	11	IGF-II mRNA-binding protein
CG1341	229	5	Rpt1
CG3455	213	3	Rpt4
CG3412	212	8	supernumerary limbs
CG1489	211	6	Pros45
CG1883	205	8	Ribosomal protein S7
CG6181	198	8	Ge-1
CG3689	184	4	CG3689
CG3612	176	5	bellwether
CG4832	176	4	centrosomin
CG3218	175	3	female sterile (1) K10
CG5934	171	2	CG5934
CG17347	171	3	lethal (2) 37Ce
CG31022	165	7	prolyl-4-hydroxylase-alpha EFB
CG6631	160	4	anastral spindle 1
CG4211	159	3	no on or off transient A
CG5726	156	2	CG5726
CG10360	153	5	refractory to sigma P
CG9212	147	5	Nipsnap
CG3981	144	2	Unc-76
CG8994	143	2	exuperantia
CG10596	143	2	Msr-110
CG17081	143	3	Cep135
CG4394	140	2	TNF-receptor-associated factor-like
CG10938	139	2	Proteasome α5 subunit
CG16916	138	2	Rpt3
CG32626	138	2	AMP deaminase
CG8472	134	3	Calmodulin
CG11984	131	2	CG11984
CG7769	131	2	piccolo
CG3595	130	3	spaghetti squash
CG10230	130	4	Rpn9
CG10732	126	3	combover
CG3379	125	3	Histone H4 replacement
CG8295	123	2	Myelodysplasia/myeloid leukemia factor
CG6831	121	3	rhea
CG3322	120	2	Laminin B2
CG4266	118	2	CG4266
CG8597	114	6	lark
CG1524	109	4	Ribosomal protein S14a
CG7961	105	2	Coat Protein (coatomer) α
CG31012	105	1	CIN85 and CD2AP orthologue
CG11198	104	1	Acetyl-CoA carboxylase
CG1242	102	3	Heat shock protein 83
CG10753	100	2	Small ribonucleoprotein particle protein SmD1
CG7915	99	2	Ect4
CG3157	97	3	γ-Tubulin at 23C
CG13277	96	2	CG13277
CG5378	94	2	Rpn7
CG3210	92	2	Dynamin related protein 1
CG2186	89	3	CG2186
CG10922	88	1	La autoantigen-like
CG33554	88	2	Nipped-A
CG8900	87	2	Ribosomal protein S18
CG3422	85	2	Proteasome 28kD subunit 1

CG14472	84	3	purity of essence
CG2025	84	3	CG2025
CG13849	84	2	Nop56
CG5374	82	1	Tcp1-like
CG9282	82	1	Ribosomal protein L24
CG5604	81	2	CG5604
CG2508	81	2	cdc23
CG2910	76	2	spenito
CG2960	75	4	Ribosomal protein L40
CG16940	75	2	CG16940
CG8578	73	1	CG8578
CG7490	71	1	Ribosomal protein LP0
CG9012	71	2	Clathrin heavy chain
CG2216	71	1	Ferritin 1 heavy chain homologue
CG6203	71	1	Fmr1
CG12264	71	1	CG12264
CG8426	71	1	lethal (2) NC136
CG5208	69	2	Protein associated with topo II related - 1
CG14207	69	2	HspB8
CG5502	68	2	Ribosomal protein L4
CG10289	68	1	CG10289
CG6815	67	2	belphegor
CG17158	66	2	capping protein beta
CG17291	66	1	Protein phosphatase 2A at 29B
CG6866	65	1	loquacious
CG4389	64	1	Mitochondrial trifunctional protein α subunit
CG7324	64	1	CG7324
CG17838	63	2	Syncrip
CG9206	62	1	Glued
CG7726	61	1	Ribosomal protein L11
CG18495	61	1	Proteasome α1 subunit
CG8055	61	1	shrub
CG7831	60	2	non-claret disjunctional
CG6223	60	2	Coat Protein (coatomer) β
CG17912	60	2	Bub3 interacting GLEBS and Zinc finger domain protein
CG6439	59	3	CG6439
CG10377	58	1	Heterogeneous nuclear ribonucleoprotein at 27C
CG8715	55	1	lingerer
CG10061	53	2	Sas-4
CG14813	52	1	Coat Protein (coatomer) δ
CG8863	52	1	DnaJ-like-2
CG10701	51	1	Moesin
CG2168	51	2	Ribosomal protein S3A
CG18174	50	1	Rpn11
CG10232	50	1	CG10232
CG18572	49	2	rudimentary
CG2033	49	1	Ribosomal protein S15Aa
CG3024	49	1	torp4a
CG10535	48	1	Elongator complex protein 1
CG5316	47	1	CG5316
CG6253	46	1	Ribosomal protein L14
CG9589	46	2	CG9589
CG1484	45	3	flightless I
CG4460	45	2	Heat shock protein 22
CG5526	44	7	Dynein heavy chain at 36C
CG6610	44	1	CG6610
CG1345	44	1	Glutamine:fructose-6-phosphate aminotransferase 2
CG6692	43	1	Cysteine proteinase-1
CG10149	43	1	Proteasome p44.5 subunit
CG9684	43	1	CG9684
CG10305	42	1	Ribosomal protein S26
CG15437	42	1	modifier of rpr and grim, ubiquitously expressed
CG15697	42	1	Ribosomal protein S30
CG2684	41	3	lodestar
CG5753	41	1	staufen
CG10851	41	2	B52
CG4164	41	1	CG4164
CG10423	41	2	Ribosomal protein S27
CG2637	40	1	Female sterile (2) Ketel
CG4898	40	2	Tropomyosin 1
CG7507	39	1	Dynein heavy chain 64C
CG1821	39	1	Ribosomal protein L31
CG11963	39	1	skpA associated protein
CG10370	38	1	Tat-binding protein-1
CG9795	38	1	CG9795
CG6779	37	1	Ribosomal protein S3
CG32138	37	1	CG32138
CG8571	35	1	smallminded
CG8588	35	1	pastrel
CG6987	35	1	SF2
CG7123	34	1	Laminin B1
CG9888	34	2	Fibrillarin
CG6509	34	2	Discs large 5
CG9769	34	1	CG9769
CG1683	33	4	Adenine nucleotide translocase 2
CG8108	33	2	CG8108
CG13349	33	1	Regulatory particle non-ATPase 13
CG7945	33	1	CG7945
CG11888	32	1	Rpn2
CG5028	32	1	CG5028
CG31048	32	1	sponge
CG33309	32	1	CG33309
CG7033	31	1	CG7033
CG6617	31	1	CG6617
CG17768	31	1	CG17768
CG14647	31	1	CG14647
CG4569	30	1	Proteasome 28kD subunit 1B
CG17286	30	1	spindle defective 2
CG8415	30	1	Ribosomal protein S23
CG5144	30	1	CG5144
CG8542	29	1	Heat shock protein cognate 5
CG5481	29	1	leak
CG4033	29	1	RNA polymerase I 135kD subunit
CG1850	29	1	CG1850
CG10102	29	1	CG10102
CG6684	29	2	Ribosomal protein S25
CG4904	28	1	Proteasome 35kD subunit
CG9450	28	1	tudor
CG4252	28	2	meiotic 41
CG13185	28	1	CG13185
CG1925	27	1	mutagen-sensitive 205
CG16944	27	3	stress-sensitive B
CG14616	27	1	lethal (1) G0196
CG16936	27	1	Glutathione S transferase E12
CG9940	27	1	CG9940
CG8332	27	1	Ribosomal protein S15
CG12027	27	1	ATP synthase, coupling factor 6-like
CG18176	27	1	deflated
CG6451	27	1	bluestreak
CG4220	26	1	elbow B
CG3395	26	1	Ribosomal protein S9
CG4257	26	1	Signal-transducer and activator of transcription protein at 92E
CG1249	26	1	Small ribonucleoprotein particle protein SmD2
CG4038	25	1	CG4038
CG17484	25	1	Adherens junction protein p120
CG2244	25	2	MTA1-like
CG15678	25	1	poor Imd response upon knock-in
CG5902	25	1	CG5902
CG32046	25	2	CG32046
CG2714	24	1	cramped
CG16983	24	1	skpA
CG5004	24	1	CG5004
CG4704	24	1	CG4704
CG9506	24	1	slow as molasses
CG12878	24	1	barentsz
CG31617	24	1	His1:CG31617
CG4097	23	1	Proteasome 26kD subunit
CG4651	23	1	Ribosomal protein L13
CG3333	23	1	Nucleolar protein at 60B
CG5888	23	1	CG5888
CG13742	23	1	CG13742
CG6327	23	1	CG6327
CG3711	23	1	CG3711
CG5154	23	1	Imaginal disc growth factor 5
CG7977	22	1	Ribosomal protein L23A
CG7762	22	1	Rpn1
CG30490	22	1	CG30490
CG33093	22	2	CG33093
CG8923	21	2	meiotic 218
CG11949	21	2	coracle
CG4258	21	1	dribble
CG4012	21	1	genghis khan
CG7144	21	1	lysine ketoglutarate reductase
CG5174	21	1	CG5174
CG3382	21	1	Organic anion transporting polypeptide 58Db
CG11261	21	1	CG11261
CG33106	21	1	multiple ankyrin repeats single KH domain
CG3001	20	1	Hexokinase A
CG2163	20	1	Pabp2
CG6375	20	1	pitchoune
CG8947	20	1	26-29kD-proteinase
CG4557	20	1	CG4557
CG10778	20	1	CG10778
CG10347	20	1	CG10347
CG7371	20	1	Vacuolar protein sorting 52
CG9316	20	1	CG9316
CG1621	20	1	Corepressor of Pangolin
CG32164	20	1	CG32164
CG32703	20	1	Extracellularly regulated kinase 7
CG9006	20	1	Enigma
CG31175	20	1	Dystrophin
CG9484	19	1	hyperplastic discs
CG13389	19	1	Ribosomal protein S13
CG6759	19	1	cdc16
CG17800	19	1	Down syndrome cell adhesion molecule
CG10094	19	1	Cyp313a2
CG33766	19	1	CG33766
CG1977	19	1	α Spectrin
CG7595	18	1	crinkled
CG10129	18	1	nudel
CG11312	18	1	inscuteable

CG4996	18	1	Vacuolar protein sorting 54L
CG3700	18	1	CG3700
CG14916	18	2	Gustatory receptor 32a
CG32351	18	1	Sperm-Leucylaminopeptidase 2

A.3 pMT-PrA-Plk4 +OA +MG132 purification from *Drosophila* cells

CG #	Score	#pep	Full name
CG33957	4029	116	cp309
CG15792	3481	76	zipper
CG1913	3173	69	α-Tubulin at 84B
CG7186	3011	111	Plk4
CG9277	2923	70	β-Tubulin at 56D
CG4264	2421	80	Heat shock protein cognate 4
CG2919	1778	53	asterless
CG6631	1776	55	anastral spindle 1
CG4147	1246	32	Heat shock protein cognate 3
CG3401	1189	32	β-Tubulin at 60D
CG17081	1107	33	Cep135
CG4027	1062	36	Actin 5C
CG18743	983	26	Heat-shock-protein-70Ab
CG5834	962	25	Hsp70Bbb
CG4463	946	27	Heat shock protein 23
CG4832	927	22	centrosomin
CG8014	785	20	Receptor mediated endocytosis 8
CG16901	780	14	squid
CG12101	710	13	Heat shock protein 60
CG10067	659	27	Actin 57B
CG5436	611	17	Heat shock protein 68
CG8280	600	21	Elongation factor 1α48D
CG16896	507	17	CG16896
CG16858	480	11	viking
CG10370	434	12	Tat-binding protein-1
CG3201	422	9	Myosin light chain cytoplasmic
CG10061	409	19	Sas-4
CG4183	378	15	Heat shock protein 26
CG6815	373	10	belphegor
CG16916	357	7	Rpt3
CG3595	354	7	spaghetti squash
CG12233	352	10	lethal (1) G0156
CG8472	347	9	Calmodulin
CG10230	328	6	Rpn9
CG1341	320	9	Rpt1
CG4466	301	7	Heat shock protein 27
CG10360	290	7	refractory to sigma P
CG3422	274	7	Proteasome 28kD subunit 1
CG5289	266	6	Proteasome 26S subunit subunit 4 ATPase
CG1548	263	4	cathD
CG10938	251	7	Proteasome α5 subunit
CG1242	243	8	Heat shock protein 83
CG18572	243	7	rudimentary
CG3455	237	4	Rpt4
CG17520	231	5	casein kinase IIα
CG10811	226	4	eukaryotic translation initiation factor 4G
CG18495	226	7	Proteasome α1 subunit
CG4145	224	6	Collagen type IV
CG5261	203	8	midline uncoordinated
CG31022	202	5	prolyl-4-hydroxylase-alpha EFB
CG4460	200	5	Heat shock protein 22
CG7762	197	8	Rpn1
CG11888	191	9	Rpn2
CG4904	183	5	Proteasome 35kD subunit
CG12000	179	3	Proteasome β7 subunit
CG5378	176	5	Rpn7
CG13162	175	3	anastral spindle 3
CG1519	174	6	Proteasome α7 subunit
CG14207	158	4	HspB8
CG4097	157	3	Proteasome 26kD subunit
CG1591	156	5	REG
CG9484	155	3	hyperplastic discs
CG9327	152	5	Proteasome 29kD subunit
CG12179	144	6	CG12179
CG17870	142	3	14-3-3ζ
CG31613	142	2	His3:CG31613
CG3412	140	5	supernumerary limbs
CG10191	140	4	Proteome of centrioles 1
CG8392	135	3	Proteasome β1 subunit
CG8262	134	2	anastral spindle 2
CG9940	131	4	CG9940
CG11963	127	2	skpA associated protein
CG15224	126	2	Casein kinase II β subunit
CG3379	124	4	Histone H4 replacement
CG4389	122	3	Mitochondrial trifunctional protein α subunit
CG5520	120	2	Glycoprotein 93
CG18174	119	2	Rpn11
CG31618	117	3	His2A:CG31618
CG2960	110	4	Ribosomal protein L40
CG10484	106	3	Regulatory particle non-ATPase 3
CG6453	106	4	Glucosidase 2 β subunit
CG1489	105	6	Pros45
CG8863	105	4	DnaJ-like-2
CG1100	104	4	Rpn5
CG3612	102	2	bellwether
CG5119	101	3	polyA-binding protein
CG7581	100	2	Bub3
CG5330	97	1	Nucleosome assembly protein 1
CG14750	96	2	Vacuolar protein sorting 25
CG5174	93	2	CG5174
CG4157	91	2	Rpn12
CG13349	91	2	Regulatory particle non-ATPase 13
CG32626	88	1	AMP deaminase
CG12184	86	4	CG12184
CG2216	85	1	Ferritin 1 heavy chain homologue
CG3157	83	3	γ-Tubulin at 23C
CG12323	82	3	Proteasome β5 subunit
CG17949	82	1	His2B:CG17949
CG7185	81	1	CG7185
CG31196	80	2	14-3-3ε
CG3662	78	1	CG3662
CG9748	72	3	belle
CG1528	72	3	Coat Protein (coatomer) γ
CG11981	71	1	Proteasome β3 subunit
CG8055	71	2	shrub
CG1683	70	1	Adenine nucleotide translocase 2
CG3981	70	1	Unc-76
CG6617	69	1	CG6617
CG10632	67	1	sosondowah
CG16983	65	2	skpA
CG6840	64	1	Rpb11
CG8368	63	1	CG8368
CG5266	61	2	Proteasome 25kD subunit
CG7033	61	1	CG7033
CG8478	61	1	CG8478
CG5825	60	1	Histone H3.3A
CG7945	60	1	CG7945
CG9281	59	1	CG9281
CG17498	59	1	mad2
CG1977	58	1	α Spectrin
CG2152	58	1	Protein-L-isoaspartate (D-aspartate) O-methyltransferase
CG5092	57	1	Target of rapamycin
CG1569	56	1	rough deal
CG2025	56	1	CG2025
CG31764	56	1	virus-induced RNA 1
CG31012	55	1	CIN85 and CD2AP orthologue
CG32138	55	1	CG32138
CG17291	55	1	Protein phosphatase 2A at 29B
CG1524	54	1	Ribosomal protein S14a
CG17158	53	1	capping protein beta
CG14648	53	1	growl
CG5934	53	1	CG5934
CG6692	52	1	Cysteine proteinase-1
CG4581	52	2	Thiolase
CG8947	51	2	26-29kD-proteinase
CG4164	51	1	CG4164
CG1883	51	1	Ribosomal protein S7
CG5374	50	1	Tcp1-like
CG6223	50	2	Coat Protein (coatomer) β
CG12019	50	1	Cdc37
CG7619	50	2	Proteasome 54kD subunit
CG3917	49	1	gamma-tubulin ring protein 84
CG10149	49	1	Proteasome p44.5 subunit
CG30147	49	1	Hillarin
CG8439	48	1	T-complex Chaperonin 5
CG10701	47	2	Moesin
CG1453	47	1	Klp10A
CG3689	47	1	CG3689
CG3751	45	1	Ribosomal protein S24
CG5450	42	1	Cytoplasmic dynein light chain 2
CG7611	42	1	CG7611
CG9853	42	1	CG9853
CG7546	40	2	CG7546
CG4042	40	1	CG4042
CG9769	40	1	CG9769
CG31739	39	1	Aspartyl-tRNA synthetase, mitochondrial
CG3416	38	1	Mov34
CG32164	38	1	CG32164
CG8309	37	2	Transport and Golgi organization 7
CG4260	36	1	Adaptor Protein complex 2, α subunit
CG9372	36	2	CG9372
CG17331	35	1	Proteasome β4 subunit
CG3074	35	1	Secreted Wg-interacting molecule
CG7107	34	2	upheld
CG5949	34	1	DNA-polymerase-δ
CG10540	34	1	capping protein alpha
CG4252	33	1	meiotic 41
CG10535	33	1	Elongator complex protein 1
CG5170	32	1	Dodeca-satellite-binding protein 1
CG4617	32	1	CG4617

CG2534	31	1	canoe
CG9155	31	1	Myosin 61F
CG5366	31	1	Cullin-associated and neddylation-dissociated 1
CG13284	31	1	CG13284
CG33694	31	1	CENP-ana
CG8194	30	1	Ribonuclease X25
CG6988	30	1	Protein disulfide isomerase
CG10975	30	1	Protein tyrosine phosphatase 69D
CG11929	30	2	CG11929
CG4003	30	1	pontin
CG30477	30	1	CG30477
CG1484	29	1	flightless I
CG5474	29	1	Signal sequence receptor β
CG5094	29	1	small glutamine-rich tetratricopeptide containing protein
CG31426	29	1	ligatin
CG7507	29	1	Dynein heavy chain 64C
CG7595	28	2	crinkled
CG7935	28	1	moleskin
CG13091	28	1	CG13091
CG10546	28	1	Cellular retinaldehyde binding protein
CG7837	28	1	CG7837
CG7439	28	1	Argonaute 2
CG1703	27	1	CG1703
CG3610	27	1	CG3610
CG14792	26	1	stubarista
CG30388	26	1	Magi
CG31149	26	1	CG31149
CG3431	25	1	Ubiquitin C-terminal hydrolase
CG16742	25	1	CG16742
CG2139	24	1	aralar1
CG8008	24	1	CG8008
CG3799	24	1	Ephexin

A.4 Act5-PrA-Asl purification from *Drosophila* cells

CG #	Score	#pep	Full name
CG6450	4816	186	lava lamp
CG16858	4302	176	viking
CG4145	3761	137	Collagen type IV
CG2919	2736	138	Asterless
CG6988	1327	47	Protein disulfide isomerase
CG4147	1247	50	Heat shock protein cognate 3
CG31022	1189	52	prolyl-4-hydroxylase-alpha EFB
CG3074	1040	56	Secreted Wg-interacting molecule
CG33957	772	29	cp309
CG2512	610	18	alpha-Tubulin at 84D
CG6199	597	26	procollagen lysyl hydroxylase
CG4264	581	25	Heat shock protein cognate 4
CG6944	540	23	Lamin
CG9282	322	7	Ribosomal protein L24
CG9277	291	21	beta-Tubulin at 56D
CG8014	259	8	Receptor mediated endocytosis 8
CG6631	229	11	anastral spindle 1
CG7808	189	3	Ribosomal protein S8
CG15792	182	5	zipper
CG8983	146	6	ERp60
CG3751	124	3	Ribosomal protein S24
CG10652	123	3	Ribosomal protein L30
CG17081	123	5	CG17081
CG4918	122	2	Ribosomal protein LP2
CG7622	121	3	Ribosomal protein L36
CG5726	116	3	CG5726
CG1821	111	2	Ribosomal protein L31
CG1883	110	5	Ribosomal protein S7
CG6253	108	2	Ribosomal protein L14
CG7490	105	4	Ribosomal protein LP0
CG12184	102	4	CG12184
CG17520	99	2	Casein kinase II alpha subunit
CG17286	97	3	spindle defective 2
CG8900	94	4	Ribosomal protein S18
CG2216	94	2	Ferritin 1 heavy chain homologue
CG8922	92	2	Ribosomal protein S5a
CG5920	90	1	string of pearls
CG3203	90	2	Ribosomal protein L17
CG4897	89	4	Ribosomal protein L7
CG2168	88	4	Ribosomal protein S3A
CG12101	82	2	Heat shock protein 60
CG14792	80	1	stubarista
CG3201	74	1	Myosin light chain cytoplasmic
CG7726	70	1	Ribosomal protein L11
CG1524	66	1	Ribosomal protein S14a
CG5718	65	3	Succinate dehydrogenase, subunit A (flavoprotein)-like
CG33102	64	2	Hex-t1
CG10732	60	2	combover
CG8507	60	1	CG8507
CG5502	57	2	Ribosomal protein L4
CG4087	57	1	Ribosomal protein LP1
CG3195	56	1	Ribosomal protein L12
CG16896	55	2	CG16896
CG32031	53	2	Arginine kinase
CG8280	53	2	Elongation factor 1alpha48D
CG2998	53	2	Ribosomal protein S28b
CG10061	52	1	lethal (3) s2214
CG11271	50	1	Ribosomal protein S12
CG5178	49	1	Actin 88F
CG8281	49	1	CG8281
CG7186	49	2	Plk4
CG5168	48	1	CG5168
CG3092	47	1	CG3092
CG17177	47	1	CG17177
CG5809	47	1	CaBP1
CG15207	46	1	CG15207
CG7603	46	1	QIL1
CG7434	45	1	Ribosomal protein L22
CG4744	45	1	CG4744
CG8200	45	1	flotillin
CG6019	44	1	mutagen-sensitive 308
CG33554	44	1	Nipped-A
CG10272	44	1	grappa
CG18076	44	1	short stop
CG6779	44	1	Ribosomal protein S3
CG3157	44	1	gamma-Tubulin at 23C
CG11276	43	1	Ribosomal protein S4
CG31195	43	1	CG31195
CG12010	43	1	CG12010
CG16833	42	1	CG16833
CG17836	42	1	CG17836
CG18102	42	1	shibire
CG31159	42	1	Elongation Factor G2
CG10423	42	1	Ribosomal protein S27
CG3314	42	1	Ribosomal protein L7A
CG8472	41	1	Calmodulin
CG33301	41	1	CG33301
CG12233	41	1	lethal (1) G0156
CG15844	40	1	Kinesin-like protein at 54D
CG4337	40	1	mitochondrial single stranded DNA-binding protein
CG8379	39	1	CG8379
CG8930	38	1	rickets
CG4078	38	1	CG4078
CG15442	37	1	Ribosomal protein L27A
CG3356	37	1	CG3356
CG41466	23	1	cp309
CG18625	0	1	CG18625
CG10107	0	1	veloren

A.5 Act5-Asl-PrA purification from *Drosophila* cells

CG #	Score	#pep	Full name
CG2919	10717	465	CG2919
CG16858	2421	82	viking
CG4145	1798	60	Collagen type IV
CG6450	1099	39	lava lamp
CG17498	875	26	mad2
CG33957	798	24	cp309
CG9277	769	43	beta-Tubulin at 56D
CG4264	736	33	Heat shock protein cognate 4
CG6631	628	26	anastral spindle 1
CG4147	597	19	Heat shock protein cognate 3
CG2512	555	19	alpha-Tubulin at 84D
CG31022	462	9	prolyl-4-hydroxylase-alpha EFB
CG3401	394	25	beta-Tubulin at 60D
CG3074	300	11	Secreted Wg-interacting molecule
CG7186	224	9	Plk4
CG6944	178	6	Lamin
CG17081	174	6	Cep135
CG6988	144	5	Protein disulfide isomerase
CG5062	125	6	CG5062
CG6199	124	3	procollagen lysyl hydroxylase
CG2960	122	4	Ribosomal protein L40
CG13800	111	3	CG13800
CG10346	108	5	Grip71

CG5718	104	7	Succinate dehydrogenase, subunit A (flavoprotein)-like
CG17286	87	4	spindle defective 2
CG9795	83	2	CG9795
CG9900	78	2	mitotic 15
CG8280	77	3	Elongation factor 1alpha48D
CG4918	74	1	Ribosomal protein LP2
CG8962	73	4	Platelet-activating factor acetylhydrolase alpha
CG10061	71	1	lethal (3) s2214
CG3203	69	1	Ribosomal protein L17
CG8983	68	2	ERp60
CG15792	66	2	zipper
CG31012	64	1	CIN85 and CD2AP orthologue
CG4744	63	3	CG4744
CG10652	61	2	Ribosomal protein L30
CG7808	60	1	Ribosomal protein S8
CG9699	60	2	Septin 4
CG4897	58	2	Ribosomal protein L7
CG33554	56	1	Nipped-A
CG11522	54	1	Ribosomal protein L6
CG9282	53	1	Ribosomal protein L24
CG33555	53	1	bitesize
CG1683	52	2	Adenine nucleotide translocase 2
CG17520	49	2	Casein kinase II alpha subunit
CG8605	48	1	RINT1 ortholog
CG6785	47	1	CG6785
CG7603	47	1	QIL1
CG40500	47	2	CG40500
CG12129	47	1	CG12129
CG31045	46	1	Myosin heavy chain-like
CG9924	46	1	roadkill
CG12753	46	1	endosomal maturation defective
CG16896	46	1	CG16896
CG31374	45	1	sarcomere length short
CG15828	45	1	Apolipoprotein lipid transfer particle
CG11999	45	1	CG11999
CG1104	44	1	CG1104
CG13359	44	1	CG13359
CG6692	43	1	Cysteine proteinase-1
CG11282	43	1	capricious
CG14025	42	1	Blastoderm-specific gene 25D
CG8900	42	1	Ribosomal protein S18
CG17927	41	1	Myosin heavy chain
CG3902	41	1	CG3902
CG18255	41	1	Stretchin-Mlck
CG6667	40	1	dorsal
CG32031	40	1	Arginine kinase
CG17839	40	1	CG17839
CG4585	40	1	CG4585
CG18572	31	1	rudimentary
CG2762	0	1	u-shaped
CG13772	0	1	neuroligin

A.6 Act5-Asl (531-994aa)-PrA purification from *Drosophila* cells

CG #	**Score**	**#pep**	**Full name**
CG2919	3340	152	Asterless
CG9277	1964	72	beta-Tubulin at 56D
CG4264	1333	47	Heat shock protein cognate 4
CG3401	1075	46	beta-Tubulin at 60D
CG33957	1057	29	cp309
CG2512	942	34	alpha-Tubulin at 84D
CG17286	616	23	spindle defective 2
CG4147	437	16	Heat shock protein cognate 3
CG7808	361	7	Ribosomal protein S8
CG17498	306	8	mad2
CG5436	272	11	Heat shock protein 68
CG6631	248	11	anastral spindle 1
CG4832	237	7	centrosomin
CG7490	230	9	Ribosomal protein LP0
CG10732	217	5	combover
CG6253	197	4	Ribosomal protein L14
CG8947	193	4	26-29kD-proteinase
CG10652	189	3	Ribosomal protein L30
CG13800	189	5	CG13800
CG3195	187	5	Ribosomal protein L12
CG8280	183	7	Elongation factor 1alpha48D
CG7622	179	4	Ribosomal protein L36
CG7977	170	6	Ribosomal protein L23A
CG17081	165	3	CG17081
CG14206	163	4	Ribosomal protein S10b
CG5502	163	7	Ribosomal protein L4
CG6779	155	4	Ribosomal protein S3
CG3751	155	4	Ribosomal protein S24
CG4918	150	2	Ribosomal protein LP2
CG9282	149	2	Ribosomal protein L24
CG31022	145	4	prolyl-4-hydroxylase-alpha EFB
CG1821	142	3	Ribosomal protein L31
CG10944	137	4	Ribosomal protein S6
CG1548	132	2	cathD
CG6453	128	4	Glucosidase 2 β subunit
CG7111	126	5	Receptor of activated protein kinase C 1
CG1883	124	3	Ribosomal protein S7
CG3661	123	4	Ribosomal protein L23
CG8900	123	4	Ribosomal protein S18
CG14792	121	3	stubarista
CG8615	120	2	Ribosomal protein L18
CG3157	118	3	gamma-Tubulin at 23C
CG4863	117	4	Ribosomal protein L3
CG2960	116	4	Ribosomal protein L40
CG4087	111	3	Ribosomal protein LP1
CG2168	108	2	Ribosomal protein S3A
CG6692	102	2	Cysteine proteinase-1
CG11271	101	2	Ribosomal protein S12
CG7939	101	2	Ribosomal protein L32
CG16858	100	2	viking
CG1263	100	2	Ribosomal protein L8
CG7283	94	2	Ribosomal protein L10Ab
CG12163	94	2	CG12163
CG1524	94	3	Ribosomal protein S14a
CG2216	93	1	Ferritin 1 heavy chain homologue
CG7726	92	1	Ribosomal protein L11
CG7014	92	1	Ribosomal protein S5b
CG1489	91	2	Pros45
CG5119	80	2	polyA-binding protein
CG2746	77	2	Ribosomal protein L19
CG9795	76	2	CG9795
CG16944	76	2	stress-sensitive B
CG16896	75	2	CG16896
CG6510	74	2	Ribosomal protein L18A
CG5289	72	1	Proteasome 26S subunit subunit 4 ATPase
CG11579	71	1	armadillo
CG17489	69	1	Ribosomal protein L5
CG4897	69	3	Ribosomal protein L7
CG2998	68	2	Ribosomal protein S28b
CG3314	67	2	Ribosomal protein L7A
CG32031	67	4	Arginine kinase
CG12184	64	2	CG12184
CG7434	64	2	Ribosomal protein L22
CG6846	63	1	Ribosomal protein L26
CG2411	63	2	patched
CG8415	62	1	Ribosomal protein S23
CG10305	61	1	Ribosomal protein S26
CG3074	60	2	Secreted Wg-interacting molecule
CG17520	60	1	Casein kinase II alpha subunit
CG2772	59	2	CG2772
CG32626	58	1	AMP deaminase
CG15697	57	1	Ribosomal protein S30
CG4525	52	1	CG4525
CG8472	52	2	Calmodulin
CG1633	51	1	thioredoxin peroxidase 1
CG12385	50	1	thetaTrypsin
CG8857	50	1	Ribosomal protein S11
CG4651	50	2	Ribosomal protein L13
CG2033	50	1	Ribosomal protein S15Aa
CG6141	49	1	Ribosomal protein L9
CG18001	49	2	Ribosomal protein L38
CG9117	49	1	CG9117
CG31915	49	1	CG31915
CG11963	48	1	skpA associated protein
CG8055	47	1	shrub
CG5920	47	1	string of pearls
CG11276	47	1	Ribosomal protein S4
CG5467	46	1	scribbled
CG10061	46	1	lethal (3) s2214
CG12233	46	1	lethal (1) G0156
CG13389	46	1	Ribosomal protein S13
CG6303	45	1	Bruce
CG3429	45	1	swallow
CG15442	44	1	Ribosomal protein L27A
CG3033	44	1	Glycosylphosphatidylinositol anchor attachment 1 ortholo
CG15548	44	1	CG15548
CG12775	44	1	Ribosomal protein L21
CG5462	44	1	scribbled
CG14304	44	1	CG14304
CG33555	44	1	bitesize
CG2928	43	1	Rhythmically expressed gene 5
CG6383	43	1	crumbs
CG8815	42	1	Sin3A
CG40500	42	1	CG40500
CG9761	42	1	Neprilysin 2
CG4399	41	1	enhanced adult sensory threshold
CG2508	41	1	cdc23
CG1695	41	1	CG1695
CG3395	41	1	Ribosomal protein S9
CG31045	41	1	Myosin heavy chain-like

CG6355	40	1	CG6355
CG6684	40	1	Ribosomal protein S25
CG10967	40	1	Autophagy-specific gene 1
CG13762	39	1	brivido-3

A.7 pMT-Ana2-PrA +MG132 purification from *Drosophila* cells

CG #	Score	#pep	Full name
CG15792	6625	131	zipper
CG8262	4562	80	anastral spindle 2
CG4264	3244	61	Heat shock protein cognate 4
CG4027	1900	54	Actin 5C
CG10067	1487	47	Actin 57B
CG9277	1339	33	β-Tubulin at 56D
CG3201	883	14	Myosin light chain cytoplasmic
CG1913	701	19	α-Tubulin at 84B
CG18743	657	14	Heat-shock-protein-70Ab
CG4147	637	24	Heat shock protein cognate 3
CG5834	631	14	Hsp70Bbb
CG5450	543	11	Cytoplasmic dynein light chain 2
CG3401	524	18	β-Tubulin at 60D
CG3595	523	12	spaghetti squash
CG8937	472	11	Heat shock protein cognate 1
CG5436	412	9	Heat shock protein 68
CG12101	409	7	Heat shock protein 60
CG4463	397	10	Heat shock protein 23
CG10641	282	6	Swiprosin-1
CG8472	267	7	Calmodulin
CG8280	265	9	Elongation factor 1α48D
CG4183	173	3	Heat shock protein 26
CG7438	173	3	Myosin 31DF
CG31618	146	2	His2A:CG31618
CG9086	140	6	Ubr1 ubiquitin ligase
CG10465	137	5	CG10465
CG1106	124	4	Gelsolin
CG14637	120	3	abstrakt
CG4145	111	4	Collagen type IV
CG12750	109	3	nucampholin
CG4898	108	3	Tropomyosin 1
CG9940	108	3	CG9940
CG17158	105	3	capping protein beta
CG31022	104	3	prolyl-4-hydroxylase-alpha EFB
CG10540	101	3	capping protein alpha
CG4087	93	2	Ribosomal protein LP1
CG5499	89	1	Histone H2A variant
CG6988	89	2	Protein disulfide isomerase
CG5934	86	1	CG5934
CG7283	81	1	Ribosomal protein L10Ab
CG8947	78	1	26-29kD-proteinase
CG9282	77	1	Ribosomal protein L24
CG11999	77	1	CG11999
CG8542	74	3	Heat shock protein cognate 5
CG2146	74	4	dilute class unconventional myosin
CG5695	72	2	jaguar
CG6341	66	1	Elongation factor 1 β
CG1548	63	1	cathD
CG9684	62	3	CG9684
CG31712	61	3	CG31712
CG11276	60	1	Ribosomal protein S4
CG6253	60	1	Ribosomal protein L14
CG1826	60	4	BTB (POZ) domain containing 9 ortholog
CG18572	54	1	rudimentary
CG2960	54	1	Ribosomal protein L40
CG9581	54	1	CG9581
CG1516	47	1	Pyruvate carboxylase
CG7808	44	1	Ribosomal protein S8
CG7791	43	1	CG7791
CG10663	43	3	CG10663
CG7144	42	2	lysine ketoglutarate reductase
CG18174	42	1	Rpn11
CG12233	41	1	lethal (1) G0156
CG10546	41	1	Cellular retinaldehyde binding protein
CG10944	41	2	Ribosomal protein S6
CG3612	40	1	bellwether
CG7985	39	1	CG7985
CG6509	39	2	Discs large 5
CG7490	37	1	Ribosomal protein LP0
CG7581	37	2	Bub3
CG5119	35	1	polyA-binding protein
CG7003	34	2	Msh6
CG10370	32	1	Tat-binding protein-1
CG1633	32	1	thioredoxin peroxidase 1
CG8978	31	1	Suppressor of profilin 2
CG9155	31	2	Myosin 61F
CG17209	31	1	CG17209
CG14996	31	1	Chd64
CG3996	30	2	CG3996
CG1539	30	1	tropomodulin
CG2168	29	1	Ribosomal protein S3A
CG1683	29	2	Adenine nucleotide translocase 2
CG6428	29	1	CG6428
CG8578	29	1	CG8578
CG5502	28	1	Ribosomal protein L4
CG10377	28	1	Heterogeneous nuclear ribonucleoprotein at 27C
CG14040	28	1	senju
CG3074	28	1	Secreted Wg-interacting molecule
CG3382	28	1	Organic anion transporting polypeptide 58Db
CG7434	27	1	Ribosomal protein L22
CG8427	27	1	Small ribonucleoprotein particle protein SmD3
CG7961	26	1	Coat Protein (coatomer) α
CG11522	26	1	Ribosomal protein L6
CG7595	25	1	crinkled
CG10071	25	1	Ribosomal protein L29
CG1484	24	1	flightless I
CG2692	24	1	gooseberry-neuro
CG10061	24	1	Sas-4
CG1403	24	1	Septin-1
CG2941	24	1	CG2941
CG10353	24	1	CG10353
CG1810	24	1	mRNA-capping-enzyme
CG9777	24	1	CG9777
CG7219	24	1	Serpin 28D
CG3711	24	1	CG3711
CG17949	24	1	His2B:CG17949
CG3836	23	1	stonewall
CG16853	23	1	CG16853
CG2767	23	1	CG2767
CG13609	23	1	CG13609
CG5432	23	1	CG5432
CG3751	23	1	Ribosomal protein S24
CG10851	22	1	B52
CG4063	22	1	ebi
CG5214	22	1	CG5214
CG18408	21	1	CAP
CG7999	21	1	Mediator complex subunit 24
CG32365	20	1	CG32365
CG11274	18	1	SRm160
CG10986	17	1	garnet

A.8 pMT-Ana2-PrA +OA +MG132 purification from *Drosophila* cells

CG #	Score	#pep	Full name
CG8262	11127	177	anastral spindle 2
CG4264	4392	98	Heat shock protein cognate 4
CG9277	1234	32	β-Tubulin at 56D
CG18743	1106	23	Heat-shock-protein-70Ab
CG6998	1065	22	cut up
CG5834	1043	21	Hsp70Bbb
CG3401	945	28	β-Tubulin at 60D
CG4147	789	21	Heat shock protein cognate 3
CG5436	781	15	Heat shock protein 68
CG1913	724	20	α-Tubulin at 84B
CG12051	681	22	Actin 42A
CG4027	678	22	Actin 5C
CG10465	599	18	CG10465
CG15792	461	13	zipper
CG10067	434	16	Actin 57B
CG8280	373	10	Elongation factor 1α48D
CG3201	364	8	Myosin light chain cytoplasmic
CG14996	274	7	Chd64
CG12101	248	4	Heat shock protein 60
CG4463	243	5	Heat shock protein 23
CG6988	239	7	Protein disulfide isomerase
CG31022	234	6	prolyl-4-hydroxylase-alpha EFB
CG31618	210	2	His2A:CG31618
CG4183	181	3	Heat shock protein 26
CG1548	179	4	cathD
CG10377	149	2	Heterogeneous nuclear ribonucleoprotein at 27C
CG14637	133	4	abstrakt
CG18572	129	4	rudimentary
CG1826	128	5	BTB (POZ) domain containing 9 ortholog

CG2960	113	3	Ribosomal protein L40
CG3937	103	2	cheerio
CG9086	87	3	Ubr1 ubiquitin ligase
CG6521	86	1	Signal transducing adaptor molecule
CG17498	85	1	mad2
CG10938	83	2	Proteasome α5 subunit
CG11143	76	3	Inos
CG5499	74	1	Histone H2A variant
CG12750	73	1	nucampholin
CG3265	69	1	Eb1
CG2050	67	1	modulo
CG5170	67	2	Dodeca-satellite-binding protein 1
CG9940	65	2	CG9940
CG1528	64	2	Coat Protein (coatomer) γ
CG31712	63	3	CG31712
CG4466	62	2	Heat shock protein 27
CG3595	60	1	spaghetti squash
CG11274	58	2	SRm160
CG9748	55	3	belle
CG9124	53	1	Eukaryotic initiation factor 3 p40 subunit
CG10191	53	2	Proteome of centrioles 1
CG8947	53	1	26-29kD-proteinase
CG17291	52	1	Protein phosphatase 2A at 29B
CG4145	51	1	Collagen type IV
CG8542	51	2	Heat shock protein cognate 5
CG1977	50	1	α Spectrin
CG9684	49	2	CG9684
CG7985	44	1	CG7985
CG5174	44	1	CG5174
CG1516	43	1	Pyruvate carboxylase
CG10546	41	1	Cellular retinaldehyde binding protein
CG10753	39	1	Small ribonucleoprotein particle protein SmD1
CG11276	38	1	Ribosomal protein S4
CG7961	38	2	Coat Protein (coatomer) α
CG10230	38	1	Rpn9
CG4904	37	1	Proteasome 35kD subunit
CG6223	37	1	Coat Protein (coatomer) β
CG6453	37	1	Glucosidase 2 β subunit
CG10663	37	2	CG10663
CG18811	37	1	Caprin
CG1683	36	3	Adenine nucleotide translocase 2
CG4087	35	1	Ribosomal protein LP1
CG6509	35	1	Discs large 5
CG10851	34	2	B52
CG6773	32	1	sec13
CG7581	32	1	Bub3
CG1341	32	1	Rpt1
CG6692	31	1	Cysteine proteinase-1
CG3379	31	1	Histone H4 replacement
CG17768	31	1	CG17768
CG1973	30	1	yata
CG1519	29	1	Proteasome α7 subunit
CG6428	29	1	CG6428
CG17209	29	1	CG17209
CG1633	29	1	thioredoxin peroxidase 1
CG7595	28	1	crinkled
CG6699	28	1	Coat Protein (coatomer) β'
CG17949	28	1	His2B:CG17949
CG2168	27	1	Ribosomal protein S3A
CG4898	26	1	Tropomyosin 1
CG17870	26	1	14-3-3ζ
CG11198	26	1	Acetyl-CoA carboxylase
CG13609	26	1	CG13609
CG9750	26	1	reptin
CG3711	26	1	CG3711
CG4063	25	1	ebi
CG1591	25	1	REG
CG2692	24	1	gooseberry-neuro
CG7144	24	1	lysine ketoglutarate reductase
CG14040	24	1	senju
CG7219	24	2	Serpin 28D
CG9934	24	1	CG9934
CG8857	24	1	Ribosomal protein S11
CG11963	24	1	skpA associated protein
CG34130	24	2	CG34130
CG6631	24	1	anastral spindle 1
CG5825	23	1	Histone H3.3A
CG2488	23	1	(6-4)-photolyase
CG6230	23	1	CG6230
CG31370	23	1	CG31370
CG6850	22	1	UDP-glucose-glycoprotein glucosyltransferase
CG18408	22	1	CAP
CG5195	22	1	artichoke
CG5406	22	1	still life
CG6944	21	1	Lamin
CG9581	21	1	CG9581
CG7434	20	1	Ribosomal protein L22
CG5708	20	2	CG5708
CG13345	20	1	RacGAP50C
CG9888	19	1	Fibrillarin
CG3836	19	1	stonewall
CG9191	19	1	Kinesin-like protein at 61F
CG8427	19	1	Small ribonucleoprotein particle protein SmD3
CG10712	19	1	Chromator
CG10986	18	1	garnet
CG10333	18	1	CG10333
CG6781	18	1	sepia
CG3382	17	1	Organic anion transporting polypeptide 58Db

A.9 pAct5-PrA-Ana2 + pMT-Plk4 +OA

CG #	Score	#pep	Full name
CG8262	7098	138	anastral spindle 2
CG15792	1987	42	zipper
CG4027	1342	39	Actin 5C
CG4264	896	21	Heat shock protein cognate 4
CG10686	846	16	trailer hitch
CG5450	662	22	Cytoplasmic dynein light chain 2
CG8280	512	15	Elongation factor 1α48D
CG11183	444	11	Decapping protein 1
CG4147	430	8	Heat shock protein cognate 3
CG5436	345	8	Heat shock protein 68
CG4063	340	9	ebi
CG5834	338	8	Hsp70Bbb
CG3201	287	5	Myosin light chain cytoplasmic
CG3595	169	6	spaghetti squash
CG9277	136	4	β-Tubulin at 56D
CG4013	130	2	Smrter
CG17002	116	3	CG17002
CG6995	115	1	Scaffold attachment factor B
CG4087	93	1	Ribosomal protein LP1
CG16858	92	1	viking
CG31022	89	1	prolyl-4-hydroxylase-alpha EFB
CG11901	78	2	Ef1γ
CG4145	74	2	Collagen type IV
CG9412	72	1	rasputin
CG1913	69	1	α-Tubulin at 84B
CG10984	69	1	CG10984
CG3195	58	1	Ribosomal protein L12
CG14648	56	1	growl
CG7434	54	1	Ribosomal protein L22
CG3922	51	1	Ribosomal protein S17
CG3821	49	1	Aspartyl-tRNA synthetase
CG1524	49	1	Ribosomal protein S14a
CG2746	47	1	Ribosomal protein L19
CG14206	47	1	Ribosomal protein S10b
CG30084	47	1	Z band alternatively spliced PDZ-motif protein 52
CG3937	44	1	cheerio
CG3661	43	1	Ribosomal protein L23
CG7622	41	1	Ribosomal protein L36
CG12306	41	1	polo
CG3314	41	1	Ribosomal protein L7A
CG17489	41	1	Ribosomal protein L5
CG17158	38	1	capping protein beta
CG4046	38	1	Ribosomal protein S16
CG2098	37	1	ferrochelatase
CG10576	37	1	CG10576
CG7985	36	1	CG7985
CG11276	35	1	Ribosomal protein S4
CG6253	35	1	Ribosomal protein L14
CG10161	34	1	Eukaryotic initiation factor 3 p66 subunit
CG5920	33	1	Ribosomal protein S2
CG6684	33	1	Ribosomal protein S25
CG7186	32	1	Plk4
CG6509	32	1	Discs large 5
CG7878	32	1	CG7878
CG9155	31	1	Myosin 61F
CG8274	31	1	Megator
CG6148	31	1	Putative Achaete Scute Target 1

A.10 pMT-Sas4-PrA +MG132 purification from *Drosophila* cells

CG #	Score	#pep	Full name
CG10061	39977	1290	Sas-4
CG9277	10982	296	β-Tubulin at 56D
CG4264	7674	292	Heat shock protein cognate 4
CG3401	4606	106	β-Tubulin at 60D
CG4463	3894	120	Heat shock protein 23
CG1913	3136	74	α-Tubulin at 84B
CG4164	1861	61	CG4164
CG5436	1437	35	Heat shock protein 68
CG18743	1427	47	Heat-shock-protein-70Ab
CG5502	1228	32	Ribosomal protein L4
CG5834	1199	36	Hsp70Bbb
CG9748	1084	30	belle
CG11999	995	35	CG11999
CG4147	982	33	Heat shock protein cognate 3
CG4183	863	29	Heat shock protein 26
CG8478	713	22	CG8478
CG12233	676	22	lethal (1) G0156
CG6815	566	14	belphegor
CG8280	562	22	Elongation factor 1α48D
CG7831	516	12	non-claret disjunctional
CG11451	492	15	Spc105-related
CG1883	490	15	Ribosomal protein S7
CG4027	464	14	Actin 5C
CG7478	439	13	Actin 79B
CG3981	378	9	Unc-76
CG31618	321	7	His2A:CG31618
CG3203	306	8	Ribosomal protein L17
CG4466	298	6	Heat shock protein 27
CG7915	297	11	Ect4
CG14207	296	7	HspB8
CG7439	294	11	Argonaute 2
CG5119	290	12	polyA-binding protein
CG8900	283	6	Ribosomal protein S18
CG31012	260	9	CIN85 and CD2AP orthologue
CG1427	257	7	CG1427
CG5654	250	6	ypsilon schachtel
CG5028	249	8	CG5028
CG5330	248	5	Nucleosome assembly protein 1
CG6143	247	3	Protein on ecdysone puffs
CG4897	246	12	Ribosomal protein L7
CG31022	240	5	prolyl-4-hydroxylase-alpha EFB
CG7863	239	8	dream
CG16858	233	4	viking
CG14648	232	8	growl
CG10811	227	4	eukaryotic translation initiation factor 4G
CG4087	219	7	Ribosomal protein LP1
CG14792	219	5	stubarista
CG4460	218	5	Heat shock protein 22
CG5174	213	6	CG5174
CG10578	212	10	DnaJ-like-1
CG6779	202	8	Ribosomal protein S3
CG8332	202	6	Ribosomal protein S15
CG7323	201	3	CG7323
CG1489	199	3	Pros45
CG1242	197	7	Heat shock protein 83
CG9281	195	8	CG9281
CG15784	191	3	CG15784
CG7808	177	3	Ribosomal protein S8
CG10230	176	4	Rpn9
CG16973	168	3	misshapen
CG2168	167	5	Ribosomal protein S3A
CG14206	167	6	Ribosomal protein S10b
CG3612	166	5	bellwether
CG11522	164	3	Ribosomal protein L6
CG11276	161	7	Ribosomal protein S4
CG3455	157	3	Rpt4
CG9188	145	3	septin interacting protein 2
CG8947	144	4	26-29kD-proteinase
CG3201	141	5	Myosin light chain cytoplasmic
CG4145	140	4	Collagen type IV
CG3379	140	5	Histone H4 replacement
CG2746	135	1	Ribosomal protein L19
CG16944	131	5	stress-sensitive B
CG12775	131	7	Ribosomal protein L21
CG9282	130	2	Ribosomal protein L24
CG3922	129	3	Ribosomal protein S17
CG32626	129	2	AMP deaminase
CG7977	128	5	Ribosomal protein L23A
CG8922	127	2	Ribosomal protein S5a
CG9325	127	3	hu li tai shao
CG3395	123	6	Ribosomal protein S9
CG4464	122	5	Ribosomal protein S19a
CG3422	121	3	Proteasome 28kD subunit 1
CG7283	120	3	Ribosomal protein L10Ab
CG16916	118	2	Rpt3
CG5499	116	2	Histone H2A variant
CG1548	116	2	cathD
CG12262	116	4	CG12262
CG2216	115	2	Ferritin 1 heavy chain homologue
CG7490	111	4	Ribosomal protein LP0
CG4157	110	2	Rpn12
CG5920	109	3	string of pearls
CG15442	106	5	Ribosomal protein L27A
CG1683	106	3	Adenine nucleotide translocase 2
CG5353	106	2	Threonyl-tRNA synthetase
CG6439	106	2	CG6439
CG7622	105	2	Ribosomal protein L36
CG5374	103	2	Tcp1-like
CG8355	102	3	slit
CG1341	100	3	Rpt1
CG2960	98	4	Ribosomal protein L40
CG2998	98	2	Ribosomal protein S28b
CG15792	97	3	zipper
CG10652	97	3	Ribosomal protein L30
CG15697	94	3	Ribosomal protein S30
CG1524	93	2	Ribosomal protein S14a
CG3024	92	3	torp4a
CG7726	91	2	Ribosomal protein L11
CG6181	91	2	Ge-1
CG8615	89	2	Ribosomal protein L18
CG10305	89	1	Ribosomal protein S26
CG10944	88	2	Ribosomal protein S6
CG7961	87	2	Coat Protein (coatomer) α
CG31045	86	3	Myosin heavy chain-like
CG2098	84	2	ferrochelatase
CG6095	84	2	exo84
CG4581	83	1	Thiolase
CG11870	80	1	CG11870
CG10753	80	1	Small ribonucleoprotein particle protein SmD1
CG6875	79	2	abnormal spindle
CG9327	79	3	Proteasome 29kD subunit
CG4389	78	2	Mitochondrial trifunctional protein α subunit
CG5474	76	2	Signal sequence receptor β
CG4651	76	4	Ribosomal protein L13
CG6253	75	2	Ribosomal protein L14
CG18174	75	2	Rpn11
CG1453	74	1	Klp10A
CG4454	74	3	borealin-related
CG17528	74	3	CG17528
CG7434	73	3	Ribosomal protein L22
CG2078	73	2	Myd88
CG7945	73	2	CG7945
CG11734	72	1	HERC2
CG17949	72	2	His2B:CG17949
CG10360	70	1	refractory to sigma P
CG6459	70	1	CG6459
CG1092	70	1	CG1092
CG5934	70	1	CG5934
CG3314	69	2	Ribosomal protein L7A
CG9124	69	1	Eukaryotic initiation factor 3 p40 subunit
CG11888	69	3	Rpn2
CG31764	69	2	virus-induced RNA 1
CG13389	68	3	Ribosomal protein S13
CG11271	68	2	Ribosomal protein S12
CG18495	67	3	Proteasome α1 subunit
CG7518	67	1	CG7518
CG9946	67	1	eukaryotic translation Initiation Factor 2α
CG3157	66	2	γ-Tubulin at 23C
CG3195	66	2	Ribosomal protein L12
CG17291	66	1	Protein phosphatase 2A at 29B
CG11963	65	1	skpA associated protein
CG4046	63	3	Ribosomal protein S16
CG6692	62	2	Cysteine proteinase-1
CG8282	62	1	Snx6
CG4863	61	1	Ribosomal protein L3
CG5094	61	1	small glutamine-rich tetratricopeptide containing protein
CG2033	60	1	Ribosomal protein S15Aa
CG15087	60	1	Vacuolar protein sorting 51
CG1569	59	2	rough deal
CG7111	59	2	Receptor of activated protein kinase C 1
CG6701	59	1	CG6701
CG14066	59	1	La related protein
CG2028	58	1	Casein kinase Iα
CG7935	58	1	moleskin
CG12264	58	2	CG12264
CG8258	57	1	CG8258
CG6699	56	1	Coat Protein (coatomer) β'
CG31617	56	2	His1:CG31617
CG9940	55	2	CG9940
CG5726	55	1	CG5726
CG4274	54	1	fizzy
CG7762	54	2	Rpn1
CG33162	53	1	Signal recognition particle receptor β
CG14482	53	1	Ubiquinol-cytochrome c reductase 6.4 kDa subunit
CG10938	52	2	Proteasome α5 subunit
CG6378	52	2	BM-40-SPARC
CG10484	51	3	Regulatory particle non-ATPase 3
CG17521	51	1	Qm
CG5378	51	2	Rpn7

CG4097	50	1	Proteasome 26kD subunit
CG1345	49	1	Glutamine:fructose-6-phosphate aminotransferase 2
CG13849	47	1	Nop56
CG9888	46	2	Fibrillarin
CG15224	45	1	Casein kinase II β subunit
CG3008	45	1	CG3008
CG7185	45	1	CG7185
CG5266	45	1	Proteasome 25kD subunit
CG3595	44	1	spaghetti squash
CG14472	44	1	purity of essence
CG1100	44	1	Rpn5
CG4320	44	1	raptor
CG13349	44	2	Regulatory particle non-ATPase 13
CG7546	44	2	CG7546
CG33106	44	1	multiple ankyrin repeats single KH domain
CG8055	44	1	shrub
CG10315	43	1	eIF2B-δ
CG7595	41	3	crinkled
CG3210	41	1	Dynamin related protein 1
CG9938	41	1	Ndc80
CG8415	41	1	Ribosomal protein S23
CG32223	41	1	CG32223
CG33715	41	2	Muscle-specific protein 300
CG6684	40	1	Ribosomal protein S25
CG5004	40	1	CG5004
CG14469	39	2	dpr12
CG31009	39	2	Cad99C
CG5170	38	2	Dodeca-satellite-binding protein 1
CG8857	38	2	Ribosomal protein S11
CG9795	38	3	CG9795
CG9775	38	1	CG9775
CG11881	38	1	dim γ-tubulin 6
CG2711	37	3	deformed wings
CG5319	37	1	lute
CG6223	36	1	Coat Protein (coatomer) β
CG1403	36	1	Septin-1
CG6141	36	1	Ribosomal protein L9
CG5316	36	1	CG5316
CG8994	35	1	exuperantia
CG12101	35	1	Heat shock protein 60
CG17286	35	1	spindle defective 2
CG12740	35	1	Ribosomal protein L28
CG3647	34	1	shuttle craft
CG1559	34	1	Upf1
CG7637	34	1	CG7637
CG6090	34	1	Ribosomal protein L34a
CG7939	33	1	Ribosomal protein L32
CG17870	33	1	14-3-3ζ
CG1657	33	1	CG1657
CG11838	33	1	Oseg3
CG6509	33	1	Discs large 5
CG2213	33	1	mitotic spindle density 5
CG1483	32	1	Microtubule-associated protein 205
CG6510	32	2	Ribosomal protein L18A
CG12245	32	1	glial cells missing
CG1591	32	1	REG
CG10663	32	1	CG10663
CG17320	31	1	Sterol carrier protein X-related thiolase
CG10269	31	1	D19A
CG3126	31	1	C3G
CG7758	31	2	pumpless
CG14446	31	1	CG14446
CG18102	30	1	shibire
CG1101	30	1	Aly
CG10379	30	1	myoblast city
CG6428	30	1	CG6428
CG13126	30	1	CG13126
CG5450	29	1	Cytoplasmic dynein light chain 2
CG1528	29	1	Coat Protein (coatomer) γ
CG6450	29	1	lava lamp
CG31426	29	1	ligatin
CG30477	29	1	CG30477
CG32191	29	1	CG32191
CG5825	28	1	Histone H3.3A
CG14816	28	1	Phosphoglycerate mutase 5
CG10370	28	1	Tat-binding protein-1
CG2253	28	1	Upf2
CG7041	28	1	HP1b
CG1691	28	1	IGF-II mRNA-binding protein
CG9091	28	1	Ribosomal protein L37a
CG3996	28	1	CG3996
CG9999	27	1	Ran GTPase activating protein
CG4297	27	1	CG4297
CG5604	27	1	CG5604
CG6116	27	1	UV-resistance associated gene
CG6042	27	1	Cyp12a4
CG10161	27	1	Eukaryotic initiation factor 3 p66 subunit
CG31792	27	1	CG31792
CG1666	26	1	Helicase
CG8571	26	1	smallminded
CG3751	26	1	Ribosomal protein S24
CG3051	25	1	SNF1A/AMP-activated protein kinase
CG6842	25	1	Vacuolar protein sorting 4
CG15255	25	1	CG15255
CG33131	25	1	SCAP

A.11 pMT-Sas4-PrA +OA +MG132 purification from *Drosophila* cells

CG #	Score	#pep	Full name
CG10061	24851	848	Sas-4
CG4264	10717	273	Heat shock protein cognate 4
CG9277	5948	176	β-Tubulin at 56D
CG1913	4682	123	α-Tubulin at 84B
CG15792	4332	95	zipper
CG4164	4043	90	CG4164
CG4183	3586	93	Heat shock protein 26
CG4463	3552	95	Heat shock protein 23
CG18743	1959	50	Heat-shock-protein-70Ab
CG5834	1901	48	Hsp70Bbb
CG5436	1767	42	Heat shock protein 68
CG3401	1704	38	β-Tubulin at 60D
CG4147	1558	39	Heat shock protein cognate 3
CG12233	1308	30	lethal (1) G0156
CG4869	1261	26	β-Tubulin at 97EF
CG10732	949	26	combover
CG10811	905	17	eukaryotic translation initiation factor 4G
CG8280	874	31	Elongation factor 1α48D
CG4027	871	27	Actin 5C
CG4466	732	23	Heat shock protein 27
CG11999	652	13	CG11999
CG9748	649	16	belle
CG10067	613	21	Actin 57B
CG2684	551	15	lodestar
CG6815	527	11	belphegor
CG3201	516	11	Myosin light chain cytoplasmic
CG17870	516	10	14-3-3ζ
CG17870	498	10	14-3-3ζ
CG7915	490	14	Ect4
CG31196	485	10	14-3-3ε
CG6450	460	11	lava lamp
CG3595	443	10	spaghetti squash
CG7439	410	13	Argonaute 2
CG14207	405	10	HspB8
CG7863	405	11	dream
CG8014	396	9	Receptor mediated endocytosis 8
CG31022	376	10	prolyl-4-hydroxylase-alpha EFB
CG4460	354	10	Heat shock protein 22
CG5353	354	9	Threonyl-tRNA synthetase
CG10578	353	13	DnaJ-like-1
CG1528	341	7	Coat Protein (coatomer) γ
CG8571	337	5	smallminded
CG16858	329	7	viking
CG1242	323	7	Heat shock protein 83
CG8863	312	10	DnaJ-like-2
CG5092	308	7	Target of rapamycin
CG1569	302	6	rough deal
CG8478	297	8	CG8478
CG2216	295	7	Ferritin 1 heavy chain homologue
CG5028	294	7	CG5028
CG3024	293	9	torp4a
CG10230	290	6	Rpn9
CG16944	289	7	stress-sensitive B
CG8947	287	7	26-29kD-proteinase
CG4260	285	6	Adaptor Protein complex 2, α subunit
CG9325	283	7	hu li tai shao
CG12306	281	9	polo
CG11963	281	5	skpA associated protein
CG1548	271	5	cathD
CG6223	267	7	Coat Protein (coatomer) β
CG16916	259	4	Rpt3
CG5330	235	4	Nucleosome assembly protein 1
CG7865	234	6	PNGase-like
CG9281	232	8	CG9281
CG4389	224	4	Mitochondrial trifunctional protein α SUt
CG10077	224	7	CG10077
CG32164	224	6	CG32164
CG4145	222	5	Collagen type IV
CG1945	220	6	fat facets
CG3422	214	5	Proteasome 28kD subunit 1
CG3210	213	5	Dynamin related protein 1
CG9012	211	6	Clathrin heavy chain
CG1489	211	6	Pros45
CG1341	210	5	Rpt1
CG5174	210	5	CG5174
CG5289	208	4	Proteasome 26S subunit subunit 4

			ATPase
CG11198	206	3	Acetyl-CoA carboxylase
CG5119	205	5	polyA-binding protein
CG18495	202	6	Proteasome α1 subunit
CG11451	199	5	Spc105-related
CG4320	195	6	raptor
CG17291	193	4	Protein phosphatase 2A at 29B
CG6439	192	7	CG6439
CG3612	189	3	bellwether
CG10596	188	2	Msr-110
CG7324	187	5	CG7324
CG10535	185	3	Elongator complex protein 1
CG8977	183	3	Cctγ
CG1559	183	6	Upf1
CG7507	177	5	Dynein heavy chain 64C
CG5974	175	4	pelle
CG6692	174	4	Cysteine proteinase-1
CG10938	169	3	Proteasome α5 subunit
CG31012	169	5	CIN85 and CD2AP orthologue
CG1883	168	4	Ribosomal protein S7
CG11870	166	2	CG11870
CG18572	164	5	rudimentary
CG1657	164	3	CG1657
CG9900	162	4	mitotic 15
CG6760	158	4	peroxin 1
CG14792	157	4	stubarista
CG31618	155	2	His2A:CG31618
CG8309	154	3	Transport and Golgi organization 7
CG14472	153	4	purity of essence
CG17520	150	4	casein kinase IIα
CG7945	149	2	CG7945
CG5520	149	4	Glycoprotein 93
CG2028	148	6	Casein kinase Iα
CG6988	147	3	Protein disulfide isomerase
CG32138	147	3	CG32138
CG17498	145	2	mad2
CG14648	145	5	growl
CG3981	145	3	Unc-76
CG5366	144	4	Cullin-associated and neddylation-dissociated 1
CG7546	144	2	CG7546
CG5650	141	2	Protein phosphatase 1 at 87B
CG9372	140	3	CG9372
CG5378	137	3	Rpn7
CG10360	135	4	refractory to sigma P
CG5170	134	4	Dodeca-satellite-binding protein 1
CG4157	132	2	Rpn12
CG6509	132	2	Discs large 5
CG33957	132	2	cp309
CG4257	131	3	Signal-transducer and activator of transcription protein at 92E
CG18174	131	3	Rpn11
CG8295	128	1	Myelodysplasia/myeloid leukemia factor
CG7033	127	3	CG7033
CG31739	127	3	Aspartyl-tRNA synthetase, mitochondrial
CG17358	126	2	TBP-associated factor 12
CG3074	126	2	Secreted Wg-interacting molecule
CG1092	125	3	CG1092
CG14750	124	4	Vacuolar protein sorting 25
CG3455	124	2	Rpt4
CG6181	124	3	Ge-1
CG1092	124	4	CG1092
CG8262	123	2	anastral spindle 2
CG1884	123	3	Not1
CG6875	121	2	abnormal spindle
CG7885	121	2	RNA polymerase II 33kD subunit
CG6392	121	2	CENP-meta
CG15087	120	2	Vacuolar protein sorting 51
CG8002	119	3	rapamycin-insensitive companion of Tor
CG6253	118	2	Ribosomal protein L14
CG17698	118	2	CG17698
CG6476	117	4	Suppressor of variegation 3-9
CG11261	117	2	CG11261
CG10711	117	3	Vacuolar protein sorting 36
CG10370	116	4	Tat-binding protein-1
CG3157	114	4	γ-Tubulin at 23C
CG16838	113	2	CG16838
CG6699	112	2	Coat Protein (coatomer) β'
CG11984	109	1	CG11984
CG33180	109	1	Ranbp16
CG5374	108	3	Tcp1-like
CG9075	104	4	Eukaryotic initiation factor 4a
CG5949	104	1	DNA-polymerase-δ
CG5525	104	3	CG5525
CG6339	103	1	rad50
CG1666	102	3	Helicase
CG1683	102	3	Adenine nucleotide translocase 2
CG7935	102	2	moleskin
CG32626	102	1	AMP deaminase
CG3661	101	3	Ribosomal protein L23
CG7961	100	4	Coat Protein (coatomer) α
CG6235	99	1	twins
CG11148	99	2	Gigyf
CG8636	97	1	eIF3g paralogue a
CG9282	96	1	Ribosomal protein L24
CG6459	96	1	CG6459
CG18102	94	2	shibire
CG7146	93	1	Vacuolar protein sorting 39
CG9124	91	1	Eukaryotic initiation factor 3 p40 subunit
CG8282	91	2	Snx6
CG16728	91	1	Git
CG17746	91	1	CG17746
CG3262	90	2	CG3262
CG11888	89	4	Rpn2
CG5934	89	1	CG5934
CG2960	88	3	Ribosomal protein L40
CG11154	88	2	ATP synthase, β subunit
CG7581	88	4	Bub3
CG3265	88	1	Eb1
CG33554	88	3	Nipped-A
CG14482	87	2	Ubiquinol-cytochrome c reductase 6.4 kDa subunit
CG31764	87	3	virus-induced RNA 1
CG4978	86	2	Minichromosome maintenance 7
CG7769	86	1	DDB1
CG7762	86	3	Rpn1
CG12108	86	1	Palmitoyl-protein thioesterase 1
CG7319	86	1	Mitochondrial Transcription Factor B1
CG31045	85	2	Myosin heavy chain-like
CG4033	84	2	RNA polymerase I 135kD subunit
CG8368	84	3	CG8368
CG3180	83	4	RNA polymerase II 140kD subunit
CG5920	83	1	string of pearls
CG6617	82	1	CG6617
CG7074	82	1	missing oocyte
CG11276	81	2	Ribosomal protein S4
CG1851	81	1	Ady43A
CG14999	81	1	Replication factor C subunit 4
CG10379	79	2	myoblast city
CG7519	79	1	CG7519
CG8351	79	1	Tcp-1η
CG3004	78	2	CG3004
CG13277	78	2	CG13277
CG9712	78	1	tumor suppressor protein 101
CG10198	78	1	Nucleoporin 98
CG4003	78	2	pontin
CG17246	77	1	Succinyl coenzyme A synthetase flavoprotein subunit
CG12262	77	2	CG12262
CG12265	77	1	Deterin
CG10701	76	2	Moesin
CG8266	76	1	sec31
CG13387	75	1	embargoed
CG8231	75	2	T-cp1ζ
CG14695	75	1	CG14695
CG30497	75	1	CG30497
CG1059	75	3	Karyopherin β 3
CG1453	74	1	Klp10A
CG15433	74	1	Elongator complex protein 3
CG7490	72	3	Ribosomal protein LP0
CG10988	72	1	lethal (1) discs degenerate 4
CG3678	72	1	CG3678
CG4849	72	1	CG4849
CG30349	72	1	CG30349
CG4799	71	2	Pendulin
CG6556	71	1	connector enhancer of ksr
CG4858	71	1	CG4858
CG10719	70	1	brain tumor
CG1100	70	2	Rpn5
CG1635	70	1	CG1635
CG2238	69	2	Elongation factor 2b
CG4087	69	1	Ribosomal protein LP1
CG6840	69	1	Rpb11
CG7791	69	1	CG7791
CG5266	69	2	Proteasome 25kD subunit
CG6095	69	1	exo84
CG3011	67	1	CG3011
CG33484	67	1	zormin
CG11228	67	1	hippo
CG10484	66	3	Regulatory particle non-ATPase 3
CG7825	66	1	Rad17
CG3278	66	1	Tif-IA
CG7558	64	1	Actin-related protein 66B
CG8715	64	1	lingerer
CG5450	64	1	Cytoplasmic dynein light chain 2
CG3356	64	2	CG3356
CG12244	64	2	licorne
CG12273	63	1	angel
CG3751	63	1	Ribosomal protein S24
CG4792	63	1	Dicer-1
CG9750	63	1	reptin
CG12532	62	3	Adaptor Protein complex 1/2, β subunit
CG7139	62	3	CG7139
CG31453	62	1	pch2
CG12163	62	2	CG12163
CG7831	61	1	non-claret disjunctional
CG7580	61	1	Ubiquinol-cytochrome c reductase ubiquinone-binding protein
CG11877	61	1	Autophagy-related 14
CG8322	60	1	ATP citrate lyase
CG6258	60	1	Replication factor C 38kD subunit
CG2038	60	1	COP9 complex homolog subunit 7

CG9446	60	1	coro
CG3295	60	1	CG3295
CG33162	59	2	Signal recognition particle receptor β
CG9940	59	2	CG9940
CG31048	59	2	sponge
CG1977	58	1	α Spectrin
CG1403	58	1	Septin-1
CG11981	58	1	Proteasome β3 subunit
CG32045	57	1	furry
CG8426	57	1	lethal (2) NC136
CG9031	56	2	icarus
CG6850	55	1	UDP-glucose-glycoprotein glucosyltransferase
CG4201	55	1	immune response deficient 5
CG8777	55	1	CG8777
CG5625	55	1	Vacuolar protein sorting 35
CG6233	55	1	Ubiquitin fusion-degradation 1-like
CG11856	55	1	Nucleoporin 358
CG3416	54	1	Mov34
CG8340	54	1	upstream of RpIII128
CG8578	54	1	CG8578
CG14211	54	1	MAPK Phosphatase 4
CG5094	54	2	small glutamine-rich tetratricopeptide containing protein
CG1104	54	1	CG1104
CG2656	54	1	CG2656
CG5723	53	1	Tenascin major
CG17158	53	1	capping protein beta
CG17331	53	1	Proteasome β4 subunit
CG7008	53	1	Tudor-SN
CG18176	53	1	deflated
CG9888	52	2	Fibrillarin
CG2168	52	1	Ribosomal protein S3A
CG4993	52	2	PRL-1
CG7838	52	1	Bub1-related kinase
CG1486	52	1	CG1486
CG6444	52	1	Dpy-30-like 1
CG4662	52	1	CG4662
CG6831	52	1	rhea
CG5688	51	1	Grip163
CG2206	51	1	lethal (1) G0193
CG9547	51	1	CG9547
CG31009	51	2	Cad99C
CG8448	50	2	mrj
CG1793	50	1	Mediator complex subunit 26
CG4904	50	2	Proteasome 35kD subunit
CG8793	50	1	lethal (3) 76BDm
CG18740	49	1	moira
CG4897	49	1	Ribosomal protein L7
CG9984	49	1	TH1
CG7238	49	1	septin interacting protein 1
CG6378	49	3	BM-40-SPARC
CG9769	49	1	CG9769
CG6369	49	1	Smg6
CG5692	49	1	rapsynoid
CG8472	48	2	Calmodulin
CG9327	48	2	Proteasome 29kD subunit
CG8402	48	1	Protein phosphatase D3
CG9155	48	1	Myosin 61F
CG8439	48	1	T-complex Chaperonin 5
CG11115	48	1	Ssl1
CG5902	48	1	CG5902
CG33175	48	1	sprint
CG8933	47	1	extradenticle
CG12184	47	1	CG12184
CG7184	47	1	Makorin 1
CG5001	47	1	CG5001
CG11577	47	1	CG11577
CG4898	46	1	Tropomyosin 1
CG10377	46	1	Heterogeneous nuclear ribonucleoprotein at 27C
CG12235	46	1	Arp11
CG9528	46	1	real-time
CG32149	46	2	RhoGAP71E
CG7725	46	1	rogdi
CG17272	46	1	CG17272
CG10539	45	1	RPS6-p70-protein kinase
CG9088	45	1	little imaginal discs
CG6453	45	1	Glucosidase 2 β subunit
CG6117	44	1	cAMP-dependent protein kinase 3
CG10109	44	1	Lobe
CG7948	44	1	spindle A
CG1616	44	1	disc proliferation abnormal
CG3917	44	2	gamma-tubulin ring protein 84
CG10306	44	1	CG10306
CG8996	43	1	walrus
CG5474	43	1	Signal sequence receptor β
CG32315	43	1	discs lost
CG5972	43	1	Arc-p20
CG9853	43	1	CG9853
CG10161	43	1	Eukaryotic initiation factor 3 p66 subunit
CG7749	43	1	kugelei
CG5502	42	1	Ribosomal protein L4
CG9450	42	2	tudor
CG32223	42	1	CG32223
CG5316	42	1	CG5316

CG10305	41	1	Ribosomal protein S26
CG8344	41	1	RNA polymerase III 128kD subunit
CG4457	41	1	Signal recognition particle protein 19
CG12264	41	2	CG12264
CG8831	41	1	Nucleoporin 54
CG6303	41	1	Bruce
CG8142	40	1	CG8142
CG10540	40	1	capping protein alpha
CG12014	40	1	CG12014
CG7073	40	1	sar1
CG3696	40	1	kismet
CG5870	39	1	β Spectrin
CG15099	39	1	CG15099
CG9191	38	1	Kinesin-like protein at 61F
CG1594	38	1	hopscotch
CG3379	38	1	Histone H4 replacement
CG2146	38	2	dilute class unconventional myosin
CG9834	38	1	endophilin B
CG9946	38	1	eukaryotic translation Initiation Factor 2α
CG7619	37	1	Proteasome 54kD subunit
CG9086	37	1	CG9086
CG8609	37	1	Mediator complex subunit 4
CG3506	36	1	vasa
CG5163	36	1	Transcription-factor-IIA-S
CG3714	36	1	CG3714
CG8877	36	1	pre-mRNA processing factor 8
CG10315	36	1	eIF2B-δ
CG10663	36	2	CG10663
CG3329	35	1	Proteasome β2 subunit
CG5313	35	1	Replication factor C subunit 3
CG6846	35	1	Ribosomal protein L26
CG17484	35	1	Adherens junction protein p120
CG15224	34	1	Casein kinase II β subunit
CG1591	34	1	REG
CG8184	34	1	CG8184
CG8605	34	1	RINT1 ortholog
CG10423	34	1	Ribosomal protein S27
CG7438	34	1	Myosin 31DF
CG2845	33	1	pole hole
CG4429	33	1	RNA-binding protein 2
CG16785	33	1	frizzled 3
CG7668	33	1	CG7668
CG9280	32	1	Glutactin
CG4097	32	1	Proteasome 26kD subunit
CG1065	32	1	Succinyl coenzyme A synthetase α subunit
CG5575	32	1	ken and barbie
CG4901	32	1	CG4901
CG10178	32	1	CG10178
CG5566	32	1	CG5566
CG4051	31	1	egalitarian
CG3949	31	1	hoi-polloi
CG1112	31	1	α-Esterase-7
CG1387	31	1	CG1387
CG2711	30	1	deformed wings
CG4297	30	1	CG4297
CG4839	30	1	CG4839
CG2078	30	1	Myd88
CG13349	30	1	Regulatory particle non-ATPase 13
CG8479	30	1	Optic atrophy 1 ortholog
CG15678	30	1	poor Imd response upon knock-in
CG12005	30	1	Mms19
CG30421	30	2	Ubiquitin specific protease 15/31
CG31659	30	1	CG31659
CG1484	29	1	flightless I
CG6382	29	1	Ef1α-like factor
CG3051	29	1	SNF1A/AMP-activated protein kinase
CG1519	29	1	Proteasome α7 subunit
CG4581	29	1	Thiolase
CG13745	29	1	Fanconi anemia complementation group I homologue
CG8187	29	1	CG8187
CG31794	29	1	Paxillin
CG13197	29	1	CG13197
CG12008	28	1	karst
CG16983	28	1	skpA
CG13284	28	1	CG13284
CG8588	28	1	pastrel
CG1081	28	1	Rheb
CG8454	28	1	Vacuolar protein sorting 16A
CG7041	27	1	HP1b
CG8008	27	1	CG8008
CG11814	27	1	mauve
CG12000	27	1	Proteasome β7 subunit
CG33106	27	1	multiple ankyrin repeats single KH domain
CG33249	27	1	CG33249
CG9273	26	1	Replication protein A2
CG13530	26	1	CG13530
CG5608	26	1	CG5608
CG30390	26	1	Sgf29
CG31018	26	1	CG31018
CG14801	25	1	CG14801
CG5004	25	1	CG5004
CG31918	25	1	CG31918
CG33139	25	1	Ranbp11

A.12 pMT-Rcd4-PrA +MG132 purification from *Drosophila* cells

CG #	Score	#pep	Full name
CG4264	3021	97	Heat shock protein cognate 4
CG9277	2548	75	β-Tubulin at 56D
CG1913	1226	34	α-Tubulin at 84B
CG3401	1131	38	β-Tubulin at 60D
CG17295	698	32	Reduction in Cnn dots 4
CG4147	668	35	Heat shock protein cognate 3
CG18743	582	17	Heat-shock-protein-70Ab
CG5834	575	17	Hsp70Bbb
CG12051	504	19	Actin 42A
CG5436	496	13	Heat shock protein 68
CG8863	481	16	DnaJ-like-2
CG4463	394	11	Heat shock protein 23
CG8280	319	11	Elongation factor 1α48D
CG4183	319	9	Heat shock protein 26
CG12101	309	8	Heat shock protein 60
CG4466	307	7	Heat shock protein 27
CG1524	304	6	Ribosomal protein S14a
CG10938	292	9	Proteasome α5 subunit
CG15792	279	10	zipper
CG5119	244	7	polyA-binding protein
CG7581	206	5	Bub3
CG13162	199	8	anastral spindle 3
CG15697	162	4	Ribosomal protein S30
CG9888	148	5	Fibrillarin
CG6253	148	3	Ribosomal protein L14
CG7808	147	3	Ribosomal protein S8
CG2168	144	6	Ribosomal protein S3A
CG7439	140	5	Argonaute 2
CG3195	139	3	Ribosomal protein L12
CG18572	131	4	rudimentary
CG2960	127	4	Ribosomal protein L40
CG14648	126	3	growl
CG10652	125	2	Ribosomal protein L30
CG4863	123	4	Ribosomal protein L3
CG6779	119	2	Ribosomal protein S3
CG10944	115	3	Ribosomal protein S6
CG6692	114	3	Cysteine proteinase-1
CG3612	113	2	bellwether
CG13389	110	3	Ribosomal protein S13
CG6143	105	2	Protein on ecdysone puffs
CG1883	105	3	Ribosomal protein S7
CG5502	104	3	Ribosomal protein L4
CG5920	104	5	string of pearls
CG6684	104	4	Ribosomal protein S25
CG5654	104	2	ypsilon schachtel
CG7490	103	2	Ribosomal protein LP0
CG5504	98	1	lethal (2) tumorous imaginal discs
CG7434	97	3	Ribosomal protein L22
CG9282	93	1	Ribosomal protein L24
CG12233	90	2	lethal (1) G0156
CG7622	89	1	Ribosomal protein L36
CG8947	89	2	26-29kD-proteinase
CG10824	88	2	Common Dpr-interacting protein
CG32315	85	2	discs lost
CG11999	85	3	CG11999
CG14066	85	1	La related protein
CG12008	83	1	karst
CG8735	83	6	CG8735
CG1591	80	1	REG
CG4119	77	1	CG4119
CG9940	76	2	CG9940
CG11154	75	1	ATP synthase, β subunit
CG4464	71	2	Ribosomal protein S19a
CG9748	70	4	belle
CG11276	70	2	Ribosomal protein S4
CG2028	70	1	Casein kinase Iα
CG8262	70	1	anastral spindle 2
CG3203	70	1	Ribosomal protein L17
CG10305	69	2	Ribosomal protein S26
CG10811	67	2	eukaryotic translation initiation factor 4G
CG8415	67	2	Ribosomal protein S23
CG17870	66	1	14-3-3ζ
CG3922	65	1	Ribosomal protein S17
CG13388	65	1	A kinase anchor protein 200
CG3201	63	2	Myosin light chain cytoplasmic
CG4897	63	1	Ribosomal protein L7
CG8615	60	3	Ribosomal protein L18
CG10663	57	3	CG10663
CG15442	56	2	Ribosomal protein L27A
CG12052	55	1	longitudinals lacking
CG1821	55	1	Ribosomal protein L31
CG6846	50	1	Ribosomal protein L26
CG33715	50	3	Muscle-specific protein 300
CG4651	49	3	Ribosomal protein L13
CG6453	49	1	Glucosidase 2 β subunit
CG13349	49	1	Regulatory particle non-ATPase 13
CG4087	48	1	Ribosomal protein LP1
CG3314	48	1	Ribosomal protein L7A
CG8571	47	2	smallminded
CG17521	43	1	Qm
CG3395	42	1	Ribosomal protein S9
CG1341	42	1	Rpt1
CG2746	41	2	Ribosomal protein L19
CG6510	41	3	Ribosomal protein L18A
CG4389	41	1	Mitochondrial trifunctional protein α subunit
CG2033	39	1	Ribosomal protein S15Aa
CG9327	38	1	Proteasome 29kD subunit
CG12264	37	1	CG12264
CG13708	37	1	CG13708
CG2146	36	1	dilute class unconventional myosin
CG31764	36	1	virus-induced RNA 1
CG14206	35	1	Ribosomal protein S10b
CG7595	34	1	crinkled
CG6090	34	1	Ribosomal protein L34a
CG13387	33	1	embargoed
CG11522	33	1	Ribosomal protein L6
CG31524	33	1	CG31524
CG7961	32	1	Coat Protein (coatomer) α
CG12775	32	1	Ribosomal protein L21
CG4046	32	1	Ribosomal protein S16
CG1242	31	1	Heat shock protein 83
CG13609	31	2	CG13609
CG3595	30	1	spaghetti squash
CG9660	30	1	toucan
CG8857	30	1	Ribosomal protein S11
CG15134	28	1	tweek
CG7283	25	1	Ribosomal protein L10Ab
CG17768	23	1	CG17768
CG10333	22	1	CG10333
CG9256	22	1	Na+/H+ hydrogen exchanger 2
CG7977	21	1	Ribosomal protein L23A

A.13 pMT-Rcd4-PrA +OA +MG132 purification from *Drosophila* cells

CG #	Score	#pep	Full name
CG15792	6816	222	zipper
CG4027	2393	83	Actin 5C
CG12051	2366	82	Actin 42A
CG10067	1631	61	Actin 57B
CG4264	1390	50	Heat shock protein cognate 4
CG9277	1238	36	β-Tubulin at 56D
CG1913	827	21	α-Tubulin at 84B
CG3201	762	21	Myosin light chain cytoplasmic
CG4898	701	23	Tropomyosin 1
CG3401	660	21	β-Tubulin at 60D
CG2146	509	18	dilute class unconventional myosin
CG17295	438	17	Reduction in Cnn dots 4
CG3595	369	11	spaghetti squash
CG8578	369	10	CG8578
CG10540	333	7	capping protein alpha
CG8280	284	9	Elongation factor 1α48D
CG9155	267	10	Myosin 61F
CG4183	259	6	Heat shock protein 26
CG5695	250	8	jaguar
CG5436	219	6	Heat shock protein 68
CG1484	210	8	flightless I
CG13162	207	8	anastral spindle 3
CG4147	205	9	Heat shock protein cognate 3
CG8472	189	7	Calmodulin
CG17158	177	6	capping protein beta
CG4466	173	5	Heat shock protein 27
CG12008	171	4	karst
CG7581	169	4	Bub3
CG7438	151	5	Myosin 31DF
CG1106	141	4	Gelsolin
CG10641	132	4	CG10641
CG8947	119	2	26-29kD-proteinase
CG4463	109	2	Heat shock protein 23
CG1977	108	4	α Spectrin
CG3379	102	4	Histone H4 replacement
CG8863	89	2	DnaJ-like-2
CG12101	87	2	Heat shock protein 60
CG32315	83	2	discs lost
CG4119	81	1	CG4119
CG5499	70	2	Histone H2A variant
CG11999	70	1	CG11999

CG5825	64	3	Histone H3.3A
CG1591	60	1	REG
CG8396	56	1	Single stranded-binding protein c31A
CG10663	56	3	CG10663
CG8735	53	4	CG8735
CG14648	52	1	growl
CG9940	51	1	CG9940
CG9888	49	1	Fibrillarin
CG10811	49	1	eukaryotic translation initiation factor 4G
CG14419	48	1	CG14419
CG17949	48	2	His2B:CG17949
CG1539	46	2	tropomodulin
CG10546	41	1	Cellular retinaldehyde binding protein
CG2207	36	2	Decondensation factor 31
CG13387	35	1	embargoed
CG2168	33	1	Ribosomal protein S3A
CG17209	30	1	CG17209
CG10539	26	1	RPS6-p70-protein kinase
CG5047	26	1	mTerf3
CG5467	23	1	scribbled
CG6355	21	1	fab1
CG7595	0	1	crinkled

A.14 pMT-PrA-Cep97 +OA +MG132 purification from *Drosophila* cells

CG #	Score	#pep	Full name
CG15792	7020	205	zipper
CG4027	2860	93	Actin 5C
CG12051	2854	93	Actin 42A
CG12008	2681	83	karst
CG10067	2132	72	Actin 57B
CG1977	1557	54	α Spectrin
CG3980	1465	50	Cep97
CG2146	978	33	dilute class unconventional myosin
CG7438	940	30	Myosin 31DF
CG3201	919	23	Myosin light chain cytoplasmic
CG9155	902	28	Myosin 61F
CG5695	666	26	jaguar
CG3595	536	17	spaghetti squash
CG1106	512	16	Gelsolin
CG10641	481	14	CG10641
CG9277	470	19	β-Tubulin at 56D
CG1913	445	17	α-Tubulin at 84B
CG4898	367	10	Tropomyosin 1
CG10540	361	9	capping protein alpha
CG4264	358	13	Heat shock protein cognate 4
CG3379	357	9	Histone H4 replacement
CG17158	326	11	capping protein beta
CG8280	298	8	Elongation factor 1α48D
CG8472	282	8	Calmodulin
CG4147	239	9	Heat shock protein cognate 3
CG1242	197	8	Heat shock protein 83
CG6998	197	5	cut up
CG14617	178	5	Cp110
CG7558	160	6	Actin-related protein 66B
CG3401	132	7	β-Tubulin at 60D
CG9446	115	3	coro
CG1258	105	2	pavarotti
CG5972	98	2	Arc-p20
CG8578	97	2	CG8578
CG8055	97	3	Vps32
CG17949	96	4	His2B:CG17949
CG3937	89	2	cheerio
CG10954	88	3	Arc-p34
CG4145	87	2	Collagen type IV
CG16858	84	2	viking
CG8978	80	2	Suppressor of profilin 2
CG32315	80	2	discs lost
CG14648	78	3	growl
CG2238	77	2	Elongation factor 2b
CG1524	66	1	Ribosomal protein S14a
CG11901	64	2	Ef1γ
CG17870	59	2	14-3-3ζ
CG10701	58	1	Moesin
CG1484	52	1	flightless I
CG5499	52	2	Histone H2A variant
CG4183	52	2	Heat shock protein 26
CG9881	50	1	p16-ARC
CG5825	47	1	Histone H3.3A
CG33957	44	1	cp309
CG8983	43	1	ERp60
CG2179	41	1	Xe7
CG10546	41	1	Cellular retinaldehyde binding protein
CG7581	40	1	Bub3
CG14897	35	1	CG14897
CG2207	31	1	Decondensation factor 31
CG13389	30	1	Ribosomal protein S13
CG4042	30	2	CG4042
CG10385	29	1	male-specific lethal 1
CG5920	28	1	string of pearls
CG1702	28	1	Glutathione S transferase T3
CG5047	26	1	mTerf3
CG6355	23	1	fab1
CG6375	21	1	pitchoune
CG5467	20	1	scribbled
CG10859	19	1	CG10859

A.15 pMT-Cep97-PrA +MG132 purification from *Drosophila* cells

CG #	Score	#pep	Full name
CG3980	7109	208	Cep97
CG9277	2480	48	β-Tubulin at 56D
CG4264	2277	45	Heat shock protein cognate 4
CG15792	1747	44	zipper
CG3401	1544	33	β-Tubulin at 60D
CG1913	1398	29	α-Tubulin at 84B
CG31012	982	23	CIN85 and CD2AP orthologue
CG12051	846	25	Actin 42A
CG4147	751	18	Heat shock protein cognate 3
CG10067	629	20	Actin 57B
CG3201	422	7	Myosin light chain cytoplasmic
CG9940	402	12	CG9940
CG5119	376	12	polyA-binding protein
CG5502	374	9	Ribosomal protein L4
CG8280	363	10	Elongation factor 1α48D
CG14207	359	7	HspB8
CG5436	350	7	Heat shock protein 68
CG5779	321	9	Black cells
CG1483	297	7	Microtubule-associated protein 205
CG5174	260	7	CG5174
CG12101	256	4	Heat shock protein 60
CG7808	252	4	Ribosomal protein S8
CG12233	235	6	lethal (1) G0156
CG8262	235	3	anastral spindle 2
CG4087	191	5	Ribosomal protein LP1
CG7915	176	9	Ect4
CG4463	171	4	Heat shock protein 23
CG1883	170	5	Ribosomal protein S7
CG6253	162	2	Ribosomal protein L14
CG5920	159	4	string of pearls
CG3203	156	2	Ribosomal protein L17
CG31618	151	2	His2A:CG31618
CG3751	133	2	Ribosomal protein S24
CG4897	132	4	Ribosomal protein L7
CG7971	132	2	CG7971
CG8571	124	1	smallminded
CG7490	122	5	Ribosomal protein LP0
CG6181	116	2	Ge-1
CG10377	113	3	Heterogeneous nuclear ribonucleoprotein at 27C
CG9282	110	1	Ribosomal protein L24
CG10944	108	3	Ribosomal protein S6
CG6779	106	3	Ribosomal protein S3
CG17498	101	2	mad2
CG7581	98	5	Bub3
CG7977	98	5	Ribosomal protein L23A
CG2960	95	2	Ribosomal protein L40
CG1341	94	3	Rpt1
CG10851	92	5	B52
CG4651	90	5	Ribosomal protein L13
CG6459	90	1	CG6459
CG10689	89	3	lethal (2) 37Cb
CG8615	89	2	Ribosomal protein L18
CG14648	89	3	growl
CG3595	87	4	spaghetti squash
CG3395	87	4	Ribosomal protein S9
CG3612	87	2	bellwether
CG11522	87	4	Ribosomal protein L6
CG13388	84	4	A kinase anchor protein 200
CG5499	82	2	Histone H2A variant
CG11276	81	2	Ribosomal protein S4
CG6988	74	2	Protein disulfide isomerase
CG8478	74	3	CG8478
CG12750	74	3	nucampholin
CG9091	73	1	Ribosomal protein L37a
CG8863	73	1	DnaJ-like-2
CG7726	70	2	Ribosomal protein L11

CG8947	70	2	26-29kD-proteinase
CG1516	69	2	Pyruvate carboxylase
CG2216	68	1	Ferritin 1 heavy chain homologue
CG3922	66	1	Ribosomal protein S17
CG5934	65	1	CG5934
CG2671	64	2	lethal (2) giant larvae
CG5094	64	1	small glutamine-rich tetratricopeptide containing protein
CG2746	62	3	Ribosomal protein L19
CG10360	62	1	refractory to sigma P
CG3126	61	4	C3G
CG7028	59	1	CG7028
CG6617	59	1	CG6617
CG4183	58	3	Heat shock protein 26
CG5450	58	2	Cytoplasmic dynein light chain 2
CG6686	58	3	CG6686
CG1821	57	1	Ribosomal protein L31
CG3981	57	1	Unc-76
CG31764	57	1	virus-induced RNA 1
CG15442	56	4	Ribosomal protein L27A
CG6692	55	2	Cysteine proteinase-1
CG1263	55	3	Ribosomal protein L8
CG7507	55	3	Dynein heavy chain 64C
CG13389	53	2	Ribosomal protein S13
CG14637	53	2	abstrakt
CG1548	53	1	cathD
CG31022	53	2	prolyl-4-hydroxylase-alpha EFB
CG7185	52	1	CG7185
CG7439	52	2	Argonaute 2
CG8922	49	1	Ribosomal protein S5a
CG17158	49	2	capping protein beta
CG9684	49	2	CG9684
CG5520	49	2	Glycoprotein 93
CG8472	47	2	Calmodulin
CG3379	47	2	Histone H4 replacement
CG5654	46	2	ypsilon schachtel
CG11963	46	1	skpA associated protein
CG8857	45	2	Ribosomal protein S11
CG6090	45	2	Ribosomal protein L34a
CG2152	45	1	Protein-L-isoaspartate (D-aspartate) O-methyltransferase
CG7622	44	1	Ribosomal protein L36
CG5422	44	1	Rox8
CG7939	43	1	Ribosomal protein L32
CG12264	43	2	CG12264
CG8542	42	2	Heat shock protein cognate 5
CG10305	42	1	Ribosomal protein S26
CG7434	42	1	Ribosomal protein L22
CG10540	42	2	capping protein alpha
CG1242	41	2	Heat shock protein 83
CG12306	41	1	polo
CG3314	41	1	Ribosomal protein L7A
CG15770	41	1	CG15770
CG10546	41	1	Cellular retinaldehyde binding protein
CG17520	40	2	casein kinase IIα
CG4898	39	1	Tropomyosin 1
CG8415	39	2	Ribosomal protein S23
CG4046	39	2	Ribosomal protein S16
CG1677	37	1	CG1677
CG3542	36	1	CG3542
CG6684	36	2	Ribosomal protein S25
CG10149	34	1	Proteasome p44.5 subunit
CG10824	34	1	Common Dpr-interacting protein
CG1633	34	1	thioredoxin peroxidase 1
CG2168	33	1	Ribosomal protein S3A
CG12775	33	1	Ribosomal protein L21
CG11856	33	1	Nucleoporin 358
CG16944	32	1	stress-sensitive B
CG1524	32	1	Ribosomal protein S14a
CG14235	32	1	Cytochrome c oxidase subunit 6B
CG10663	32	2	CG10663
CG3836	31	1	stonewall
CG11949	30	1	coracle
CG17949	30	2	His2B:CG17949
CG6428	29	1	CG6428
CG5916	29	1	CG5916
CG1977	29	1	α Spectrin
CG6510	28	1	Ribosomal protein L18A
CG1489	27	1	Pros45
CG32680	27	2	sprint
CG2692	26	1	gooseberry-neuro
CG3661	26	1	Ribosomal protein L23
CG34130	26	2	CG34130
CG7111	25	1	Receptor of activated protein kinase C 1
CG7961	25	1	Coat Protein (coatomer) α
CG17521	24	1	Qm
CG8476	24	1	CG8476
CG1683	23	1	Adenine nucleotide translocase 2
CG4164	23	1	CG4164
CG7219	23	1	Serpin 28D
CG18522	23	1	Aldehyde oxidase 1
CG7595	22	1	crinkled
CG4918	22	1	Ribosomal protein LP2
CG4215	22	1	spellchecker1
CG6773	22	1	sec13
CG33715	22	1	Muscle-specific protein 300
CG10071	21	1	Ribosomal protein L29
CG4863	21	1	Ribosomal protein L3
CG11143	21	1	Inos
CG3711	21	1	CG3711
CG4863	20	2	Ribosomal protein L3
CG17209	20	1	CG17209
CG12070	19	1	Saposin-related
CG8715	19	1	lingerer
CG6699	19	1	Coat Protein (coatomer) β'
CG4678	19	1	CG4678
CG11274	19	1	SRm160
CG6169	19	1	Decapping protein 2
CG32688	18	1	Hyperkinetic
CG9888	18	2	Fibrillarin

A.16 pMT-Cep97-PrA +OA +MG132 purification from *Drosophila* cells

CG #	Score	#pep	Full name
CG3980	16796	437	Cep97
CG15792	2652	65	zipper
CG4264	1993	41	Heat shock protein cognate 4
CG9277	1433	33	β-Tubulin at 56D
CG4027	1180	30	Actin 5C
CG1913	921	25	α-Tubulin at 84B
CG3401	902	21	β-Tubulin at 60D
CG10067	851	26	Actin 57B
CG3201	753	12	Myosin light chain cytoplasmic
CG4147	722	21	Heat shock protein cognate 3
CG31618	616	9	His2A:CG31618
CG5834	448	9	Hsp70Bbb
CG5436	446	8	Heat shock protein 68
CG8280	344	9	Elongation factor 1α48D
CG14617	330	11	Cp110
CG8472	281	9	Calmodulin
CG12101	246	5	Heat shock protein 60
CG5499	241	6	Histone H2A variant
CG12233	179	4	lethal (1) G0156
CG10641	179	6	Swiprosin-1
CG10377	156	2	Heterogeneous nuclear ribonucleoprotein at 27C
CG9940	148	5	CG9940
CG10540	139	3	capping protein alpha
CG14637	131	4	abstrakt
CG5450	131	4	Cytoplasmic dynein light chain 2
CG3595	120	4	spaghetti squash
CG9155	118	3	Myosin 61F
CG14207	118	2	HspB8
CG6453	117	3	Glucosidase 2 β subunit
CG2216	106	1	Ferritin 1 heavy chain homologue
CG3379	105	2	Histone H4 replacement
CG9282	93	1	Ribosomal protein L24
CG5779	91	4	Black cells
CG33332	89	1	CG33332
CG11963	85	3	skpA associated protein
CG1242	84	2	Heat shock protein 83
CG16901	74	1	squid
CG17498	73	1	mad2
CG3612	70	2	bellwether
CG18572	69	2	rudimentary
CG15770	67	2	CG15770
CG10689	59	2	lethal (2) 37Cb
CG1341	58	1	Rpt1
CG8947	57	1	26-29kD-proteinase
CG8578	57	1	CG8578
CG8542	56	3	Heat shock protein cognate 5
CG3203	56	1	Ribosomal protein L17
CG10851	55	3	B52
CG6509	55	2	Discs large 5
CG12750	54	1	nucampholin
CG8863	54	2	DnaJ-like-2
CG7507	53	1	Dynein heavy chain 64C
CG17158	52	1	capping protein beta
CG6692	52	1	Cysteine proteinase-1
CG5422	49	2	Rox8
CG5119	49	2	polyA-binding protein
CG5520	47	2	Glycoprotein 93
CG9888	46	3	Fibrillarin
CG31764	46	1	virus-induced RNA 1
CG1483	44	1	Microtubule-associated protein 205

CG10546	41	1	Cellular retinaldehyde binding protein
CG14648	40	1	growl
CG17949	40	2	His2B:CG17949
CG4463	37	1	Heat shock protein 23
CG9075	37	1	Eukaryotic initiation factor 4a
CG5174	37	1	CG5174
CG9684	36	1	CG9684
CG31012	35	2	CIN85 and CD2AP orthologue
CG31022	35	1	prolyl-4-hydroxylase-alpha EFB
CG3662	34	1	CG3662
CG10596	33	2	Msr-110
CG7762	33	1	Rpn1
CG6617	33	1	CG6617
CG9748	32	1	belle
CG2960	32	1	Ribosomal protein L40
CG5825	32	1	Histone H3.3A
CG7915	32	1	Ect4
CG4145	31	1	Collagen type IV
CG2175	31	1	defective chorion 1
CG12306	31	1	polo
CG6341	31	1	Elongation factor 1 β
CG1548	31	1	cathD
CG6428	31	1	CG6428
CG17209	31	1	CG17209
CG2152	30	1	Protein-L-isoaspartate (D-aspartate) O-methyltransferase
CG2168	30	1	Ribosomal protein S3A
CG10663	30	2	CG10663
CG7611	30	1	CG7611
CG10360	29	1	refractory to sigma P
CG3836	29	1	stonewall
CG3661	29	1	Ribosomal protein L23
CG4651	29	2	Ribosomal protein L13
CG15784	29	1	CG15784
CG4064	29	1	CG4064
CG4164	29	1	CG4164
CG32196	29	1	CG32196
CG7581	28	1	Bub3
CG17768	28	1	CG17768
CG3382	27	1	Organic anion transporting polypeptide 58Db
CG4087	26	1	Ribosomal protein LP1
CG7144	26	1	lysine ketoglutarate reductase
CG8677	26	1	CG8677
CG1883	26	1	Ribosomal protein S7
CG11123	25	1	CG11123
CG14996	25	1	Chd64
CG33715	25	1	Muscle-specific protein 300
CG1524	24	1	Ribosomal protein S14a
CG10385	24	1	male-specific lethal 1
CG1683	24	1	Adenine nucleotide translocase 2
CG3711	24	1	CG3711
CG34130	24	2	CG34130
CG5330	23	1	Nucleosome assembly protein 1
CG7219	23	1	Serpin 28D
CG1869	23	1	Cht7
CG4289	23	1	Peroxin 14
CG7595	22	1	crinkled
CG31196	22	1	14-3-3ε
CG4678	22	1	CG4678
CG7971	22	1	CG7971
CG13833	22	1	CG13833
CG32680	22	1	sprint
CG3561	22	1	KH1
CG2146	22	1	dilute class unconventional myosin
CG2692	21	2	gooseberry-neuro
CG12775	20	1	Ribosomal protein L21
CG4849	20	1	CG4849
CG32688	19	2	Hyperkinetic
CG5502	19	1	Ribosomal protein L4
CG18255	19	1	Stretchin-Mlck
CG33715	19	1	Muscle-specific protein 300
CG10986	18	1	garnet
CG4183	18	1	Heat shock protein 26
CG9934	18	1	CG9934
CG5432	18	1	CG5432
CG33464	18	1	slit

A.17 pMT-PrA-CP110 +MG132 purification from *Drosophila* cells

CG #	Score	#pep	Full name
CG4027	85941	1322	Actin 5C
CG12051	85843	1313	Actin 42A
CG15792	47870	840	zipper
CG18290	17848	580	Actin 87E
CG3595	8513	158	spaghetti squash
CG1977	4876	98	α Spectrin
CG3201	4751	95	Myosin light chain cytoplasmic
CG9155	4575	99	Myosin 61F
CG4264	3673	76	Heat shock protein cognate 4
CG6831	3631	77	rhea
CG7438	2988	84	Myosin 31DF
CG9277	2841	74	β-Tubulin at 56D
CG8472	2757	46	Calmodulin
CG10540	2698	89	capping protein alpha
CG1913	2261	43	α-Tubulin at 84B
CG17158	2155	46	capping protein beta
CG1539	2111	40	tropomodulin
CG8280	2093	45	Elongation factor 1α48D
CG14617	2046	46	Cp110
CG2146	2015	46	dilute class unconventional myosin
CG12008	1938	67	karst
CG1484	1854	41	flightless I
CG3401	1676	45	β-Tubulin at 60D
CG9325	1673	33	hu li tai shao
CG10641	1622	46	CG10641
CG3937	1394	31	cheerio
CG5870	1346	32	β Spectrin
CG31618	1294	18	His2A:CG31618
CG7558	1224	25	Actin-related protein 66B
CG5695	1080	26	jaguar
CG1106	1066	30	Gelsolin
CG8578	976	28	CG8578
CG4147	914	15	Heat shock protein cognate 3
CG31196	862	16	14-3-3ε
CG1883	850	16	Ribosomal protein S7
CG7490	733	12	Ribosomal protein LP0
CG4087	586	9	Ribosomal protein LP1
CG1242	556	14	Heat shock protein 83
CG18572	541	13	rudimentary
CG4463	535	10	Heat shock protein 23
CG5499	528	8	Histone H2A variant
CG5502	453	15	Ribosomal protein L4
CG14792	416	6	stubarista
CG3299	412	7	Vinculin
CG9901	409	12	Actin-related protein 14D
CG10922	396	6	La autoantigen-like
CG31794	386	6	Paxillin
CG17291	379	7	Protein phosphatase 2A at 29B
CG2238	376	13	Elongation factor 2b
CG7507	373	7	Dynein heavy chain 64C
CG4145	333	8	Collagen type IV
CG10954	332	6	Arc-p34
CG3203	327	6	Ribosomal protein L17
CG4897	315	7	Ribosomal protein L7
CG8978	312	8	Suppressor of profilin 2
CG9881	311	6	p16-ARC
CG9748	305	8	belle
CG9012	303	11	Clathrin heavy chain
CG8055	303	3	shrub
CG8977	299	4	Cctγ
CG15784	295	9	CG15784
CG8309	278	7	Transport and Golgi organization 7
CG1258	276	7	pavarotti
CG7033	276	4	CG7033
CG7283	275	9	Ribosomal protein L10Ab
CG7595	268	7	crinkled
CG9282	266	4	Ribosomal protein L24
CG18076	248	6	short stop
CG4560	241	6	Arpc3A
CG5119	235	8	polyA-binding protein
CG11522	233	6	Ribosomal protein L6
CG1059	233	4	Karyopherin β 3
CG8900	229	6	Ribosomal protein S18
CG33484	229	4	zormin
CG7380	227	4	barrier to autointegration factor
CG5825	225	5	Histone H3.3A
CG31764	220	4	virus-induced RNA 1
CG4376	214	8	α actinin
CG31613	212	5	His3:CG31613
CG17272	208	4	CG17272
CG5020	207	4	Cytoplasmic linker protein 190
CG3379	204	5	Histone H4 replacement
CG17949	202	8	His2B:CG17949
CG30349	199	3	CG30349
CG8332	198	5	Ribosomal protein S15
CG2331	193	2	TER94
CG1782	192	5	Ubiquitin activating enzyme 1
CG10811	189	3	eukaryotic translation initiation factor 4G
CG18076	188	3	short stop
CG8439	179	4	T-complex Chaperonin 5
CG4183	173	4	Heat shock protein 26
CG3751	168	5	Ribosomal protein S24
CG12030	167	5	UDP-galactose 4'-epimerase
CG7439	167	3	Argonaute 2
CG1263	165	3	Ribosomal protein L8

CG6253	162	4	Ribosomal protein L14
CG8983	162	4	ERp60
CG1822	161	6	bifocal
CG40045	160	2	CG40045
CG3314	159	7	Ribosomal protein L7A
CG4466	158	4	Heat shock protein 27
CG11271	158	3	Ribosomal protein S12
CG1524	157	4	Ribosomal protein S14a
CG1483	149	5	Microtubule-associated protein 205
CG17489	148	4	Ribosomal protein L5
CG33957	148	5	cp309
CG11276	147	3	Ribosomal protein S4
CG12740	146	2	Ribosomal protein L28
CG16916	145	2	Rpt3
CG4898	144	5	Tropomyosin 1
CG16858	143	4	viking
CG5525	143	2	CG5525
CG3455	141	2	Rpt4
CG12363	140	2	Dynein light chain 90F
CG32164	138	2	CG32164
CG14207	134	4	HspB8
CG6522	134	4	Testin ortholog
CG31352	133	5	CG31352
CG9075	131	3	Eukaryotic initiation factor 4a
CG6148	130	2	Putative Achaete Scute Target 1
CG5520	127	2	Glycoprotein 93
CG7581	126	2	Bub3
CG11888	126	2	Rpn2
CG5972	126	3	Arc-p20
CG3949	124	3	hoi-polloi
CG3821	122	2	Aspartyl-tRNA synthetase
CG10596	122	5	Msr-110
CG6779	119	2	Ribosomal protein S3
CG3922	119	3	Ribosomal protein S17
CG5374	117	3	Tcp1-like
CG17654	115	5	Enolase
CG7261	114	1	tubulin folding cofactor D
CG4912	112	1	eEF1δ
CG2168	108	4	Ribosomal protein S3A
CG6988	104	6	Protein disulfide isomerase
CG15717	99	1	CG15717
CG17521	98	2	Qm
CG7935	98	3	moleskin
CG13849	98	1	Nop56
CG7765	97	2	Kinesin heavy chain
CG4799	97	3	Pendulin
CG9281	96	2	CG9281
CG31852	95	1	Two A-associated protein of 42kDa
CG31012	94	3	CIN85 and CD2AP orthologue
CG3195	94	3	Ribosomal protein L12
CG2746	92	2	Ribosomal protein L19
CG10652	92	1	Ribosomal protein L30
CG5920	91	2	string of pearls
CG8351	91	2	Tcp-1η
CG13389	90	2	Ribosomal protein S13
CG7967	90	1	CG7967
CG9769	88	2	CG9769
CG6684	87	3	Ribosomal protein S25
CG5384	87	2	Ubiquitin specific protease 14
CG3333	84	2	Nucleolar protein at 60B
CG10230	82	2	Rpn9
CG32075	82	1	CG32075
CG9888	81	3	Fibrillarin
CG4665	81	1	Dihydropteridine reductase
CG3172	81	2	twinfilin
CG3523	80	2	Fatty acid synthase 1
CG10990	80	1	Programmed cell death 4 ortholog
CG3011	78	1	CG3011
CG14066	78	1	La related protein
CG33715	77	2	Muscle-specific protein 300
CG14206	77	5	Ribosomal protein S10b
CG6603	76	1	Hsc70Cb
CG1345	76	3	Glutamine:fructose-6-phosphate aminotransferase 2
CG5170	75	4	Dodeca-satellite-binding protein 1
CG6453	75	4	Glucosidase 2 β subunit
CG9446	75	5	coro
CG6238	74	1	slingshot
CG15693	73	2	Ribosomal protein S20
CG3265	72	1	Eb1
CG8258	72	2	CG8258
CG7831	70	1	non-claret disjunctional
CG4863	69	2	Ribosomal protein L3
CG7961	69	1	Coat Protein (coatomer) α
CG6699	68	1	Coat Protein (coatomer) β'
CG9674	68	1	CG9674
CG14750	67	1	Vacuolar protein sorting 25
CG1528	66	3	Coat Protein (coatomer) γ
CG7635	66	2	Mec2
CG8588	66	1	pastrel
CG6673	66	2	Glutathione S transferase O2
CG12233	65	1	lethal (1) G0156
CG13388	65	1	A kinase anchor protein 200
CG9328	65	1	CG9328
CG12005	65	2	Mms19
CG8495	65	2	Ribosomal protein S29

CG4225	65	2	Heavy metal tolerance factor 1
CG4265	63	1	Ubiquitin carboxy-terminal hydrolase
CG12262	63	1	CG12262
CG4800	63	1	Translationally controlled tumor protein
CG11527	62	2	Tiggrin
CG3981	62	1	Unc-76
CG6842	61	3	Vacuolar protein sorting 4
CG32306	61	2	CG32306
CG13391	60	1	Alanyl-tRNA synthetase
CG4046	60	2	Ribosomal protein S16
CG6846	60	1	Ribosomal protein L26
CG4429	59	1	RNA-binding protein 2
CG18408	59	1	CAP
CG4759	59	2	Ribosomal protein L27
CG10701	58	1	Moesin
CG31363	58	1	Jupiter
CG6598	57	1	Formaldehyde dehydrogenase
CG1404	57	1	ran
CG10944	57	2	Ribosomal protein S6
CG12306	56	1	polo
CG10385	56	5	male-specific lethal 1
CG7977	56	1	Ribosomal protein L23A
CG3262	55	1	CG3262
CG18174	54	1	Rpn11
CG15100	53	1	CG15100
CG12713	53	3	CG12713
CG10522	52	1	sticky
CG8882	52	1	Trip1
CG6223	51	2	Coat Protein (coatomer) β
CG9633	51	1	Replication Protein A 70
CG5433	51	1	Kinesin light chain
CG5688	51	1	Grip163
CG1837	51	2	pretaporter
CG2767	51	1	CG2767
CG1542	50	1	CG1542
CG30084	50	1	Z band alternatively spliced PDZ-motif protein 52
CG6944	49	2	Lamin
CG3752	49	1	Aldehyde dehydrogenase
CG7808	49	2	Ribosomal protein S8
CG7762	48	2	Rpn1
CG31022	48	1	prolyl-4-hydroxylase-alpha EFB
CG7915	48	1	Ect4
CG31617	47	2	His1:CG31617
CG3416	45	1	Mov34
CG5353	45	2	Threonyl-tRNA synthetase
CG6751	45	2	no child left behind
CG14996	45	1	Chd64
CG7913	44	1	PP2A-B'
CG11949	43	1	coracle
CG4651	43	2	Ribosomal protein L13
CG7434	43	1	Ribosomal protein L22
CG4236	43	1	Chromatin assembly factor 1 subunit
CG3226	43	2	CG3226
CG1666	41	1	Helicase
CG2033	41	1	Ribosomal protein S15Aa
CG6961	40	1	CG6961
CG9354	40	2	Ribosomal protein L34b
CG31453	40	1	pch2
CG8431	39	1	Cysteinyl-tRNA synthetase
CG3395	38	2	Ribosomal protein S9
CG1877	38	1	lin-19-like
CG1516	38	1	Pyruvate carboxylase
CG12244	38	1	licorne
CG7109	37	1	microtubule star
CG31289	37	1	Diphthamide methyltransferase
CG4523	37	1	PTEN-induced putative kinase 1
CG4954	37	1	eIF3-S8
CG7891	37	2	novel GTPase indispensable for equal segregation of chromosomes
CG1956	36	1	Roughened
CG9735	36	1	Tryptophanyl-tRNA synthetase
CG17528	36	1	CG17528
CG11228	36	1	hippo
CG6378	35	1	BM-40-SPARC
CG3415	35	1	peroxisomal Multifunctional enzyme type 2
CG17337	35	1	CG17337
CG8427	34	1	Small ribonucleoprotein particle protein SmD3
CG9436	34	1	CG9436
CG13345	34	2	tumbleweed
CG1065	33	1	Succinyl coenzyme A synthetase α subunit
CG10527	33	1	CG10527
CG10191	33	1	Proteome of centrioles 1
CG3127	32	1	Phosphoglycerate kinase
CG1088	32	1	Vacuolar H+-ATPase 26kD E subunit
CG10539	32	1	RPS6-p70-protein kinase
CG13955	32	2	CG13955
CG7722	32	2	Serpin 47C
CG8615	32	1	Ribosomal protein L18
CG8036	32	1	CG8036
CG4164	31	1	CG4164
CG31918	31	1	CG31918
CG5482	31	2	CG5482

CG18490	31	1	CG18490
CG14648	31	1	growl
CG15697	31	1	Ribosomal protein S30
CG4464	30	1	Ribosomal protein S19a
CG10206	30	1	nop5
CG17286	30	1	spindle defective 2
CG4535	30	1	FK506-binding protein FKBP59
CG12202	30	1	Nat1
CG17599	30	1	CG17599
CG12775	30	1	Ribosomal protein L21
CG6050	29	1	Elongation factor Tu mitochondrial
CG1387	29	1	CG1387
CG11154	28	1	ATP synthase, β subunit
CG6948	28	1	Clathrin light chain
CG5394	27	1	Glutamyl-prolyl-tRNA synthetase
CG6084	27	1	CG6084
CG2099	27	1	Ribosomal protein L35A
CG6904	27	1	Glycogen synthase
CG5857	27	1	Ndc1 ortholog
CG31549	27	1	CG31549
CG5915	26	1	Rab-protein 7
CG9983	25	1	Heterogeneous nuclear ribonucleoprotein at 98DE
CG7111	25	1	Receptor of activated protein kinase C 1
CG5726	25	1	CG5726
CG6822	25	1	ergic53
CG5366	24	1	Cullin-associated and neddylation-dissociated 1
CG1810	24	1	mRNA-capping-enzyme
CG10859	24	2	CG10859
CG8187	24	1	CG8187
CG7003	24	1	Msh6
CG5432	23	1	CG5432
CG17520	22	1	casein kinase IIα
CG7939	22	1	Ribosomal protein L32
CG8014	22	1	Receptor mediated endocytosis 8
CG3097	22	1	CG3097
CG10778	22	2	CG10778
CG4428	22	1	Autophagy-specific gene 4
CG6510	21	1	Ribosomal protein L18A
CG7269	21	1	Helicase at 25E
CG6382	21	1	Ef1α-like factor
CG4199	21	1	CG4199
CG14442	21	1	CG14442
CG4774	21	1	Cardiolipin synthase
CG1721	20	1	Phosphoglyceromutase
CG7144	20	1	lysine ketoglutarate reductase
CG8231	20	1	T-cp1ζ
CG4218	19	1	CG4218
CG3382	19	1	Organic anion transporting polypeptide 58Db
CG1475	19	1	Ribosomal protein L13A
CG10845	19	1	CG10845
CG8443	18	1	clueless
CG14457	18	3	CG14457
CG13213	17	1	fbl6

A.18 pMT-PrA-Cp110 +OA +MG132 purification from *Drosophila* cells

CG #	Score	#pep	Full name
CG4027	73719	1157	Actin 5C
CG12051	72277	1105	Actin 42A
CG15792	48614	826	zipper
CG18290	16058	477	Actin 87E
CG10067	16052	478	Actin 57B
CG3595	6610	131	spaghetti squash
CG3201	3457	57	Myosin light chain cytoplasmic
CG7438	3089	80	Myosin 31DF
CG10540	2707	99	capping protein alpha
CG9155	2486	57	Myosin 61F
CG4264	2440	54	Heat shock protein cognate 4
CG7558	1961	35	Actin-related protein 66B
CG1484	1806	42	flightless I
CG9277	1673	38	β-Tubulin at 56D
CG1913	1659	39	α-Tubulin at 84B
CG17158	1637	37	capping protein beta
CG31618	1511	20	His2A:CG31618
CG14617	1506	33	Cp110
CG2146	1496	40	dilute class unconventional myosin
CG10641	1336	37	CG10641
CG8280	1252	26	Elongation factor 1α48D
CG5695	1202	35	jaguar
CG1106	1201	36	Gelsolin
CG1977	1164	24	α Spectrin
CG1539	1133	21	tropomodulin
CG31196	1122	18	14-3-3ε
CG8472	1065	17	Calmodulin
CG8578	1046	31	CG8578
CG3401	1018	23	β-Tubulin at 60D
CG12008	996	31	karst
CG6831	860	14	rhea
CG9325	702	12	hu li tai shao
CG5499	685	11	Histone H2A variant
CG1242	550	21	Heat shock protein 83
CG9901	502	11	Actin-related protein 14D
CG3937	489	12	cheerio
CG8978	468	12	Suppressor of profilin 2
CG9748	435	8	belle
CG4147	396	6	Heat shock protein cognate 3
CG17291	389	6	Protein phosphatase 2A at 29B
CG4560	353	9	Arpc3A
CG4087	340	6	Ribosomal protein LP1
CG5870	337	7	β Spectrin
CG10954	333	8	Arc-p34
CG15784	315	8	CG15784
CG17870	314	6	14-3-3ζ
CG2331	310	5	TER94
CG4376	298	8	α actinin
CG4463	287	4	Heat shock protein 23
CG9012	281	6	Clathrin heavy chain
CG1258	275	4	pavarotti
CG6148	268	5	Putative Achaete Scute Target 1
CG10811	251	3	eukaryotic translation initiation factor 4G
CG1883	250	6	Ribosomal protein S7
CG1782	245	6	Ubiquitin activating enzyme 1
CG18572	244	6	rudimentary
CG7033	230	4	CG7033
CG8983	217	7	ERp60
CG9881	214	4	p16-ARC
CG8309	213	6	Transport and Golgi organization 7
CG4898	212	5	Tropomyosin 1
CG5502	210	5	Ribosomal protein L4
CG4145	203	4	Collagen type IV
CG5119	194	8	polyA-binding protein
CG12030	191	4	UDP-galactose 4'-epimerase
CG4183	189	6	Heat shock protein 26
CG5825	183	4	Histone H3.3A
CG31613	177	5	His3:CG31613
CG14996	175	2	Chd64
CG3379	174	4	Histone H4 replacement
CG11522	170	4	Ribosomal protein L6
CG5972	167	4	Arc-p20
CG14792	165	2	stubarista
CG7507	165	2	Dynein heavy chain 64C
CG7490	160	4	Ribosomal protein LP0
CG1263	152	3	Ribosomal protein L8
CG31617	146	5	His1:CG31617
CG4265	144	3	Ubiquitin carboxy-terminal hydrolase
CG3751	143	4	Ribosomal protein S24
CG17654	139	5	Enolase
CG4466	136	3	Heat shock protein 27
CG7073	134	2	sar1
CG3523	124	2	Fatty acid synthase 1
CG17272	124	4	CG17272
CG5020	123	2	Cytoplasmic linker protein 190
CG14207	122	3	HspB8
CG3011	121	2	CG3011
CG6699	120	2	Coat Protein (coatomer) β'
CG2238	118	4	Elongation factor 2b
CG7762	118	3	Rpn1
CG8055	111	1	shrub
CG7967	110	2	CG7967
CG1528	108	2	Coat Protein (coatomer) γ
CG8977	101	2	Cctγ
CG16858	101	2	viking
CG9423	99	2	karyopherin α3
CG3455	99	1	Rpt4
CG32164	98	2	CG32164
CG17521	97	2	Qm
CG9281	96	3	CG9281
CG10922	94	2	La autoantigen-like
CG15717	93	1	CG15717
CG9282	92	1	Ribosomal protein L24
CG10652	92	1	Ribosomal protein L30
CG8900	90	2	Ribosomal protein S18
CG40045	89	1	CG40045
CG5374	87	2	Tcp1-like
CG14709	86	1	Multidrug resistance protein 4 ortholog
CG4897	85	2	Ribosomal protein L7
CG3314	85	4	Ribosomal protein L7A
CG10230	85	2	Rpn9
CG17949	82	4	His2B:CG17949
CG9579	80	1	Annexin X
CG3299	79	1	Vinculin
CG1059	77	6	Karyopherin β 3
CG8922	76	3	Ribosomal protein S5a
CG3949	75	2	hoi-polloi
CG30349	75	1	CG30349
CG15099	73	1	CG15099

CG9311	73	1	myopic
CG6944	72	2	Lamin
CG6598	72	1	Formaldehyde dehydrogenase
CG9888	71	2	Fibrillarin
CG10377	71	2	Heterogeneous nuclear ribonucleoprotein at 27C
CG7961	71	3	Coat Protein (coatomer) α
CG10527	71	2	CG10527
CG3821	70	1	Aspartyl-tRNA synthetase
CG8439	69	1	T-complex Chaperonin 5
CG13345	69	3	RacGAP50C
CG7831	67	1	non-claret disjunctional
CG7595	66	2	crinkled
CG3922	65	2	Ribosomal protein S17
CG13388	65	2	A kinase anchor protein 200
CG10990	65	1	Programmed cell death 4 ortholog
CG6522	65	2	Testin ortholog
CG8351	65	1	Tcp-1η
CG6988	63	3	Protein disulfide isomerase
CG7935	63	1	moleskin
CG4157	63	1	Rpn12
CG13849	63	1	Nop56
CG9429	61	1	Calreticulin
CG11276	61	2	Ribosomal protein S4
CG3416	59	2	Mov34
CG10385	59	5	male-specific lethal 1
CG15693	59	2	Ribosomal protein S20
CG12262	59	1	CG12262
CG4878	58	1	eIF3-S9
CG4759	58	2	Ribosomal protein L27
CG17489	58	2	Ribosomal protein L5
CG14206	58	2	Ribosomal protein S10b
CG1524	56	1	Ribosomal protein S14a
CG4799	56	2	Pendulin
CG10596	56	2	Msr-110
CG13391	56	1	Alanyl-tRNA synthetase
CG4912	56	1	eEF1δ
CG12005	56	1	Mms19
CG31764	56	1	virus-induced RNA 1
CG9075	55	2	Eukaryotic initiation factor 4a
CG7439	54	1	Argonaute 2
CG2092	54	1	scraps
CG10522	53	1	sticky
CG10863	52	1	CG10863
CG5170	50	1	Dodeca-satellite-binding protein 1
CG8235	49	1	aaRS-interacting multifunctional protein 1
CG31453	48	1	pch2
CG6223	47	1	Coat Protein (coatomer) β
CG10944	47	2	Ribosomal protein S6
CG1837	46	1	pretaporter
CG9436	46	1	CG9436
CG6090	46	1	Ribosomal protein L34a
CG13389	45	1	Ribosomal protein S13
CG11527	45	1	Tiggrin
CG16916	45	2	Rpt3
CG4046	44	1	Ribosomal protein S16
CG1877	43	1	lin-19-like
CG14066	42	1	La related protein
CG8231	41	1	T-cp1ζ
CG11271	41	1	Ribosomal protein S12
CG13349	40	1	Regulatory particle non-ATPase 13
CG3195	40	1	Ribosomal protein L12
CG14648	40	3	growl
CG2767	40	1	CG2767
CG4429	39	1	RNA-binding protein 2
CG8332	38	1	Ribosomal protein S15
CG1345	38	4	Glutamine:fructose-6-phosphate aminotransferase 2
CG6684	37	1	Ribosomal protein S25
CG17599	37	1	CG17599
CG15100	37	1	Methionyl-tRNA synthetase
CG1387	36	1	CG1387
CG4225	36	1	Heavy metal tolerance factor 1
CG1542	36	1	CG1542
CG10161	36	1	Eukaryotic initiation factor 3 p66
			subunit
CG3226	35	1	CG3226
CG7722	35	4	Serpin 47C
CG7182	34	1	CG7182
CG2216	33	1	Ferritin 1 heavy chain homologue
CG4863	33	1	Ribosomal protein L3
CG10191	33	1	Proteome of centrioles 1
CG11984	33	1	CG11984
CG5450	32	1	Cytoplasmic dynein light chain 2
CG4535	32	1	FK506-binding protein FKBP59
CG6846	32	1	Ribosomal protein L26
CG8036	31	2	CG8036
CG15697	31	1	Ribosomal protein S30
CG5394	29	1	Glutamyl-prolyl-tRNA synthetase
CG6092	29	1	Dak1
CG11888	28	1	Rpn2
CG15102	28	1	Juvenile hormone epoxide hydrolase 2
CG8615	28	1	Ribosomal protein L18
CG3333	28	1	Nucleolar protein at 60B
CG4651	27	1	Ribosomal protein L13
CG3203	27	2	Ribosomal protein L17
CG9819	26	1	Calcineurin A at 14F
CG3186	26	1	eIF-5A
CG8588	26	1	pastrel
CG2168	25	1	Ribosomal protein S3A
CG5720	25	1	CG5720
CG9273	25	1	Replication protein A2
CG7891	25	1	novel GTPase indispensable for equal segregation of chromosomes
CG8863	25	1	DnaJ-like-2
CG9553	24	1	chickadee
CG1065	24	1	Succinyl coenzyme A synthetase α subunit
CG1721	24	1	Phosphoglyceromutase
CG1444	24	1	CG1444
CG1810	24	1	mRNA-capping-enzyme
CG10638	24	1	CG10638
CG7003	24	1	Msh6
CG14457	24	1	CG14457
CG9738	23	1	MAP kinase kinase 4
CG7999	23	1	Mediator complex subunit 24
CG3996	23	1	CG3996
CG5432	23	1	CG5432
CG3981	23	1	Unc-76
CG30115	23	2	Guanine nucleotide exchange factor in mesoderm
CG2050	22	1	modulo
CG5353	22	1	Threonyl-tRNA synthetase
CG1691	22	1	IGF-II mRNA-binding protein
CG31332	22	1	unc-115
CG15804	21	1	Dynein heavy chain at 62B
CG5352	21	1	Small ribonucleoprotein particle protein SmB
CG2830	20	1	Heat shock protein 60 related
CG1822	20	1	bifocal
CG5726	20	1	CG5726
CG3382	20	1	Organic anion transporting polypeptide 58Db
CG4832	19	1	centrosomin
CG7207	19	1	ceramide transfer protein
CG10778	19	1	CG10778
CG32458	19	1	neuromusculin
CG3661	18	1	Ribosomal protein L23
CG12532	18	1	Adaptor Protein complex 1/2, β subunit
CG18076	18	1	short stop
CG4236	18	1	Chromatin assembly factor 1 subunit
CG2774	18	1	Sorting nexin 1
CG17028	17	1	CG17028

A.19 pMT-CP110-PrA +OA +MG132 purification from *Drosophila* cells

CG #	Score	#pep	Full name
CG1913	8208	282	α-Tubulin at 84B
CG15792	7953	167	zipper
CG4183	7393	128	Heat shock protein 26
CG4264	7345	181	Heat shock protein cognate 4
CG9277	6607	224	β-Tubulin at 56D
CG4027	4349	110	Actin 5C
CG14617	2607	72	Cp110
CG4463	2549	53	Heat shock protein 23
CG18572	2293	56	rudimentary
CG3401	2154	41	β-Tubulin at 60D
CG10067	1811	58	Actin 57B
CG5834	1472	34	Hsp70Bbb
CG18743	1396	32	Heat-shock-protein-70Ab
CG4869	1225	26	β-Tubulin at 97EF
CG12101	1225	24	Heat shock protein 60
CG5436	1185	26	Heat shock protein 68
CG4147	1109	26	Heat shock protein cognate 3
CG6453	1068	31	CG6453
CG8280	983	23	Elongation factor 1α48D
CG17291	851	16	Protein phosphatase 2A at 29B
CG3595	818	19	spaghetti squash
CG12233	797	19	lethal (1) G0156
CG6815	693	14	belphegor
CG3201	661	12	Myosin light chain cytoplasmic
CG31618	660	9	His2A:CG31618
CG1569	640	14	rough deal
CG1528	624	14	Coat Protein (coatomer) γ

CG10811	617	10	eukaryotic translation initiation factor 4G
CG5366	616	16	CG5366
CG14476	615	16	CG14476
CG7507	603	15	Dynein heavy chain 64C
CG11963	581	10	skpA associated protein
CG17870	567	9	14-3-3ζ
CG9155	534	15	Myosin 61F
CG1548	523	9	cathD
CG31196	510	11	14-3-3ε
CG7961	509	21	Coat Protein (coatomer) α
CG7769	509	8	piccolo
CG1242	501	15	Heat shock protein 83
CG7935	498	12	moleskin
CG7439	490	20	Argonaute 2
CG32164	488	9	CG32164
CG6223	481	13	Coat Protein (coatomer) β
CG9748	479	12	belle
CG4466	444	14	Heat shock protein 27
CG1884	441	7	Not1
CG5520	426	10	Glycoprotein 93
CG31022	423	13	prolyl-4-hydroxylase-alpha EFB
CG9012	421	11	Clathrin heavy chain
CG5252	420	8	Ranbp9
CG6699	405	11	Coat Protein (coatomer) β'
CG1059	404	7	Karyopherin β 3
CG8947	390	7	26-29kD-proteinase
CG9674	388	10	CG9674
CG10535	380	6	Elongator complex protein 1
CG8571	375	5	smallminded
CG16916	370	8	Rpt3
CG1977	352	10	α Spectrin
CG9888	344	12	Fibrillarin
CG14472	339	9	purity of essence
CG17870	328	8	14-3-3ζ
CG2238	319	16	Elongation factor 2b
CG8309	262	6	Transport and Golgi organization 7
CG10938	250	3	Proteasome α5 subunit
CG10360	248	6	refractory to sigma P
CG3210	247	6	Dynamin related protein 1
CG14792	241	4	stubarista
CG10370	241	8	Tat-binding protein-1
CG10206	240	6	nop5
CG11154	236	5	ATP synthase, β subunit
CG2331	235	7	TER94
CG7438	233	8	Myosin 31DF
CG5330	222	4	Nucleosome assembly protein 1
CG10596	220	4	Msr-110
CG1516	217	5	CG1516
CG4389	217	9	CG4389
CG8863	215	6	DnaJ-like-2
CG8472	214	6	Calmodulin
CG11943	213	5	CG11943
CG14637	205	4	abstrakt
CG11198	201	2	Acetyl-CoA carboxylase
CG14648	201	6	growl
CG6476	200	5	Suppressor of variegation 3-9
CG10540	200	6	capping protein alpha
CG5949	196	4	DNA-polymerase-δ
CG16944	195	7	stress-sensitive B
CG10080	190	6	mahjong
CG5934	190	2	CG5934
CG2146	189	6	dilute class unconventional myosin
CG12008	188	5	karst
CG1341	186	7	Rpt1
CG18174	185	4	Rpn11
CG1591	185	4	REG
CG9282	184	2	Ribosomal protein L24
CG10289	183	2	CG10289
CG1883	179	4	Ribosomal protein S7
CG4145	178	5	Collagen type IV
CG3422	177	3	Proteasome 28kD subunit 1
CG32626	177	2	AMP deaminase
CG9946	173	5	eukaryotic translation Initiation Factor 2α
CG11888	173	5	Rpn2
CG4164	172	3	CG4164
CG4581	171	8	Thiolase
CG10230	171	3	Rpn9
CG9819	169	7	Calcineurin A at 14F
CG7762	167	8	Rpn1
CG9842	166	5	Protein phosphatase 2B at 14D
CG13849	160	5	Nop56
CG14996	157	4	Chd64
CG1851	153	2	Ady43A
CG6439	153	5	CG6439
CG5499	152	3	Histone H2A variant
CG5119	151	4	polyA-binding protein
CG9539	150	3	Sec61 α subunit
CG6303	149	3	Bruce
CG2960	147	4	Ribosomal protein L40
CG11700	146	5	CR11700
CG8963	142	2	CG8963
CG6050	140	3	Elongation factor Tu mitochondrial
CG10641	138	4	CG10641
CG1683	137	6	Adenine nucleotide translocase 2
CG1489	136	4	Pros45
CG3612	133	4	bellwether
CG8351	133	3	Tcp-1η
CG9325	132	4	hu li tai shao
CG5064	128	2	Srp68
CG11793	127	2	Superoxide dismutase
CG3455	127	2	Rpt4
CG2216	126	2	Ferritin 1 heavy chain homologue
CG3379	125	4	Histone H4 replacement
CG6459	125	1	CG6459
CG11228	125	2	hippo
CG8996	124	1	walrus
CG32210	124	2	Listerin E3 ubiquitin protein ligase 1
CG8231	123	4	T-cp1ζ
CG7033	123	3	CG7033
CG9900	122	4	mitotic 15
CG3523	122	3	Fatty acid synthase 1
CG3961	120	2	CG3961
CG6988	119	3	Protein disulfide isomerase
CG5504	117	3	lethal (2) tumorous imaginal discs
CG7885	117	2	RNA polymerase II 33kD subunit
CG8798	117	2	Lon protease
CG9327	117	3	Proteasome 29kD subunit
CG8287	116	2	Rab-protein 8
CG17158	115	4	capping protein beta
CG31764	115	3	virus-induced RNA 1
CG3937	114	2	cheerio
CG8715	114	1	lingerer
CG14207	113	3	HspB8
CG7070	112	3	Pyruvate kinase
CG7808	112	2	Ribosomal protein S8
CG5374	111	3	Tcp1-like
CG33162	111	3	Signal recognition particle receptor β
CG4260	111	3	Adaptor Protein complex 2, α subunit
CG33180	110	2	Ranbp16
CG10753	109	2	Small ribonucleoprotein particle protein SmD1
CG10630	106	2	blanks
CG15433	105	1	Elongator complex protein 3
CG4087	104	2	Ribosomal protein LP1
CG12306	104	5	polo
CG4858	104	2	CG4858
CG12005	104	3	Mms19
CG1666	103	3	Helicase
CG8882	102	3	Trip1
CG31794	101	3	Paxillin
CG7831	99	2	non-claret disjunctional
CG3725	98	2	Calcium ATPase at 60A
CG5266	98	2	Proteasome 25kD subunit
CG8977	98	3	Cctγ
CG3949	98	2	hoi-polloi
CG14813	98	4	Coat Protein (coatomer) δ
CG10198	98	1	Nucleoporin 98
CG3265	97	1	Eb1
CG3180	96	4	RNA polymerase II 140kD subunit
CG6692	96	3	Cysteine proteinase-1
CG1092	95	2	CG1092
CG11999	95	3	CG11999
CG12202	93	1	Nat1
CG10484	93	2	Regulatory particle non-ATPase 3
CG9677	92	3	Int6 homologue
CG4878	91	2	eIF3-S9
CG11984	91	1	CG11984
CG3981	91	1	Unc-76
CG10701	90	2	Moesin
CG6617	90	1	CG6617
CG5028	89	4	CG5028
CG17484	88	2	Adherens junction protein p120
CG2637	87	2	Female sterile (2) Ketel
CG9124	87	2	Eukaryotic initiation factor 3 p40 subunit
CG7144	86	3	lysine ketoglutarate reductase
CG6521	86	1	Signal transducing adaptor molecule
CG15784	86	2	CG15784
CG3980	84	3	Cep97
CG4033	83	2	RNA polymerase I 135kD subunit
CG11276	83	1	Ribosomal protein S4
CG10805	83	4	lethal (2) k09022
CG5684	83	4	Pop2
CG3585	82	2	Rabconnectin-3A
CG4897	81	2	Ribosomal protein L7
CG7619	81	1	Proteasome 54kD subunit
CG16858	81	3	viking
CG33554	81	2	Nipped-A
CG13349	79	1	Regulatory particle non-ATPase 13
CG5651	79	2	pixie
CG5170	78	2	Dodeca-satellite-binding protein 1
CG3752	77	1	Aldehyde dehydrogenase
CG18495	77	1	Proteasome α1 subunit
CG9484	75	2	hyperplastic discs
CG7074	75	1	missing oocyte
CG6756	75	1	Translocase of outer membrane 70
CG2118	75	1	CG2118
CG30084	75	2	Z band alternatively spliced PDZ-motif protein 52
CG4254	74	1	twinstar

CG13387	74	1	embargoed
CG31739	74	2	Aspartyl-tRNA synthetase, mitochondrial
CG7490	73	3	Ribosomal protein LP0
CG3661	73	2	Ribosomal protein L23
CG8900	73	2	Ribosomal protein S18
CG2206	73	3	lethal (1) G0193
CG4659	72	1	Signal recognition particle protein 54k
CG31137	72	1	twin
CG8578	72	2	CG8578
CG5650	71	1	Protein phosphatase 1 at 87B
CG6948	71	2	Clathrin light chain
CG7558	70	1	Actin-related protein 66B
CG6998	70	3	cut up
CG5604	70	2	CG5604
CG12264	70	5	CG12264
CG11856	70	1	Nucleoporin 358
CG10149	69	2	Proteasome p44.5 subunit
CG17746	69	1	CG17746
CG4738	69	1	Nucleoporin 160
CG5974	68	2	pelle
CG9769	68	1	CG9769
CG12163	68	2	CG12163
CG1600	67	2	Death resistor Adh domain containing target
CG10527	67	4	CG10527
CG5394	65	1	Glutamyl-prolyl-tRNA synthetase
CG12792	65	1	lethal (2) 09851
CG1987	65	1	Rbp1-like
CG3751	65	1	Ribosomal protein S24
CG5495	65	3	Thioredoxin-like
CG4003	65	2	pontin
CG5363	64	1	cdc2
CG1524	64	1	Ribosomal protein S14a
CG4257	64	1	Signal-transducer and activator of transcription protein at 92E
CG9088	64	2	little imaginal discs
CG9750	64	1	reptin
CG7726	63	1	Ribosomal protein L11
CG4821	63	2	Tequila
CG7375	63	1	Ubiquitin conjugating enzyme E2M
CG12532	62	2	Adaptor Protein complex 1/2, β subunit
CG14750	62	2	Vacuolar protein sorting 25
CG6095	62	1	exo84
CG5920	61	2	string of pearls
CG6235	61	1	twins
CG17498	61	1	mad2
CG4800	60	1	Translationally controlled tumor protein
CG12019	59	1	Cdc37
CG5838	59	1	DNA replication-related element factor
CG12737	59	1	Calmodulin-binding protein related to a Rab3 GDP/GTP exchange protein
CG15618	59	1	CG15618
CG5608	59	2	CG5608
CG17272	59	1	CG17272
CG6944	58	1	Lamin
CG2520	58	1	like-AP180
CG9086	58	2	Ubr1 ubiquitin ligase
CG7945	58	1	CG7945
CG18596	58	1	CG18596
CG5837	57	1	HEM-protein
CG9940	57	2	CG9940
CG6840	57	1	Rpb11
CG1657	56	1	CG1657
CG8266	56	2	sec31
CG6904	56	1	Glycogen synthase
CG3423	55	1	Stromalin
CG9351	55	1	falafel
CG1049	55	1	CTP:phosphocholine cytidylyltransferase 1
CG17654	54	1	Enolase
CG1484	54	2	flightless I
CG10663	54	4	CG10663
CG13388	53	1	A kinase anchor protein 200
CG2099	53	1	Ribosomal protein L35A
CG4747	53	2	CG4747
CG5502	52	2	Ribosomal protein L4
CG32075	52	1	CG32075
CG1106	51	2	Gelsolin
CG12244	51	2	licorne
CG10376	51	1	CG10376
CG32138	50	2	CG32138
CG10392	50	1	super sex combs
CG10305	49	1	Ribosomal protein S26
CG9805	49	2	eIF3-S10
CG9684	49	1	CG9684
CG8978	48	1	Suppressor of profilin 2
CG8439	48	1	T-complex Chaperonin 5
CG3373	48	1	Hemomucin
CG6092	48	2	Dak1
CG5525	48	1	CG5525
CG5902	48	1	CG5902
CG11522	48	1	Ribosomal protein L6
CG10161	48	1	Eukaryotic initiation factor 3 p66 subunit
CG7863	47	1	dream
CG13900	47	2	CG13900
CG7324	47	2	CG7324
CG4931	47	2	specifically Rac1-associated protein 1
CG10652	46	1	Ribosomal protein L30
CG6444	46	1	Dpy-30-like 1
CG3209	46	1	CG3209
CG7870	46	1	wollknaeuel
CG6148	45	1	Putative Achaete Scute Target 1
CG7398	45	2	Transportin
CG7915	45	2	Ect4
CG2097	45	2	Symplekin
CG8542	44	1	Heat shock protein cognate 5
CG6647	44	1	porin
CG9901	44	1	Actin-related protein 14D
CG4199	44	1	CG4199
CG5378	44	1	Rpn7
CG4898	43	1	Tropomyosin 1
CG11981	43	1	Proteasome β3 subunit
CG8478	43	1	CG8478
CG9423	42	1	karyopherin α3
CG8368	42	1	CG8368
CG18102	41	1	shibire
CG4046	41	1	Ribosomal protein S16
CG8588	41	2	pastrel
CG3061	41	1	CG3061
CG31332	41	1	unc-115
CG9633	40	1	Replication Protein A 70
CG7917	40	1	Nucleoplasmin
CG6768	40	1	DNA polymerase ε 255kD subunit
CG9581	40	1	CG9581
CG17949	40	2	His2B:CG17949
CG17520	39	2	casein kinase IIα
CG10385	39	2	male-specific lethal 1
CG5422	39	1	Rox8
CG7581	39	2	Bub3
CG40478	39	1	Dyrk3
CG3756	39	1	CG3756
CG7791	39	1	CG7791
CG4954	39	1	eIF3-S8
CG1651	38	2	Ankyrin
CG9543	38	1	Coat Protein (coatomer) ε
CG8415	38	1	Ribosomal protein S23
CG16908	38	1	CG16908
CG2684	37	1	lodestar
CG4978	37	1	Minichromosome maintenance 7
CG4261	37	1	Helicase 89B
CG1782	37	1	Ubiquitin activating enzyme 1
CG8740	37	1	CG8740
CG1945	36	1	fat facets
CG3957	36	1	wing morphogenesis defect
CG8036	36	1	CG8036
CG7434	35	1	Ribosomal protein L22
CG5092	35	2	Target of rapamycin
CG5972	35	1	Arc-p20
CG13389	34	1	Ribosomal protein S13
CG6378	34	1	BM-40-SPARC
CG3186	34	2	eIF-5A
CG4153	33	1	Eukaryotic initiation factor 2β
CG4429	33	1	RNA-binding protein 2
CG5695	33	3	jaguar
CG2028	33	1	Casein kinase Iα
CG11092	33	1	Nucleoporin 93kD-1
CG10212	33	1	SMC2
CG9031	33	1	icarus
CG1387	33	4	CG1387
CG6831	33	1	rhea
CG10236	32	1	Laminin A
CG9209	32	1	vacuolar peduncle
CG1810	32	2	mRNA-capping-enzyme
CG5688	31	1	Grip163
CG2064	31	1	CG2064
CG10315	31	1	eIF2B-δ
CG2692	30	2	gooseberry-neuro
CG16973	30	2	misshapen
CG6177	30	1	ldlCp-related protein
CG7041	30	1	HP1b
CG3004	30	1	CG3004
CG3714	30	1	CG3714
CG6509	30	1	Discs large 5
CG13277	30	1	CG13277
CG1512	30	1	Cullin-2
CG8632	30	1	Zinc transporter 49B
CG15099	30	1	CG15099
CG7595	29	1	crinkled
CG9999	29	1	Ran GTPase activating protein
CG15693	29	1	Ribosomal protein S20
CG1100	29	2	Rpn5
CG12225	29	1	Spt6
CG2941	29	1	CG2941
CG6428	29	1	CG6428
CG7865	29	1	PNGase-like
CG8983	29	1	ERp60
CG3996	29	2	CG3996
CG12070	28	1	Saposin-related
CG16721	28	1	CG16721
CG9281	28	1	CG9281

CG10306	28	1	CG10306
CG12262	28	1	CG12262
CG3308	28	2	CG3308
CG4960	28	1	CG4960
CG10992	27	1	Cathepsin B1
CG8002	27	1	rapamycin-insensitive companion of Tor
CG33926	27	1	CG33926
CG2210	26	1	abnormal wing discs
CG6899	26	1	Protein tyrosine phosphatase 4E
CG4651	26	1	Ribosomal protein L13
CG1428	26	1	CG1428
CG6543	26	1	CG6543
CG12030	26	1	UDP-galactose 4'-epimerase
CG2767	26	1	CG2767
CG1708	25	1	costa
CG12348	25	1	Shaker
CG10944	25	1	Ribosomal protein S6
CG13745	25	1	Fanconi anemia complementation group I homologue
CG4729	25	1	CG4729
CG2917	24	1	Origin recognition complex subunit 4
CG9060	24	1	Zpr1
CG14224	24	1	Ubiquilin
CG7219	24	2	Serpin 28D
CG31551	24	1	CG31551
CG1721	23	1	Phosphoglyceromutase
CG17528	23	1	CG17528
CG7003	23	1	Msh6
CG2929	23	1	Pi4KIIα
CG13609	23	1	CG13609
CG5432	23	1	CG5432
CG9983	22	1	Heterogeneous nuclear ribonucleoprotein at 98DE
CG1483	22	1	Microtubule-associated protein 205
CG6545	22	1	ladybird early
CG4083	22	1	Mo25
CG5168	22	1	CG5168
CG6751	22	2	no child left behind
CG8487	22	1	gartenzwerg
CG8443	22	1	clueless
CG4572	22	1	CG4572
CG11790	22	1	CG11790
CG1800	22	1	partner of drosha
CG4097	21	1	Proteasome 26kD subunit

CG3431	21	1	Ubiquitin C-terminal hydrolase
CG2168	21	1	Ribosomal protein S3A
CG5796	21	1	Protoporphyrinogen oxidase
CG9291	21	1	Elongin C
CG15667	21	1	Smad anchor for receptor activation
CG4994	21	1	Mitochondrial phosphate carrier protein
CG4218	21	1	CG4218
CG10778	21	1	CG10778
CG14213	21	1	Required for cell differentiation 1 ortholog
CG17593	21	1	CG17593
CG11887	21	2	Elongator complex protein 2
CG18176	21	1	deflated
CG3711	21	1	CG3711
CG33715	21	1	Muscle-specific protein 300
CG6551	20	1	fused
CG1112	20	1	α-Esterase-7
CG9212	20	1	Nipsnap
CG13096	20	1	CG13096
CG8709	20	1	Lipin
CG8332	20	1	Ribosomal protein S15
CG3382	20	1	Organic anion transporting polypeptide 58Db
CG6432	20	1	CG6432
CG4849	20	1	CG4849
CG12750	20	1	nucampholin
CG11471	19	1	Isoleucyl-tRNA synthetase
CG5729	19	1	Dgp-1
CG6718	19	1	calcium-independent phospholipase A2 VIA
CG10585	19	1	CG10585
CG6042	19	1	Cyp12a4
CG10712	19	1	Chromator
CG15105	18	1	another B-box affiliate
CG6811	18	1	RhoGAP68F
CG3359	18	1	midline fasciclin
CG8014	17	1	Receptor mediated endocytosis 8
CG13325	17	1	CG13325
CG34130	17	1	CG34130

Appendix B: Autoradiograms of *in vitro* studies.

A-H showing autoradiographic signals from binding assays of ^{35}S-Methionine-labelled centriole duplication proteins with (A) GST-Ana2, (B) Asl-GST, (C) GST-Cep97, (D) GST-CP110 1/3, (E) GST-CP110 3/3, (F) MBP-Plk4, (G) GST-Rcd4, and (H) GST-Sas4 immobilised on resin; the according negative control (GST- or MBP-alone immobilised on resin; and 1% input of the ^{35}S-Methionine-labelled centriole duplication protein used in each binding assay. Autoradiographic signals were applied to categorise the analysed direct protein-protein interactions into weak, good, strong and no interaction in Table 3-3.

A) *In vitro* interaction with GST-Ana2

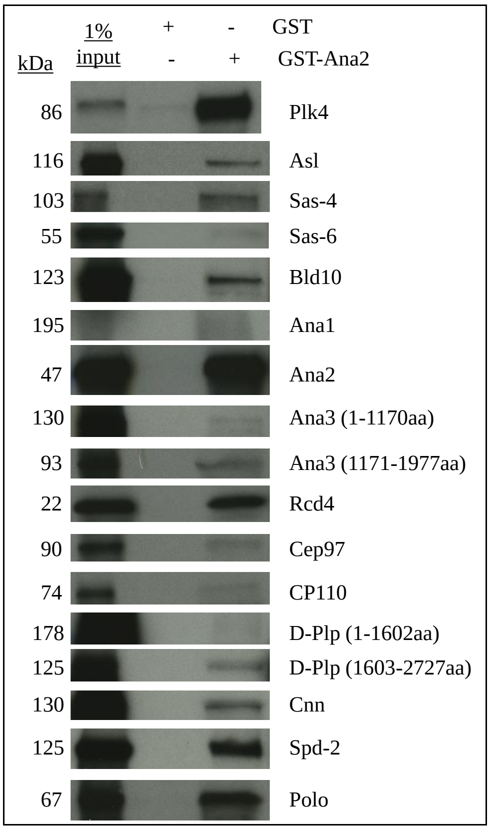

B) *In vitro* Interaction with Asl-GST

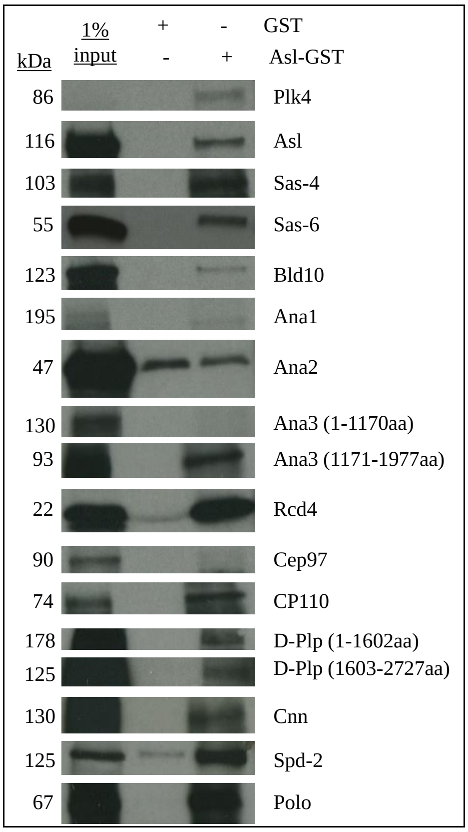

C) *In vitro* interaction with GST-Cep97

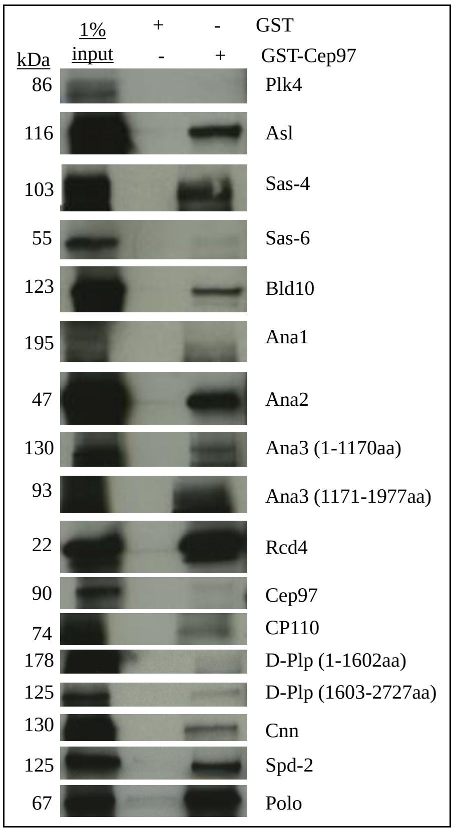

D) *In vitro* Interaction with GST-CP110 1/3

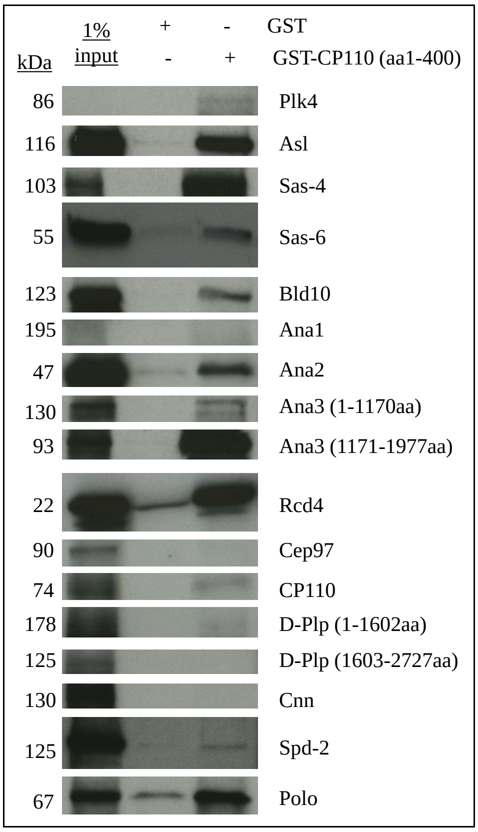

E) *In vitro* interaction with GST-CP110 2/3

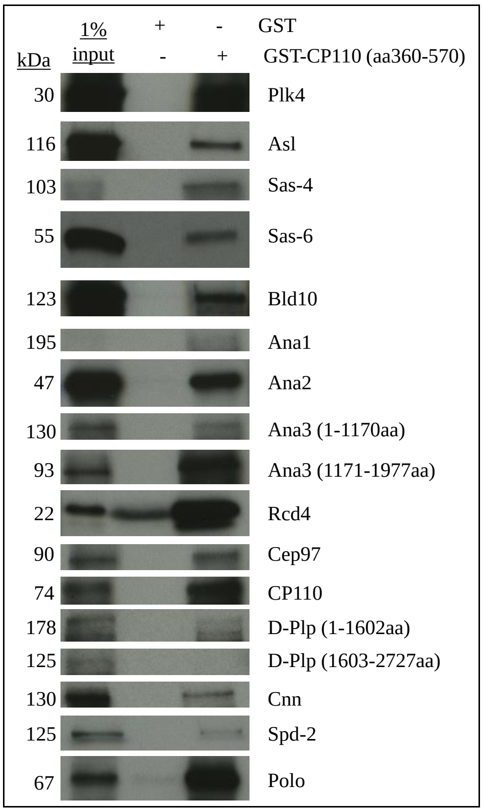

F) *In vitro* Interaction with MBP-Plk4

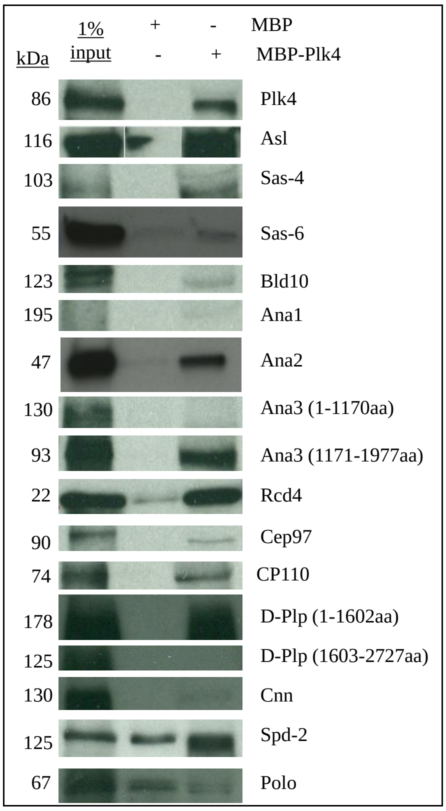

G) *In vitro* interaction with GST-Rcd4

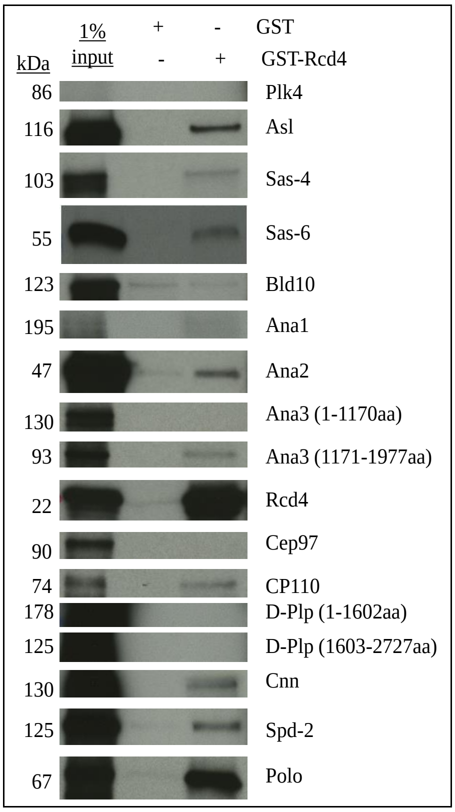

H) *In vitro* Interaction with GST-Sas4

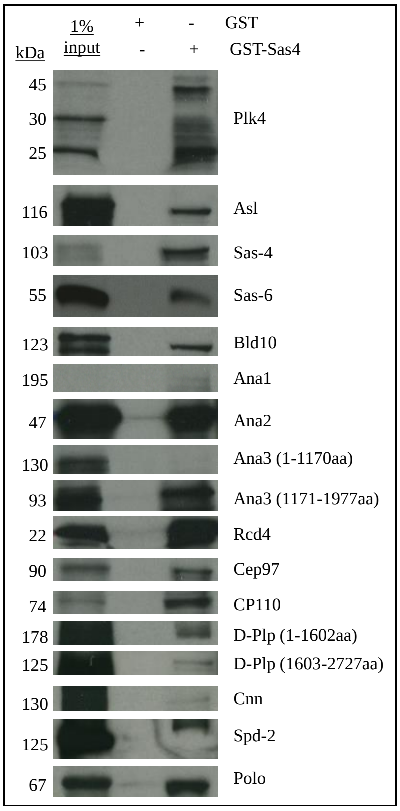

Appendix C: Mass spectrometry results from purifications of centriole duplication proteins from cultured *Drosophila* cells and syncytial *Drosophila* embryos.

Tables show the full list of hits identified from the stated purification; indicating CG numbers, Mascot scores, Number of peptides (#pep), and the Full name of the protein if available. Tables are supplementary to Table 5-1 and Table 5-2.

C.1 pMT-PrA-Sas6 +MG132 purification from *Drosophila* cells

CG #	Score	#pep	Full name
CG15524	4576	281	spindle assembly abnormal 6
CG4264	1587	111	Heat shock protein cognate 4
CG9277	1404	51	β-Tubulin at 56D
CG1913	919	47	α-Tubulin at 84B
CG3401	329	19	β-Tubulin at 60D
CG5834	299	23	Hsp70Bbb
CG1524	223	6	Ribosomal protein S14a
CG4463	198	9	Heat shock protein 23
CG7434	175	6	Ribosomal protein L22
CG2960	139	4	Ribosomal protein L40
CG12051	114	5	Actin 42A
CG4466	94	3	Heat shock protein 27
CG11522	87	3	Ribosomal protein L6
CG8274	84	2	Megator
CG15697	84	3	Ribosomal protein S30
CG4183	83	3	Heat shock protein 26
CG3201	81	3	Myosin light chain cytoplasmic
CG6684	76	2	Ribosomal protein S25
CG10944	76	4	Ribosomal protein S6
CG12775	73	1	Ribosomal protein L21
CG33052	69	5	CG33052
CG7808	64	3	Ribosomal protein S8
CG6253	62	3	Ribosomal protein L14
CG9282	61	3	Ribosomal protein L24
CG13389	60	2	Ribosomal protein S13
CG11276	59	1	Ribosomal protein S4
CG1354	59	3	CG1354
CG9795	57	1	CG9795
CG4087	56	2	Ribosomal protein LP1
CG2746	56	1	Ribosomal protein L19
CG3395	54	3	Ribosomal protein S9
CG10824	54	1	Common Dpr-interacting protein
CG8900	52	1	Ribosomal protein S18
CG10465	50	2	CG10465
CG1873	49	1	Elongation factor 1α100E
CG15442	49	1	Ribosomal protein L27A
CG7622	48	1	Ribosomal protein L36
CG12109	47	2	Caf1-180
CG2168	46	2	Ribosomal protein S3A
CG11734	46	1	HERC2
CG5119	44	1	polyA-binding protein
CG4651	44	1	Ribosomal protein L13
CG1821	44	1	Ribosomal protein L31
CG3203	44	1	Ribosomal protein L17
CG8615	44	2	Ribosomal protein L18
CG2050	42	2	modulo
CG4863	42	1	Ribosomal protein L3
CG9680	41	1	Dead box protein 73D
CG2998	41	1	Ribosomal protein S28b
CG17521	40	1	Qm
CG4897	38	2	Ribosomal protein L7
CG14025	37	1	Blastoderm-specific gene 25D
CG5920	35	1	string of pearls
CG3253	35	1	CG3253
CG7490	34	1	Ribosomal protein LP0
CG4631	34	2	CG4631
CG8735	34	1	CG8735
CG17034	34	1	CG17034
CG7946	31	1	CG7946
CG6846	30	1	Ribosomal protein L26
CG8415	29	1	Ribosomal protein S23
CG8947	28	1	26-29kD-proteinase
CG1506	27	1	Ac3
CG31551	27	2	CG31551
CG7283	25	1	Ribosomal protein L10Ab
CG6773	0	1	sec13

C.2 pMT-PrA-Sas6 +OA +MG132 purification from *Drosophila* cells

CG #	Score	#pep	Full name
CG15524	4606	280	spindle assembly abnormal 6
CG15792	1530	86	zipper
CG4264	1499	83	Heat shock protein cognate 4
CG4027	974	45	Actin 5C
CG1913	710	36	α-Tubulin at 84B
CG10067	558	23	Actin 57B
CG9277	296	16	β-Tubulin at 56D
CG2960	263	8	Ribosomal protein L40
CG3201	261	14	Myosin light chain cytoplasmic
CG3595	122	6	spaghetti squash
CG4183	102	5	Heat shock protein 26
CG8274	81	3	Megator
CG2050	64	4	modulo
CG8578	61	1	CG8578
CG4145	58	1	Collagen type IV
CG4463	55	1	Heat shock protein 23
CG33052	55	2	CG33052
CG8472	54	2	Calmodulin
CG7438	42	2	Myosin 31DF
CG17158	41	1	capping protein beta
CG4466	39	1	Heat shock protein 27
CG8280	38	1	Elongation factor 1α48D
CG5588	38	1	Mig-2-like
CG8735	37	2	CG8735
CG13708	36	1	CG13708
CG17034	34	1	CG17034
CG13624	32	1	Repressed by TOR
CG32025	32	1	desert
CG33958	31	1	CG33958
CG4898	30	1	Tropomyosin 1
CG7595	29	1	crinkled
CG11384	29	1	CG11384
CG3253	29	1	CG3253
CG31551	26	2	CG31551
CG4444	25	1	plexus
CG6428	0	1	CG6428

C.3 pUb-Sas6-GFP purification from syncytial *Drosophila* embryos

CG #	Score	#pep	Full name
CG15524	13751	272	spindle assembly abnormal 6
CG33052	6514	105	CG33052
CG4264	1134	25	Heat shock protein cognate 4
CG11129	1022	14	Yolk protein 3
CG2985	719	13	Yolk protein 1
CG9277	619	10	β-Tubulin at 56D
CG9277	549	8	β-Tubulin at 56D
CG9277	549	8	β-Tubulin at 56D
CG1913	482	10	α-Tubulin at 84B

CG8280	473	10	Elongation factor 1α48D
CG2979	462	8	Yolk protein 2
CG9359	441	6	β-Tubulin at 85D
CG4634	407	6	Nucleosome remodeling factor - 38kD
CG5261	354	8	CG5261
CG5261	337	7	CG5261
CG9476	306	7	α-Tubulin at 85E
CG7660	283	4	pxt
CG8937	243	6	Heat shock protein cognate 1
CG5436	229	5	Heat shock protein 68
CG8251	221	2	Phosphoglucose isomerase
CG8262	219	4	anastral spindle 2
CG4147	207	5	Heat shock 70-kDa protein cognate 3
CG8937	181	3	Heat shock protein cognate 1
CG8937	181	3	Heat shock protein cognate 1
CG7756	178	4	Heat shock protein cognate 2
CG1873	169	4	Elongation factor 1α100E
CG1873	169	4	Elongation factor 1α100E
CG1873	169	4	Elongation factor 1α100E
CG1873	169	4	Elongation factor 1α100E
CG4869	164	2	β-Tubulin at 97EF
CG8963	146	2	CG8963
CG8439	136	2	T-complex Chaperonin 5
CG5366	134	2	Cullin-associated and neddylation-dissociated 1
CG11793	121	1	Superoxide dismutase
CG1633	119	3	thioredoxin peroxidase 1
CG1782	114	2	Ubiquitin activating enzyme 1
CG5252	105	1	Ranbp9
CG4898	104	2	Tropomyosin 1
CG1489	101	1	Regulatory particle triple-A ATPase 6
CG11876	101	2	CG11876
CG12233	99	2	lethal (1) G0156
CG17246	97	3	Succinate dehydrogenase A
CG4169	96	1	Ubiquinol-cytochrome c reductase core protein 2
CG4254	95	1	twinstar
CG3024	95	1	Torsin
CG8947	90	1	26-29kD-proteinase
CG6439	88	2	CG6439
CG4898	87	1	Tropomyosin 1
CG4898	87	1	Tropomyosin 1
CG4898	87	1	Tropomyosin 1
CG4898	87	1	Tropomyosin 1
CG7010	85	1	lethal (1) G0334
CG3751	85	1	Ribosomal protein S24
CG4581	78	1	Thiolase
CG8351	78	1	Tcp-1η
CG5374	75	2	Tcp1-like
CG3612	75	1	bellwether
CG9124	74	1	Eukaryotic initiation factor 3 p40 subunit
CG14792	73	1	stubarista
CG3455	72	1	Regulatory particle triple-A ATPase 4
CG17754	72	3	CG17754
CG2960	71	2	Ribosomal protein L40
CG6186	71	1	Transferrin 1
CG2982	66	1	CG2982
CG11276	65	1	Ribosomal protein S4
CG32855	64	7	CG32855
CG10811	63	1	eukaryotic translation initiation factor 4G
CG14648	62	1	growl
CG8893	61	1	Glyceraldehyde 3 phosphate dehydrogenase 2
CG3203	61	1	Ribosomal protein L17
CG2048	59	1	discs overgrown
CG4916	59	1	maternal expression at 31B
CG8231	56	1	T-cp1ζ
CG1242	55	1	Heat shock protein 83
CG10489	55	1	Pole2
CG7583	52	1	C-terminal Binding Protein
CG17333	51	1	CG17333
CG12708	51	2	CG12708
CG7490	49	2	Ribosomal protein LP0
CG8308	49	1	α-Tubulin at 67C
CG5330	48	1	Nucleosome assembly protein 1
CG6598	47	1	Formaldehyde dehydrogenase
CG2151	47	1	Thioredoxin reductase-1
CG5119	47	1	polyA-binding protein
CG3201	44	1	Myosin light chain cytoplasmic
CG7425	42	1	effete
CG10045	41	1	Glutathione S transferase D1
CG11512	41	1	Glutathione S transferase D4
CG8542	36	1	Heat shock protein cognate 5
CG8740	35	1	CG8740
CG8905	34	1	Superoxide dismutase 2 (Mn)
CG5371	34	1	Ribonucleoside diphosphate reductase large subunit
CG4200	33	1	small wing
CG2168	33	1	Ribosomal protein S3A
CG9913	33	1	Kinesin family member 19A ortholog
CG11522	33	1	Ribosomal protein L6
CG13387	32	1	embargoed
CG12836	32	1	CG12836
CG17870	31	1	14-3-3ζ
CG32683	31	1	CG32683
CG2925	30	1	noisette
CG14206	30	1	Ribosomal protein S10b
CG5098	30	1	CG5098

C.4 pUb-Sas6-GFP purification from syncytial *Drosophila* embryos with 440mM NaCl concentration (high salt)

CG #	Score	#pep	Full name
CG15524	5900	123	spindle assembly abnormal 6
CG33052	1641	27	CG33052
CG4264	933	21	Heat shock protein cognate 4
CG1913	458	7	α-Tubulin at 84B
CG2979	455	8	Yolk protein 2
CG8280	440	11	Elongation factor 1α48D
CG4634	436	8	Nucleosome remodeling factor - 38kD
CG9277	433	10	β-Tubulin at 56D
CG4634	407	7	Nucleosome remodeling factor - 38kD
CG7808	361	6	Ribosomal protein S8
CG9277	326	9	β-Tubulin at 56D
CG9476	323	5	α-Tubulin at 85E
CG4916	311	7	maternal expression at 31B
CG11129	309	4	Yolk protein 3
CG1782	309	6	Ubiquitin activating enzyme 1
CG1873	280	7	Elongation factor 1α100E
CG1873	280	7	Elongation factor 1α100E
CG1873	280	7	Elongation factor 1α100E
CG1873	280	7	Elongation factor 1α100E
CG17246	276	5	Succinyl coenzyme A synthetase flavoprotein subunit
CG9277	273	8	β-Tubulin at 56D
CG9277	273	8	β-Tubulin at 56D
CG7660	268	3	pxt
CG4147	258	4	Heat shock protein cognate 3
CG8937	226	4	Heat shock protein cognate 1
CG8251	216	3	Phosphoglucose isomerase
CG2985	216	4	Yolk protein 1
CG16944	212	4	stress-sensitive B
CG2168	207	5	Ribosomal protein S3A
CG8308	201	2	α-Tubulin at 67C
CG8937	191	3	Heat shock protein cognate 1
CG8937	191	3	Heat shock protein cognate 1
CG5252	191	2	Ranbp9
CG4169	186	2	CG4169
CG9359	179	6	β-Tubulin at 85D
CG5920	173	3	Ribosomal protein S2
CG7033	173	2	CG7033
CG10489	168	2	Pole2
CG5436	166	2	Heat shock protein 68
CG3922	166	4	Ribosomal protein S17
CG8947	166	2	26-29kD-proteinase
CG8262	164	2	anastral spindle 2
CG7014	155	2	Ribosomal protein S5b
CG6439	153	4	CG6439
CG2168	148	3	Ribosomal protein S3A
CG6235	145	2	twins
CG1349	144	3	dj-1β
CG4863	139	3	Ribosomal protein L3
CG10686	136	2	trailer hitch
CG8900	134	3	Ribosomal protein S18
CG17521	133	1	Ribosomal protein L10
CG9748	124	1	belle
CG8231	115	2	T-cp1ζ
CG4254	114	1	twinstar
CG5371	113	3	Ribonucleoside diphosphate reductase large subunit
CG6779	112	2	Ribosomal protein S3
CG5366	112	1	Cullin-associated and neddylation-dissociated 1
CG2238	111	2	Elongation factor 2b
CG3195	111	2	Ribosomal protein L12
CG6253	110	2	Ribosomal protein L14
CG1633	110	2	thioredoxin peroxidase 1
CG8439	106	2	T-complex Chaperonin 5
CG7490	105	2	Ribosomal protein LP0
CG10535	101	1	Elongator complex protein 1

CG11276	99	2	Ribosomal protein S4
CG8857	94	2	Ribosomal protein S11
CG13281	93	1	CAS/CSE1 segregation protein
CG11943	93	2	Nucleoporin 205
CG3612	92	1	bellwether
CG10652	92	1	Ribosomal protein L30
CG3752	91	1	Aldehyde dehydrogenase
CG1837	91	1	pretaporter
CG8893	90	1	Glyceraldehyde 3 phosphate dehydrogenase 2
CG33180	88	1	Ranbp16
CG2960	87	2	Ribosomal protein L40
CG8415	87	1	Ribosomal protein S23
CG11522	87	1	Ribosomal protein L6
CG7340	87	1	granny smith
CG3661	84	2	Ribosomal protein L23
CG6543	84	1	CG6543
CG3751	84	1	Ribosomal protein S24
CG11793	83	1	Superoxide dismutase
CG1129	83	1	CG1129
CG12101	82	1	Heat shock protein 60
CG6186	82	1	Transferrin 1
CG1372	81	1	yolkless
CG2151	81	1	Thioredoxin reductase-1
CG2046	80	1	CG2046
CG9075	79	1	Eukaryotic initiation factor 4a
CG3203	79	1	Ribosomal protein L17
CG8922	77	1	Ribosomal protein S5a
CG17286	76	1	spindle defective 2
CG17291	75	1	Protein phosphatase 2A at 29B
CG3401	74	1	β-Tubulin at 60D
CG4869	74	1	β-Tubulin at 97EF
CG4869	74	1	β-Tubulin at 97EF
CG11154	74	1	ATP synthase, β subunit
CG6180	74	1	CG6180
CG8963	74	1	CG8963
CG1218	73	1	CG1218
CG6513	73	1	endosulfine
CG9677	70	1	Int6 homologue
CG12202	68	1	Nat1
CG12233	67	2	lethal (1) G0156
CG4898	65	2	Tropomyosin 1
CG1945	65	1	fat facets
CG15442	65	1	Ribosomal protein L27A
CG4087	64	1	Ribosomal protein LP1
CG6141	61	1	Ribosomal protein L9
CG4581	61	1	Thiolase
CG9769	61	1	CG9769
CG11001	60	1	FK506-binding protein 2
CG7111	60	1	Receptor of activated protein kinase C 1
CG17333	60	1	CG17333
CG9282	60	1	Ribosomal protein L24
CG3379	59	1	Histone H4 replacement
CG3455	58	1	Regulatory particle triple-A ATPase 4
CG17566	55	1	γ-Tubulin at 37C
CG6852	54	1	CG6852
CG10198	54	1	Nucleoporin 98-96
CG8740	53	4	CG8740
CG1683	52	1	Adenine nucleotide translocase 2
CG1683	52	1	Adenine nucleotide translocase 2
CG15697	52	1	Ribosomal protein S30
CG1524	49	1	Ribosomal protein S14a
CG2982	49	1	CG2982
CG6904	48	1	Glycogen synthase
CG4046	47	1	Ribosomal protein S16
CG8495	47	1	Ribosomal protein S29
CG11064	45	1	Retinoid- and fatty acid-binding glycoprotein
CG9012	44	1	Clathrin heavy chain
CG18572	44	1	rudimentary
CG3395	44	1	Ribosomal protein S9
CG13822	44	1	Gamma-interferon-inducible lysosomal thiol reductase 3
CG17754	42	1	CG17754
CG4408	42	1	CG4408
CG1569	41	1	rough deal
CG31618	41	1	His2A:CG31618
CG18001	40	1	Ribosomal protein L38
CG10944	40	1	Ribosomal protein S6
CG1242	39	1	Heat shock protein 83
CG12708	39	1	CG12708
CG17870	38	1	14-3-3ζ
CG7400	38	1	Fatty acid (long chain) transport protein
CG10045	37	1	Glutathione S transferase D1
CG2048	37	1	discs overgrown
CG6177	37	2	ldlCp-related protein
CG7439	37	1	Argonaute 2
CG8036	36	1	CG8036
CG1009	36	1	Puromycin sensitive aminopeptidase
CG7437	36	1	mushroom-body expressed
CG15693	35	1	Ribosomal protein S20
CG4898	34	1	Tropomyosin 1
CG4898	34	1	Tropomyosin 1
CG4898	34	1	Tropomyosin 1
CG4898	34	1	Tropomyosin 1
CG4898	34	1	Tropomyosin 1
CG4898	34	1	Tropomyosin 1
CG4898	34	1	Tropomyosin 1
CG4898	34	1	Tropomyosin 1
CG4898	34	1	Tropomyosin 1
CG17904	34	1	CG17904
CG10538	34	1	CdGAPr
CG2171	34	1	Triose phosphate isomerase
CG5122	33	1	CG5122
CG34015	33	1	CG34015
CG12836	32	1	CG12836
CG10306	32	1	CG10306
CG6084	32	1	CG6084
CG12359	31	1	Ulp1
CG32855	31	1	CG32855
CG31062	30	1	sidestep
CG6509	30	1	Discs large 5
CG32683	30	1	CG32683

C.5 pUb-Sas6-GFP +OA purification from syncytial *Drosophila* embryos with 440mM NaCl concentration (high salt)

CG #	**Score**	**#pep**	**Full name**
CG15524	4677	131	spindle assembly abnormal 6
CG33052	1380	27	CG33052
CG4264	586	12	Heat shock protein cognate 4
CG8280	292	7	Elongation factor 1α48D
CG4634	253	4	Nucleosome remodeling factor - 38kD
CG1913	210	4	α-Tubulin at 84B
CG1873	173	4	Elongation factor 1α100E
CG1873	173	4	Elongation factor 1α100E
CG1873	173	4	Elongation factor 1α100E
CG1873	173	4	Elongation factor 1α100E
CG8937	170	3	Heat shock protein cognate 1
CG9277	145	3	β-Tubulin at 56D
CG8937	138	2	Heat shock protein cognate 1
CG8937	138	2	Heat shock protein cognate 1
CG17246	135	3	Succinate dehydrogenase A
CG17521	123	2	Ribosomal protein L10
CG6235	114	1	twins
CG4147	112	1	Heat shock protein cognate 3
CG4147	112	1	Heat shock protein cognate 3
CG4147	112	1	Heat shock protein cognate 3
CG4147	112	1	Heat shock protein cognate 3
CG5436	112	1	Heat shock protein 68
CG2979	104	3	Yolk protein 2
CG3751	98	2	Ribosomal protein S24
CG6779	90	2	Ribosomal protein S3
CG4916	90	2	maternal expression at 31B
CG9359	85	2	β-Tubulin at 85D
CG5920	85	1	Ribosomal protein S2
CG8251	82	1	Phosphoglucose isomerase
CG10652	82	1	Ribosomal protein L30
CG3203	79	1	Ribosomal protein L17
CG2960	78	2	Ribosomal protein L40
CG10045	76	1	Glutathione S transferase D1
CG11512	76	1	Glutathione S transferase D4
CG5371	75	1	Ribonucleoside diphosphate reductase large subunit
CG8900	74	1	Ribosomal protein S18
CG6253	72	1	Ribosomal protein L14
CG9476	69	2	α-Tubulin at 85E
CG7660	68	1	Peroxinectin-like
CG3661	67	1	Ribosomal protein L23
CG4863	63	2	Ribosomal protein L3
CG8857	62	1	Ribosomal protein S11
CG10944	58	2	Ribosomal protein S6
CG1633	58	1	thioredoxin peroxidase 1
CG11276	56	1	Ribosomal protein S4
CG2168	54	1	Ribosomal protein S3A
CG11129	50	1	Yolk protein 3
CG10811	49	1	eukaryotic translation initiation factor 4G
CG7340	48	1	granny smith
CG8495	47	1	Ribosomal protein S29
CG10489	43	1	Pole2

CG4466	41	1	Heat shock protein 27
CG4898	39	1	Tropomyosin 1
CG12708	39	1	CG12708
CG10538	38	1	CdGAPr
CG8963	38	1	CG8963
CG2668	37	1	Protein ejaculatory bulb
CG3922	37	1	Ribosomal protein S17
CG17870	36	1	14-3-3ζ
CG4863	35	1	Ribosomal protein L3
CG4863	35	1	Ribosomal protein L3
CG8740	35	1	CG8740
CG4046	34	1	Ribosomal protein S16
CG32082	34	1	CG32082
CG6509	33	1	Discs large 5
CG12836	33	1	CG12836
CG6177	32	1	ldlCp-related protein

C.6 pUb-GFP-Dragon purification from *Drosophila* cells

CG #	Score	#pep	Full name
CG33052	18036	290	CG33052
CG4264	4556	65	Heat shock protein cognate 4
CG9277	4140	56	β-Tubulin at 56D
CG9277	3875	52	β-Tubulin at 56D
CG1913	3031	48	α-Tubulin at 84B
CG8280	2423	38	Elongation factor 1α48D
CG17949	2364	37	His2B:CG17949
CG4147	2315	35	Heat shock 70-kDa protein cognate 3
CG3401	2055	34	β-Tubulin at 60D
CG9476	1947	32	α-Tubulin at 85E
CG1528	1792	29	Coat Protein (coatomer) γ
CG12051	1712	26	Actin 42A
CG4027	1575	25	Actin 5C
CG31613	1557	42	His3:CG31613
CG12065	1513	30	CG12065
CG3379	1458	29	Histone H4 replacement
CG2238	1426	22	Elongation factor 2
CG9359	1367	29	β-Tubulin at 85D
CG8937	1334	14	Heat shock protein cognate 1
CG33869	1314	25	His4:CG33869
CG5825	1290	42	Histone H3.3A
CG6223	1263	19	Coat Protein (coatomer) β
CG12065	1259	28	CG12065
CG10067	1255	17	Actin 57B
CG31618	1200	20	His2A:CG31618
CG7478	1157	15	Actin 79B
CG5520	1146	20	Glycoprotein 93
CG5178	1112	16	Actin 88F
CG7961	1106	26	Coat Protein (coatomer) α
CG9748	1062	17	belle
CG8937	1038	9	Heat shock protein cognate 1
CG1873	1032	19	Elongation factor 1α100E
CG6718	1016	21	calcium-independent phospholipase A2 VIA
CG3752	903	11	Aldehyde dehydrogenase
CG7439	899	14	Argonaute 2
CG2216	886	16	Ferritin 1 heavy chain homologue
CG10279	874	11	Rm62
CG4869	861	17	β-Tubulin at 97EF
CG2216	829	15	Ferritin 1 heavy chain homologue
CG9888	773	16	Fibrillarin
CG9012	763	14	Clathrin heavy chain
CG5825	754	37	Histone H3.3A
CG2331	740	13	TER94
CG2216	711	14	Ferritin 1 heavy chain homologue
CG18743	706	8	Heat-shock-protein-70Ab
CG6871	694	10	Catalase
CG32626	671	16	AMP deaminase
CG7583	655	11	C-terminal Binding Protein
CG4897	622	10	Ribosomal protein L7
CG7756	620	9	Heat shock protein cognate 2
CG5261	619	11	midline uncoordinated
CG12030	598	14	UDP-galactose 4'-epimerase
CG5119	587	9	polyA-binding protein
CG2151	586	8	Thioredoxin reductase-1
CG1250	582	7	sec23
CG10701	562	13	Moesin
CG12389	541	7	Farnesyl pyrophosphate synthase
CG5502	537	10	Ribosomal protein L4
CG1349	536	7	dj-1β
CG10701	527	12	Moesin
CG16944	526	14	stress-sensitive B
CG18212	510	8	aluminum tubes
CG11522	494	10	Ribosomal protein L6
CG1242	487	10	Heat shock protein 83
CG9075	486	9	Eukaryotic initiation factor 4a
CG8983	484	10	ERp60
CG4581	483	11	Thiolase
CG4347	478	7	UGP
CG10206	473	8	nop5
CG1973	456	6	yata
CG5353	428	6	Threonyl-tRNA synthetase
CG5371	425	7	Ribonucleoside diphosphate reductase large subunit
CG4863	425	5	Ribosomal protein L3
CG7380	424	8	barrier to autointegration factor
CG2331	419	6	TER94
CG5261	402	7	midline uncoordinated
CG5920	395	5	Ribosomal protein S2
CG10922	392	5	La autoantigen-like
CG4863	387	4	Ribosomal protein L3
CG11276	384	7	Ribosomal protein S4
CG1489	384	7	Regulatory particle triple-A ATPase 6
CG6988	382	7	Protein disulfide isomerase
CG1472	382	6	Sec24AB ortholog (H. sapiens)
CG6779	362	8	Ribosomal protein S3
CG6543	362	7	CG6543
CG4389	361	9	Mitochondrial trifunctional protein α subunit
CG3612	355	5	bellwether
CG14648	353	6	lost
CG3314	352	6	Ribosomal protein L7A
CG5499	351	8	Histone H2A variant
CG4916	345	5	maternal expression at 31B
CG1404	340	6	Ran
CG9577	328	5	CG9577
CG10944	323	6	Ribosomal protein S6
CG6699	322	8	Coat Protein (coatomer) β'
CG1475	320	7	Ribosomal protein L13A
CG2918	318	4	CG2918
CG2098	317	7	Ferrochelatase
CG7762	313	5	Regulatory particle non-ATPase 1
CG10990	310	5	Programmed cell death 4 ortholog
CG10882	309	6	stenosis
CG7111	308	8	Receptor of activated protein kinase C 1
CG8615	308	6	Ribosomal protein L18
CG8036	307	5	CG8036
CG2168	305	7	Ribosomal protein S3A
CG4199	301	5	CG4199
CG31363	301	4	Jupiter
CG9244	296	4	Aconitase
CG17291	296	5	Protein phosphatase 2A at 29B
CG6513	295	3	endosulfine
CG1422	294	5	p115
CG7808	291	5	Ribosomal protein S8
CG1633	291	5	thioredoxin peroxidase 1
CG9805	288	5	eIF3-S10
CG5366	285	4	Cullin-associated and neddylation-dissociated 1
CG4878	278	7	eIF3-S9
CG32549	278	5	CG32549
CG5374	276	4	Tcp1-like
CG1516	276	5	Pyruvate carboxylase
CG3661	272	5	Ribosomal protein L23
CG2098	271	6	Ferrochelatase
CG2241	270	5	Regulatory particle triple-A ATPase 6-related
CG2098	270	5	Ferrochelatase
CG3751	267	5	Ribosomal protein S24
CG8036	266	4	CG8036
CG12775	260	5	Ribosomal protein L21
CG8900	258	6	Ribosomal protein S18
CG17420	257	4	Ribosomal protein L15
CG3922	255	4	Ribosomal protein S17
CG1883	254	3	Ribosomal protein S7
CG6253	253	3	Ribosomal protein L14
CG9124	253	4	Eukaryotic initiation factor 3 p40 subunit
CG1263	249	3	Ribosomal protein L8
CG4747	240	6	CG4747
CG6235	239	3	twins
CG8877	235	4	pre-mRNA processing factor 8
CG6831	234	4	rhea
CG2522	233	4	GTP-binding protein
CG17246	233	3	Succinyl coenzyme A synthetase flavoprotein subunit
CG42668	232	6	CG42668
CG31196	231	6	14-3-3ε
CG5289	218	4	Regulatory particle triple-A ATPase 2
CG11198	212	3	Acetyl-CoA carboxylase
CG2922	210	4	krasavietz
CG1483	209	4	Microtubule-associated protein 205
CG7935	209	4	moleskin
CG2621	207	4	shaggy
CG8893	206	2	Glyceraldehyde 3 phosphate dehydrogenase 2
CG15784	205	4	CG15784
CG9282	205	3	Ribosomal protein L24
CG9705	203	4	CG9705
CG8857	199	4	Ribosomal protein S11
CG14792	198	3	stubarista

CG8332	198	1	Ribosomal protein S15
CG42668	198	4	CG42668
CG8542	196	4	Heat shock protein cognate 5
CG2168	196	5	Ribosomal protein S3A
CG6084	196	3	CG6084
CG6510	195	5	Ribosomal protein L18A
CG4747	194	5	CG4747
CG32549	194	3	CG32549
CG4651	193	4	Ribosomal protein L13
CG10652	193	2	Ribosomal protein L30
CG13343	193	18	Ubiquitin activating enzyme 3
CG14207	191	1	CG14207
CG7897	190	4	Gp210 ortholog (H. sapiens)
CG3523	189	4	Fatty acid synthase 1
CG5934	189	3	CG5934
CG10691	188	2	lethal (2) 37Cc
CG3107	188	5	CG3107
CG31764	188	5	virus-induced RNA 1
CG6143	187	3	Protein on ecdysone puffs
CG1403	187	4	Septin 1
CG9677	184	4	Int6 homologue
CG1548	184	2	cathD
CG2050	182	3	modulo
CG8322	181	5	ATP citrate lyase
CG8857	180	3	Ribosomal protein S11
CG4994	179	2	Mitochondrial phosphate carrier protein
CG1345	179	4	Glutamine:fructose-6-phosphate aminotransferase 2
CG1524	178	4	Ribosomal protein S14a
CG8415	177	3	Ribosomal protein S23
CG17737	177	3	CG17737
CG3186	176	2	eIF-5A
CG6838	176	3	ADP-ribosylation factor GTPase activating protein 3
CG2637	172	4	Female sterile (2) Ketel
CG1782	170	3	Ubiquitin activating enzyme 1
CG9273	169	1	Replication protein A2
CG6439	169	4	CG6439
CG10504	168	3	Integrin linked kinase
CG7507	167	5	Dynein heavy chain 64C
CG6988	167	2	Protein disulfide isomerase
CG8705	166	4	peanut
CG15717	164	4	CG15717
CG10377	163	2	Heterogeneous nuclear ribonucleoprotein at 27C
CG15433	163	3	Elongator complex protein 3
CG3320	162	3	Rab1
CG10223	160	3	Topoisomerase 2
CG4659	159	3	Signal recognition particle protein 54k
CG11963	159	3	skpA associated protein
CG15524	159	4	Spindle assembly abnormal 6 ortholog (C. elegans)
CG34407	159	2	Not1
CG1092	154	2	CG1092
CG3395	153	4	Ribosomal protein S9
CG9160	153	3	mitochondrial acyl carrier protein 1
CG5838	152	4	DNA replication-related element factor
CG7483	152	2	eIF4AIII
CG14999	151	2	Replication-factor-C 40kD subunit
CG6501	151	1	Nucleostemin ortholog (H. sapiens) 2
CG1943	151	2	CG1943
CG3731	151	1	Ubiquinol-cytochrome c reductase core protein 1
CG7831	149	4	non-claret disjunctional
CG11444	148	1	CG11444
CG2033	146	4	Ribosomal protein S15Aa
CG7471	146	4	Rpd3
CG12101	145	3	Heat shock protein 60
CG31289	145	2	Diphthamide methyltransferase
CG10691	144	1	lethal (2) 37Cc
CG33162	144	2	Signal recognition particle receptor β
CG4257	143	3	Signal-transducer and activator of transcription protein at 92E
CG5175	142	1	kugelkern
CG13388	141	1	A kinase anchor protein 200
CG9983	140	3	Heterogeneous nuclear ribonucleoprotein at 98DE
CG10370	140	3	Regulatory particle triple-A ATPase 5
CG7581	138	5	Bub3
CG7224	138	1	Starvation-upregulated protein
CG12749	136	2	Heterogeneous nuclear ribonucleoprotein at 87F
CG31012	136	2	CIN85 and CD2AP orthologue
CG3529	136	3	CG3529
CG1683	135	3	Adenine nucleotide translocase 2
CG31363	134	2	Jupiter
CG4046	133	3	Ribosomal protein S16
CG13849	133	3	Nop56
CG2061	131	2	CG2061
CG8309	131	3	Transport and Golgi organization 7
CG11779	131	4	CG11779
CG11154	130	3	ATP synthase, β subunit
CG4457	130	2	Signal recognition particle protein 19
CG6189	129	2	lethal (1) 1Bi
CG1059	129	2	Karyopherin β 3

CG3800	128	2	CG3800
CG31617	128	4	His1:CG31617
CG42668	128	4	CG42668
CG1691	128	4	IGF-II mRNA-binding protein
CG7843	127	4	Ars2
CG6084	127	2	CG6084
CG8552	125	3	Phosphatidic Acid Phospholipase A1
CG3762	125	4	Vacuolar H+ ATPase 68 kDa subunit 2
CG17654	123	2	Enolase
CG31137	123	2	twin
CG4799	122	2	Pendulin
CG11567	122	2	Cytochrome P450 reductase
CG9423	120	2	karyopherin α3
CG7726	119	2	Ribosomal protein L11
CG3024	119	1	Torsin
CG8532	118	3	liquid facets
CG10630	118	3	blanks
CG2746	117	2	Ribosomal protein L19
CG3644	116	2	bicaudal
CG17870	116	3	14-3-3ζ
CG3821	115	2	Aspartyl-tRNA synthetase
CG4001	115	1	Phosphofructokinase
CG11888	115	2	Regulatory particle non-ATPase 2
CG4821	113	4	Tequila
CG5252	113	2	Ranbp9
CG7834	113	2	CG7834
CG30349	113	2	CG30349
CG6375	113	3	pitchoune
CG7033	112	2	CG7033
CG17611	111	1	eIF6
CG4169	111	3	Ubiquinol-cytochrome c reductase core protein 2
CG6846	111	2	Ribosomal protein L26
CG17489	111	3	Ribosomal protein L5
CG7490	110	3	Ribosomal protein LP0
CG4464	110	1	Ribosomal protein S19a
CG8732	110	2	Acyl-CoA synthetase long-chain
CG4620	109	1	unkempt
CG15081	109	1	Prohibitin 2
CG1100	109	2	Regulatory particle non-ATPase 5
CG5642	109	3	CG5642
CG3524	109	2	v(2)k05816
CG11661	108	1	Neural conserved at 73EF
CG2064	108	2	CG2064
CG2803	108	3	Troponin C-akin-1
CG10824	108	3	Common Dpr-interacting protein
CG8266	106	2	Sec31 ortholog (S. cerevisiae)
CG16916	105	2	Regulatory particle triple-A ATPase 3
CG13387	104	2	embargoed
CG8439	103	3	T-complex Chaperonin 5
CG8759	103	1	Nascent polypeptide associated complex protein alpha subunit
CG9916	102	1	Cyclophilin 1
CG3455	102	2	Regulatory particle triple-A ATPase 4
CG4729	102	1	CG4729
CG6815	102	2	belphegor
CG4145	100	2	Collagen type IV
CG9999	100	2	Ran GTPase activating protein
CG7269	100	2	Helicase at 25E
CG5215	100	1	Zn72D
CG6050	100	1	Elongation factor Tu mitochondrial
CG3127	99	2	Phosphoglycerate kinase
CG4429	98	2	RNA-binding protein 2
CG4954	98	2	eIF3-S8
CG7113	97	1	scully
CG9543	96	2	Coat Protein (coatomer) ε
CG4069	96	1	CG4069
CG8507	96	2	CG8507
CG31694	96	1	CG31694
CG4738	96	2	Nucleoporin 160kD
CG5848	95	1	cactus
CG18174	95	2	Regulatory particle non-ATPase 11
CG1837	93	2	pretaporter
CG7461	93	3	CG7461
CG6226	92	3	FK506-binding protein 1
CG17060	92	1	Rab10
CG10302	92	2	bicoid stability factor
CG7434	91	1	Ribosomal protein L22
CG6782	91	2	scheggia
CG6382	90	3	Ef1α-like factor
CG17521	90	3	Ribosomal protein L10
CG15609	89	2	Eps15 homology domain containing protein-binding protein 1
CG8430	88	2	Glutamate oxaloacetate transaminase 1
CG4993	88	2	PRL-1
CG6904	88	1	Glycogen synthase
CG4821	87	2	Tequila
CG7144	87	1	lysine ketoglutarate reductase
CG12085	87	2	poly U binding factor 68kD
CG11107	87	1	DHX15 ortholog
CG10161	87	2	Eukaryotic initiation factor 3 p66 subunit
CG8975	86	1	Ribonucleoside diphosphate reductase small subunit
CG2691	86	2	CG2691

CG7404	86	2	estrogen-related receptor
CG7878	86	2	CG7878
CG5417	86	1	Signal recognition particle protein 14
CG15792	85	2	zipper
CG3664	85	1	Rab5
CG6203	85	1	Fmr1
CG8890	85	1	GDP-mannose 4,6-dehydratase
CG9373	85	1	rumpelstiltskin
CG4254	84	1	twinstar
CG6692	84	2	Cysteine proteinase-1
CG9738	84	2	MAP kinase kinase 4
CG9246	84	2	CG9246
CG7920	84	2	CG7920
CG3949	83	1	hoi-polloi
CG6072	83	1	sarah
CG16901	83	1	squid
CG8553	82	1	Selenide,water dikinase
CG1453	81	1	Kinesin-like protein at 10A
CG12202	81	2	NAT1 ortholog (S. cerevisiae)
CG33129	81	3	CG33129
CG42641	81	1	Regulatory particle non-ATPase 3
CG1274	80	3	thioredoxin peroxidase 2
CG30122	80	1	CG30122
CG17489	80	1	Ribosomal protein L5
CG7622	79	2	Ribosomal protein L36
CG9148	79	2	supercoiling factor
CG8262	79	1	anastral spindle 2
CG8258	79	1	CG8258
CG8231	78	1	T-cp1ζ
CG4800	78	1	Translationally controlled tumor protein ortholog (H. sapiens)
CG12163	77	2	CG12163
CG16858	76	2	viking
CG8649	76	2	Fimbrin
CG12324	76	2	Ribosomal protein S15Ab
CG3593	75	2	rudimentary-like
CG9680	75	1	Dead box protein 73D
CG10077	75	1	CG10077
CG3902	75	1	CG3902
CG5844	75	1	CG5844
CG15442	74	2	Ribosomal protein L27A
CG12233	74	2	lethal (1) G0156
CG9412	73	1	rasputin
CG1341	73	2	Regulatory particle triple-A ATPase 1
CG7632	73	2	CG7632
CG6143	72	1	Protein on ecdysone puffs
CG12085	72	1	poly U binding factor 68kD
CG2469	72	1	CG2469
CG7375	72	1	Ubiquitin conjugating enzyme 12
CG8351	72	1	Tcp-1η
CG8787	71	7	Additional sex combs
CG3395	70	2	Ribosomal protein S9
CG1081	70	1	Ras homolog enriched in brain ortholog (H. sapiens)
CG5394	69	1	Glutamyl-prolyl-tRNA synthetase
CG10160	68	1	Ecdysone-inducible gene L3
CG10596	68	1	Msr-110
CG6708	68	1	Oxysterol binding protein
CG12275	68	1	Ribosomal protein S10a
CG10306	68	1	CG10306
CG3981	68	1	Unc-76
CG8922	67	2	Ribosomal protein S5a
CG31022	67	1	prolyl-4-hydroxylase-alpha EFB
CG4584	67	1	Deoxyuridine triphosphatase
CG17369	66	2	Vacuolar H+-ATPase 55kD subunit
CG9155	66	2	Myosin 61F
CG12532	66	1	Adaptor Protein complex 1/2, β subunit
CG6453	65	1	Glucosidase 2 β subunit
CG1600	65	1	Death resistor Adh domain containing target
CG10897	65	2	toutatis
CG7338	65	1	Tsr1 ribosome assembly factor
CG12750	65	1	nucampholin
CG7254	64	1	Glycogen phosphorylase
CG9556	64	1	alien
CG11092	64	1	Nucleoporin 93kD-1
CG4094	64	1	lethal (1) G0255
CG6907	64	1	CG6907
CG7235	64	1	Hsp60C
CG4598	64	1	CG4598
CG3195	64	1	Ribosomal protein L12
CG14066	64	1	La related protein
CG1651	63	1	Ankyrin
CG1721	63	1	Phosphoglyceromutase
CG3861	63	1	knockdown
CG3606	62	1	cabeza
CG3265	62	1	Eb1
CG9088	62	1	little imaginal discs
CG9188	62	1	septin interacting protein 2
CG8590	61	1	Kinesin-like protein at 3A
CG7977	61	2	Ribosomal protein L23A
CG5654	60	2	ypsilon schachtel
CG12076	60	1	YT521-B
CG11901	60	1	Ef1γ
CG14407	60	1	CG14407

CG3074	60	2	Secreted Wg-interacting molecule
CG8756	60	4	vermiform
CG5728	60	1	CG5728
CG33129	59	1	CG33129
CG5931	59	1	lethal (3) 72Ab
CG13628	58	1	Rpb10
CG1828	57	1	dre4
CG1416	57	1	CG1416
CG7816	57	1	Zinc/iron regulated transporter-related protein 99C
CG33456	57	2	muscle wasted
CG4785	56	3	Integrator 14
CG12050	56	2	CG12050
CG4752	56	4	CG4752
CG9674	56	2	CG9674
CG18102	55	1	shibire
CG18076	55	3	short stop
CG3572	55	1	visceral mesodermal armadillo-repeats
CG9581	55	1	CG9581
CG5972	55	2	Actin-related protein 2/3 complex, subunit 4
CG9302	55	1	CG9302
CG5641	55	1	CG5641
CG12512	54	1	CG12512
CG4016	54	1	Serine palmitoyltransferase subunit I
CG3201	53	1	Myosin light chain cytoplasmic
CG8340	53	1	upstream of RpIII128
CG8174	53	1	SRPK
CG11856	53	1	Nucleoporin 358kD
CG7392	53	1	Connector of kinase to AP-1
CG11804	52	2	ced-6
CG9635	51	1	Rho guanine nucleotide exchange factor 2
CG5809	51	1	calcium-binding protein 1
CG6778	51	1	Glycyl-tRNA synthetase
CG2957	51	1	mitochondrial ribosomal protein S9
CG6987	51	2	SF2
CG8977	50	1	Cctγ
CG4912	50	1	eEF1δ
CG5214	50	1	CG5214
CG8882	49	1	Trip1
CG7010	49	2	lethal (1) G0334
CG6891	49	1	CG6891
CG2803	49	1	Troponin C-akin-1
CG7852	49	1	CG7852
CG4821	48	2	Tequila
CG6819	48	1	members only
CG7985	48	3	CG7985
CG8683	48	1	mon2
CG8545	48	1	CG8545
CG17494	48	1	Sarcolemma associated protein
CG2194	48	1	suppressor of rudimentary
CG5650	47	1	Protein phosphatase 1 at 87B
CG10130	47	1	Sec61 β subunit
CG6743	47	1	Nucleoporin 107kD
CG5733	47	1	Nucleoporin 75kD
CG8286	47	1	P58IPK
CG6042	47	1	Cyp12a4
CG4236	47	1	Chromatin assembly factor 1 subunit
CG4260	47	2	Adaptor Protein complex 2, α subunit
CG12262	46	1	CG12262
CG4173	45	1	Septin 2
CG7610	45	1	ATP synthase, γ subunit
CG12770	45	1	Vacuolar protein sorting 28
CG6181	45	1	Ge-1 ortholog (H. sapiens)
CG9674	45	1	CG9674
CG33097	45	1	CG33097
CG8947	45	1	26-29kD-proteinase
CG30498	44	1	boca
CG10719	44	1	brain tumor
CG6155	44	1	Roe1
CG31794	44	1	Paxillin
CG4337	43	1	mitochondrial single stranded DNA-binding protein
CG4111	43	1	Ribosomal protein L35
CG8475	43	1	CG8475
CG3351	43	1	mitochondrial ribosomal protein L11
CG5442	43	1	SC35
CG7752	43	1	putzig
CG32528	42	1	parvin
CG1725	41	1	discs large 1
CG11427	41	1	ruby
CG13389	41	1	Ribosomal protein S13
CG1101	41	1	RNA and export factor binding protein 1
CG8103	41	1	Mi-2
CG3433	41	1	Coproporphyrinogen oxidase
CG16936	41	1	Glutathione S transferase E12
CG10851	40	1	B52
CG10811	40	1	eukaryotic translation initiation factor 4G
CG11324	40	1	homer
CG5014	40	1	VAMP-associated protein of 33kDa ortholog A
CG8282	40	1	Sorting nexin 6
CG6251	40	1	Nucleoporin 62kD

CG14271	39	2	Growth arrest specific protein 8
CG4320	39	1	raptor
CG7277	39	1	CG7277
CG7003	39	1	Msh6
CG8798	39	1	Lon protease
CG6000	39	1	CG6000
CG31817	38	2	CG31817
CG6450	38	1	lava lamp
CG10194	38	2	CG10194
CG1316	38	1	CG1316
CG33180	38	1	Ranbp16
CG1646	37	1	CG1646
CG8610	36	1	Cell division cycle 27 ortholog
CG5726	36	1	CG5726
CG18519	36	1	Aldehyde oxidase 2
CG1915	36	1	sallimus
CG8014	35	1	Receptor mediated endocytosis 8
CG1210	35	1	Phosphoinositide-dependent kinase 1
CG14786	35	1	Leucine-rich pentatricopeptide repeat containing 2
CG5723	34	1	Tenascin major
CG8355	34	1	slit
CG5680	33	1	basket
CG3416	33	1	Regulatory particle non-ATPase 8
CG5105	33	1	Phospholipase A2 activator protein
CG1591	33	1	REG
CG4853	33	1	CG4853
CG3362	33	1	cytosolic 5'-nucleotidase IIIB
CG7014	33	1	Ribosomal protein S5b
CG11148	33	1	Gigyf
CG8189	32	1	ATP synthase, subunit b
CG10869	32	1	CG10869
CG9674	32	1	CG9674
CG12983	32	1	CG12983
CG6420	32	1	CG6420
CG1945	31	1	fat facets
CG4038	31	1	CG4038
CG11943	31	1	Nucleoporin 205kD
CG8360	31	1	CG8360
CG42670	31	1	pasilla
CG9735	30	1	Tryptophanyl-tRNA synthetase
CG10617	30	1	Synaptotagmin 12

C.7 pUb-GFP-Dragon +OA purification from *Drosophila* cells

CG #	Score	#pep	Full name
CG33052	61897	766	CG33052
CG4264	4605	65	Heat shock protein cognate 4
CG7583	3502	47	C-terminal Binding Protein
CG9277	3400	47	β-Tubulin at 56D
CG7583	3329	45	C-terminal Binding Protein
CG9277	3183	44	β-Tubulin at 56D
CG4027	2995	47	Actin 5C
CG12051	2930	46	Actin 42A
CG4147	2726	42	Heat shock 70-kDa protein cognate 3
CG1913	2613	41	α-Tubulin at 84B
CG10067	2227	34	Actin 57B
CG8280	2070	34	Elongation factor 1α48D
CG7478	2042	30	Actin 79B
CG5178	1970	31	Actin 88F
CG15524	1961	37	Spindle assembly abnormal 6 ortholog (C. elegans)
CG9476	1738	27	α-Tubulin at 85E
CG3401	1565	26	β-Tubulin at 60D
CG9359	1478	26	β-Tubulin at 85D
CG8937	1259	13	Heat shock protein cognate 1
CG1528	1171	22	Coat Protein (coatomer) γ
CG9748	1115	16	belle
CG15792	1096	20	zipper
CG17949	1077	17	His2B:CG17949
CG4869	1072	21	β-Tubulin at 97EF
CG8937	1070	10	Heat shock protein cognate 1
CG6871	900	11	Catalase
CG1349	874	14	dj-1β
CG5436	868	10	Heat shock protein 68
CG18743	852	9	Heat-shock-protein-70Ab
CG15792	849	18	zipper
CG12065	812	15	CG12065
CG2216	811	16	Ferritin 1 heavy chain homologue
CG6718	738	7	calcium-independent phospholipase A2 VIA
CG2238	728	13	Elongation factor 2
CG1873	724	12	Elongation factor 1α100E
CG7439	700	11	Argonaute 2
CG3752	685	4	Aldehyde dehydrogenase
CG3379	672	15	Histone H4 replacement
CG32626	659	15	AMP deaminase
CG33869	659	14	His4:CG33869
CG5261	655	14	midline uncoordinated
CG5502	645	12	Ribosomal protein L4
CG31613	637	11	His3:CG31613
CG12065	619	13	CG12065
CG10701	616	14	Moesin
CG7961	606	13	Coat Protein (coatomer) α
CG7756	604	7	Heat shock protein cognate 2
CG6223	582	9	Coat Protein (coatomer) β
CG5825	572	10	Histone H3.3A
CG10701	542	12	Moesin
CG1250	532	6	sec23
CG10279	497	8	Rm62
CG5261	497	11	midline uncoordinated
CG31618	486	10	His2A:CG31618
CG8309	461	7	Transport and Golgi organization 7
CG2216	453	10	Ferritin 1 heavy chain homologue
CG5371	451	8	Ribonucleoside diphosphate reductase large subunit
CG2151	444	5	Thioredoxin reductase-1
CG1548	441	5	cathD
CG18212	435	6	aluminum tubes
CG14648	403	7	lost
CG9888	402	9	Fibrillarin
CG8542	395	5	Heat shock protein cognate 5
CG12163	368	5	CG12163
CG4897	367	5	Ribosomal protein L7
CG10944	364	5	Ribosomal protein S6
CG8322	355	5	ATP citrate lyase
CG4799	338	4	Pendulin
CG3612	328	7	bellwether
CG4863	327	5	Ribosomal protein L3
CG10630	327	6	blanks
CG1403	322	3	Septin 1
CG6253	307	4	Ribosomal protein L14
CG8922	304	4	Ribosomal protein S5a
CG2331	299	6	TER94
CG4634	283	3	Nucleosome remodeling factor - 38kD
CG4389	283	7	Mitochondrial trifunctional protein α subunit
CG3265	273	6	Eb1
CG1489	272	4	Regulatory particle triple-A ATPase 6
CG5920	271	5	Ribosomal protein S2
CG1973	269	4	yata
CG8893	267	3	Glyceraldehyde 3 phosphate dehydrogenase 2
CG12233	255	4	lethal (1) G0156
CG2050	253	5	modulo
CG3201	250	4	Myosin light chain cytoplasmic
CG8983	247	5	ERp60
CG4199	244	5	CG4199
CG2922	242	5	extra bases
CG6510	240	5	Ribosomal protein L18A
CG11276	239	4	Ribosomal protein S4
CG7808	239	3	Ribosomal protein S8
CG3455	231	4	Regulatory particle triple-A ATPase 4
CG1100	231	4	Regulatory particle non-ATPase 5
CG31363	229	4	Jupiter
CG7430	227	3	CG7430
CG4863	225	3	Ribosomal protein L3
CG8996	222	3	walrus
CG2168	222	6	Ribosomal protein S3A
CG17246	216	3	Succinate dehydrogenase A
CG1341	215	4	Regulatory particle triple-A ATPase 1
CG7977	213	3	Ribosomal protein L23A
CG33206	213	3	Golgi microtubule-associated protein
CG6699	212	3	Coat Protein (coatomer) β'
CG3523	212	4	Fatty acid synthase 1
CG5353	209	3	Threonyl-tRNA synthetase
CG3661	208	3	Ribosomal protein L23
CG5520	207	4	Glycoprotein 93
CG5000	206	3	mini spindles
CG17420	206	3	Ribosomal protein L15
CG15442	206	3	Ribosomal protein L27A
CG3024	205	3	Torsin
CG2746	204	2	Ribosomal protein L19
CG3644	195	3	bicaudal
CG5499	192	5	Histone H2A variant
CG6819	191	3	members only
CG1782	190	3	Ubiquitin activating enzyme 1
CG16944	189	5	stress-sensitive B
CG13349	189	2	Regulatory particle non-ATPase 13
CG1404	187	3	Ran
CG16916	187	2	Regulatory particle triple-A ATPase 3
CG6235	186	3	twins
CG10377	184	2	Heterogeneous nuclear ribonucleoprotein at 27C
CG10990	184	3	Programmed cell death 4 ortholog
CG11888	181	3	Regulatory particle non-ATPase 2
CG8590	180	1	Kinesin-like protein at 3A
CG6831	180	2	rhea
CG31764	179	4	virus-induced RNA 1
CG6988	178	3	Protein disulfide isomerase
CG6084	178	3	CG6084

CG10161	176	3	Eukaryotic initiation factor 3 p66 subunit
CG9075	174	4	Eukaryotic initiation factor 4a
CG4347	173	2	UGP
CG5215	171	2	Zn72D
CG10206	171	3	nop5
CG1475	170	3	Ribosomal protein L13A
CG11856	170	3	Nucleoporin 358kD
CG6543	169	3	CG6543
CG3314	167	3	Ribosomal protein L7A
CG17333	167	2	CG17333
CG8351	167	2	Tcp-1η
CG11154	165	3	ATP synthase, β subunit
CG42670	165	3	pasilla
CG13343	165	15	Ubiquitin activating enzyme 3
CG12389	164	1	Farnesyl pyrophosphate synthase
CG15784	163	3	CG15784
CG32549	163	2	CG32549
CG6988	162	2	Protein disulfide isomerase
CG4581	158	3	Thiolase
CG5654	154	1	ypsilon schachtel
CG5374	153	2	Tcp1-like
CG7490	152	2	Ribosomal protein LP0
CG9412	152	3	rasputin
CG6439	152	4	CG6439
CG10811	151	2	eukaryotic translation initiation factor 4G
CG8877	151	1	pre-mRNA processing factor 8
CG7111	150	3	Receptor of activated protein kinase C 1
CG9983	149	2	Heterogeneous nuclear ribonucleoprotein at 98DE
CG8900	148	3	Ribosomal protein S18
CG4651	148	3	Ribosomal protein L13
CG1472	147	3	Sec24AB ortholog (H. sapiens)
CG9805	147	4	eIF3-S10
CG4916	144	3	maternal expression at 31B
CG8975	144	2	Ribonucleoside diphosphate reductase small subunit
CG2522	143	2	GTP-binding protein
CG11943	143	2	Nucleoporin 205kD
CG10535	142	1	Elongator complex protein 1
CG7831	141	1	non-claret disjunctional
CG10305	138	3	Ribosomal protein S26
CG18190	138	2	CG18190
CG2098	136	3	Ferrochelatase
CG13389	133	2	Ribosomal protein S13
CG10882	133	3	stenosis
CG5825	130	6	Histone H3.3A
CG6084	130	2	CG6084
CG4800	130	2	Translationally controlled tumor protein ortholog (H. sapiens)
CG7507	130	3	Dynein heavy chain 64C
CG8439	129	2	T-complex Chaperonin 5
CG10223	127	3	Topoisomerase 2
CG31363	126	2	Jupiter
CG14206	126	2	Ribosomal protein S10b
CG10691	125	1	lethal (2) 37Cc
CG12532	125	3	Adaptor Protein complex 1/2, β subunit
CG7185	123	1	CG7185
CG13849	123	2	Nop56
CG6815	121	2	belphegor
CG2168	120	4	Ribosomal protein S3A
CG30176	120	2	within bgcn
CG1483	119	1	Microtubule-associated protein 205
CG4169	119	2	Ubiquinol-cytochrome c reductase core protein 2
CG3902	116	1	CG3902
CG3606	115	2	cabeza
CG8266	115	2	Sec31 ortholog (S. cerevisiae)
CG10922	113	2	La autoantigen-like
CG9124	111	3	Eukaryotic initiation factor 3 p40 subunit
CG10160	110	2	Ecdysone-inducible gene L3
CG13387	110	2	embargoed
CG9012	108	3	Clathrin heavy chain
CG7398	108	2	Transportin
CG11793	107	1	Superoxide dismutase
CG3107	107	2	CG3107
CG4584	107	2	Deoxyuridine triphosphatase
CG1242	106	2	Heat shock protein 83
CG8073	106	3	Phosphomannomutase 45A
CG8571	105	2	smallminded
CG4236	105	1	Chromatin assembly factor 1 subunit
CG4259	104	1	CG4259
CG1453	103	2	Kinesin-like protein at 10A
CG10230	101	2	Regulatory particle non-ATPase 9
CG8615	101	2	Ribosomal protein L18
CG8798	101	2	Lon protease
CG18102	100	1	shibire
CG6692	100	1	Cysteine proteinase-1
CG8857	99	1	Ribosomal protein S11
CG7766	98	1	CG7766
CG8831	97	2	Nucleoporin 54kD
CG4878	97	3	eIF3-S9
CG6513	97	1	endosulfine
CG7726	96	1	Ribosomal protein L11
CG6617	96	1	CG6617
CG17654	95	1	Enolase
CG3351	95	4	mitochondrial ribosomal protein L11
CG9999	94	2	Ran GTPase activating protein
CG1633	94	1	thioredoxin peroxidase 1
CG2033	93	3	Ribosomal protein S15Aa
CG5170	93	3	Dodeca-satellite-binding protein 1
CG1683	92	2	Adenine nucleotide translocase 2
CG9543	92	2	Coat Protein (coatomer) ε
CG1129	92	1	CG1129
CG2918	91	1	CG2918
CG6180	91	1	CG6180
CG4463	90	1	Heat shock protein 23
CG7637	90	2	CG7637
CG11522	90	1	Ribosomal protein L6
CG4003	90	1	pontin
CG10652	89	1	Ribosomal protein L30
CG4598	89	2	CG4598
CG4257	88	3	Signal-transducer and activator of transcription protein at 92E
CG8553	88	1	selenide,water dikinase
CG12775	88	2	Ribosomal protein L21
CG9916	87	1	Cyclophilin 1
CG33162	87	1	Signal recognition particle receptor β
CG3320	86	1	Rab1
CG6050	86	1	Elongation factor Tu mitochondrial
CG5175	86	1	kugelkern
CG34407	86	1	Not1
CG3333	86	1	Nucleolar protein at 60B
CG3152	85	2	Trap1
CG10370	85	2	Regulatory particle triple-A ATPase 5
CG4954	85	1	eIF3-S8
CG3395	84	2	Ribosomal protein S9
CG8882	84	1	Trip1
CG7340	83	1	granny smith
CG5394	82	1	Glutamyl-prolyl-tRNA synthetase
CG12324	82	2	Ribosomal protein S15Ab
CG10077	82	2	CG10077
CG31196	81	1	14-3-3ε
CG2061	81	1	CG2061
CG5446	81	1	CG5446
CG2098	80	2	Ferrochelatase
CG2098	80	1	Ferrochelatase
CG1263	79	1	Ribosomal protein L8
CG12275	79	1	Ribosomal protein S10a
CG5366	79	1	Cullin-associated and neddylation-dissociated 1
CG9493	79	1	Pez
CG8552	79	1	Phosphatidic Acid Phospholipase A1
CG9373	78	1	rumpelstiltskin
CG3593	77	2	rudimentary-like
CG1837	77	2	pretaporter
CG12013	77	1	PHGPx
CG7033	76	1	CG7033
CG5064	76	1	Signal recognition particle protein 68
CG11579	75	1	armadillo
CG9680	75	1	Dead box protein 73D
CG9282	75	1	Ribosomal protein L24
CG7697	74	1	Cleavage stimulation factor 64 kilodalton subunit
CG10504	74	1	Integrin linked kinase
CG2331	73	1	TER94
CG4111	73	1	Ribosomal protein L35
CG5389	73	1	male sterile (3) 72Dt
CG33456	73	4	muscle wasted
CG42668	73	1	CG42668
CG8443	72	1	clueless
CG5119	72	1	polyA-binding protein
CG7144	71	2	lysine ketoglutarate reductase
CG10198	71	1	Nucleoporin 98-96kD
CG11271	71	1	Ribosomal protein S12
CG2637	71	2	Female sterile (2) Ketel
CG7765	70	1	Kinesin heavy chain
CG11661	70	2	Neural conserved at 73EF
CG4173	70	2	Septin 2
CG4993	70	1	PRL-1
CG9148	70	1	supercoiling factor
CG1422	70	1	p115
CG8705	69	1	peanut
CG14996	69	2	Chd64
CG6521	68	1	Signal transducing adaptor molecule
CG10777	68	1	maheshvara
CG2064	68	2	CG2064
CG7392	68	1	Connector of kinase to AP-1
CG9273	67	1	Replication protein A2
CG11811	67	1	CG11811
CG3949	66	1	hoi-polloi
CG31012	66	1	CIN85 and CD2AP orthologue
CG10992	66	1	Cathepsin B1
CG8890	66	1	GDP-mannose 4,6-dehydratase
CG2158	66	2	Nucleoporin 50kD
CG2803	66	1	Troponin C-akin-1
CG8231	65	1	T-cp1ζ
CG1516	65	1	Pyruvate carboxylase
CG9088	65	1	little imaginal discs
CG6779	64	1	Ribosomal protein S3

CG7762	64	2	Regulatory particle non-ATPase 1
CG3714	64	2	CG3714
CG7626	64	1	Spt5
CG1943	63	1	CG1943
CG4817	62	1	Structure specific recognition protein
CG7935	62	1	moleskin
CG11198	62	2	Acetyl-CoA carboxylase
CG8610	61	5	Cell division cycle 27 ortholog
CG12101	61	1	Heat shock protein 60
CG4567	61	1	iconoclast
CG1524	60	1	Ribosomal protein S14a
CG3922	60	1	Ribosomal protein S17
CG5289	60	2	Regulatory particle triple-A ATPase 2
CG1088	60	1	Vacuolar H+-ATPase 26kD subunit
CG14224	60	2	Ubiquilin
CG4046	60	2	Ribosomal protein S16
CG33180	60	2	Ranbp16
CG3203	58	1	Ribosomal protein L17
CG4679	58	1	CG4679
CG33129	58	2	CG33129
CG10641	57	1	Swiprosin-1
CG7939	56	1	Ribosomal protein L32
CG5838	56	1	DNA replication-related element factor
CG10753	56	1	Small ribonucleoprotein particle protein SmD1
CG4538	56	1	CG4538
CG6907	55	1	CG6907
CG32533	55	2	CG32533
CG4183	54	1	Heat shock protein 26
CG6850	54	1	UDP-glucose-glycoprotein glucosyltransferase
CG7074	54	1	missing oocyte
CG7581	53	1	Bub3
CG42708	53	1	Glutaminase
CG5931	53	1	lethal (3) 72Ab
CG9244	52	1	Aconitase
CG4457	52	1	Signal recognition particle protein 19
CG9423	52	1	karyopherin α3
CG8683	52	1	mon2
CG5733	52	1	Nucleoporin 75kD
CG17870	51	1	14-3-3ζ
CG2916	51	1	Septin 5
CG8963	51	1	CG8963
CG9325	51	1	hu li tai shao
CG17255	50	2	no circadian temperature entrainment
CG9160	49	1	mitochondrial acyl carrier protein 1
CG4821	49	1	Tequila
CG12030	48	2	UDP-galactose 4'-epimerase
CG8390	48	1	vulcan
CG2674	47	1	S-adenosylmethionine Synthetase
CG11738	47	1	lethal (1) G0004
CG7461	47	1	CG7461
CG1945	46	1	fat facets
CG9577	45	1	CG9577
CG8036	45	1	CG8036
CG6042	45	1	Cyp12a4
CG33129	45	1	CG33129
CG10596	44	1	Msr-110
CG6375	44	1	pitchoune
CG14792	43	1	stubarista
CG4252	43	1	meiotic 41
CG3395	43	1	Ribosomal protein S9
CG4752	43	2	CG4752
CG10824	43	1	Common Dpr-interacting protein
CG7985	42	2	CG7985
CG15717	42	1	CG15717
CG3262	42	1	CG3262
CG5723	41	1	Tenascin major
CG8609	41	1	Mediator complex subunit 4
CG4931	41	1	specifically Rac1-associated protein 1
CG2171	40	1	Triose phosphate isomerase
CG6226	40	1	FK506-binding protein 1
CG16827	40	2	Integrin alphaPS4 subunit
CG8787	40	2	Additional sex combs
CG4211	39	1	no on or off transient A
CG7404	38	1	estrogen-related receptor
CG5642	38	1	CG5642
CG31739	37	1	Aspartyl-tRNA synthetase, mitochondrial
CG3821	36	1	Aspartyl-tRNA synthetase
CG1071	36	1	E2F transcription factor 2
CG6546	36	1	Brahma associated protein 55kD
CG4785	36	1	Integrator 14
CG10194	36	1	CG10194
CG12223	35	1	Dorsal switch protein 1
CG9854	35	1	hiiragi
CG6339	35	1	rad50
CG5916	35	1	CG5916
CG15697	35	1	Ribosomal protein S30
CG7834	35	1	CG7834
CG31550	35	1	CG31550
CG7558	35	1	Actin-related protein 3
CG4035	34	1	Eukaryotic initiation factor 4E
CG7917	34	1	Nucleoplasmin
CG12264	34	1	CG12264
CG5728	34	1	CG5728
CG6946	34	1	glorund
CG15811	33	1	Ras opposite
CG30349	33	1	CG30349
CG15822	32	1	CG15822
CG7546	32	1	CG7546
CG6418	32	1	CG6418
CG5519	32	1	Prp19
CG4032	31	1	Abl tyrosine kinase
CG9553	31	1	chickadee
CG7070	31	1	Pyruvate kinase
CG7434	31	1	Ribosomal protein L22
CG2658	31	1	CG2658
CG8677	31	1	CG8677
CG10863	31	1	CG10863
CG3328	31	1	CG3328
CG13708	31	1	CG13708
CG10289	31	1	CG10289
CG4747	31	1	CG4747
CG31367	31	1	CG31367
CG6790	30	1	CG6790
CG14317	30	1	CG14317
CG31794	30	1	Paxillin

C.8 pMT-Dragon-GFP purification from *Drosophila* cells

CG #	Size	#pep	Full name
CG15792	227633	701	zipper
CG15792	237395	696	zipper
CG15792	232241	696	zipper
CG15792	228521	696	zipper
CG15792	233676	696	zipper
CG15792	227529	695	zipper
CG33052	37855	253	CG33052
CG4027	42194	173	Actin 5C
CG12051	42196	172	Actin 42A
CG10067	42207	157	Actin 57B
CG7478	42159	126	Actin 79B
CG5178	42072	129	Actin 88F
CG1484	144959	40	flightless I
CG9155	119657	44	Myosin 61F
CG3201	16717	41	Myosin light chain cytoplasmic
CG4898	29336	42	Tropomyosin 1
CG7438	117649	35	Myosin 31DF
CG4898	29248	39	Tropomyosin 1
CG4898	32537	37	Tropomyosin 1
CG4898	32795	34	Tropomyosin 1
CG8280	50561	25	Elongation factor 1α48D
CG4898	80290	32	Tropomyosin 1
CG4898	53394	32	Tropomyosin 1
CG4898	32783	32	Tropomyosin 1
CG4898	32783	32	Tropomyosin 1
CG4898	54666	32	Tropomyosin 1
CG4898	32783	32	Tropomyosin 1
CG4898	32783	32	Tropomyosin 1
CG10540	32853	18	capping protein alpha
CG1913	50561	28	α-Tubulin at 84B
CG2146	138912	22	dilute class unconventional myosin
CG4264	71372	17	Heat shock protein cognate 4
CG7595	251804	16	crinkled
CG1539	41524	19	tropomodulin
CG5825	15376	14	Histone H3.3A
CG6450	316451	21	lava lamp
CG5695	144349	20	jaguar
CG7583	42738	22	C-terminal Binding Protein
CG9476	50619	19	α-Tubulin at 85E
CG4145	175391	13	Collagen type IV
CG5502	45112	12	Ribosomal protein L4
CG12008	472720	9	karst
CG16858	194685	14	viking
CG3595	19999	16	spaghetti squash
CG4897	29591	10	Ribosomal protein L7
CG5409	42459	11	Actin-related protein 53D
CG4898	48168	9	Tropomyosin 1
CG4898	74950	9	Tropomyosin 1
CG4898	48168	9	Tropomyosin 1
CG4898	18518	9	Tropomyosin 1
CG8937	70871	5	Heat shock protein cognate 1
CG8937	61480	5	Heat shock protein cognate 1
CG8937	61480	5	Heat shock protein cognate 1

CG18572	248796	3	rudimentary
CG9277	51720	11	β-Tubulin at 56D
CG14792	30266	6	stubarista
CG4147	72330	11	Heat shock 70-kDa protein cognate 3
CG1106	82648	12	Gelsolin
CG31613	15436	11	His3:CG31613
CG9277	42619	10	β-Tubulin at 56D
CG9277	42619	10	β-Tubulin at 56D
CG18212	95266	5	aluminum tubes
CG3401	51387	7	β-Tubulin at 60D
CG1977	279101	5	α Spectrin
CG1883	22156	6	Ribosomal protein S7
CG8014	274770	5	Receptor mediated endocytosis 8
CG6699	103618	4	Coat Protein (coatomer) β'
CG1973	97727	6	CG1973
CG32138	133702	4	CG32138
CG9901	44959	2	Actin-related protein 2
CG8615	21822	6	Ribosomal protein L18
CG17158	31572	6	capping protein beta
CG3752	57325	3	Aldehyde dehydrogenase
CG9359	50408	8	β-Tubulin at 85D
CG3751	15095	7	Ribosomal protein S24
CG7765	110901	4	Kinesin heavy chain
CG7558	47459	6	Actin-related protein 66B
CG8309	44515	3	Transport and Golgi organization 7
CG10160	35800	4	Ecdysone-inducible gene L3
CG10938	27094	1	Proteasome α5 subunit
CG15693	13593	4	Ribosomal protein S20
CG3379	11374	8	Histone H4 replacement
CG8578	45489	6	CG8578
CG6223	108308	4	Coat Protein (coatomer) β
CG33869	11356	7	His4:CG33869
CG33877	11356	7	His4:CG33877
CG33879	11356	7	His4:CG33879
CG33881	11356	7	His4:CG33881
CG1873	51030	10	Elongation factor 1α100E
CG1873	51030	10	Elongation factor 1α100E
CG1873	51030	10	Elongation factor 1α100E
CG1873	51030	10	Elongation factor 1α100E
CG5436	70043	4	Heat shock protein 68
CG8922	25760	4	Ribosomal protein S5a
CG5825	13687	10	Histone H3.3A
CG6831	308914	2	rhea
CG7762	103010	1	Regulatory particle non-ATPase 1
CG10223	165034	5	Topoisomerase 2
CG2168	30549	7	Ribosomal protein S3A
CG31618	13355	8	His2A:CG31618
CG3455	45111	4	Regulatory particle triple-A ATPase 4
CG4863	47285	3	Ribosomal protein L3
CG17489	34244	7	Ribosomal protein L5
CG7111	36109	3	Receptor of activated protein kinase C 1
CG1691	62376	2	IGF-II mRNA-binding protein
CG3937	240799	5	cheerio
CG6253	19219	3	Ribosomal protein L14
CG15099	293740	3	CG15099
CG5920	29110	5	Ribosomal protein S2
CG2168	18546	6	Ribosomal protein S3A
CG4863	18295	2	Ribosomal protein L3
CG4863	15772	2	Ribosomal protein L3
CG9282	17623	4	Ribosomal protein L24
CG12592	75824	1	CG12592
CG17420	24424	7	Ribosomal protein L15
CG3203	21922	3	Ribosomal protein L17
CG7507	532987	2	Dynein heavy chain 64C
CG10652	12398	2	Ribosomal protein L30
CG17333	26997	1	CG17333
CG5119	70110	3	polyA-binding protein
CG7490	34295	3	Ribosomal protein LP0
CG8439	59697	1	T-complex Chaperonin 5
CG17949	13688	5	His2B:CG17949
CG11276	29230	6	Ribosomal protein S4
CG9748	85371	4	belle
CG4466	23659	2	Heat shock protein 27
CG10370	48005	3	Regulatory particle triple-A ATPase 5
CG18076	629346	2	short stop
CG7283	24429	3	Ribosomal protein L10Ab
CG17611	26649	1	eIF6
CG12052	76161	1	longitudinals lacking
CG3395	22610	7	Ribosomal protein S9
CG5170	144929	2	Dodeca-satellite-binding protein 1
CG32626	82610	3	AMP deaminase
CG3922	15332	4	Ribosomal protein S17
CG16916	47083	1	Regulatory particle triple-A ATPase 3
CG4869	59217	4	β-Tubulin at 97EF
CG4869	51733	4	β-Tubulin at 97EF
CG4759	15893	3	Ribosomal protein L27
CG3314	30884	2	Ribosomal protein L7A
CG5330	43026	1	Nucleosome assembly protein 1
CG11522	27738	3	Ribosomal protein L6
CG3416	38180	2	Regulatory particle non-ATPase 8
CG7626	120226	1	Spt5
CG6779	27682	4	Ribosomal protein S3
CG5289	49464	2	Regulatory particle triple-A ATPase 2
CG13388	88252	1	A kinase anchor protein 200
CG5482	45005	1	CG5482
CG5000	227956	2	mini spindles
CG7756	70078	2	Heat shock protein cognate 2
CG3299	107034	5	Vinculin
CG6846	17270	3	Ribosomal protein L26
CG9325	128772	2	hu li tai shao
CG1569	242390	3	rough deal
CG1994	113659	1	lethal (1) G0020
CG1528	98470	3	Coat Protein (coatomer) γ
CG2050	60387	3	modulo
CG17521	26024	2	Ribosomal protein L10
CG14996	20859	2	Chd64
CG10377	44970	1	Heterogeneous nuclear ribonucleoprotein at 27C
CG9012	192937	2	Clathrin heavy chain
CG8332	17026	2	Ribosomal protein S15
CG17291	66067	3	Protein phosphatase 2A at 29B
CG4651	25050	4	Ribosomal protein L13
CG10305	13543	3	Ribosomal protein S26
CG8705	60448	1	peanut
CG1115	24361	1	CG1115
CG7977	29445	2	Ribosomal protein L23A
CG31794	66128	1	Paxillin
CG12030	39071	2	UDP-galactose 4'-epimerase
CG3164	79017	2	CG3164
CG4463	20730	1	Heat shock protein 23
CG10811	184570	2	eukaryotic translation initiation factor 4G
CG15524	55135	2	Spindle assembly abnormal 6 ortholog (C. elegans)
CG2238	95424	4	Elongation factor 2
CG4464	17394	3	Ribosomal protein S19a
CG8715	135935	1	lingerer
CG3074	50124	1	Secreted Wg-interacting molecule
CG14206	17867	3	Ribosomal protein S10b
CG12532	101914	1	Adaptor Protein complex 1/2, β subunit
CG18076	624270	1	short stop
CG18076	620997	1	short stop
CG18076	590626	1	short stop
CG18076	992421	1	short stop
CG18076	623815	1	short stop
CG18076	590733	1	short stop
CG18076	620997	1	short stop
CG18076	623898	1	short stop
CG6684	13193	3	Ribosomal protein S25
CG3661	15041	2	Ribosomal protein L23
CG1559	131256	1	Upf1
CG18102	93371	1	shibire
CG4046	16878	2	Ribosomal protein S16
CG8900	17658	2	Ribosomal protein S18
CG11228	75518	1	hippo
CG6757	63584	1	SH3PX1
CG15697	14633	2	Ribosomal protein S30
CG2621	59192	1	shaggy
CG5499	14972	5	Histone H2A variant
CG4183	23208	1	Heat shock protein 26
CG4289	30843	1	Peroxin 14
CG9888	34673	2	Fibrillarin
CG7961	140952	2	Coat Protein (coatomer) α
CG12512	65788	1	CG12512
CG6987	28447	2	SF2
CG6831	236962	1	rhea
CG6831	236962	1	rhea
CG1821	14581	4	Ribosomal protein L31
CG3008	69634	1	CG3008
CG11888	113754	1	Regulatory particle non-ATPase 2
CG12775	18521	1	Ribosomal protein L21
CG43063	15533	2	CG43063
CG6143	78570	2	Protein on ecdysone puffs
CG1104	87942	1	CG1104
CG1242	82099	2	Heat shock protein 83
CG2699	57734	1	Pi3K21B
CG11527	257403	3	Tiggrin
CG13389	17168	2	Ribosomal protein S13
CG7014	25985	1	Ribosomal protein S5b
CG43119	178970	2	Ectoderm-expressed 4
CG10944	24795	1	Ribosomal protein S6
CG11943	234806	1	Nucleoporin 205kD
CG1489	45999	2	Regulatory particle triple-A ATPase 6
CG11471	141979	1	Isoleucyl-tRNA synthetase
CG13387	123746	1	embargoed
CG6811	55220	1	Rho GTPase activating protein at 68F
CG3644	17727	1	bicaudal
CG6238	132323	1	slingshot
CG14648	59934	3	growl
CG42807	31558	1	CG42807
CG12306	67614	1	polo
CG7269	49077	2	Helicase at 25E
CG10279	78956	1	Rm62

CG4111	14498	2	Ribosomal protein L35
CG6815	68489	2	belphegor
CG3195	17891	1	Ribosomal protein L12
CG10535	143580	1	Elongator complex protein 1
CG2033	14933	2	Ribosomal protein S15Aa
CG6522	91901	2	Testin ortholog
CG17272	17239	1	CG17272
CG6439	40698	1	CG6439
CG42611	548180	1	Megalin
CG8571	105000	1	smallminded
CG3529	57852	1	CG3529
CG6199	82914	1	procollagen lysyl hydroxylase
CG9805	134425	1	eIF3-S10
CG17489	15603	2	Ribosomal protein L5
CG6944	71371	2	Lamin
CG3178	75045	1	Recombination repair protein 1
CG2998	7529	1	Ribosomal protein S28b
CG32086	56258	3	CG32086
CG42668	70815	1	CG42668
CG4602	58673	1	Srp54
CG12324	14903	1	Ribosomal protein S15Ab
CG14549	26223	3	Sld5
CG3587	33919	1	CG3587
CG42595	93624	1	unextended
CG6143	11598	1	Protein on ecdysone puffs
CG1399	69173	1	Leucine-rich repeat
CG6476	72926	1	Suppressor of variegation 3-9
CG1945	314766	1	fat facets
CG17766	170592	1	Rabconnectin-3B
CG15899	354966	1	Ca^{2+}-channel protein α_1 subunit
CG16932	134507	1	Epidermal growth factor receptor pathway substrate clone 15
CG12292	42714	1	spichthyin
CG15100	113269	1	Methionyl-tRNA synthetase
CG11981	23618	1	Proteasome β3 subunit
CG1263	27989	1	Ribosomal protein L8
CG10840	127638	2	eIF5B
CG31012	57268	1	CIN85 and CD2AP orthologue
CG1059	125078	1	Karyopherin β 3
CG10501	57555	4	α methyl dopa-resistant
CG1524	16312	1	Ribosomal protein S14a
CG4079	22135	1	TBP-associated factor 11
CG14804	52794	1	Vacuolar protein sorting 26
CG3210	83085	1	Dynamin related protein 1
CG15784	62634	1	CG15784
CG4217	29945	1	mitochondrial transcription factor A
CG5515	28702	1	CG5515
CG4918	11750	1	Ribosomal protein LP2
CG1345	77403	1	Glutamine:fructose-6-phosphate aminotransferase 2
CG6976	245267	1	Myosin 28B1
CG6976	245258	1	Myosin 28B1
CG6976	120117	1	Myosin 28B1
CG6976	120126	1	Myosin 28B1
CG32075	62202	1	CG32075
CG8857	18262	1	Ribosomal protein S11
CG6977	218051	1	Cadherin 87A
CG42318	83573	1	approximated
CG12065	76897	1	CG12065
CG1810	75461	2	mRNA-capping-enzyme
CG14224	58798	1	Ubiquilin
CG15398	35388	2	CG15398
CG5525	57764	1	CG5525
CG18467	28173	1	CG18467
CG2241	45255	1	Regulatory particle triple-A ATPase 6-related
CG8472	16800	1	Calmodulin
CG2746	24154	1	Ribosomal protein L19
CG9281	70085	1	CG9281
CG1702	27130	1	Glutathione S transferase T3
CG12740	16019	1	Ribosomal protein L28
CG1599	25211	1	Vesicle-associated membrane protein 7
CG13813	49728	3	CG13813
CG5870	266316	1	β Spectrin
CG33979	45975	1	capulet
CG15249	21072	1	CG15249
CG9188	69081	1	septin interacting protein 2
CG8258	59795	1	CG8258
CG1475	23803	1	Ribosomal protein L13A
CG4560	20349	1	Actin-related protein 2/3 complex, subunit 3A
CG5378	45524	1	Regulatory particle non-ATPase 7
CG17209	156467	1	CG17209
CG7380	10338	1	barrier to autointegration factor
CG18437	369614	1	CG18437
CG9603	9895	1	Cytochrome c oxidase subunit 7A
CG7324	147970	1	CG7324
CG7808	23859	1	Ribosomal protein S8
CG30115	172806	1	Guanine nucleotide exchange factor in mesoderm
CG3724	52971	1	Phosphogluconate dehydrogenase
CG5371	92889	1	Ribonucleoside diphosphate reductase large subunit
CG9124	38725	1	Eukaryotic initiation factor 3 p40 subunit
CG4633	114629	3	mitochondrial alanyl-tRNA synthetase
CG4954	106158	1	eIF3-S8
CG13809	198915	1	osm-1
CG1359	16959	1	BET5 ortholog
CG18026	173429	1	Calcium activated protein for secretion
CG6946	61359	1	glorund
CG4214	51818	1	Syntaxin 5
CG7843	107612	1	Ars2
CG3608	60164	1	aarF domain containing kinase
CG1347	153384	1	Atg17
CG9983	39014	1	Heterogeneous nuclear ribonucleoprotein at 98DE
CG16880	26279	1	Nimrod C3
CG1683	34007	1	Adenine nucleotide translocase 2
CG3961	79621	1	CG3961
CG31617	26400	1	His1:CG31617
CG32549	82093	1	CG32549
CG32683	88166	2	CG32683
CG4257	71722	1	Signal-transducer and activator of transcription protein at 92E
CG9945	58896	1	CG9945
CG9394	77002	1	CG9394
CG12499	239542	1	CG12499
CG6059	104413	1	CG6059
CG17514	296460	1	CG17514
CG1422	93094	1	p115
CG32743	366260	1	no-on-and-no-off transient C
CG14168	81739	1	Zasp67
CG30021	67089	1	menage a trois
CG2121	57687	1	CG2121

C.9 pMT-Dragon-GFP +OA purification from *Drosophila* cells

CG #	Score	#pep	Full name
CG15792	36530	566	zipper
CG15792	36311	564	zipper
CG15792	36311	564	zipper
CG15792	36311	564	zipper
CG15792	36311	564	zipper
CG15792	36266	563	zipper
CG33052	24140	337	CG33052
CG4027	9568	145	Actin 5C
CG12051	9532	143	Actin 42A
CG10067	7953	122	Actin 57B
CG7478	7380	103	Actin 79B
CG5178	5060	100	Actin 88F
CG3201	2730	51	Myosin light chain cytoplasmic
CG9155	2495	47	Myosin 61F
CG9155	2483	46	Myosin 61F
CG9155	2483	46	Myosin 61F
CG9155	2483	46	Myosin 61F
CG7583	2262	40	C-terminal Binding Protein
CG7583	1984	38	C-terminal Binding Protein
CG4264	1796	35	Heat shock protein cognate 4
CG1973	1584	20	yata
CG5695	1513	29	jaguar
CG4898	1404	33	Tropomyosin 1
CG5695	1401	26	jaguar
CG8280	1367	31	Elongation factor 1α48D
CG9012	1347	22	Clathrin heavy chain
CG4898	1313	31	Tropomyosin 1
CG7438	1280	26	Myosin 31DF
CG9277	1220	18	β-Tubulin at 56D
CG1913	1201	25	α-Tubulin at 84B
CG9277	1176	17	β-Tubulin at 56D
CG3595	1144	27	spaghetti squash
CG9277	1117	16	β-Tubulin at 56D
CG9277	1117	16	β-Tubulin at 56D
CG4898	1113	25	Tropomyosin 1
CG1484	1107	21	flightless I
CG4898	1022	23	Tropomyosin 1
CG16858	1014	16	viking
CG4145	984	15	Collagen type IV
CG5825	748	6	Histone H3.3A
CG9476	747	16	α-Tubulin at 85E
CG17158	745	12	capping protein beta
CG12065	708	15	CG12065

CG4898	697	16	Tropomyosin 1
CG4898	697	16	Tropomyosin 1
CG4898	697	16	Tropomyosin 1
CG4898	697	16	Tropomyosin 1
CG4898	697	16	Tropomyosin 1
CG4898	697	16	Tropomyosin 1
CG4898	697	16	Tropomyosin 1
CG2146	673	20	dilute class unconventional myosin
CG18743	628	9	Heat-shock-protein-70Ab
CG5436	600	8	Heat shock protein 68
CG31449	600	8	Heat-shock-protein-70Ba
CG31359	600	8	Heat-shock-protein-70Bb
CG6489	600	8	Heat-shock-protein-70Bc
CG5834	600	8	Hsp70Bbb
CG6223	590	12	Coat Protein (coatomer) β
CG10938	566	2	Proteasome α5 subunit
CG4898	549	10	Tropomyosin 1
CG4898	549	10	Tropomyosin 1
CG4898	549	10	Tropomyosin 1
CG4898	549	10	Tropomyosin 1
CG5502	548	11	Ribosomal protein L4
CG1539	548	10	tropomodulin
CG2146	523	16	dilute class unconventional myosin
CG4634	508	5	Nucleosome remodeling factor - 38kD
CG3752	506	2	Aldehyde dehydrogenase
CG1528	488	8	Coat Protein (coatomer) γ
CG2331	481	10	TER94
CG31618	481	8	His2A:CG31618
CG7885	470	2	RNA polymerase II 33kD subunit
CG9325	463	5	hu li tai shao
CG3401	458	7	β-Tubulin at 60D
CG6699	441	6	Coat Protein (coatomer) β'
CG9359	428	10	β-Tubulin at 85D
CG12052	425	5	longitudinals lacking
CG8937	410	4	Heat shock protein cognate 1
CG8937	410	4	Heat shock protein cognate 1
CG8937	410	4	Heat shock protein cognate 1
CG1873	407	15	Elongation factor 1α100E
CG1873	407	15	Elongation factor 1α100E
CG1873	407	15	Elongation factor 1α100E
CG1873	407	15	Elongation factor 1α100E
CG1242	378	8	Heat shock protein 83
CG6831	378	3	rhea
CG3016	373	4	Ubiquitin specific protease 30
CG6871	372	5	Catalase
CG10160	365	5	Ecdysone-inducible gene L3
CG7595	363	6	crinkled
CG10370	333	4	Regulatory particle triple-A ATPase 5
CG12008	330	3	karst
CG7961	329	11	Coat Protein (coatomer) α
CG32549	317	7	CG32549
CG10540	301	6	capping protein alpha
CG5499	294	6	Histone H2A variant
CG14996	294	8	Chd64
CG6148	289	4	Putative Achaete Scute Target 1
CG1106	287	7	Gelsolin
CG11143	285	4	Inos
CG2238	284	7	Elongation factor 2
CG6815	276	7	belphegor
CG3937	275	7	cheerio
CG8014	274	4	Receptor mediated endocytosis 8
CG6439	272	6	CG6439
CG4897	265	4	Ribosomal protein L7
CG9748	262	8	belle
CG8472	261	7	Calmodulin
CG4147	261	5	Heat shock 70-kDa protein cognate 3
CG7878	259	2	CG7878
CG4799	258	4	Pendulin
CG32549	257	6	CG32549
CG1977	256	3	α Spectrin
CG10223	256	9	Topoisomerase 2
CG1883	256	5	Ribosomal protein S7
CG6450	251	5	lava lamp
CG2331	235	4	TER94
CG6253	232	6	Ribosomal protein L14
CG4389	232	3	Mitochondrial trifunctional protein α subunit
CG5482	232	2	CG5482
CG7765	228	3	Kinesin heavy chain
CG6831	228	2	rhea
CG6831	228	2	rhea
CG5409	225	4	Actin-related protein 53D
CG15524	223	7	Spindle assembly abnormal 6 ortholog (C. elegans)
CG8266	214	3	sec31
CG12819	214	3	slender lobes
CG3265	213	6	Eb1
CG5170	211	4	Dodeca-satellite-binding protein 1
CG3074	207	2	Secreted Wg-interacting molecule
CG4858	206	1	CG4858
CG8309	200	2	Transport and Golgi organization 7
CG8922	198	4	Ribosomal protein S5a
CG12233	198	3	lethal (1) G0156
CG12592	198	1	CG12592
CG32626	198	6	AMP deaminase
CG9633	194	1	Replication Protein A 70
CG17521	194	1	Ribosomal protein L10
CG4634	190	2	Nucleosome remodeling factor - 38kD
CG2621	189	2	shaggy
CG13389	188	4	Ribosomal protein S13
CG11943	188	2	Nucleoporin 205kD
CG17333	178	2	CG17333
CG18740	177	3	moira
CG3714	177	2	CG3714
CG18572	176	1	rudimentary
CG1782	175	2	Ubiquitin activating enzyme 1
CG30122	175	3	CG30122
CG8578	173	4	CG8578
CG1064	172	1	Snf5-related 1
CG2252	171	2	female sterile (1) homeotic
CG3379	171	5	Histone H4 replacement
CG5289	171	2	Regulatory particle triple-A ATPase 2
CG16944	170	8	stress-sensitive B
CG8036	168	2	CG8036
CG7726	167	3	Ribosomal protein L11
CG18190	167	4	CG18190
CG8615	167	3	Ribosomal protein L18
CG16932	165	2	Epidermal growth factor receptor pathway substrate clone 15
CG4878	163	4	eIF3-S9
CG6339	163	2	rad50
CG31048	162	1	sponge
CG6617	160	2	CG6617
CG14299	157	1	CG14299
CG7756	154	2	Heat shock protein cognate 2
CG5371	154	2	Ribonucleoside diphosphate reductase large subunit
CG12532	153	4	Adaptor Protein complex 1/2, β subunit
CG8439	153	1	T-complex Chaperonin 5
CG10986	152	1	garnet
CG1548	151	4	cathD
CG9805	151	3	eIF3-S10
CG5920	149	3	Ribosomal protein S2
CG1683	147	6	Adenine nucleotide translocase 2
CG1683	147	6	Adenine nucleotide translocase 2
CG17654	146	1	Enolase
CG9888	146	4	Fibrillarin
CG18102	146	3	shibire
CG11856	146	2	Nucleoporin 358kD
CG16916	145	1	Regulatory particle triple-A ATPase 3
CG5378	144	3	Regulatory particle non-ATPase 7
CG9282	144	2	Ribosomal protein L24
CG1345	144	2	Glutamine:fructose-6-phosphate aminotransferase 2
CG15693	143	2	Ribosomal protein S20
CG9901	141	1	Actin-related protein 2
CG1403	139	1	Septin 1
CG9543	138	1	Coat Protein (coatomer) ε
CG10306	138	2	CG10306
CG4169	138	2	Ubiquinol-cytochrome c reductase core protein 2
CG17949	138	2	His2B:CG17949
CG3416	135	2	Regulatory particle non-ATPase 8
CG1691	135	2	IGF-II mRNA-binding protein
CG8954	134	1	Smg5
CG3203	134	3	Ribosomal protein L17
CG3821	133	1	Aspartyl-tRNA synthetase
CG6258	132	3	Replication factor C 38kD subunit
CG4003	131	1	pontin
CG2216	130	3	Ferritin 1 heavy chain homologue
CG5704	129	1	CG5704
CG8443	129	1	clueless
CG15820	129	1	CG15820
CG3395	127	3	Ribosomal protein S9
CG6773	127	3	Sec13 ortholog (S. cerevisiae)
CG8334	127	1	Ubiquitin specific protease 32
CG4877	124	1	RING-associated factor 2
CG8322	123	1	ATP citrate lyase
CG9181	119	2	Protein tyrosine phosphatase 61F
CG9999	119	1	Ran GTPase activating protein
CG6946	119	4	glorund
CG12234	117	1	Ranbp21
CG1489	116	3	Regulatory particle triple-A ATPase 6
CG6235	115	2	twins
CG8705	115	1	peanut
CG1591	115	2	REG
CG17489	115	3	Ribosomal protein L5
CG34407	115	2	Not1
CG1341	113	3	Regulatory particle triple-A ATPase 1
CG5014	112	2	Vap-33-1
CG7846	112	1	Actin-related protein 8
CG3606	111	1	cabeza
CG8230	111	2	CG8230
CG17272	111	2	CG17272
CG3661	109	2	Ribosomal protein L23
CG7809	109	1	Grasp65
CG10811	108	2	eukaryotic translation initiation factor 4G
CG10230	108	1	Regulatory particle non-ATPase 9
CG3299	107	2	Vinculin
CG10377	107	1	Heterogeneous nuclear ribonucleoprotein at 27C

CG8332	107	2	Ribosomal protein S15
CG1646	107	2	CG1646
CG17498	106	3	mad2
CG7808	106	4	Ribosomal protein S8
CG7762	104	2	Regulatory particle non-ATPase 1
CG4429	103	4	RNA-binding protein 2
CG9281	103	2	CG9281
CG9881	103	1	Actin-related protein 2/3 complex, subunit 5
CG4869	102	2	β-Tubulin at 97EF
CG4869	102	2	β-Tubulin at 97EF
CG5434	102	1	Signal recognition particle protein 72
CG6779	101	4	Ribosomal protein S3
CG8542	100	3	Heat shock protein cognate 5
CG7558	100	2	Actin-related protein 66B
CG12030	100	2	UDP-galactose 4'-epimerase
CG5000	98	2	mini spindles
CG1633	98	3	thioredoxin peroxidase 1
CG4260	98	1	Adaptor Protein complex 2, α subunit
CG3922	97	2	Ribosomal protein S17
CG43119	97	3	Ectoderm-expressed 4
CG4046	96	3	Ribosomal protein S16
CG7014	96	2	Ribosomal protein S5b
CG1349	96	3	dj-1β
CG7111	94	2	Receptor of activated protein kinase C 1
CG10944	92	2	Ribosomal protein S6
CG6948	92	2	Clathrin light chain
CG3455	91	2	Regulatory particle triple-A ATPase 4
CG3751	91	2	Ribosomal protein S24
CG1250	91	1	Sec23 ortholog (S. cerevisiae)
CG4157	90	1	Regulatory particle non-ATPase 12
CG12262	90	1	CG12262
CG7283	90	1	Ribosomal protein L10Ab
CG2905	90	1	Nipped-A
CG6315	89	1	female lethal d
CG17291	89	2	Protein phosphatase 2A at 29B
CG5119	88	2	polyA-binding protein
CG4033	88	2	RNA polymerase I 135kD subunit
CG3523	88	3	Fatty acid synthase 1
CG5261	88	2	midline uncoordinated
CG4931	88	1	specifically Rac1-associated protein 1
CG17420	87	4	Ribosomal protein L15
CG3612	86	3	bellwether
CG14792	85	2	stubarista
CG5825	84	2	Histone H3.3A
CG31613	84	2	His3:CG31613
CG33803	84	2	His3:CG33803
CG33806	84	2	His3:CG33806
CG33809	84	2	His3:CG33809
CG33812	84	2	His3:CG33812
CG33815	84	2	His3:CG33815
CG33818	84	2	His3:CG33818
CG33821	84	2	His3:CG33821
CG33824	84	2	His3:CG33824
CG33827	84	2	His3:CG33827
CG33830	84	2	His3:CG33830
CG33833	84	2	His3:CG33833
CG33836	84	2	His3:CG33836
CG33839	84	2	His3:CG33839
CG33842	84	2	His3:CG33842
CG33845	84	2	His3:CG33845
CG33848	84	2	His3:CG33848
CG33851	84	2	His3:CG33851
CG33854	84	2	His3:CG33854
CG33857	84	2	His3:CG33857
CG33860	84	2	His3:CG33860
CG33863	84	2	His3:CG33863
CG33866	84	2	His3:CG33866
CG4863	82	1	Ribosomal protein L3
CG10423	82	2	Ribosomal protein S27
CG3724	81	1	Phosphogluconate dehydrogenase
CG17611	81	1	eIF6
CG2699	80	1	Pi3K21B
CG7324	80	1	CG7324
CG8947	80	1	26-29kD-proteinase
CG3314	79	1	Ribosomal protein L7A
CG8231	79	2	T-cp1ζ
CG1994	79	1	lethal (1) G0020
CG5028	79	3	CG5028
CG5330	78	1	Nucleosome assembly protein 1
CG2774	78	1	Sorting nexin 1
CG3587	77	2	CG3587
CG16817	77	1	CG16817
CG5726	76	1	CG5726
CG8351	76	2	Tcp-1η
CG4173	75	1	Septin 2
CG12512	75	1	CG12512
CG4217	74	1	mitochondrial transcription factor A
CG33979	74	3	capulet
CG6476	73	2	Suppressor of variegation 3-9
CG7439	73	3	Argonaute 2
CG4464	72	1	Ribosomal protein S19a
CG3226	72	1	CG3226
CG14206	72	2	Ribosomal protein S10b
CG5271	70	1	Ribosomal protein S27A
CG4364	70	1	CG4364
CG6684	69	2	Ribosomal protein S25
CG3333	69	1	Nucleolar protein at 60B
CG6782	69	2	scheggia
CG5028	69	2	CG5028
CG11901	68	1	Ef1γ
CG13349	68	1	Regulatory particle non-ATPase 13
CG14549	68	4	Sld5
CG16973	67	2	misshapen
CG3210	67	1	Dynamin related protein 1
CG5366	67	1	Cullin-associated and neddylation-dissociated 1
CG6203	67	1	Fmr1
CG3539	66	1	SLY-1 homologous
CG6543	66	1	CG6543
CG5174	66	1	CG5174
CG6646	65	1	DJ-1α
CG2050	64	1	modulo
CG11228	64	1	hippo
CG12306	63	2	polo
CG8977	63	2	Cctγ
CG2168	63	1	Ribosomal protein S3A
CG11276	62	2	Ribosomal protein S4
CG18212	62	1	aluminum tubes
CG6937	62	1	CG6937
CG2216	61	2	Ferritin 1 heavy chain homologue
CG6842	61	1	Vacuolar protein sorting 4
CG16901	61	1	squid
CG7490	60	1	Ribosomal protein LP0
CG10701	60	2	Moesin
CG2508	60	1	Cell division cycle 23 ortholog
CG10944	58	1	Ribosomal protein S6
CG6341	58	1	Elongation factor 1 β
CG3967	58	1	CG3967
CG6718	58	1	calcium-independent phospholipase A2 VIA
CG9769	58	1	CG9769
CG31617	58	1	His1:CG31617
CG32066	58	1	CG32066
CG6603	56	1	Hsc70Cb
CG7843	56	3	Ars2
CG4211	55	1	no on or off transient A
CG4916	55	1	maternal expression at 31B
CG8103	55	2	Mi-2
CG2982	55	1	CG2982
CG6846	55	1	Ribosomal protein L26
CG8649	54	2	Fimbrin
CG1911	54	1	CAP-D2 condensin subunit
CG10161	54	1	Eukaryotic initiation factor 3 p66 subunit
CG12163	54	2	CG12163
CG3879	53	2	Multi drug resistance 49
CG9680	52	2	Dead box protein 73D
CG7269	51	1	Helicase at 25E
CG9124	51	1	Eukaryotic initiation factor 3 p40 subunit
CG6084	51	1	CG6084
CG6854	51	1	CTP synthase
CG7070	50	1	Pyruvate kinase
CG12775	50	1	Ribosomal protein L21
CG8728	50	1	CG8728
CG4994	49	1	Mitochondrial phosphate carrier protein
CG6582	49	1	Aac11
CG1406	49	1	U2A
CG4954	49	1	eIF3-S8
CG34126	49	1	CG34126
CG10279	48	1	Rm62
CG3320	48	1	Rab1
CG3162	48	1	Large Subunit 2
CG4800	47	1	Translationally controlled tumor protein ortholog (H. sapiens)
CG5433	46	1	Kinesin light chain
CG14472	46	1	purity of essence
CG1821	46	2	Ribosomal protein L31
CG4043	46	1	Rrp46
CG5602	46	1	DNA ligase I
CG15784	45	1	CG15784
CG10354	45	1	Rat1
CG1945	44	3	fat facets
CG2061	44	1	CG2061
CG6907	44	1	CG6907
CG6199	44	1	procollagen lysyl hydroxylase
CG4759	44	1	Ribosomal protein L27
CG30084	44	1	Z band alternatively spliced PDZ-motif protein 52
CG8882	43	1	Trip1
CG15899	43	3	Ca^{2+}-channel protein α_1 subunit T
CG6876	43	1	Prp31
CG4651	42	1	Ribosomal protein L13
CG1524	41	1	Ribosomal protein S14a
CG11715	41	1	Cyp4g15
CG9446	41	1	coro
CG7057	40	1	AP-50
CG5642	40	1	CG5642
CG8233	39	1	Reduction in Cnn dots 1
CG10363	39	1	Thioester-containing protein 4

CG32086	39	2	CG32086
CG6944	38	1	Lamin
CG8340	38	1	upstream of RpIII128
CG4257	38	1	Signal-transducer and activator of transcription protein at 92E
CG17023	38	1	Dead box protein 80
CG11888	38	1	Regulatory particle non-ATPase 2
CG9940	38	1	CG9940
CG5348	38	3	CG5348
CG4079	37	1	TBP-associated factor 11
CG3585	37	1	Rabconnectin-3A
CG9677	37	1	Int6 homologue
CG17280	37	1	levy
CG10587	37	2	CG10587
CG6946	37	2	glorund
CG5515	37	1	CG5515
CG16880	36	3	Nimrod C3
CG31045	36	1	Myosin heavy chain-like
CG14648	36	1	lost
CG5374	35	1	Tcp1-like
CG17766	35	1	Rabconnectin-3B
CG10327	35	1	TAR DNA-binding protein-43 homolog
CG12264	35	1	CG12264
CG16868	35	1	CG16868
CG9712	35	1	tumor suppressor protein 101
CG1943	35	1	CG1943
CG6213	34	1	Vacuolar H+ ATPase 13kD subunit
CG15523	34	1	Vacuolar protein sorting 13B
CG10539	33	1	RPS6-p70-protein kinase
CG8571	33	1	smallminded
CG4829	33	1	CG4829
CG9188	33	1	septin interacting protein 2
CG10501	32	2	α methyl dopa-resistant
CG7467	32	1	osa
CG2807	32	1	CG2807
CG6668	32	1	atlastin
CG31188	32	1	CG18749
CG32854	32	1	mitochondrial ribosomal protein S21
CG9191	31	1	Kinesin-like protein at 61F
CG11064	31	1	Retinoid- and fatty-acid binding protein
CG10840	31	1	eIF5B
CG15249	31	1	CG15249
CG4744	31	1	CG4744
CG12734	31	1	Girdin
CG10630	31	1	blanks
CG13601	31	1	CG13601
CG2112	31	1	CG2112
CG3762	31	1	Vacuolar H+ ATPase 68 kDa subunit 2
CG6476	31	1	Suppressor of variegation 3-9
CG2904	30	2	echinus
CG8975	30	2	Ribonucleoside diphosphate reductase small subunit
CG9635	30	1	Rho guanine nucleotide exchange factor 2
CG4004	30	2	CG4004
CG6279	30	2	CG6279
CG13813	30	1	CG13813
CG15442	30	1	Ribosomal protein L27A
CG10305	29	1	Ribosomal protein S26
CG4337	29	1	mitochondrial single stranded DNA-binding protein
CG32809	29	2	CG32809
CG6092	29	1	Dak1
CG3002	29	1	Golgi-localized, γ-adaptin ear containing, ARF binding protein
CG9406	29	1	CG9406
CG14168	29	2	Zasp67
CG1347	29	1	Atg17
CG43318	29	1	CG43318
CG1554	28	1	RNA polymerase II 215kD subunit
CG10922	28	1	La autoantigen-like
CG11020	28	1	no mechanoreceptor potential C
CG15848	28	1	Sarcoplasmic calcium-binding protein 1
CG11471	28	1	Isoleucyl-tRNA synthetase
CG5252	28	1	Ranbp9
CG2522	27	1	GTP-binding protein
CG5183	27	1	KDEL receptor
CG4633	27	1	mitochondrial alanyl-tRNA synthetase
CG12499	27	1	CG12499
CG17510	27	1	Fis1
CG32146	27	1	dally-like
CG32683	27	1	CG32683
CG31175	27	1	Dystrophin
CG17870	26	1	14-3-3ζ
CG8749	26	1	small ribonucleoprotein particle U1 subunit 70K
CG7405	26	1	Cyclin H
CG17838	26	1	Syncrip
CG33233	26	1	CG33233
CG8793	26	1	lethal (3) 76BDm
CG4001	25	1	Phosphofructokinase
CG10859	25	1	CG10859
CG32016	25	1	eIF4E-Transporter
CG43063	25	1	CG43063
CG14816	23	1	Phosphoglycerate mutase 5
CG31116	23	2	Chloride channel-a
CG32210	23	1	Listerin E3 ubiquitin protein ligase 1
CG42327	23	1	CG42327
CG18176	21	1	deflated
CG1716	20	1	Set2

C.10 pUb-GFP-Dragon purification from syncytial *Drosophila* embryos

CG #	Score	#pep	Full name
CG33052	2764	50	CG33052
CG4264	1590	25	Heat shock protein cognate 4
CG8280	1028	15	Elongation factor 1α48D
CG15524	752	18	Spindle assembly abnormal 6 ortholog (C. elegans)
CG9277	731	17	β-Tubulin at 56D
CG9277	656	14	β-Tubulin at 56D
CG9359	506	11	β-Tubulin at 85D
CG4147	439	6	Heat shock 70-kDa protein cognate 3
CG8937	438	5	Heat shock protein cognate 1
CG8937	389	4	Heat shock protein cognate 1
CG18743	386	4	Heat-shock-protein-70Ab
CG2979	345	6	Yolk protein 2
CG4466	321	6	Heat shock protein 27
CG11129	315	7	Yolk protein 3
CG3401	308	9	β-Tubulin at 60D
CG1349	307	4	dj-1β
CG1873	300	6	Elongation factor 1α100E
CG7756	277	3	Heat shock protein cognate 2
CG4169	254	4	Ubiquinol-cytochrome c reductase core protein 2
CG10521	241	58	Netrin-B
CG4869	233	7	β-Tubulin at 97EF
CG7660	232	3	Peroxinectin-like
CG1913	215	5	α-Tubulin at 84B
CG17246	179	2	Succinate dehydrogenase A
CG9476	177	4	α-Tubulin at 85E
CG17291	173	3	Protein phosphatase 2A at 29B
CG3283	169	4	Succinate dehydrogenase B
CG5366	161	2	Cullin-associated and neddylation-dissociated 1
CG4916	141	3	maternal expression at 31B
CG8863	139	2	DnaJ-like-2
CG4183	133	2	Heat shock protein 26
CG33129	129	19	CG33129
CG4634	126	2	Nucleosome remodeling factor - 38kD
CG15825	121	1	fondue
CG10377	118	1	Heterogeneous nuclear ribonucleoprotein at 27C
CG12233	116	3	lethal (1) G0156
CG1263	114	1	Ribosomal protein L8
CG12306	113	1	polo
CG16944	110	6	stress-sensitive B
CG7349	104	2	Succinate dehydrogenase, subunit B (iron-sulfur)-like
CG6235	101	2	twins
CG14648	100	3	lost
CG1548	97	2	cathD
CG5371	94	2	Ribonucleoside diphosphate reductase large subunit
CG5499	88	2	Histone H2A variant
CG5261	87	2	midline uncoordinated
CG13422	87	1	GNBP-like 3
CG12262	83	1	CG12262
CG11181	80	1	cup
CG2985	80	4	Yolk protein 1
CG2168	77	1	Ribosomal protein S3A
CG8947	77	1	26-29kD-proteinase
CG11793	69	2	Superoxide dismutase
CG4916	69	2	maternal expression at 31B
CG1372	67	1	yolkless
CG15693	66	1	Ribosomal protein S20
CG8308	64	2	α-Tubulin at 67C
CG1683	64	1	Adenine nucleotide translocase 2
CG3203	64	1	Ribosomal protein L17
CG1242	59	1	Heat shock protein 83
CG1782	59	2	Ubiquitin activating enzyme 1
CG12244	58	2	licorne
CG7361	57	1	Rieske iron-sulfur protein

CG4193	56	1	deadhead
CG4863	56	1	Ribosomal protein L3
CG5504	53	1	lethal (2) tumorous imaginal discs
CG11276	53	1	Ribosomal protein S4
CG5502	52	1	Ribosomal protein L4
CG3024	52	1	Torsin
CG4651	51	1	Ribosomal protein L13
CG12052	50	1	longitudinals lacking
CG8415	50	1	Ribosomal protein S23
CG33456	50	2	muscle wasted
CG12369	49	12	Lachesin
CG6782	49	1	scheggia
CG5252	47	1	Ranbp9
CG9738	44	1	MAP kinase kinase 4
CG7977	44	1	Ribosomal protein L23A
CG13671	44	9	CG13671
CG1633	42	1	thioredoxin peroxidase 1
CG31884	41	1	thioredoxin-2
CG32164	40	1	CG32164
CG8905	37	1	Superoxide dismutase 2 (Mn)
CG5261	37	1	midline uncoordinated
CG4752	37	5	CG4752
CG31038	35	3	CG31038
CG2048	34	1	discs overgrown
CG4683	34	2	Testis EndoG-Like 4
CG10718	33	1	nebbish
CG9012	32	1	Clathrin heavy chain
CG6453	32	1	Glucosidase 2 β subunit
CG1821	31	1	Ribosomal protein L31
CG12163	31	1	CG12163
CG5263	30	1	smaug
CG2982	29	1	CG2982
CG9769	29	1	CG9769
CG7985	28	1	CG7985
CG33322	28	1	CG33322
CG32599	28	1	CG32599
CG42333	28	1	Synaptotagmin β
CG8246	27	1	Pox neuro
CG40478	27	1	Dual-specificity tyrosine phosphorylation-regulated kinase 3
CG14961	27	2	CG14961
CG10617	27	1	Synaptotagmin 12
CG8900	26	1	Ribosomal protein S18
CG2179	26	1	Xe7
CG16827	26	1	Integrin alphaPS4 subunit
CG31029	26	1	CG31029
CG12079	26	1	NADH dehydrogenase (ubiquinone) Fe-S protein 3
CG10594	25	2	spook
CG12164	25	1	CG12164
CG8907	25	2	CG8907
CG7413	24	1	Retinoblastoma-family protein
CG9809	24	1	spargel
CG8201	23	2	par-1
CG16983	22	1	skpA
CG5762	22	2	CG5762
CG2050	21	1	modulo
CG9537	21	2	Daxx-like protein
CG7369	21	1	CG7369
CG34434	21	1	CG34434
CG12055	20	1	Glyceraldehyde 3 phosphate dehydrogenase 1
CG9081	20	1	Cyp4s3
CG10021	19	1	brother of odd with entrails limited
CG9674	19	1	CG9674
CG1842	18	1	Dynein heavy chain at 89D
CG9159	18	2	Kruppel homolog 2
CG15744	18	1	CG15744
CG42346	18	1	CG42346
CG8817	17	1	lilliputian
CG30281	17	1	CG30281
CG7378	16	1	CG7378
CG12836	16	1	CG12836
CG3350	16	1	bigmax
CG17632	15	1	brown
CG11387	15	1	cut
CG11254	15	1	maelstrom
CG8322	15	1	ATP citrate lyase
CG6509	15	1	Discs large 5
CG11107	15	1	DHX15 ortholog
CG9168	15	1	CG9168
CG30484	15	1	CG30484
CG10375	14	1	CG10375

Appendix D

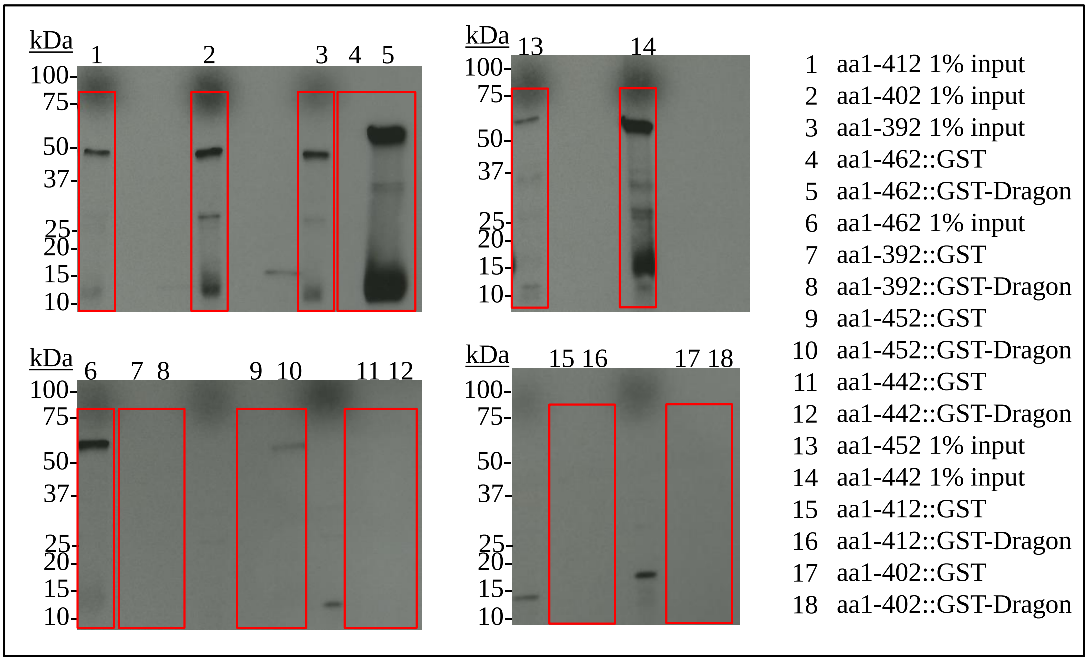

D.1 Original autoradiogram of four gels with indicated boxes that were cropped for Figure 5-12C. Numbers are explained in figure legend on the right. Domains of Sas6 in aa (amino acids); 1% input of ^{35}S-Methionine-labelled Sas6 fragment that was used for each binding assay; binding assays of ^{35}S-Methionine-labelled Sas6 fragment with GST-alone immobilised on resin (::GST) or GST-N-terminally tagged Dragon immobilised on resin (::GST-Dragon).